Multivalent antibody-scTRAIL fusion proteins for tumor therapy

–

Impact of format and targeting

Von der Fakultät Energie-, Verfahrens- und Biotechnik
der Universität Stuttgart zur Erlangung der Würde eines Doktors der Naturwissenschaften (Dr. rer. nat.) genehmigte Abhandlung

Vorgelegt von
Meike Hutt
aus Schorndorf

Hauptberichter: Prof. Dr. Roland Kontermann
Mitberichter: Prof. Dr. Ralf Takors

Tag der mündlichen Prüfung: 15.02.2017

Institut für Zellbiologie und Immunologie
Universität Stuttgart

2017

Table of Contents

Abbreviations

aa	amino acid
Ab	antibody
ABD	albumin-binding domain
ADAM	a disintegrin and metalloproteinase
Ag	antigen
AICD	activation-induced cell death
ALT	alanine transaminase
amp	ampicillin
APAF-1	apoptotic protease-activating factor 1
Apo2L	Apo2 ligand
APS	ammonium persulfate
AU	absorbance unit
AUC	area under the curve
BAD	BCL-2 antagonist of cell death
BAK	BCL-2 antagonist or killer
BAX	BCL-2-associated X protein
BCL-2	B cell lymphoma 2
BCL-XL	BCL extra large
BH3	BCL-2 homology 3
BID	BH3-interacting domain death agonist
BIM	BCL-2-interacting mediator of cell death
BLAST	basic local alignment search tool
BZB	Bortezomib
CD	cluster of differentiation
CDR	complementarity-determining region
CEA	carcinoembryonic antigen
cFLIP	cellular FLICE-like inhibitory protein
$cFLIP_L$	cFLIP-long
$cFLIP_R$	cFLIP-Raji
$cFLIP_S$	cFLIP-short
C_H	constant domain of the heavy chain
CLL1	C-type lectin-like molecule-1
CRD	cysteine-rich domain
Db	Diabody
DcR	decoy receptor
DIABLO	direct inhibitor of apoptosis binding protein with low pI
DISC	death-inducing signaling complex
DNA	deoxyribonucleic acid
dNTP	deoxynucleotide
DR	death receptor
dsDb	disulfide-stabilized diabody
EC_{50}	half-maximal effective concentration
EDA	alternatively-spliced EDA domain of fibronectin
EDTA	ethylenediaminetetraacetic acid
EGFR	epidermal growth factor receptor
EHD2	IgE heavy chain domain 2
ELISA	enzyme-linked immunosorbent assay
EpCAM	epithelial cell adhesion molecule
EPR	enhanced permeability and retention
ER	endoplasmic reticulum
ERKs	extracellular regulated kinases
FADD	Fas-associated death domain protein
FAP	fibroblast activation protein
FasL	Fas ligand
FBS	fetal bovine serum
Fc	fragment crystallizable
FcRn	neonatal Fc receptor
FcγR	IgG Fc receptor
FLAG-tag	DYKDDDDK-tag
FLICE	FADD-like IL-1β-converting enzyme
FPLC	fast protein liquid chromatography
GITRL	ligand of glucocorticoid-induced TNF-receptor-related protein
glc	glucose
GM-CSF	granulocyte macrophage colony-stimulating factor
GPI	glycosylphosphatidylinositol
HEK	human embryonic kidney
HER2/3/4	human epidermal growth factor receptor 2/3/4
His-tag	hexahistidine-tag
HPLC	high-performance liquid chromatography
HRP	horseradish peroxidase
HSA	human serum albumin
hu	human
HUMSC	human umbilical cord derived mesenchymal stem cell
Ig	immunoglobulin
IL	interleukin
ILZ	isoleucine zipper
IMAC	immobilized metal ion affinity chromatography
IMS	intermembrane space

IPTG	isopropyl β-D-1-thiogalactopyranoside
JNKs	c-Jun N-terminal kinases
LB	lysogeny broth
LPS	lipopolysaccharide
mAb	monoclonal antibody
MAPKs	mitogen-activated protein kinases
MCL-1	myeloid cell leukemia 1
MCSP	melanoma-associated chondroitin sulfate proteoglycan
MFI	median fluorescence intensity
mo	mouse
MOM	mitochondrial outer membrane
MOMP	MOM permeabilization
MPBS	non-fat dry milk powder in PBS
NEMO	NF-κB essential modulator
NF-κB	nuclear factor κ-light-chain-enhancer of activated B cells
NTA	nitrilotriacetic acid
OD	optical density
OPG	osteoprotegerin
P/S	penicillin-streptomycin
PAA	polyacrylamide
PAGE	polyacrylamide gel electrophoresis
PARA	pro-apoptotic receptors agonist
PBA	PBS, 2 % (v/v) FBS, 0.02 % (w/v) NaN_3
PBS	phosphate-buffered saline
PBST	PBS with TWEEN 20
PCR	polymerase chain reaction
PCSK9	proprotein convertase subtilisin kexin type 9
PD	pharmacodynamics
PD-L1	programmed death ligand 1
PE	phycoerythrin
PEG	polyethylene glycol
pI	isoelectric point
PI3K	phosphatidylinositide 3-kinases
PIK3CA	phosphatidylinositol-4, 5-bisphosphate 3-kinase, catalytic subunit alpha
PK	pharmacokinetics
PKC	protein kinase C
PLAD	pre-ligand assembly domain
PPB	periplasmic preparation buffer
pre-BCR	pre-B cell receptor
PUMA	p53 upregulated modulator of apoptosis
RBC	red blood cell
RBD	receptor-binding domain
RIP1/3	receptor-interacting protein 1/3
RLU	relative light units
RPMI	Roswell Park Memorial Institute
s	soluble
sc	single-chain
scDb	single-chain diabody
scFv	single-chain fragment variable
scTRAIL	single-chain tumor necrosis factor-related apoptosis-inducing ligand
$scTRAIL_{281\text{-}G\text{-}118}$	scTRAIL consisting of aa 118 to 281 with linkers of a single glycine connecting the TRAIL monomers
SD	standard deviation
SDS	sodium dodecyl sulfate
SEC	size exclusion chromatography
sEpCAM	soluble EpCAM
SMAC	second mitochondria-derived activator of caspases
S_r	Stokes radius
sTRAIL	soluble TRAIL
$t_{1/2}\alpha$	initial half-life
$t_{1/2}\beta$	terminal half-life
TAA	tumor-associated antigen
TAE	Tris-acetate-EDTA
TAK1	TGF-β-activated kinase 1
tBID	truncated BID
TEMED	tetramethylethylenediamine
Tf	transferrin
TGF-α/-β	transforming growth factor-α/-β
THD	TNF homology domain
T_M	melting point
TMB	3,3',5,5'-tetramethylbenzidine
TMTP1	tumor molecular targeted peptide 1
TNC	trimerization domain of tenascin-C
TNF	tumor necrosis factor
TNF-R	TNF receptor
TNFRSF	TNF receptor superfamily
TNFSF	TNF superfamily
TRADD	TNF receptor-associated death domain protein
TRAF2	TNF receptor-associated factor 2
TRAIL	tumor necrosis factor-related apoptosis-inducing ligand
TRAIL-R	TRAIL receptor
Tris	Tris(hydroxymethyl)aminomethane
TY	tryptone yeast
V_H	variable domain of the heavy chain
V_L	variable domain of the light chain
wt	wild-type
XIAP	X-linked inhibitor of apoptosis protein

Abstract

Using death ligands to induce apoptosis is an attractive concept for the treatment of cancer. By triggering the extrinsic apoptosis pathway, death ligands are independent of intrinsic apoptosis induction, which is frequently impaired in tumor cells. Due to its unique selectivity properties, tumor necrosis factor-related apoptosis-inducing ligand (TRAIL) has been considered as an especially promising candidate to exploit this approach. Clinical trials, however, were largely disappointing, provoking the development of manifold second generation TRAIL-based therapeutics with improved efficacy. Extensive investigations revealed the particularly high potential of increased TRAIL valency and targeted delivery as improvement strategies. This study was performed to comparatively analyze different formats of scTRAIL fusion proteins employing the concepts of increased valency and tumor targeting to further guide therapeutic development.

Based on an optimized single-chain version of TRAIL (scTRAIL), the investigated set of dimeric antibody-scTRAIL fusion proteins included the already described Db-scTRAIL and scFv-EHD2-scTRAIL formats and was extended by a disulfide-stabilized version of the diabody molecule (dsDb-scTRAIL) and scFv-Fc-scTRAIL. These four formats were generated comprising targeting moieties directed against EGFR, HER2, HER3, and EpCAM. Additionally, non-targeted monomeric scTRAIL as well as non-targeted dimeric EHD2-scTRAIL and Fc-scTRAIL were included. Consistent with previous studies, dimeric EHD2-scTRAIL and Fc-scTRAIL exerted significantly increased cell death induction compared to scTRAIL. The different formats of dimeric antibody-scTRAIL fusion proteins were equipotent with respect to binding activities and *in vitro* cell death induction in two colorectal cancer cell lines. However, by displaying enhanced properties regarding production, thermal stability, reliable dimer formation, *in vivo* half-life, and pharmacodynamic effects, scFv-Fc-scTRAIL emerged as superior protein format. Comparative analysis of scFv-Fc-scTRAIL fusion proteins comprising different targeting moieties revealed major differences in binding activity and *in vitro* cell death induction. Interestingly, only three of the five analyzed antibody units improved the cytotoxic activity of the respective targeted molecule compared to Fc-scTRAIL in a partly cell line-dependent manner. Correlation of cell death induction with binding properties indicated the relevance of improved cell binding of scFv-Fc-scTRAIL compared to Fc-scTRAIL for targeting effects *in vitro*. This appeared to be determined by strong antigen binding of the antibody part and sufficient

antigen expression levels. Surprisingly, despite strong efficacy, the targeting effects observed for three scFv-Fc-scTRAIL molecules *in vitro* did not translate into an increased anti-tumor activity compared to non-targeted Fc-scTRAIL in a Colo205 xenograft model. Further investigations will therefore be required to identify the factors underlying the discrepancy of *in vitro* and *in vivo* data. In conclusion, this study demonstrated the potent activity of non-targeted Fc-scTRAIL that further provides a platform for combination with tumor-targeting ligands as fusion partners, thereby offering the opportunity for tumor-tailored optimization.

Zusammenfassung

Ein attraktiver Ansatz zur Behandlung von Krebs ist die Verwendung von Todesliganden. Diese induzieren Apoptose über den extrinsischen Weg und sind damit unabhängig von intrinsischer Apoptoseinduktion, welche in Tumorzellen häufig beeinträchtig ist. Aufgrund seiner Selektivität für Tumorzellen gilt TRAIL (Tumornekrosefaktor-verwandter Apoptose-induzierender Ligand) als besonders vielversprechender Kandidat für die Umsetzung dieses Konzepts. Klinische Studien lieferten allerdings weitgehend enttäuschende Ergebnisse, was zur Weiterentwicklung TRAIL-basierter Therapeutika führte und eine Vielzahl verbesserter Varianten generierte. Besonders effektive Verbesserungsstrategien stellen dabei die Steigerung der Valenz von TRAIL sowie die Modifikation zur gezielten Tumorzellbindung (sogenanntes *Targeting*) dar. Ziel dieser Arbeit war die Untersuchung unterschiedlicher Formate von scTRAIL Fusionsproteinen, die auf den Konzepten der Valenzsteigerung und zielgerichteten Tumorzellbindung basierten und deren systematischer Vergleich der Unterstützung weiterer Entwicklungsschritte dienen sollte.

Unter Verwendung einer optimierten TRAIL-Version, die alle TRAIL-Untereinheiten auf einer Polypeptidkette verbindet (sogenanntes *single-chain* TRAIL; scTRAIL), wurden verschiedene dimere Antikörper-scTRAIL Fusionsproteine hergestellt. Dazu zählten, neben den etablierten Formaten Db-scTRAIL und scFv-EHD2-scTRAIL, eine Disulfid-stabilisierte Form des Diabody-Moleküls (dsDb-scTRAIL) sowie scFv-Fc-scTRAIL. Als zusätzliche Varianten ohne *Targeting*-Einheiten wurden sowohl monomeres scTRAIL als auch dimere EHD2-scTRAIL und Fc-scTRAIL Fusionsproteine generiert. Verglichen mit scTRAIL zeigten EHD2-scTRAIL und Fc-scTRAIL in Übereinstimmung mit vorangegangenen Untersuchungen eine signifikant stärkere Induktion von Zelltod. Für die unterschiedlichen Formate der dimeren Antikörper-scTRAIL Fusionsproteine wurden vergleichbare Eigenschaften hinsichtlich der Bindungsaktivität sowie der Zelltodinduktion in zwei kolorektalen Tumorzelllinien bestimmt. Weitere Untersuchungen zeigten jedoch eine verbesserte Produktion, erhöhte thermische Stabilität, verlässlichere Ausbildung der dimeren Form, verlängerte *in vivo* Halbwertszeit sowie stärkere pharmakodynamische Effekte für scFv-Fc-scTRAIL. Dies verdeutlicht die überlegenen Eigenschaften dieses Formats. Deutliche Unterschiede in der Bindungsaktivität und Induktion von Zelltod ergaben sich für scFv-Fc-scTRAIL Fusionsproteine mit unterschiedlichen *Targeting*-Einheiten. Nur drei der fünf eingesetzten Antikörper-Module verbesserten dabei die

zytotoxische Aktivität des jeweiligen scFv-Fc-scTRAIL Moleküls im Vergleich zu Fc-scTRAIL, zum Teil in Abhängigkeit von der Zelllinie. Die Korrelation von Zelltodinduktion mit Bindungseigenschaften deutete darauf hin, dass eine verstärkte Zellbindung von scFv-Fc-scTRAIL verglichen mit Fc-scTRAIL notwendig ist, um *Targeting*-Effekte *in vitro* zu erzielen. Dies wiederum schien auf einer starken Antigenbindung durch den Antikörper und einer ausreichenden Antigenexpression zu beruhen. Ein Colo205 Xenotransplantat-Modell bestätigte die hohe Wirksamkeit der Proteine. Allerdings führten die *in vitro Targeting*-Effekte, die für drei scFv-Fc-scTRAIL Moleküle gezeigt wurden, nicht zu einer Erhöhung der antitumoralen Aktivität im Vergleich zu Fc-scTRAIL *in vivo*. Weitere Untersuchungen sind daher erforderlich, um die Faktoren zu bestimmen, die dieser Diskrepanz von *in vitro* und *in vivo* Daten zu Grunde liegen. Zusammenfassend verdeutlichte diese Arbeit die hohe Wirksamkeit von Fc-scTRAIL, das zudem eine Plattform zur weiteren Verknüpfung mit Tumor bindenden Liganden als Fusionspartnern bietet und auf diese Weise eine dem jeweiligen Tumor angepasste Optimierung ermöglicht.

1 Introduction

One hallmark of cancer development and progression is the dysregulation of a cell's machinery to induce controlled death, a mechanism essential to determine cell fate upon severe damage. The mutations underlying this phenotypic alteration are diverse, but frequently affect the p53 status, thereby hampering the induction of the intrinsic apoptotic pathway (see 1.1). These modifications contribute to resistance towards classical treatment approaches, like chemo- and radiotherapy (reviewed by Ashkenazi, 2008; Cotter, 2009; Johnstone *et al.*, 2002). Therefore, strategies inducing death of malignant cells independent of these alterations are promising therapeutic concepts. Using death ligands, in particular the tumor necrosis factor-related apoptosis-inducing ligand (TRAIL), to exploit the extrinsic apoptotic pathway (see 1.1) for tumor cell killing is an attractive approach to circumvent the necessity of p53-dependent apoptosis induction (Galligan *et al.*, 2005). Limitations of classical therapy do not only arise due to intrinsic or acquired resistance mechanisms and thus insufficient efficacy, but are also caused by the lack of selectivity for cancer cells often leading to severe side effects (reviewed by Ashkenazi, 2002). Besides benefitting from death ligand-specific selectivity properties, the advances achieved in targeted cancer therapy offer great potential to further restrict the cytotoxic activity of death ligands to tumor cells.

1.1 Apoptosis

The sequence of programmed cell death, termed apoptosis, is crucial during development, in immune reactions, and for tissue homeostasis of multicellular organisms. The involvement in these processes already implicates the detrimental effects that can be caused by its dysregulation. Besides the afore-mentioned role in malignant cell transformation due to process-impairing alterations, also increased rates of programmed cell death contribute to the development of diseases, such as neurodegeneration. In general, two pathways, the intrinsic and the extrinsic apoptosis induction that are both characterized by sequential activation of caspases (cysteine-aspartic proteases) are distinguished (reviewed by Elmore, 2007; Tait and Green, 2010). The intrinsic or mitochondrial pathway is triggered upon deprivation of anti-apoptotic stimuli or detection of severe damage (e.g. induced by chemotherapeutics or irradiation). Subsequently, regulation of BCL-2 family members by p53 results in mitochondrial outer membrane permeabilization (MOMP; Figure 1.2; reviewed by Hemann and Lowe, 2006;

Vaseva and Moll, 2009). The BCL-2 family comprises pro- as well as anti-apoptotic proteins. The pro-apoptotic members BAX and BAK promote MOMP and are negatively regulated by anti-apoptotic members, like BCL-2, BCL-XL, and MCL-1 that in turn are antagonized by BH3-only members, including PUMA, NOXA, BIM, and BAD. This complex regulation is further extended by the capability of some BH3-only proteins to directly interact with and activate the effector proteins BAX and BAK (reviewed by Chipuk *et al.*, 2010). MOMP via pore formation by BAX and BAK leads to the release of pro-apoptotic proteins from the intermembrane space (IMS) into the cytosol. Binding of released cytochrome c to APAF-1 induces heptamerization and recruitment of procaspase-9. Formation of this platform, called apoptosome, enables proteolytic activation of initiator caspase-9 that subsequently activates executioner caspases. Release of other pro-apoptotic proteins, like SMAC/DIABLO further supports this activation cascade by antagonizing caspase-inhibiting XIAP (reviewed by Tait and Green, 2010).

The extrinsic or death receptor pathway is activated by binding of death ligands, i.e. tumor necrosis factor superfamily (TNFSF) members TNF, FasL, and TRAIL, to the respective death receptors (DRs), i.e. TNF receptor superfamily (TNFRSF) members TNF-R1, CD95, TRAIL-R1 and -R2 (Figure 1.2; reviewed by Elmore, 2007). The triggered signaling cascade is characterized by homotypic interactions of protein domains. Upon ligand binding, the death receptors recruit the adaptor protein FADD via homotypic interactions of so-called death domains. This occurs either directly (CD95, TRAIL-R1, TRAIL-R2) or indirectly via TRADD and RIP1 that together with TRAF2 dissociate from the receptor to form a cytoplasmic platform (TNF-R1; Micheau and Tschopp, 2003). Mediated by homotypic interactions of death effector domains, FADD subsequently associates with procaspase-8 or -10 leading to the formation of the death-inducing signaling complex (DISC). Homodimerization of procaspases-8 or -10 at the DISC provokes conformational changes that expose the active site to allow autocatalytic activation. Activated initiator caspases then cleave and activate further procaspase-8 and -10 molecules. In type I cells, activation of caspases-8 and -10 is sufficient to trigger apoptosis, whereas type II cells require an additional amplification loop that links the extrinsic to the intrinsic apoptotic pathway. Here, cleavage of the pro-apoptotic BH3-only BCL-2 family member BID by caspase-8 generates truncated BID (tBID). TBID mediates the insertion of BAX and BAK into the mitochondrial outer membrane, inducing the release of cytochrome c and SMAC into the cytosol and thus activating caspase-9 (reviewed by de Miguel *et al.*, 2016).

Both the intrinsic and extrinsic pathway share the same execution pathway, which starts with activation of executioner caspases-3, -6, and -7 by initiator caspases. Activated executioner caspases cleave various cellular substrates and thereby e.g. activate endonucleases and proteases. Morphological changes that characterize apoptotic cell death comprise cell shrinkage, chromatin condensation, membrane blebbing, and nuclear fragmentation concluding with the formation of apoptotic bodies that are rapidly removed by phagocytosis. Thus, a cell undergoing apoptosis stays intact during the whole process (reviewed by Elmore, 2007).

1.2 Structural and functional properties of TRAIL and TRAIL receptors

TRAIL, also known as CD253, TNFSF10, and Apo2L, is expressed as a 281 amino acids long type II transmembrane protein, i.e. with an intracellular N-terminus and an extracellular C-terminus connected via a single transmembrane domain (Wiley *et al.*, 1995). As a member of the TNFSF, TRAIL comprises a conserved C-terminal domain, the so-called TNF homology domain (THD) that exhibits a jelly roll structure consisting of two anti-parallel β-sheets (Figure 1.1A; Cha *et al.*, 1999; Cha *et al.*, 2000). The THD mediates homotrimeric assembly of the ligand into a bell-like shape and defines receptor binding properties (reviewed by Bodmer *et al.*, 2002; Locksley *et al.*, 2001). In contrast to other TNFSF members, homotrimerization of TRAIL requires coordination of a zinc ion by three unpaired cysteine residues (Cys230 of each monomer) at the trimer interface, which is essential for stability, solubility, and activity (Bodmer *et al.*, 2000; Hymowitz *et al.*, 2000). A stalk region links the transmembrane domain to the THD and can be subject to proteolytic processing of TRAIL into a soluble homotrimeric form. The receptor binding sites are located at the interface formed by two monomers, thus enabling simultaneous binding of three receptors (Figure 1.1B,C; Hymowitz *et al.*, 1999; Ramamurthy *et al.*, 2015). Physiologically, TRAIL is expressed on various tissues and on cells of the innate and adaptive immune system, like dendritic cells, monocytes, natural killer cells, and T cells, assigning TRAIL an important role in immune surveillance. This includes anti-viral and anti-tumoral activity as well as mediation of activation-induced cell death (AICD) to avoid autoimmune reactivity (reviewed by Almasan and Ashkenazi, 2003; de Miguel *et al.*, 2016).

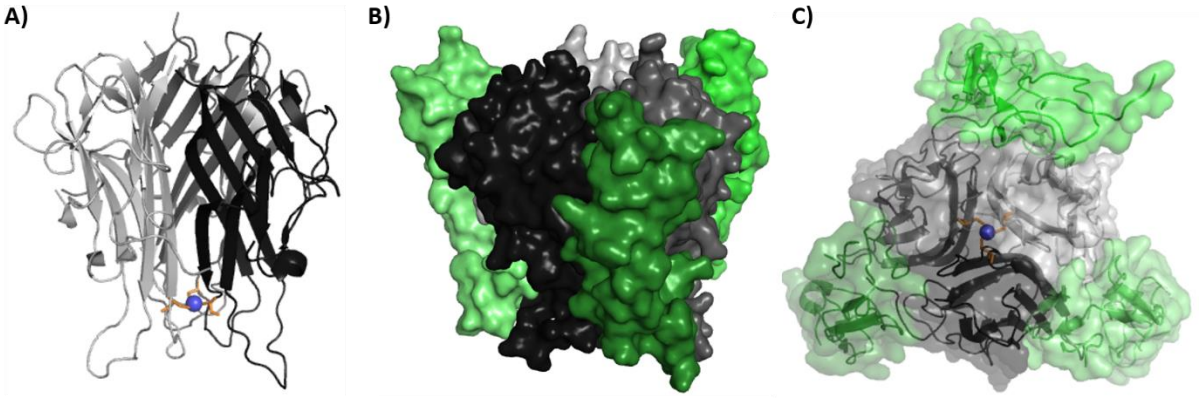

Figure 1.1: Crystal structure of TRAIL in complex with TRAIL-R2. A) Secondary structure elements of the THD of homotrimeric TRAIL are represented as cartoon. B) Surface of homotrimeric TRAIL in complex with three TRAIL-R2 chains is visualized. C) Surface and cartoon representation of the $TRAIL_3$ – $TRAIL\text{-}R2_3$ complex is shown facing the C-terminal side of TRAIL-R2. Visualization of PDB 1DU3 (Cha *et al.*, 2000) was performed using PyMOL. TRAIL monomers are shown in light gray, gray, and dark gray, while the TRAIL-R2 chains are colored in different shades of green. The zinc ion is represented as blue sphere coordinated by Cys230 of each TRAIL monomer highlighted as orange sticks.

TRAIL is able to bind to five receptors of the TNFRSF. Generally, TNFRSF members are characterized by an elongated extracellular part composed of cysteine-rich domains (CRDs) that mediate ligand binding (reviewed by Ashkenazi, 2002; Holland, 2013; de Miguel *et al.*, 2016). TRAIL-R1 (DR4, TNFRSF10A) and TRAIL-R2 (DR5, TNFRSF10B, Apo2, KILLER, TRICK2) are type I transmembrane proteins that comprise a C-terminal cytoplasmic death domain equipping them with the capability to induce apoptosis (Pan *et al.*, 1997a; Pan *et al.*, 1997b). While TRAIL-R1 is activated upon ligation with membrane-bound as well as soluble TRAIL, TRAIL-R2 signaling requires higher order receptor clustering, which is only induced by the membrane-bound form (Figure 1.3A; Mühlenbeck *et al.*, 2000; Wajant *et al.*, 2001). TRAIL-R3 (DcR1, TNFRSF10C) lacks a transmembrane and cytoplasmic domain and is linked to the cell surface via a glycosylphosphatidylinositol (GPI) anchor (Degli-Esposti *et al.*, 1997a). In contrast, TRAIL-R4 (DcR2, TNFRSF10D) contains both a transmembrane and cytoplasmic death domain, the latter however in a truncated form, which precludes apoptotic signaling (Degli-Esposti *et al.*, 1997b; Pan *et al.*, 1998). Both TRAIL-R3 and TRAIL-R4 are described to function as decoy receptors negatively regulating TRAIL-R1- and TRAIL-R2-mediated apoptosis by competing for ligand binding. Additionally, TRAIL-R4 is reported to trap TRAIL-R1 and TRAIL-R2 in signaling-incompetent receptor complexes either in a TRAIL-dependent manner or independent of ligand binding by interactions of the pre-ligand assembly domains (PLADs) that are present in those receptors. Besides these inhibitory interactions, negative regulation of TRAIL-induced apoptosis has been proposed through non-apoptotic pro-survival signaling by TRAIL-R4. However, the physiological role of TRAIL-R3 and -R4 is far from being completely

understood and might furthermore vary for different cell types (Mérino *et al.*, 2006; Neumann *et al.*, 2014). Due to a low binding affinity at physiological temperatures, the relevance of the interaction of TRAIL with a fifth TNFRSF member, the soluble decoy receptor osteoprotegerin (OPG), is still unclear (Emery *et al.*, 1998). Physiologically, TRAIL receptors are expressed on various tissues (Spierings *et al.*, 2004). Besides their localization at the plasma membrane, in secretory vesicles, endosomes, and lysosomes, TRAIL receptors are furthermore found in the nucleus, in autophagosomes, as well as in a soluble cytosolic form. Elevated expression levels in these non-membranous intracellular compartments have been reported for cancer cells and associated with TRAIL resistance and higher malignancy (reviewed by Bertsch *et al.*, 2014).

1.3 TRAIL-mediated signaling and its regulation

Being already implicated in its name, the canonical signaling pathway induced by TRAIL is apoptosis. Modulation of the afore-mentioned extrinsic or death receptor pathway (see 1.1) is possible and occurs on several levels (Figure 1.2; reviewed by Azijli *et al.*, 2013; de Miguel *et al.*, 2016). Besides the expression of decoy receptors that is able to regulate TRAIL signaling extracellularly (see 1.2), an important factor influencing intracellular signal transduction is cFLIP. CFLIP exists as three splice variants, $cFLIP_L$, $cFLIP_S$, and $cFLIP_R$, all comprising two death effector domains structurally similar to those of procaspase-8 and -10. While $cFLIP_S$ and $cFLIP_R$ are dominant-negative inhibitors of caspase-8 and -10 activation by competing for binding to FADD, the effects of $cFLIP_L$ are more complex. Depending on the ratio to caspase-8, $cFLIP_L$ either exerts anti-apoptotic properties (at high $cFLIP_L$ levels) or exhibits substrate specificity-modulating effects on caspase-8 (at lower $cFLIP_L$ levels). In the latter case, the caspase-8/$cFLIP_L$ heterodimer retains proteolytic activity that is even increased for certain substrates (Chang *et al.*, 2002; Golks *et al.*, 2005; Krueger *et al.*, 2001; Micheau *et al.*, 2002). Additional mechanisms that regulate apoptotic TRAIL signaling include the expression of XIAP (that inhibits caspases-3, -7, and -9; Deveraux *et al.*, 1997) and anti-apoptotic BCL-2 family members (Clohessy *et al.*, 2006; Hinz *et al.*, 2000; Munshi *et al.*, 2001), post-translational modifications of DISC proteins, like O-glycosylation (Wagner *et al.*, 2007) and ubiquitination (Gonzalvez *et al.*, 2012; Jin *et al.*, 2009), as well as endocytosis (Austin *et al.*, 2006; Kohlhaas *et al.*, 2007). Downregulation of pro- and upregulation of anti-apoptotic proteins is often found in TRAIL-resistant cancer cells. Commonly, resistance is not caused by a single alteration, but by simultaneous modifications of multiple factors (reviewed by Amarante-Mendes and Griffith, 2015).

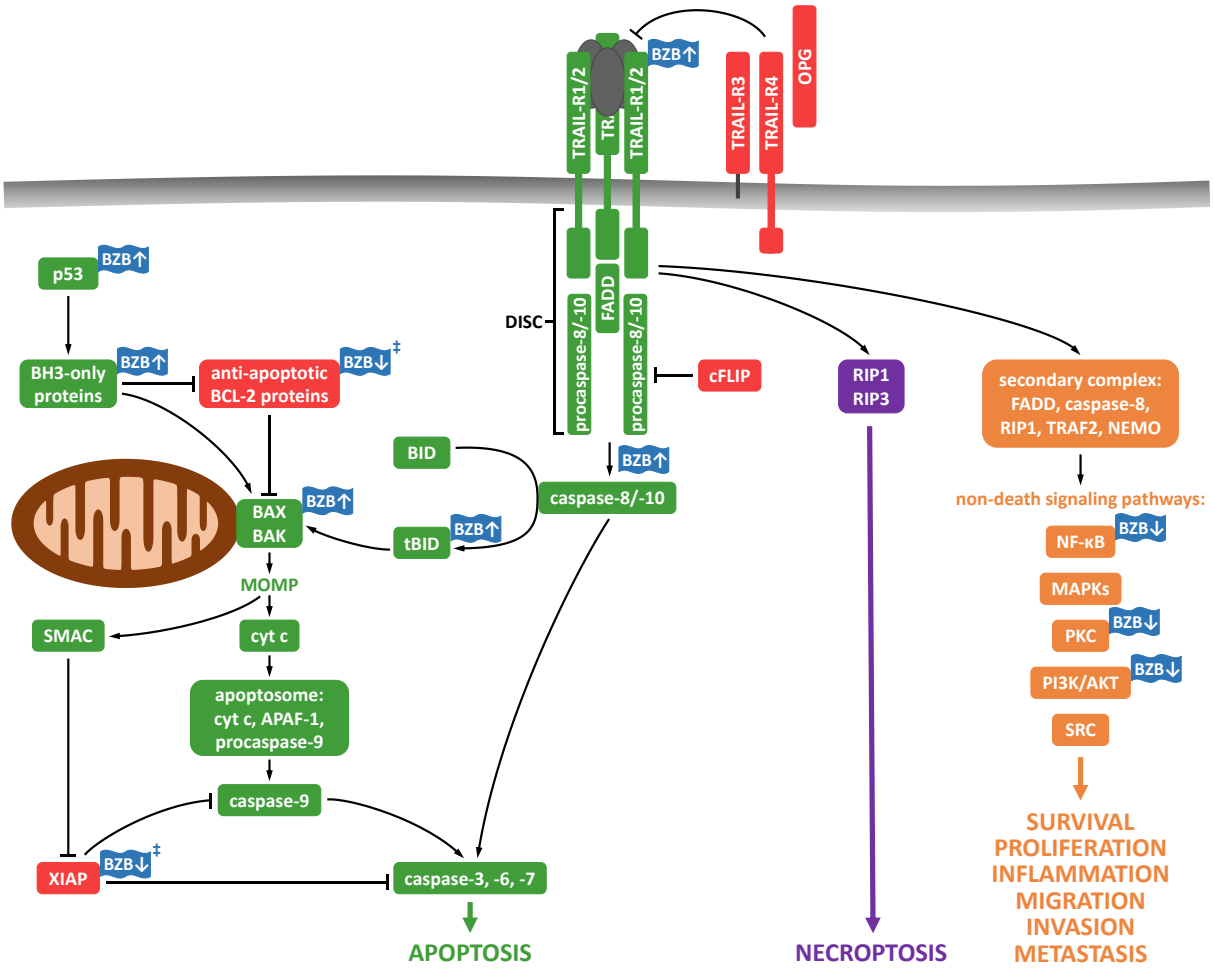

Figure 1.2: Apoptosis, non-canonical TRAIL signaling, and possible levels of interference of bortezomib. Predominant signaling induced by TRAIL is the extrinsic apoptosis pathway that in type II cells is linked to intrinsic apoptotic signaling via cleavage of BID to tBID. Alternatively, TRAIL is able to induce necroptosis and non-cell death signaling pathways. Potential influence of bortezomib (BZB) treatment on TRAIL-mediated signaling is indicated. For a more detailed explanation of apoptosis, non-canonical TRAIL signaling pathways, and impact of BZB see 1.1, 1.3, and 1.4.3, respectively. Figure is modified based on Ashkenazi, 2008; Azijli *et al.*, 2013; de Wilt *et al.*, 2013. cyt c, cytochrome c. ‡, impact of BZB is dependent on rate of proteasomal degradation and influence on new synthesis.

Besides classical signaling, TRAIL is able to induce non-canonical non-apoptotic signal transduction pathways in a cell type-dependent manner (Figure 1.2). Under circumstances of cell stress (e.g. acidic extracellular pH) combined with inhibition of caspases, TRAIL has been reported to induce necroptotic death in tumor cells. Necroptosis is an alternative form of programmed cell death phenotypically resembling necrosis, but being a strictly regulated process like apoptosis. This signaling pathway crucially involves the kinases RIP1 and RIP3. The contribution of necroptosis to TRAIL-induced anti-tumoral effects, however, is still unclear (Jouan-Lanhouet *et al.*, 2012; Voigt *et al.*, 2014). In addition to apoptosis and necroptosis induction, TRAIL is able to trigger non-cell death signaling that has been associated with conditions of blocked apoptosis and is thus observed in TRAIL-resistant tumor as well as non-

transformed cells. Following DISC assembly, these non-canonical signal transductions are characterized by TRAIL-R clustering outside lipid rafts and the formation of a secondary complex containing FADD, caspase-8, RIP1, TRAF2, and NEMO. Various signaling pathways have been found to be activated upon assembly of this secondary complex, including NF-κB, MAPKs (JNKs, p38, ERKs, TAK1), PKC, PI3K/AKT, and SRC. Activation of these kinase cascades not only contributes to inhibition of TRAIL-induced apoptosis and therefore increased survival, but additionally promotes malignancy of tumor cells by enhancing proliferation, migration, invasion, and metastasis. Instead of leading to tumor cell killing, therapeutic application of TRAIL in TRAIL-resistant tumors may thus enforce malignant progression (reviewed by Azijli *et al.*, 2013; Bertsch *et al.*, 2014; de Miguel *et al.*, 2016).

1.4 TRAIL and its receptors in cancer therapy

As outlined above, triggering the extrinsic apoptotic pathway is a promising strategy to kill tumor cells independent of their p53 status and intrinsic apoptosis induction. Various therapeutics based on this concept were thus developed and termed pro-apoptotic receptor agonists (PARAs; reviewed by Ashkenazi, 2015). Historically, first exploitation of this strategy occurred in 1891, when William Coley administered extracts of gram-negative bacteria to treat sarcoma patients (Coley, 1891). Almost a century later, the anti-tumoral effects of Coley's toxins were attributed to LPS-induced TNF (Carswell *et al.*, 1975). Systemic application of TNF for tumor therapy, however, led to severe toxicity (Kimura *et al.*, 1987). Similarly, the observation of lethal hepatotoxic effects in mice upon triggering of the death receptor Fas (Ogasawara *et al.*, 1993) hampered the translation of PARAs into the clinic. In contrast to TNF and FasL, TRAIL was found to selectively induce apoptosis in malignant cells without harming healthy tissue (Ashkenazi *et al.*, 1999; Walczak *et al.*, 1999). Due to this unique property, TRAIL has been extensively investigated and considered as a promising anti-cancer therapeutic. The mechanisms underlying the selectivity of TRAIL for tumor cells are still not completely understood, but might involve the protection of normal cells via high expression levels of decoy receptors (Marsters *et al.*, 1997; Sheridan *et al.*, 1997; see 1.2) as well as specific post-translational modifications in cancer cells, e.g. clustering-promoting O-glycosylation of TRAIL-R1 and -R2 (Wagner *et al.*, 2007). In addition to its tumor-selective activity, further factors encouraged the evaluation of TRAIL for tumor therapy. These include the possibility to exploit the complex TRAIL – TRAIL receptor system to design tumor-specific drugs, expression

of TRAIL-R1 and -R2 on various tumor types (Daniels *et al.*, 2005), and most importantly the promising effects seen in preclinical models (Ashkenazi *et al.*, 1999; Walczak *et al.*, 1999). Besides a soluble form of recombinant human TRAIL (see 1.4.2), agonistic monoclonal antibodies targeting either TRAIL-R1 or TRAIL-R2 (see 1.4.1) have been developed and evaluated in clinical studies. Despite good tolerability of those therapies (Camidge *et al.*, 2010; Herbst *et al.*, 2010; Tolcher *et al.*, 2007), the results were largely disappointing. Only few patients benefitted from treatment (reviewed by den Hollander *et al.*, 2013). Apart from the observation that many human tumors are TRAIL-resistant (reviewed by Dimberg *et al.*, 2013; Thorburn *et al.*, 2008; Zhang and Fang, 2005), this limited success has been attributed to an insufficient activity of those first generation TRAIL receptor agonists. There are several properties of the TRAIL – TRAIL receptor system that partially underlie this low efficacy and challenge the translation into the clinic. On the one hand, these factors concern the ligand and include that it is naturally expressed as a transmembrane protein that exhibits a distinct activity profile compared to the soluble version, the short serum half-life of the soluble form and its limited capability to induce clustering of DRs. On the other hand, further challenges are linked to the receptors and concern the complexity of the receptor system, the expression of death receptors on healthy tissue, and the possible induction of non-cell death signaling potentially provoking antagonistic effects (reviewed by de Bruyn *et al.*, 2013; de Miguel *et al.*, 2016; Wajant *et al.*, 2013). Strategies that address these limitations include the development of agonists with improved activity (see 1.4.1, 1.4.2), combinatorial treatments to overcome TRAIL resistance (see 1.4.3), as well as careful selection of patients likely to benefit from the respective treatment (see 1.4.4).

1.4.1 Agonistic TRAIL-R1- and TRAIL-R2-specific antibodies

There is sound scientific rationale for the use of monoclonal antibodies (mAbs) to activate TRAIL-R1 and TRAIL-R2, despite the disadvantage of potentially inducing lower levels of apoptosis due to targeting of only one of the death receptors. Besides the vast experience concerning development, production, and approval of antibodies in general, agonistic TRAIL-R1- or TRAIL-R2-specific antibodies benefit from several properties. These include the lack of binding to decoy receptors and the fact that in many tumors apoptosis is selectively triggered via either TRAIL-R1 or -R2 (Kelley *et al.*, 2005; Lemke *et al.*, 2010; MacFarlane *et al.*, 2005a; MacFarlane *et al.*, 2005b), which allows a tumor type-dependent adaptation of the antibody

specificity. Additionally, the use of mAbs circumvents the problem of low stability and short *in vivo* half-life of the homotrimeric ligand (reviewed by Lemke *et al.*, 2014; Wajant, 2015). Therefore, clinical studies have been performed evaluating one anti-TRAIL-R1 antibody (mapatumumab) and several antibodies targeting TRAIL-R2 (lexatumumab, conatumumab, drozitumab, tigatuzumab, LBY135). These trials verified the extended half-life typically seen for antibodies ranging from 19 to 26 days for mapatumumab and 6 to 19 days for the TRAIL-R2-specific antibodies (reviewed by den Hollander *et al.*, 2013). As outlined above, apart from safety and good tolerability, the conducted clinical studies did not confirm the promising effects seen in preclinical models (Chuntharapai *et al.*, 2001; Ichikawa *et al.*, 2001; Kaplan-Lefko *et al.*, 2010). These findings encouraged further clinical studies analyzing these antibodies in combinatorial treatment approaches to enhance efficacy (see 1.4.3).

Antibodies are bivalent and thus incapable of inducing receptor trimerization or even organization into supramolecular clusters. Investigations of antibodies targeting other TNFRSF members revealed the impact of antibody valency on agonistic activity. For example, pentameric IgM directed against TNFR1 or CD95 has been shown to exert superior agonistic properties compared to bivalent forms (Espevik *et al.*, 1990; Fadeel *et al.*, 1997). Likewise, a recent study on a TRAIL-R1-targeting antibody reported considerably enhanced apoptosis induction upon switching the isotype from IgG to IgM (Piao *et al.*, 2016). Similar effects have been documented for secondary cross-linking of bivalent antibodies (Li *et al.*, 2008; Natoni *et al.*, 2007; Yada *et al.*, 2008). These observations explain the low activity found in clinical trials, but fail to describe the discrepancy with the data obtained from preclinical models. Further studies have been performed to elucidate these differences and revealed that the efficacy seen in mouse models crucially depends on FcγR-mediated cross-linking of the antibodies. Via binding to the Fc part of the respective antibodies, FcγRs expressed on immune cells of the tumor microenvironment mediate clustering of TRAIL receptors and thereby enable efficient DISC formation and apoptotic signaling (Figure 1.3B; Haynes *et al.*, 2010; Li and Ravetch, 2012; Li and Ravetch, 2013; Wilson *et al.*, 2011). Since most preclinical studies were performed in athymic mice lacking significant levels of endogenous immunoglobulins, a sufficient amount of FcγRs is available to cross-link the applied antibodies. This is in sharp contrast to clinical trials, where treated patients exhibit high levels of endogenous IgG, strongly competing with the administered antibodies for FcγR binding. Additionally, varying infiltration of the tumor

with leukocytes as well as binding to FcγR-expressing cells in the circulation are factors that may influence *in vivo* activity.

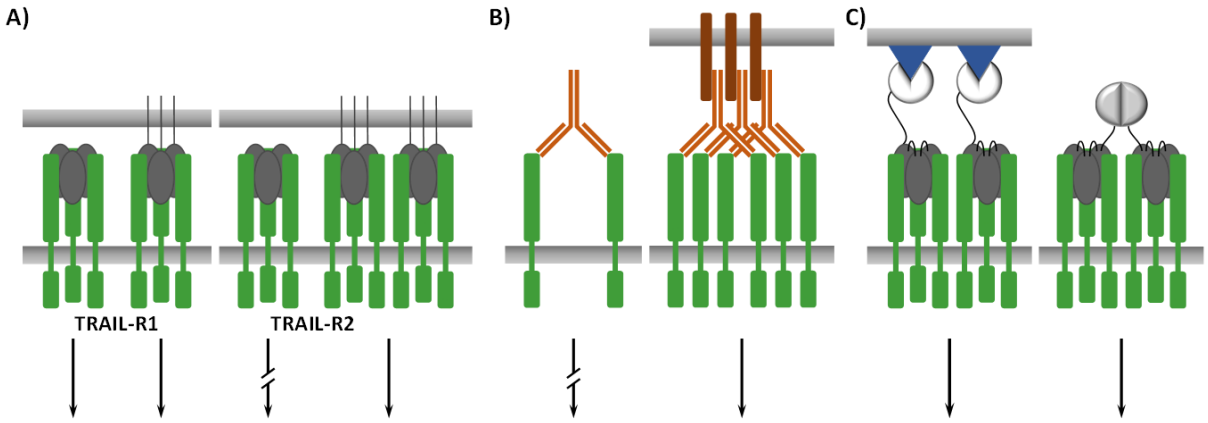

Figure 1.3: Requirements for efficient apoptosis induction. A) Physiologically, TRAIL is expressed as a transmembrane protein that can be cleaved into a soluble form. While TRAIL-R1 is activated by both forms, only membrane-bound TRAIL efficiently activates TRAIL-R2 (Wajant *et al.*, 2001). B) Agonistic antibodies targeting TRAIL-R1 or -R2 are poor activators of apoptosis due to their bivalent nature. Via binding to the Fc part, FcγRs expressed on immune cells of the tumor microenvironment mediate efficient TRAIL receptor clustering and apoptosis induction (reviewed by Wajant, 2015). C) Activity of soluble TRAIL (here in a single-chain form) is considerably enhanced by combination with fusion partners that bind to membrane-attached structures or by increasing TRAIL valency (reviewed by de Miguel *et al.*, 2016).

The importance of receptor clustering for efficient apoptotic signaling was furthermore confirmed by studies demonstrating a strong synergism of soluble TRAIL and conatumumab that are both poorly active as single agents. Conatumumab is thought to cross-link homotrimeric TRAIL – TRAIL-R complexes, thereby promoting the formation of hexagonal honeycomb-like supramolecular structures. A prerequisite for this activity is that conatumumab and TRAIL bind to non-overlapping epitopes on TRAIL-R2, thus allowing simultaneous binding (Graves *et al.*, 2014; Tuthill *et al.*, 2015). Based on these studies, highlighting the insufficient capability of the investigated antibodies alone to induce receptor clustering, effort was made to develop new therapeutics overcoming this limitation. Besides defined oligomerization of TRAIL receptor-binding units (see 1.4.2), a TRAIL-R2-specific antibody (KMTR2) has been reported to induce superoligomerization independent of additional cross-linking. Investigations of the crystal structure of KMTR2 in complex with TRAIL-R2 suggested clustering of PLAD-mediated TRAIL-R2 homodimers via two paratopes of the antibody. Binding of KMTR2 to TRAIL-R2 is supposed to generate a second paratope allowing concomitant association with another antibody molecule to induce linear oligomerization (Tamada *et al.*, 2015). Addressing the issue of targeting only one death receptor, a recent study described the generation of a pre-BCR-derived so-called Surrobody™

exhibiting agonistic activity on TRAIL-R1 and -R2 (Milutinovic *et al.*, 2016). Newest concepts employing TRAIL receptor-targeting antibodies make use of TAA (tumor-associated antigen) binding-dependent hyperclustering of especially TRAIL-R2. Bispecific antibodies incorporating binding units directed against MCSP or FAP in addition to TRAIL-R2-specific domains demonstrated efficient apoptosis induction without the necessity of secondary cross-linking (Brünker *et al.*, 2016; He *et al.*, 2016).

1.4.2 Evolution of recombinant TRAIL therapeutics

Concerning the development of therapeutics based on the natural homotrimeric ligand, mainly three strategies are pursued to overcome the limited success of soluble recombinant human TRAIL (dulanermin) seen in clinical trials (Herbst *et al.*, 2010; Soria *et al.*, 2011). These approaches comprise improving the stability, enhancing the valency, as well as targeted delivery. Based on the poor pharmacokinetic properties of dulanermin (Kelley *et al.*, 2001) and supported by the observation that other TNFSF members (like TNF or GITRL) are inactivated due to dissociation of the homotrimer (Chattopadhyay *et al.*, 2007; Corti *et al.*, 1992), first improvements addressed the stability. Via fusion to protein sequences that enforce homotrimerization, including leucine zippers (Rozanov *et al.*, 2015; Walczak *et al.*, 1999), an isoleucine zipper (Ganten *et al.*, 2006), and the trimerization domains of tenascin-C (Berg *et al.*, 2007) or human adenovirus type 5 fiber protein (Yan *et al.*, 2016), not only stability, but also activity of the respective variants have been enhanced. Compared to a half-life of only 3 to 5 min in mice reported for dulanermin (Kelley *et al.*, 2001), the leucine zipper-fused protein shows an elongated PK profile with a terminal half-life of 4.8 h (Walczak *et al.*, 1999). Due to safety concerns however, the stabilized formulations did not enter clinical investigations. These concerns were raised by the toxicities experienced with TNF and FasL on the one hand (Kimura *et al.*, 1987; Ogasawara *et al.*, 1993), and by toxic effects observed for other TRAIL preparations on the other. Early forms of TRAIL were expressed containing a His- or FLAG-tag, mainly due to purification purposes. Unfortunately, His-tagged versions as well as cross-linked FLAG-TRAIL induced apoptosis not only in tumor cells, but also in hepatocytes. This hepatotoxicity was associated with the presence of aggregates either intentionally induced by cross-linking or caused by interference of the His-tag with proper zinc coordination and assembly (Ganten *et al.*, 2006; Lawrence *et al.*, 2001). This highlighted the importance of using stably assembled and non-aggregated forms of TRAIL. Based on studies of TNF (Krippner-

Heidenreich *et al.*, 2008), another strategy for increased stability was adopted. Fusion of the extracellular domains of three TRAIL monomers (via short peptide linkers) allowed the development of single-chain versions of TRAIL (Schneider *et al.*, 2010; Spitzer *et al.*, 2010). These single-chain formats show improved properties with respect to stability, aggregation propensity, PK, and activity without demonstrating toxicity. Additionally and in contrast to homotrimeric versions with limited options of fusion partners, conversion of TRAIL into a monomeric sequence permits a wide variety of possible combination types. Further optimization of the single-chain format was reported by a recent study comprehensively analyzing versions comprising variations in TRAIL and linker sequences (Siegemund *et al.*, 2016). Besides improvements of the intrinsic stability of TRAIL, additional strategies are applied to specifically extend pharmacokinetic properties. Classical approaches include PEGylation and fusion to long-circulating serum proteins, such as HSA. Both concepts have been employed successfully. Terminal half-lives of PEGylated forms range from 1 h up to 20 h depending on PEG size, conjugation chemistry and site, as well as TRAIL version (Chae *et al.*, 2010; Kim *et al.*, 2011a; Pan *et al.*, 2013). An HSA-TRAIL conjugate and an HSA-TNC-TRAIL fusion protein also exhibit elongated half-lives of 6.2 h and 15 h, respectively (Byeon *et al.*, 2014; Müller *et al.*, 2010). Similarly, fusion of TRAIL to an albumin-binding domain prolonged the half-life to 14.1 h (Li *et al.*, 2016). These extended pharmacokinetic properties in turn translated into improved therapeutic activity *in vivo*.

Generally, targeting approaches are applied to enhance the bioactivity of a therapeutic by increasing its concentration at the tumor and to simultaneously decrease the exposure to healthy tissue, thereby reducing possible side effects. Respective strategies are categorized into passive and active targeting concepts. Passive targeting makes use of the improved half-lives of macromolecular structures with sizes exceeding the threshold for renal filtration as well as the enhanced permeability and retention (EPR) effect. Due to leakiness of the tumor vasculature and impaired lymphatic drainage, macromolecular therapeutics are released and enriched at the tumor site (reviewed by Iyer *et al.*, 2006). In order to exploit the EPR effect, TRAIL has been either encapsulated in or attached to the surface of nanoparticles. While encapsulation allows sustained release (Kim *et al.*, 2011b; Kim *et al.*, 2013; Lim *et al.*, 2011), surface-attached TRAIL exerts increased bioactivity by mimicking the membrane-bound form, thus being capable of inducing higher order receptor clustering and activation of TRAIL-R2 (de Miguel *et al.*, 2015; Nair *et al.*, 2015; Perlstein *et al*., 2013). Various compounds have been

used as nanoparticulate carriers of TRAIL. Most extensively, liposomal formulations have been employed and additionally modified (reviewed by de Miguel *et al.*, 2016). For example, liposomes loaded with chemotherapeutics are able to simultaneously deliver drugs enhancing the pro-apoptotic activity of TRAIL (Guo *et al.*, 2011a; Guo *et al.*, 2011b; Sun *et al.*, 2012). Exploitation of active targeting by functionalization with scFvs directed against TAAs or with other ligands further increases tumor-specific enrichment or the cytotoxic activity of immune cells (Mitchell *et al.*, 2014; Seifert *et al.*, 2014b; Wayne *et al.*, 2016).

The observation that cross-linking of soluble versions of TRAIL readily converts these forms into highly active inducers of apoptosis highlighted the importance of spatial preorganization to efficiently cluster and activate TRAIL receptors (Mühlenbeck *et al.*, 2000; Wiley *et al.*, 1995). Physiologically, this is achieved by expression of a membrane-bound form of TRAIL. Thus, active targeting of TRAIL to membrane-bound structures not only determines its localization, but can be additionally used to confer properties of the membrane-expressed variant on soluble TRAIL (Figure 1.3C; Wajant *et al.*, 2001). Furthermore, the fusion partner itself can be used to support anti-tumor effects, e.g. by activation or inhibition of signaling pathways triggered by the respective target structure. Most commonly, scFv molecules directed against various TAAs have been fused to TRAIL or scTRAIL, which allows killing of target-positive, but also target-negative tumor cells (bystander effect). Besides direct targeting of cancer cells, fusion partners binding to the tumor vasculature or immune cells are used to either disrupt tumor supply or to increase the cytotoxic potential of the respective immune cell (reviewed by de Bruyn *et al.*, 2013; de Miguel *et al.*, 2016; Holland, 2014). Additionally, receptor-specific mutants of TRAIL are used to optimize apoptosis induction by minimizing binding to decoy receptors (O'Leary *et al.*, 2016) and specifically targeting the relevant death receptor of the corresponding tumor type (reviewed by Wajant *et al.*, 2013). An overview of the broad variety of TRAIL fusion proteins exploiting active targeting is given in Table 1.1.

The concept of improving TRAIL-based therapeutics by a stable and defined increase in valency (Figure 1.3C) is again inspired by the importance of efficient receptor clustering and furthermore supported by the observation that other TNFRSF members require cross-linking of two TNFSF trimers for optimal activation (Holler *et al.*, 2003; Wyzgol *et al.*, 2009). In fact, fusion of a single-chain version of TRAIL to dimerization modules (Gieffers *et al.*, 2013; Seifert *et al.*, 2014a; Siegemund *et al.*, 2012) or combination of soluble TRAIL with an isoleucine zipper

hexamerization motif (Han *et al.*, 2016) considerably enhanced apoptosis induction (Table 1.1). Consistent with these data, oligomerization of TRAIL-R2-agonistic antibody fragments or scaffolds to an at least tetravalent form generated active therapeutics (Huet *et al.*, 2014; Liu *et al.*, 2015; Swers *et al.*, 2013; Wang *et al.*, 2013), while trimerization was sufficient for a TRAIL-R1-specific protein (Allen *et al.*, 2012).

Table 1.1: Variety of TRAIL fusion proteins exploiting active targeting and/or increased valency. Name of fusion protein, its format, target, and described effects are listed. Table is modified based on de Miguel *et al.*, 2016.

Fusion protein (Format)	Target	Main effects	Reference
Targeting of tumor cells and tumor vasculature – trivalent TRAIL forms			
anti-CD47:TRAIL (scFv-sTRAIL)	CD47	active targeting, increased bioactivity, blocking of "don't eat me" signal	Wiersma *et al.*, 2014
anti-MCSP:TRAIL (scFv-sTRAIL)	MCSP	active targeting, increased bioactivity, inhibition of MCSP signaling, no side effects *in vivo*	de Bruyn *et al.*, 2010
anti-PD-L1:TRAIL (scFv-sTRAIL)	PD-L1	active targeting, increased bioactivity, enhanced T cell activation, conversion of suppressive myeloid cells into pro-apoptotic effector cells	Hendriks *et al.*, 2016
CD19L-sTRAIL (ligand-sTRAIL)	CD19	active targeting, increased bioactivity, no side effects *in vivo*	Uckun *et al.*, 2015
CD40ed-TRAILed (receptor-sTRAIL)	CD40L	active targeting, increased bioactivity	Assohou-Luty *et al.*, 2006
F8-TRAIL (scFv-sTRAIL)	EDA	active targeting	Hemmerle *et al.*, 2014
Fn14•TRAIL (receptor-sTRAIL)	TWEAK	increased bioactivity, no side effects *in vivo*	Aronin *et al.*, 2013
MBOS4-TRAIL (scFv-C_H3-sTRAIL)	FAP	active targeting, increased bioactivity	Wajant *et al.*, 2001
MSC.scFvCD20-sTRAIL (scFv-sTRAIL delivered by HUMSCs)	CD20	active targeting, increased bioactivity, no side effects *in vivo*	Yan *et al.*, 2013
RGD-L-TRAIL (peptide-sTRAIL)	Integrins	active targeting, increased bioactivity, no side effects *in vivo*	Cao *et al.*, 2008
scFv425:sTRAIL (scFv-sTRAIL, wt, TRAIL-R1- + -R2-specific)	EGFR	active targeting, increased bioactivity, reduced EGFR activation	Bremer *et al.*, 2005a, Bremer *et al.*, 2008a
$scFv_{\alpha EGFR}$-scTRAIL (scFv-scTRAIL)	EGFR	active targeting, increased bioactivity, no side effects *in vivo*	Siegemund *et al.*, 2012
$scFv_{\alpha ErbB2}$-scTRAIL (scFv-scTRAIL)	HER2	active targeting, increased bioactivity, no side effects *in vivo*	Schneider *et al.*, 2010
scFvC54:sTRAIL (scFv-sTRAIL)	EpCAM	active targeting, increased bioactivity	Bremer *et al.*, 2004a; Bremer *et al.*, 2004b
scFvCD7:sTRAIL (scFv-scTRAIL)	CD7	active targeting, increased bioactivity	Bremer *et al.*, 2005b
scFvCD19:sTRAIL (scFv-sTRAIL)	CD19	active targeting, increased bioactivity, no side effects *in vivo*	Stieglmaier *et al.*, 2008
scFvCD33:sTRAIL (scFv-sTRAIL)	CD33	active targeting, increased bioactivity	ten Cate *et al.*, 2009

Fusion protein (Format)	Target	Main effects	Reference
Targeting of tumor cells and tumor vasculature – trivalent TRAIL forms			
scFv:lαhCD70-TNC-TRAIL (scFv-TNC-TRAIL, wt, TRAIL-R1-, -R2-specific)	CD70	active targeting, increased bioactivity, inhibition of immunosuppressive effects of CD70	Trebing *et al.*, 2014
SS-TR3 (scFv-scTRAIL)	Mesothelin	active targeting, increased bioactivity	Tatzel *et al.*, 2016
sTRAIL-TMTP1 (sTRAIL-peptide)	highly metastatic tumor cells	active targeting, increased bioactivity, no side effects *in vivo*	Liu *et al.*, 2014
Tf-PEG-TRAIL (ligand-PEG-sTRAIL, conjugate)	Tf receptor	active targeting, increased bioactivity, no side effects *in vivo*	Kim *et al.*, 2012
Modulation of immune cells – trivalent TRAIL forms			
Anti-CD3:TRAIL (scFv-sTRAIL)	CD3	active targeting, increased bioactivity, enhanced cytotoxic activity of T cells, no side effects *in vivo*	de Bruyn *et al.*, 2011
CLL1:TRAIL (scFv-sTRAIL)	CLL1	active targeting, increased bioactivity, enhanced cytotoxic activity of granulocytes	Wiersma *et al.*, 2015
K12:TRAIL (ligand-sTRAIL)	CD7	active targeting, increased bioactivity, enhanced cytotoxic activity of T cells, no side effects *in vivo*	de Bruyn *et al.*, 2011
scFv:G28-TRAILmutRs (scFv-TNC-TRAIL, wt, TRAIL-R1-, -R2-specific)	CD40	active targeting, increased bioactivity, maturation of dendritic cells	El-Mesery *et al.*, 2013
scFvRBC-TR3 (scFv-scTRAIL)	glycophorin A on mouse RBC	active targeting, increased bioactivity, no side effects *in vivo*	Spitzer *et al.*, 2010
Increased valency – hexavalent TRAIL forms			
EHD2-scTRAIL (EHD2-scTRAIL)	-	increased bioactivity, no side effects *in vivo*	Seifert *et al.*, 2014a
ILz(6):TRAIL (hexameric ILZ-TRAIL)	-	increased bioactivity	Han *et al.*, 2016
scTRAIL-RBD-IgG1-Fc (scTRAIL-Fc)	-	increased bioactivity, no side effects *in vivo*	Gieffers *et al.*, 2013
Targeting of tumor cells combined with increased valency – hexavalent TRAIL forms			
$Db_{\alpha EGFR}$-scTRAIL (Db-scTRAIL)	EGFR	active targeting, increased bioactivity, reduced EGFR activation, no side effects *in vivo*	Siegemund *et al.*, 2012; Siegemund *et al.*, 2016
$scFv_{\alpha EGFR}$-EHD2-scTRAIL (scFv-EHD2-scTRAIL)	EGFR	active targeting, increased bioactivity, no side effects *in vivo*	Seifert *et al.*, 2014a

CLL1, C-type lectin-like molecule-1; EDA, alternatively-spliced EDA domain of fibronectin; HUMSCs, human umbilical cord derived mesenchymal stem cells; ILZ, isoleucine zipper; RBC, red blood cell; RBD, receptor-binding domain; Tf, transferrin; TMTP1, tumor molecular targeted peptide 1; TNC, trimerization domain of tenascin-C.

Furthermore, alternative approaches, like adenoviral expression (Bremer *et al.*, 2008b; Griffith and Broghammer, 2001; Liu *et al.*, 2011) and delivery of TRAIL molecules by mesenchymal stem cells (reviewed by Attar *et al.*, 2014) were developed. Besides the outlined strategies, especially concepts combining tumor targeting and increased TRAIL valency (Table 1.1) seem

to be promising to overcome the limitations of first generation TRAIL therapeutics. Two concepts employing targeted delivery and increased valency have been reported previously. In a first study, these properties were realized by fusion of scTRAIL to a diabody (Db; Siegemund *et al.*, 2012). While a diabody combines tumor targeting and non-covalent dimeric assembly in one molecule, another study described the use of separate targeting and dimerization modules. Applying an scFv for targeting and the IgE heavy chain domain 2 (EHD2) for covalent homodimerization, targeted dimeric scFv-EHD2-scTRAIL fusion proteins were generated (Seifert *et al.*, 2014a). Both Db-scTRAIL and scFv-EHD2-scTRAIL exerted remarkable activity *in vitro* and *in vivo*, showing half-lives of 3.5 h and 7.2 h (Seifert, 2014), respectively.

In order to exploit the promising effects of tumor-targeted TRAIL fusion proteins, an important step in the generation of the respective therapeutics is the selection of a suitable tumor-associated antigen. The TAAs targeted by the antibody-scTRAIL fusion proteins evaluated in this study are EGFR, HER2, HER3 (see 1.4.2.1), and EpCAM (see 1.4.2.2) and have been partly employed in similar constructs (Table 1.1).

1.4.2.1 HER family members as targets in antibody-based tumor therapy

The human epidermal growth factor receptor family comprises four members, EGFR (HER1, ERBB1), HER2 (NEU, ERBB2), HER3 (ERBB3), and HER4 (ERBB4). All receptors consist of an extracellular part, a transmembrane domain, and a cytoplasmic region. The extracellular part is composed of four domains that are responsible for ligand binding. The ligand-unbound receptor adopts a closed (or tethered) conformation that is characterized by the interaction of domains II and IV. Upon ligand binding, which is mediated by domains I and III, the dimerization interface of domain II is exposed (open or extended conformation) allowing receptor homo- and heterodimerization and activation of the tyrosine-kinase domain in the cytoplasmic region. Recruitment of proteins to phosphorylated tyrosine residues in the cytoplasmic tail finally leads to activation of downstream signaling, including MAPK and PI3K/AKT pathways. Physiologically, HER family members are expressed on epithelial, mesenchymal, and neuronal cells, and their activation is tightly controlled by a temporally and spatially restricted expression of the respective ligands. However, extensive HER signaling as a result of receptor or ligand overexpression or activating mutations has been found in various human tumors and associated with tumor development and progression (reviewed by Hynes and Lane, 2005; Roskoski, 2014). EGFR is overexpressed on a broad range of tumor types and

represents an established target molecule for antibody-based therapeutic approaches (reviewed by Ciardiello and Tortora, 2003; Seshacharyulu *et al.*, 2012). The EGFR-targeting antibody domains used in this study are derived from cetuximab. Cetuximab is a chimeric human-mouse IgG1 antibody that binds to domain III of EGFR in the closed conformation, thereby inhibiting ligand binding and adoption of the open conformation (Li *et al.*, 2005). Cetuximab is approved for the treatment of metastatic colorectal carcinoma and squamous cell carcinoma of the head and neck (reviewed by Arteaga and Engelman, 2014). HER2 differs from other family members, since it does not bind to a ligand, but permanently adopts an open conformation due to a lacking interaction of domains II and IV. Therefore, HER2 is the preferred heterodimerization partner of other family members. Although present in an open conformation, HER2 is only constitutively active when overexpressed. HER2 has been extensively evaluated as target structure, especially for the treatment of breast cancer, but high expression levels are also found for other tumor types, like gastric, ovarian, and prostate cancer (reviewed by Roskoski, 2014; Tai *et al.*, 2010). In this study, the variable domains of the HER2-targeting humanized IgG1 antibody trastuzumab are employed in different molecules. Trastuzumab binds to domain IV of HER2, reduces its signaling activity, and is approved for the treatment of HER2-overexpressing breast cancer and HER2-overexpressing metastatic gastric or gastroesophageal junction adenocarcinoma (reviewed by Arteaga and Engelman, 2014). For decades, HER3 has not been considered as a target structure for tumor therapy due to its impaired tyrosine kinase activity. Recently, it has been found, however, that HER3 has an important role in cancer progression and mediating resistance towards EGFR- and HER2-targeting approaches by heterodimerization with these family members (reviewed by Hsieh and Moasser, 2007; Kol *et al.*, 2014). Some of the HER3-binding molecules generated in this study are based on the HER3-targeting fully human IgG2 antibody MM-121 (seribantumab). Via binding to domain I of HER3, MM-121 inhibits ligand-dependent activation (Schoeberl *et al.*, 2009; Schoeberl *et al.*, 2010). MM-121 has already been analyzed in several clinical trials with promising results and is currently assessed in a phase II study in combinatorial treatment approaches of non-small cell lung cancer (http://www.clinicaltrials.gov, status September 2016). Compared to the other family members, the role of HER4, which is not used as target in this study, in tumor development and progression is more complex. Further investigations of the influence of different isoforms and mutations will help to evaluate its potential as target for tumor therapy (reviewed by Arteaga and Engelman, 2014; Veikkolainen *et al.*, 2011).

1.4.2.2 EpCAM as target in antibody-based tumor therapy

Epithelial cell adhesion molecule (EpCAM, CD326) is a glycosylated type I transmembrane protein consisting of 314 amino acids. Its extracellular region (EpEX) constitutes the major part of the protein and consists of an EGF-like and thyroglobulin repeat domain, while the intracellular domain (EpICD) comprises only 26 amino acids. As implicated by its name, EpCAM is expressed on various epithelial tissues, where it is involved in the formation of homotypic cell-cell contacts. With respect to expression on malignant tissue, EpCAM is one of the most frequently and strongly expressed TAAs showing high levels on almost all adenocarcinomas, but also on squamous cell carcinoma, retinoblastoma, and hepatocellular carcinoma. Additionally, normal stem cells as well as cancer stem cells express EpCAM. In contrast to the homogeneous distribution of EpCAM on the surface of tumor cells, the accessibility of EpCAM on normal cells is limited, representing a favorable characteristic for the use as target in antibody-based therapies (reviewed by Baeuerle and Gires, 2007; Patriarca *et al.*, 2012). Besides mediating cell adhesion, EpCAM has been found to induce mitogenic signaling. Upon activation, regulated intramembrane proteolysis releases EpEX and EpICD. While EpEX serves as soluble agonist for EpCAM-positive cells, EpICD becomes part of a multiprotein complex and transcriptionally regulates genes involved in cell growth, cell cycle, proliferation, and cell death (Maaser *et al.*, 2008; Maetzel *et al.*, 2009). This signaling activity has been discovered to be important for the phenotypic characteristics of normal and cancer stem cells. Thus, EpCAM is a promising target not only due to its strong expression on a wide range of tumor types, but also because of its presence on cancer stem cells potentially allowing selective eradication of the tumor cell subpopulation responsible for disease relapse. Additionally, blocking of EpCAM's mitogenic signaling activity may support treatment efficacy (reviewed by Munz *et al.*, 2009). The EpCAM-binding antibody domains used in this study are based on the mouse monoclonal IgG1 antibody 323/A3 that has been shown to exert anti-tumoral activity in preclinical mouse models (Edwards *et al.*, 1986; Velders *et al.*, 1995). Currently, only one EpCAM-targeting antibody (anti-EpCAMxCD3, catumaxomab; Seimetz *et al.*, 2010) is approved in Europe (reviewed by Ecker *et al.*, 2015).

1.4.3 TRAIL and sensitizers

The combination of TRAIL with sensitizing agents aims at improving several shortcomings of TRAIL-R-targeting therapies. These include the in general low activity, resistance, and the

potential induction of anti-apoptotic signaling. Exploitation of the cross-talk between extrinsic and intrinsic apoptosis induction by combination with various conventional chemotherapeutics induces synergistic effects and sensitizes tumor cells in preclinical settings. Based on these observations, combinatorial treatment approaches with dulanermin and TRAIL-R1/-R2-targeting antibodies have been analyzed in clinical studies, comprising combinations with single cytotoxic agents, multiple cytotoxic agents, targeted therapeutics, as well as mixtures of cytotoxic and targeted agents. However, no beneficial effects of TRAIL-R-targeting therapeutics could be demonstrated. In general, the lacking efficacy of these combinatorial approaches is supposed to result from insufficient activity of either TRAIL-R-targeting agents, sensitizers, or both. Further analysis of various sensitizers and their molecular effects indicated the requirement of simultaneous modulation of multiple levels of TRAIL signaling to overcome resistance (reviewed by den Hollander *et al.*, 2013; Newsom-Davis *et al.*, 2009). An example for a potent and meanwhile extensively evaluated sensitizer is bortezomib, a proteasome inhibitor that reversibly binds to the β5 subunit of the 26S proteasome, thereby blocking its chymotrypsin-like proteolytic activity. Bortezomib (VELCADE, PS-341) is approved both as single agent and as combination therapy for the treatment of multiple myeloma and mantle cell lymphoma. Via inhibition of the proteasome, bortezomib affects various factors of the TRAIL pathway (Figure 1.2), on the one hand directly enhancing apoptosis, while on the other hand suppressing anti-apoptotic TRAIL signaling. The explicit mechanisms that are involved in sensitization depend on the respective tumor type, but include enhanced cell surface expression of TRAIL-R1 and -R2, increased activation of caspase-8, modulation of cFLIP levels, suppression of NF-κB activation, inhibition of NF-κB-dependent XIAP, BCL-2, and BCL-XL expression, increased levels of pro-apoptotic BCL-2 family members, p53, p21, and p27, as well as inhibition of PKC and AKT signaling (reviewed by Chen *et al.*, 2011; de Wilt *et al.*, 2013). Investigations on potential toxicity revealed that co-treatment with TRAIL and high concentrations of bortezomib kills primary human hepatocytes, yet with clearly lower sensitivity than the examined cancer cell lines, thus providing a therapeutic window for combinatorial application (Ganten *et al.*, 2005; Koschny *et al.*, 2007a). Despite the potent activity of TRAIL-R-targeting agents and bortezomib in mouse models and on primary tumor cells, a phase II randomized-controlled trial of mapatumumab and bortezomib failed to confirm superior effects of the combination (Belch *et al.*, 2010). However, the lacking efficacy might again result from the insufficient activity of the applied

TRAIL-R-agonistic therapeutic. In order to develop more sensitizers with high potency and specificity, effort has been made to unravel the mechanisms underlying TRAIL resistance (see 1.3). Counteracting high levels of XIAP or anti-apoptotic BCL-2 family members, molecules mimicking the antagonizing activity of SMAC and BH3-only proteins have been developed and shown to sensitize cancer cells to TRAIL-induced apoptosis. Several other strategies have been successfully applied, including inhibition of histone deacetylases, cyclin-dependent kinase 9, or the molecular chaperone Hsp90, as well as induction of ER stress (reviewed by Lemke *et al.*, 2014; Stolfi *et al.*, 2012).

1.4.4 Prognostic value of expression levels

Independent of sensitivity towards TRAIL-R-targeting therapies, TRAIL and TRAIL receptor expression levels have been evaluated as potential prognostic markers for disease progression. Several studies have been published reporting a correlation between high TRAIL receptor expression and poor prognosis (reviewed by Bertsch *et al.*, 2014). For instance, TRAIL-R1 expression was associated with higher tumor grade in breast cancer (Sanlioglu *et al.*, 2007), while TRAIL-R2 was identified as negative prognostic marker in several tumor entities, also including breast cancer (Ganten *et al.*, 2009). In contrast, TRAIL receptor expression levels were also found to be associated with better prognosis in other tumor types, e.g. high TRAIL-R1 expression in colorectal carcinoma (Sträter *et al.*, 2002), high TRAIL-R2 levels in melanoma (Zhuang *et al.*, 2006), and high levels of both death receptors in bladder cancer (Li *et al.*, 2012). Other studies, however, could not identify any correlation, e.g. for cervical cancer (Maduro *et al.*, 2009). Mostly, overall TRAIL receptor expression has been determined without differentiating distinct localizations. With respect to the different roles depending on localization, strictly compartment-specific determination of TRAIL receptor expression seems to be important to appropriately evaluate their potential as prognostic markers (reviewed by Bertsch *et al.*, 2014). Additional studies were performed analyzing the predictive value of decoy receptor levels. In colon carcinomas for example, expression of neither TRAIL-R3 nor TRAIL-R4 showed prognostic relevance (Sträter *et al.*, 2002). Further investigations aimed at evaluating the potential prognostic significance of TRAIL itself or molecules of the signaling pathway. High levels of TRAIL were identified as negative prognostic marker, e.g. in colorectal cancer (McLornan *et al.*, 2010). In gastric carcinoma, no significant correlation was found for full-length TRAIL. However, high expression of its truncated non-apoptotic splice variant

TRAIL-γ was demonstrated to be predictive for improved survival (Krieg *et al.*, 2013). An example of a signaling-involved molecule as prognostic marker is cFLIP that has been shown to be associated with a decrease in relapse-free survival in colorectal cancer (McLornan *et al.*, 2010). These studies clearly illustrate the tumor type dependence of the prognostic impact of molecules involved in TRAIL signaling and the importance of specific, e.g. localization- or variant-defined, determinations.

As outlined above, clinical studies of dulanermin and TRAIL-R1/-R2-targeting antibodies both alone and in combination with sensitizers were disappointing. However, promising effects were seen for few individual patients, even in the absence of additional cytotoxic agents (reviewed by den Hollander *et al.*, 2013). These observations underline the importance of unraveling factors that determine responsiveness to TRAIL-R-targeting therapies to allow selection of patients likely to benefit. Since O-glycosylation of TRAIL-R2 promotes DISC formation and apoptosis induction, the O-glycosylation enzyme GALNT14 has been analyzed as potential biomarker for TRAIL sensitivity. While a predictive value of GALNT14 expression for TRAIL sensitivity was demonstrated for several cancer cell lines and primary tumor samples (Wagner *et al*., 2007), a clinical study failed to identify a significant correlation of GALNT14 expression and effects of dulanermin (Soria *et al.*, 2011). In addition to the analysis of potential biomarkers, imaging studies using labeled TRAIL receptor-targeting antibodies provide helpful data on the bioavailability of the therapeutic at the tumor (Ciprotti *et al.*, 2015; Oldenhuis *et al.*, 2009). Recent approaches achieved promising results in predicting TRAIL sensitivity of tumor cell lines by using models that integrate the expression levels of a panel of genes (Chen *et al.*, 2012; O'Reilly *et al.*, 2014) or proteins (Passante *et al.*, 2013; Weyhenmeyer *et al.*, 2016). Further evaluation of these models on primary tumor cells and *in vivo*, however, is required to finally confirm their predictive capacity. Based on the progress in the field of high-throughput technologies, determination of gene and protein expression profiles of individual patients may help guiding TRAIL-R-targeting therapies in terms of selecting appropriate patients as well as suitable sensitizers.

1.5 Aim of the study

Recent advances in improving TRAIL-based therapeutics highlight the superior activity induced via tumor targeting and increased valency. These observations enforced the development of a meanwhile long list of promising second generation TRAIL molecules (Table 1.1). However,

no comprehensive study has been performed yet to comparatively analyze those diverse forms of fusion proteins. Therefore, this study focuses on different versions of scTRAIL-based molecules that incorporate the most efficient improvement approaches – tumor targeting and increased valency – and aims at systematically comparing the generated fusion proteins, thereby ideally revealing the characteristics crucial for optimization. Initially, four different dimeric recombinant antibody formats were generated and evaluated for the potential use as fusion partners of scTRAIL. Besides the diabody (Db) and scFv-EHD2 that have been previously combined with scTRAIL (Seifert *et al.*, 2014a; Siegemund *et al.*, 2012), two other formats were selected to create a more diverse spectrum. Attempting to further stabilize the non-covalently associated chains of a diabody, cysteine residues were introduced to covalently connect the two chains yielding a disulfide-stabilized diabody (dsDb). Additionally, scFv-Fc was included representing a format that is able to exploit FcRn-mediated recycling. Further differences in the format properties comprise flexibility and size. While altered flexibilities are especially assumed between the diabody molecules and the formats containing separate targeting and dimerization modules connected by a flexible linker, size is a factor influencing PK properties. The various formats were directed against four therapeutically relevant tumor-associated antigens (EGFR, HER2, HER3, and EpCAM) and characterized in terms of thermal stability, binding properties, and effects on cell viability. The established dimeric recombinant antibody formats were subsequently employed to generate the respective sets of dimeric antibody-scTRAIL fusion proteins (Db-scTRAIL, dsDb-scTRAIL, scFv-EHD2-scTRAIL, scFv-Fc-scTRAIL). Analysis of those molecules together with non-targeted monomeric and dimeric forms of scTRAIL was performed with respect to product quality, stability, binding properties, cell death-inducing activity *in vitro*, pharmacokinetics, and *in vivo* anti-tumor activity. Using these data, comparison of different formats directed against the same TAA and of a selected format comprising different targeting moieties allows conclusions about the impact of i) the protein format and ii) the targeting moieties on these properties, respectively. Finally, aiming at further improvement of dimeric antibody-scTRAIL fusion proteins, a new format was developed enabling simultaneous targeting of two different tumor-associated antigens. Four combinations of the above mentioned TAAs (EGFRxHER3, EpCAMxEGFR, HER2xEGFR, HER2xHER3) were realized and characterized regarding potential improvements.

2 Materials and Methods

2.1 Materials

2.1.1 General consumables

Laboratory plastics were purchased from Greiner Bio-One (Frickenhausen, Germany). Chemicals were obtained from Carl Roth (Karlsruhe, Germany), Merck (Darmstadt, Germany), Sigma-Aldrich (St. Louis, MO, USA), or Roche (Basel, Switzerland). Consumables purchased from any different source are explicitly specified.

2.1.2 Antibodies and sera

Antibodies and sera were obtained from Santa Cruz Biotechnology (Dallas, TX, USA), Sigma-Aldrich (St. Louis, MO, USA), Miltenyi Biotec (Bergisch Gladbach, Germany), BioLegend (San Diego, CA, USA), R&D Systems (Minneapolis, MN, USA), Pineda Antikörper-Service (Berlin, Germany), Dr. Margarete Fischer-Bosch-Institute of Clinical Pharmacology (IKP; Stuttgart, Germany), and ImmunoTools (Friesoythe, Germany) (Table 2.1).

Table 2.1: Antibodies and sera used in ELISA, flow cytometry, blocking studies, and PK.

Antibody or serum	Isotype	Application	Source
Anti-DYKDDDDK-PE	Monoclonal	Flow cytometry (1:200)	Miltenyi Biotec
Anti-EGFR-PE	Mouse IgG2b	Flow cytometry (1:100)	Santa Cruz Biotechnology
Anti-FLAG® M2-HRP	Mouse IgG1	ELISA (1:15,000)	Sigma-Aldrich
Anti-HER2-PE	Mouse IgG1	Flow cytometry (1:100)	Santa Cruz Biotechnology
Anti-HER3-PE	Mouse IgG2a, κ	Flow cytometry (1:100)	BioLegend
Anti-HER4-PE	Mouse IgG2a	Flow cytometry (1:100)	R&D Systems
Anti-His-PE	Mouse IgG1	Flow cytometry (1:200)	Miltenyi Biotec
Anti-human CD326 (EpCAM)-PE	Mouse IgG2b, κ	Flow cytometry (1:100)	BioLegend
Anti-human IgG (Fc specific)-Peroxidase	Goat polyclonal	ELISA (1:5,000)	Sigma-Aldrich
Anti-human IgG (γ-chain specific) R-PE	Goat polyclonal	Flow cytometry (1:500)	Sigma-Aldrich
Anti-human TRAIL-R1	Mouse IgG1	Flow cytometry (1:100)	R&D Systems
Anti-human TRAIL-R2	Mouse IgG2b	Flow cytometry (1:100)	R&D Systems
Anti-human TRAIL-R3	Mouse IgG1	Flow cytometry (1:100)	R&D Systems
Anti-human TRAIL-R4	Mouse IgG1	Flow cytometry (1:100)	R&D Systems
Anti-mouse IgG (whole molecule) R-PE	Goat polyclonal	Flow cytometry (1:100)	Sigma-Aldrich
Anti-rabbit IgG (whole molecule)-Peroxidase	Goat polyclonal	ELISA (1:5,000)	Sigma-Aldrich
Anti-scDbCEAxCD3-PEG	Rabbit polyclonal	ELISA (1:1,000)	Pineda Antikörper-Service
Cetuximab	Human IgG1, κ	Blocking studies, PK	IKP
His-probe (H-3) HRP	Mouse IgG1	ELISA (1:1,000)	Santa Cruz Biotechnology
Mouse IgG1 control PE	Mouse IgG1	Flow cytometry (1:100)	ImmunoTools

Antibody or serum	Isotype	Application	Source
Mouse IgG2a control PE	Mouse IgG2a	Flow cytometry (1:100)	ImmunoTools
PE Mouse IgG2b, κ Isotype Ctrl	Mouse IgG2b, κ	Flow cytometry (1:100)	BioLegend
Trastuzumab	Human IgG1, κ	Blocking studies	IKP

2.1.3 Buffers and solutions

If not stated otherwise, all components were dissolved in water.

Bradford reagent (5x)	Bio-Rad protein assay (Bio-Rad, Munich, Germany)
Coomassie staining solution	0.008 % (w/v) Coomassie Brilliant Blue G-250 (SERVA Electrophoresis, Heidelberg, Germany), 35 mM HCl
Crystal violet staining solution	0.5 % (w/v) crystal violet, 20 % (v/v) methanol
DNA loading dye (6x)	10 mM Tris-HCl pH 7.6, 0.03 % (w/v) xylene cyanol FF, 0.03 % (w/v) bromophenol blue, 60 mM EDTA, 60 % (v/v) glycerol (Thermo Fisher Scientific, Waltham, MA, USA)
DPBS (1x)	GIBCO® Dulbecco's phosphate-buffered saline (Thermo Fisher Scientific, Waltham, MA, USA)
ELISA blocking buffer (MPBS)	2 % (w/v) non-fat dry milk powder in 1x PBS
ELISA substrate solution	100 mM sodium acetate pH 6.0, 0.1 mg/ml TMB, 0.006 % (v/v) H_2O_2
ELISA wash buffer (PBST)	0.005 % (v/v) TWEEN 20 in 1x PBS
HPLC running buffer	0.1 M Na_2HPO_4/NaH_2PO_4, 0.1 M Na_2SO_4, pH 6.7
IMAC elution buffer	250 mM imidazole in 1x sodium phosphate buffer
IMAC wash buffer	25 mM imidazole in 1x sodium phosphate buffer
Laemmli loading buffer (5x)	non-reducing: 25 % (v/v) glycerol, 10 % (w/v) SDS, 0.05 % (w/v) bromophenol blue in 312.5 mM Tris-HCl pH 6.8; reducing: non-reducing, 12.5 % (v/v) β-mercaptoethanol
PBA	2 % (v/v) FBS, 0.02 % (w/v) NaN_3 in 1x PBS
PBS (10x)	80.6 mM Na_2HPO_4, 14.7 mM KH_2PO_4, 1.37 M NaCl, 26.7 mM KCl; used as 1x PBS pH 7.5
Periplasmic preparation buffer	30 mM Tris-HCl pH 8.0, 20 % (w/v) sucrose, 1 mM EDTA
Protein A elution buffer	100 mM glycine-HCl pH 3.0
Protein A wash buffer	100 mM Tris-HCl pH 7.5
SDS-PAGE running buffer	192 mM glycine, 25 mM Tris, 0.1 % (w/v) SDS, pH 8.3
Sodium phosphate buffer (5x, 250 mM)	210 mM Na_2HPO_4, 40 mM NaH_2PO_4, 1.25 M NaCl, pH 7.5
TAE buffer (50x)	2 M Tris, 1 M glacial acetic acid, 50 mM EDTA, pH 8.0

2.1.4 Enzymes and other proteins

Receptor-Fc fusion proteins kindly provided by Sina Fellermeier and Lisa Marquardt (both Institute of Cell Biology and Immunology, University of Stuttgart, Germany) are indicated.

EGFR-Fc	extracellular domain (aa 25-645) fused to the human Fcγ1 chain (Seifert *et al.*, 2012)
FastAP Thermosensitive Alkaline Phosphatase	1 U/µl (Thermo Fisher Scientific, Waltham, MA, USA)
HER2-Fc	extracellular domain (aa 23-652) fused to the human Fcγ1 chain (Seifert *et al.*, 2012)
HER3-Fc	extracellular domain (aa 20-643) fused to the human Fcγ1 chain (Seifert *et al.*, 2012); kindly provided by Sina Fellermeier
Human OPG-Fc	extracellular domain (aa 22-186) fused to the human Fcγ1 chain; kindly provided by Lisa Marquardt
Human TRAIL-R1-Fc	extracellular domain (aa 24-239) fused to the human Fcγ1 chain (Seifert *et al.*, 2014a); kindly provided by Lisa Marquardt
Human TRAIL-R2-Fc	extracellular domain (aa 52-212) fused to the human Fcγ1 chain (Seifert *et al.*, 2014a); kindly provided by Lisa Marquardt
Human TRAIL-R3-Fc	extracellular domain (aa 25-240) fused to the human Fcγ1 chain (Seifert *et al.*, 2014a); kindly provided by Lisa Marquardt
Human TRAIL-R4-Fc	extracellular domain (aa 56-212) fused to the human Fcγ1 chain (Seifert *et al.*, 2014a); kindly provided by Lisa Marquardt
Lysozyme	Muramidase from hen egg white (Roche Diagnostics, Mannheim, Germany)
Mouse DcTRAIL-R1-Fc	extracellular domain (aa 32-158) fused to the human Fcγ1 chain; kindly provided by Lisa Marquardt
Mouse DcTRAIL-R2-Fc	extracellular domain (aa 42-168) fused to the human Fcγ1 chain; kindly provided by Lisa Marquardt
Mouse OPG-Fc	extracellular domain (aa 22-186) fused to the human Fcγ1 chain; kindly provided by Lisa Marquardt
Mouse TRAIL-R2-Fc	extracellular domain (aa 53-180) fused to the human Fcγ1 chain; kindly provided by Lisa Marquardt
Mouse TRAIL-R2-Fc-His	extracellular domain (aa 1-177) fused to a C-terminally polyhistidine-tagged human Fcγ1 chain (Sino Biological, Beijing, China)
Pfu DNA Polymerase (native)	2.5 U/µl (Thermo Fisher Scientific, Waltham, MA, USA)

Protein L-HRP	used in ELISA as 1:1,000 dilution (Genscript, Piscataway, NJ, USA)
Restriction enzymes	AgeI, ApaI, BamHI, BspEI, EcoRI, KpnI, NotI, SfiI, SgsI, XbaI, XhoI: 10 U/µl (Thermo Fisher Scientific, Waltham, MA, USA) PspXI: 5 U/µl (New England Biolabs, Ipswich, MA, USA)
sEpCAM	extracellular domain (aa 24-265) fused to a FLAG-tag (Seifert *et al.*, 2012); kindly provided by Sina Fellermeier
T4 DNA Ligase	5 U/µl (Thermo Fisher Scientific, Waltham, MA, USA)

2.1.5 Markers and kits

Alanine Transaminase Activity Assay kit	(abcam, Cambridge, UK)
Amylase Assay kit	(abcam, Cambridge, UK)
BD OptEIA™ human TRAIL ELISA Set	(BD Biosciences, San Diego, CA, USA)
Caspase-Glo® 3/7 Assay	(Promega, Madison, WI, USA)
Caspase-Glo® 8 Assay	(Promega, Madison, WI, USA)
GeneRuler™ DNA Ladder Mix	(Thermo Fisher Scientific, Waltham, MA, USA)
NucleoBond® Xtra Midi	(Macherey-Nagel, Düren, Germany)
NucleoSpin® Gel & PCR Clean-up	(Macherey-Nagel, Düren, Germany)
NucleoSpin® Plasmid	(Macherey-Nagel, Düren, Germany)
PageRuler™	Prestained Protein Ladder (Thermo Fisher Scientific, Waltham, MA, USA)

2.1.6 Special implements

Anti-FLAG® M2 affinity gel	(Sigma-Aldrich, St. Louis, MO, USA)
Bortezomib	*in vitro* studies (UBPBio, Aurora, USA); *in vivo* studies: VELCADE® (Dr. Margarete Fischer-Bosch-Institute of Clinical Pharmacology, Stuttgart, Germany)
Bottle Top Filter	CA Low Protein binding, 500 ml, 0.2 µm/0.45 µm (Corning Incorporated, Tewksbury, MA, USA)
Centrifuge tubes	13 ml, PP (Sarstedt, Nümbrecht , Germany)
Chromatography columns	Poly-Prep® (Bio-Rad, Munich, Germany)
Counting chamber	Neubauer improved (Marienfeld Superior, Paul Marienfeld GmbH & Co. KG, Lauda-Königshofen, Germany)
Cuvette	12 mm O.D. square glass cell with cap (Malvern Instruments, Malvern, Worcestershire, UK)
Dialysis membrane	High retention seamless cellulose tubing, 23 mm, MWCO 12,400 (Sigma-Aldrich, St. Louis, MO, USA)

Dialysis membrane	ZelluTrans, MWCO 6,000-8,000, 40 mm; ZelluTrans, MWCO 3,500, 46 mm (Carl Roth, Karlsruhe, Germany)
FLAG peptide	5 mg/ml (peptides&elephants, Potsdam, Germany)
FPLC column	Superdex 200 10/300 GL (GE Healthcare, Little Chalfont, Buckinghamshire, UK)
HPLC column	Yarra™ 3 µm SEC-2000, Yarra™ 3 µm SEC-3000 (Phenomenex, Torrance, CA, USA)
Human plasma	from healthy donors (blood bank, Klinikum Stuttgart, Germany)
Protein A affinity resin	TOYOPEARL® AF-rProtein A-650F (Tosoh Bioscience, Griesheim, Germany)
Reaction tubes	1.5 ml, 2 ml Safe-Lock (Eppendorf AG, Hamburg, Germany)
REDTaq® ReadyMix™	PCR Reaction Mix (Sigma-Aldrich, St. Louis, MO, USA)
Syringe filter	Acrodisc® 13 mm, 0.2 µm, HT Tuffryn® Membrane (Pall Corporation, Port Washington, NY, USA)
TripleFlask™	500 cm², Nunclon™ Delta Surface (Thermo Fisher Scientific, Waltham, MA, USA)
Ultrafiltration spin columns	Vivaspin 500, 30,000 MWCO PES (Sartorius, Göttingen, Germany)

2.1.7 Prokaryotic and eukaryotic cell lines

Escherichia coli TG1	Genotype: *supE thi-1* Δ(*lac-proAB*) Δ(*mcrB-hsdSM*)*5* (r_K-m_K-) [F' *traD36 proAB lacI^{q}ZΔM15*] (Stratagene, La Jolla, CA, USA)
HEK293T	Human embryonic kidney
A-431	Human epidermoid carcinoma
SKBR3	Human breast adenocarcinoma
MCF7	Human breast adenocarcinoma
Colo205	Human colorectal adenocarcinoma
HCT116	Human colorectal carcinoma

2.1.8 Media and supplements for prokaryotic and eukaryotic cell culture

2xTY medium	1.6 % (w/v) peptone, 1 % (w/v) yeast extract, 0.5 % (w/v) NaCl in H_2O
Ampicillin (1000x)	100 mg/ml in H_2O
Cryopreservation solution	10 % (v/v) dimethyl sulfoxide in FBS
Eosin staining solution	0.4 % (w/v) eosin G, 0.02 % (w/v) NaN_3 in 1x PBS pH 7.4
FBS	FBS Premium (PAN Biotech, Aidenbach, Germany)
IPTG (1000x)	1 M isopropyl β-D-1-thiogalactopyranoside in H_2O

$LB_{amp,glc}$ agar plates	LB medium, 2 % (w/v) agar; after autoclaving: addition of 1 % (w/v) D-glucose and 100 µg/ml ampicillin
LB medium	1 % (w/v) peptone, 0.5 % (w/v) yeast extract, 0.5 % (w/v) NaCl in H_2O
Lipofectamine® 2000	(Thermo Fisher Scientific, Waltham, MA, USA)
Opti-MEM®	Reduced Serum Medium (Thermo Fisher Scientific, Waltham, MA, USA)
Penicillin-Streptomycin (100x)	10,000 U/ml penicillin, 10,000 µg/ml streptomycin (Thermo Fisher Scientific, Waltham, MA, USA)
Puromycin	(Sigma-Aldrich, St. Louis, MO, USA)
RPMI Medium 1640 (1x)	+ L-Glutamine (Thermo Fisher Scientific, Waltham, MA, USA)
Trypsin-EDTA (10x)	0.5 % Trypsin-EDTA, diluted to 1x in sterile PBS (Thermo Fisher Scientific, Waltham, MA, USA)
Zeocin™ Selection Reagent	100 mg/ml (Thermo Fisher Scientific, Waltham, MA, USA)
$ZnCl_2$	100 mM in H_2O, sterile filtered

2.1.9 Mice

CD-1®	Crl:CD1 (ICR) (Charles River, Wilmington, MA, USA)
NMRI nude	Crl:NMRI-*Foxn1*^{nu} (Charles River, Wilmington, MA, USA)

2.1.10 Plasmids

Plasmids developed at the Institute of Cell Biology and Immunology (University of Stuttgart, Germany) are indicated.

pAB1	Vector for prokaryotic protein expression and secretion into the periplasm of *E. coli* (Kontermann *et al.*, 1997)
pAB1-scFv323/A3hu3	(Sina Fellermeier, 2012, Institute of Cell Biology and Immunology)
pAB1-scFvhu225	(Anja Nusser, 2008, Institute of Cell Biology and Immunology)
pAB1-scFvMM-6	(Sina Fellermeier, 2011, Institute of Cell Biology and Immunology)
pAB1-scFvMOC31hu2	(Sina Fellermeier, 2012, Institute of Cell Biology and Immunology)
pIRESpuro3	Bicistronic mammalian expression vector (Clontech Laboratories, Mountain View, CA, USA)
pIRESpuro-L-F-scTRAIL$_{281\text{-}G\text{-}118}$	(Martin Siegemund, 2013, Institute of Cell Biology and Immunology)

pSecTagA	Vector for eukaryotic protein expression and secretion (Thermo Fisher Scientific, Waltham, MA, USA)
pSecTagAHis	Modification of pSecTagA lacking the *myc* epitope (Gerhard Trunk, 2005, Institute of Cell Biology and Immunology)
pSecTagAHis-Db4D5-HPR	(Heike Lill, 2009, Institute of Cell Biology and Immunology)
pSecTagAHis-Dbhu225-HPR	(Heike Lill, 2009, Institute of Cell Biology and Immunology)
pSecTagAHis-scDb4D5xhu225	(Aline Plappert, 2011, Institute of Cell Biology and Immunology)
pSecTagAHis-scDbhu225xCD3	(Sina Fellermeier, 2010, Institute of Cell Biology and Immunology)
pSecTagAHis-scDbMocBxhu225	(Aline Plappert, 2011, Institute of Cell Biology and Immunology)
pSecTagAHis-scFv4D5	(Heike Lill, 2009, Institute of Cell Biology and Immunology)
pSecTagAL1	Modification of pSecTagAHis with an additional AgeI restriction site in the Igκ chain leader sequence (Julia Seitter, 2007, Institute of Cell Biology and Immunology)

2.1.11 Primers

Primers used for DNA sequencing, colony screening, and cloning were synthesized by Sigma-Aldrich (St. Louis, MO, USA). Primers were dissolved in water to a concentration of 50 µM and stored at -20 °C.

Table 2.2: Primers used for cloning, PCR screening, and sequencing.

#	Name	Sequence (5'→3')	Application
61	LMB4	GCAAGGCGATTAAGTTGG	Reverse primer for pAB1
88	LMB3	CAGGAAACAGCTATGACC	Forward primer for pAB1
89	pET-Seq1	TAATACGACTCACTATAGG	Forward primer for pSecTagA
91	pSec-Seq2	TAGAAGGCACAGTCGAGG	Reverse primer for pSecTagA
910	AgeI-scFvhu225-back	AAAACCGGTGAAGTGCAGCTGGTTGAAA	Cloning: (ds)Dbhu225
911	AgeI-VH4D5-back	AAAACCGGTGAAGTGCAGCTCGTCGAA	Cloning: scFv4D5, (ds)Db4D5
912	BamHI-VH4D5-for	AAAGGATCCTCCGCCTCCTGAGCCAC	Cloning: scFv4D5
913	BamHI-VL4D5-back	AAAGGATCCGACATCCAGATGACCCAG	Cloning: scFv4D5
942	AgeI-scFvMM-6-back	AAAACCGGTGAAGTGCAGCTGCTGGAA	Cloning: scFv3M6, dsDb3M6
944	KpnI-VHhu225-back	AAAGGTACCGAAGTGCAGCTGGTTGAAA	Cloning: hu225 scTRAIL molecules
945	KpnI-VH4D5-back	AAAGGTACCGAAGTGCAGCTCGTCGAA	Cloning: 4D5 scTRAIL molecules
947	KpnI-VH3M6-back	AAAGGTACCGAAGTGCAGCTGCTGGAA	Cloning: 3M6 scTRAIL molecules
953	NotI-VLMM-6-Ser-for	AAATGCGGCCGCCAGCACGGTCACTTTGGTGCCAC CTCCGAAGATCACGAAGATGCTGCTGCCGGCGTAG CTGGAGCAGTAGTAGTCGGCCTC	Cloning: scFv3M6
954	VHhu225-Cys44-for	CCCAGCCATTCCAGACATTTGCCCGGTGCCTGAC	Cloning: dsDbhu225
955	VHhu225-Cys44-back	AGGCACCGGGCAAATGTCTGGAATGGCTGGGCGT	Cloning: dsDbhu225
956	BamHI-GGGGS-VHhu255-for	AAAGGATCCACCGCCACCG	Cloning: dsDbhu225

#	Name	Sequence (5'→3')	Application
957	BamHI-VLhu225-back	AAAGGATCCGATATTCAGCTGA	Cloning: dsDbhu225
958	NotI-VLhu225-Cys100-for	AAAGGCGGCCGCACGTTTAATTTCCAGTTTGGTGCC GCAACCAAAGGTGGTCGGCC	Cloning: dsDbhu225
959	VH4D5-Cys44-for	GCGACCCACTCCAAACACTTTCCAGGAGCTTGCCT	Cloning: dsDb4D5
960	VH4D5-Cys44-back	AAGCTCCTGGAAAGTGTTTGGAGTGGGTCGCTAGG	Cloning: dsDb4D5
961	BspEI-VH4D5-for	AAATCCGGAACTGACGGTCAC	Cloning: dsDb4D5
962	BspEI-VL4D5-back	AAATCCGGAGGAGGGGGTAG	Cloning: dsDb4D5
963	NotI-VL4D5-Cys100-for	AAATGCGGCCGCACGCTTGATCTCGACCTTCGTTCC GCAACCGAAGGTTGGAGGAGT	Cloning: dsDb4D5
986	ApaI-scTRAIL118-for	AAAGGGCCCTCTAGACGTACGTCAACCC	Cloning: pSecTagFLAG-linker-EHD2-scTRAIL
987	XhoI-linker-scTRAIL118-back	AAAGCCTCGAGCGGCGGCGGCCCCCAG	Cloning: pSecTagFLAG-linker-EHD2-scTRAIL
992	BamHI-linker-VH3M6-for	AAAGGATCCGCCTCCCCCACTCGAGACTGTGACCAG	Cloning: Db3M6
1015	NotI-linker-scTRAIL118-back	ATAAGAATGCGGCCGCCGGGGGAAGCGGCGGCGG CCCCCAG	Cloning: pSecTagFLAG-linker-scTRAIL
1016	EcoRI-scTRAIL118-for	CCGGAATTCTCTAGACGTACGTCAACCC	Cloning: scTRAIL vectors
1019	XhoI-linker-scTRAIL118-back	CCGGCCTCGAGCGGCGGCGGCCCCCAG	Cloning: pSecTagFLAG-EHD2-scTRAIL
1050	VH3M6-Cys44-for	GACACCCATTCCAGACACTTGCCAGGGGCCTGTC	Cloning: dsDb3M6
1051	VH3M6-Cys44-back	AGGCCCCTGGCAAGTGTCTGGAATGGGTGTCCAGC	Cloning: dsDb3M6
1052	BamHI-GGGGS-VH3M6-for	AAAGGATCCGCCTCCCCCA	Cloning: dsDb3M6
1053	BamHI-VL3M6-back	AAAGGATCCCAGTCTGCCCT	Cloning: dsDb3M6
1054	NotI-VL3M6-Cys100-for	AAAGGCGGCCGCCAGCACGGTCACTTTGGTGCCGC ATCCGAAGATCACGAAGATG	Cloning: dsDb3M6
1081	XhoI-G-Fc(Q)-for	AAAGCTCGAGCCACCGCCGCTTCCCCCCTGACCCGG AGACAGGGAG	Cloning: optimized Fc-linker for scTRAIL molecules
1210	KpnI-Fc(Q)-back	AAAGGTACCGACAAAACTCACACATGCC	Cloning: Fc-scTRAIL
1212	BamHI-VL323A3hu3-back	AAAGGATCCGAGATCGTGCTGACACAG	Cloning: Db323/A3hu3
1213	KpnI-VH323A3hu3-back	AAAGGTACCCAAGTGCAGCTGGTGCAG	Cloning: 323/A3hu3 scTRAIL molecules
1214	XhoI-linker-VL3M6-back	AAACTCGAGTGGCGGTGGCGGATCGCAGTCTGCCC TGACACAG	Cloning: scDbhu225x3M6
1215	SgsI-linker-VL3M6-for	AAAGGCGCGCCCACCGCTGCCACCGCCTCCCAGCAC GGTCACTTTGGT	Cloning: scDbhu225x3M6
1216	SgsI-linker-VH3M6-back	AAAGGCGCGCCTCGGGCGGAGGTGGCTCAGAAGT GCAGCTGCTGGAA	Cloning: scDbhu225x3M6
1217	BamHI-linker-VH3M6-for	AAAGGATCCCCCGCCTCCACTCGAGACTGTGACCAG	Cloning: scDbhu225x3M6
1245	AgeI-VH3-43-back	AAAACCGGTCAGGTGCAGCTGCAGCA	Cloning: Db3-43
1246	BamHI-GGGGS-VL3-43-for	AAAGGATCCGCCTCCCCCTGAAGAGACGGTGACCA TT	Cloning: Db3-43
1247	BamHI-VL3-43-back	AAAGGATCCCAGGCTGGGCTGACTCA	Cloning: Db3-43
1248	NotI-VL3-43-for	AAAGGCGGCCGCTAGGACGGTCAGCTTGGT	Cloning: Db3-43
1249	KpnI-VH3-43-back	AAAGGTACCCAAGTGCAGCTGCAGCAG	Cloning: 3-43 scTRAIL molecules
1306	BamHI-(GGGGS)3-VH3-43-for	AAAGGATCCACCGCCGCCACTTCCACCTCCCCCAGA TCCTCCCCCGCCAGAGGACACTGTGACCAT	Cloning: scFv3-43

2.1.12 Instruments

Centrifuges	Centrifuges 5415D, 5810R (Eppendorf, Hamburg, Germany); Rotanta 460 RF (Hettich Zentrifugen, Tuttlingen, Germany); J2-MC and Avanti® J-30I with rotors JA-10, JA-14, JA-20, JA-30.50 Ti; Avanti® J-26XP with rotor JLA-8.1000 (Beckman Coulter, Krefeld, Germany)
CO_2 incubator for cell culture	Varocell 140 (varolab GmbH, Giesen, Germany)
Electrophoresis systems	Mini-PROTEAN® Tetra Cell, Mini-Sub® Cell GT, PowerPac™ Basic and HC power supply (Bio-Rad, Munich, Germany)
Flow cytometer	MACSQuant® Analyzer 10, MACSQuant® VYB (Miltenyi Biotec, Bergisch Gladbach, Germany)
FPLC	ÄKTApurifier (GE Healthcare, Little Chalfont, Buckinghamshire, UK)
Gel documentation	Transilluminator, ImageSystem Felix® (biostep, Jahnsdorf, Germany)
HPLC	Waters 2695 Separations Module, Waters 2489 UV/Visible Detector (Waters Corporation, Milford, MA, USA)
Incubator for bacteria	Infors HT Multitron (Infors AG, Bottmingen, Switzerland)
Laminar flow cabinet	Variolab Mobilien W90 Sicherheitswerkbank (Waldner Laboreinrichtungen, Wangen, Germany)
Microplate reader	Infinite M200 (Tecan Group, Männedorf, Switzerland)
PCR cycler	RoboCycler® 96 (Stratagene, La Jolla, CA, USA)
Spectrophotometer	NanoDrop™ ND-1000 (Thermo Fisher Scientific, Waltham, MA, USA)
Zetasizer	Zetasizer Nano ZS (Malvern Instruments, Malvern, Worcestershire, UK)

2.1.13 Software and online tools

Antibody sequence numbering	Abnum (http://www.bioinf.org.uk/abs/abnum/) IMGT (http://www.imgt.org/IMGTScientificChart/Numbering/Hu_IGHGnber.html)
Cleavage site analysis	ExPASy PeptideCutter (http://web.expasy.org/peptide_cutter/)
Data evaluation	GraphPad Prism® 5.00 for Windows (GraphPad Software, La Jolla, CA, USA); Microsoft Excel 2013 (Microsoft, Redmond, WA, USA)
Flow cytometry	MACSQuantify 2.6 (Miltenyi Biotec, Bergisch Gladbach, Germany); FlowJo 7.6.5 (Tree Star Inc., Ashland, OR, USA)
Molecular biology software	SerialCloner 2.6.1 (http://serialbasics.free.fr/Serial_Cloner.html)
Molecular visualization	PyMOL™ v0.99 (DeLano Scientific, San Francisco, CA, USA)

Protein databases	UniProt (http://www.uniprot.org/) PDB (http://www.rcsb.org/pdb/home/home.do)
Protein parameter determination	ExPASy ProtParam (http://web.expasy.org/protparam/)
Sequence alignment	BLAST (http://blast.ncbi.nlm.nih.gov/Blast.cgi)

2.2 Cloning techniques

2.2.1 Polymerase chain reaction

PCR was performed to specifically modify existing DNA sequences. 1 µl of forward and 1 µl of reverse primer (both 10 µM) were mixed with 1 µl of template DNA (10 ng/µl to 5 µg/µl), 2.5 µl of dNTP mix (5 mM each), 5 µl 10x Pfu buffer containing $MgSO_4$, 1 µl Pfu DNA polymerase, and 38.5 µl nuclease-free water. DNA fragments were amplified using a standard PCR protocol, composed of an initial denaturation phase (94 °C, 5 min), followed by 30 cycles of denaturation (94 °C, 1 min), annealing (temperature depending on the melting point of the primers, 1 min) and elongation (72 °C, time adjusted to the length of the amplified fragment). PCR was completed with a final elongation step (72 °C, 5 min). The elongation time in the PCR cycles was adapted based on the synthesis rate of the Pfu DNA polymerase of 500 nucleotides per min and the length of the expected fragment. Amplified DNA fragments were subjected to agarose gel electrophoresis and subsequent gel extraction (see 2.2.2).

In order to introduce mutations that are not located near to restrictions sites, fusion-PCR was used. Initially, two separate polymerase chain reactions were performed based on the standard protocol described above to amplify two overlapping fragments containing the desired mutation. These DNA fragments were purified by preparative gel electrophoresis, and extracted DNA was eluted in 30 µl nuclease-free water (see 2.2.2). 15 µl of each PCR product were mixed, and 2.5 µl of dNTP mix (5 mM each), 5 µl 10x Pfu buffer containing $MgSO_4$, 1 µl Pfu DNA polymerase, and 11.5 µl nuclease-free water were added. The fusion-PCR protocol consisted of an initial denaturation phase (94 °C, 5 min) and 5 cycles of denaturation (94 °C, 0.5 min), annealing (50 °C, 0.5 min) and elongation (72 °C, 1 min). After the last elongation step, the PCR sample was held at 94 °C and directly transferred on ice. After 3 min, 1 µl of forward and 1 µl of reverse primer (both 10 µM) as well as 2.5 µl of dNTP mix (5 mM each) were added, and a final standard PCR was run to amplify the fused fragment.

2.2.2 Agarose gel electrophoresis and gel extraction

PCR products and DNA fragments generated by restriction digestion were analyzed by horizontal agarose gel electrophoresis (80 V according to 1 V/cm, 40 min). 1 % (w/v) agarose was dissolved in 1x TAE buffer by heating, and ethidium bromide was added to a final concentration of 1 µg/ml to visualize DNA bands by exposure to UV light. DNA samples containing 1x DNA loading dye were analyzed together with GeneRuler™ DNA Ladder Mix. DNA fragments desired for further cloning were excised, and DNA was extracted using NucleoSpin® Gel & PCR Clean-up kit according to the manufacturer's instructions.

2.2.3 Restriction digestion and ligation

Plasmid DNA or purified PCR products were digested by preparing a reaction mixture of DNA (10 µg or complete amount of PCR product), 1 µl restriction enzyme, and the corresponding buffer at the indicated concentration. Sample volume was adjusted to 50 µl with water. Digestion was done at the working temperature of the respective enzyme for at least 2 h. Prior to digestion with the second enzyme, buffer was exchanged using NucleoSpin® Gel & PCR Clean-up kit. Double digest was only performed, when recommended by the manufacturer. To prevent religation, vector DNA was dephosphorylated by adding 1 µl FastAP and incubation at 37 °C for at least 1 h. Agarose gel electrophoresis was run and desired DNA fragments were extracted using NucleoSpin® Gel & PCR Clean-up kit (see 2.2.2). Ligation was prepared with purified insert and vector DNA (100 ng to 200 ng vector DNA, typically in molar ratios of 3:1 and 5:1 of insert to vector), 2 µl ligase buffer, and 1 µl T4 DNA ligase. Sample volume was adjusted to 20 µl with water. Ligation was performed at room temperature for at least 1 h.

2.2.4 Transformation

E. coli TG1 were transformed with purified plasmid DNA (100 ng) or ligation preparations (20 µl) by heat shock. Chemically competent bacteria were thawed on ice, mixed with DNA, and incubated on ice for 15 min. Heat shock was performed for 1 min at 42 °C. Bacteria were transferred back on ice for 1 min, and LB medium (1 ml) was added. Bacteria were incubated shaking at 37°C for 1 h and subsequently plated on $LB_{amp,glc}$ agar plates for overnight culture at 37 °C.

2.2.5 Colony Screening

Transformed bacteria colonies were screened for positive clones by PCR. The reaction mix consisted of 50 % (v/v) REDTaq® ReadyMix™, 0.2 µM of forward and 0.2 µM of reverse primer in water. Samples of 20 µl reaction mix were inoculated with single picked colonies that were subsequently plated on $LB_{amp,glc}$ agar plates and incubated at 37 °C for at least 6 h. DNA fragments were amplified by PCR (see 2.2.1) and analyzed on agarose gels (see 2.2.2) to identify clones showing bands of the desired size.

2.2.6 Plasmid DNA preparation

LB medium containing 1 % (w/v) glucose and 100 µg/ml ampicillin was inoculated with transformed bacteria and incubated shaking overnight at 37 °C. Plasmid DNA was prepared using NucleoSpin® Plasmid (Mini-preparation, 6 ml overnight culture) and NucleoBond® Xtra Midi kits (Midi-preparation, 150 ml overnight culture) according to the manufacturer's protocol.

2.2.7 Determination of DNA concentration and sequence analysis

DNA concentration was determined by measuring the absorbance at 260 nm using NanoDrop™ ND-1000. DNA mixed with the respective primer at the recommended concentrations was sent to GATC (Constance, Germany) for sequence analysis. BLAST was used to compare the sequencing result with the virtually cloned DNA sequence.

2.3 Cloning strategies

2.3.1 Cloning of scFv

ScFvhu225 was generated by humanization of the anti-EGFR antibody C225 (Goldstein *et al.*, 1995) by complementarity-determining region grafting (Seifert *et al.*, 2012). ScFv4D5, scFvMM-6, and scFv323/A3 were derived from previously published data (Carter *et al.*, 1992; Schoeberl *et al.*, 2009; Edwards *et al.*, 1986 and Roovers *et al.*, 1998). Humanization of scFv323/A3 required sequential analysis of several humanized forms finally developing scFv323/A3hu3 (Fellermeier *et al.*, 2016). ScFv3-43 was selected from a human scFv phage display library using HER3-Fc as target structure (Stefan Dübel, Technical University of Braunschweig, Germany). V_H and V_L sequences of 3-43 codon-optimized for eukaryotic expression were ordered from GeneArt® Gene Synthesis (Thermo Fisher Scientific GENEART

GmbH, Regensburg, Germany). ScFv sequences were cloned into pAB1 for periplasmic expression in *E. coli*. Sequences of scFvhu225, scFvMM-6, and scFv323/A3hu3 in pAB1 were already available. The sequence of scFv4D5 containing an alternative linker was modified to generate an scFv with the standard $(GGGGS)_3$ linker. AgeI-V_H4D5-linker-BamHI and BamHI-V_L4D5-NotI fragments were amplified by PCR (primers #911/912 and #913/91, Table 2.2), followed by digestion with the respective restriction enzymes and substitution of the scFv in pAB1-scFvMOC31hu2. ScFvMM-6 was modified by mutation of the cysteine residue at position 89 (Kabat numbering scheme) in the CDR-L3 loop to serine generating scFv3M6 (mutated MM-6). The C89S mutation was introduced by PCR generating an AgeI-scFv3M6-NotI fragment (primers #942/953, Table 2.2) and subsequent transfer into pAB1. ScFv3-43 was cloned based on Db3-43 (see 2.3.2) by PCR amplification of an AgeI-V_H3-43-linker-BamHI fragment containing a $(GGGGS)_3$ linker (primers #89/1306, Table 2.2) and substitution of the V_H-linker part of the diabody via AgeI/BamHI digestion.

2.3.2 Cloning of Db

All diabody sequences were cloned into pSecTagAL1 for eukaryotic expression. Dbhu225 was amplified by PCR from pSecTagAHis-Dbhu225-HPR adding an AgeI restriction site (primers #910/91, Table 2.2) and transferred to pSecTagAL1 via AgeI/NotI digestion. Generation of pSecTagAL1-Db4D5 was performed according to the Dbhu225 construct using pSecTagAHis-Db4D5-HPR as template in PCR (primers #911/91, Table 2.2). Db3M6 was generated based on scFv3M6 by substituting the V_H-linker part with PCR amplified AgeI-V_H3M6-linker-BamHI containing a GGGGS linker (primers #89/992, Table 2.2). pSecTagAL1-Db323/A3hu3 was constructed by substitution of the V_H of pSecTagAL1-Dbhu225 with the V_H of pAB1-scFv323/A3hu3 via AgeI/XhoI prior to replacing the V_L with PCR amplified BamHI-V_L323/A3hu3-NotI (primers #1212/61, Table 2.2). Db3-43 was cloned by generating AgeI-V_H3-43-linker-BamHI and BamHI-V_L3-43-NotI fragments using the sequence synthesized by GeneArt® as template in PCR (primers #1245/1246 and #1247/1248, Table 2.2) and subsequent transfer into pSecTagAL1.

2.3.3 Cloning of dsDb

Disulfide-stabilized versions of the diabodies were cloned into pSecTagAL1 for eukaryotic expression. One amino acid in the V_H domain and one amino acid in the V_L domain located at

positions allowing the formation of interchain disulfide bonds were specifically mutated to cysteines (reviewed by Reiter *et al.*, 1996). One cysteine residue was introduced at position 44 in the V_H domain (Kabat numbering scheme) by fusion-PCR (primers #910/954 and #955/956 for hu225, #911/959 and #960/961 for 4D5, #942/1050 and #1051/1052 for 3M6, Table 2.2). Another cysteine residue was introduced in the V_L domain at position 100 (Kabat numbering scheme) by standard PCR (primers #957/958 for hu225, #962/963 for 4D5, #1053/1054 for 3M6, Table 2.2). V_H and V_L domains of the diabodies were sequentially substituted with the corresponding mutated domains via AgeI/BamHI and BamHI/NotI (hu225, 3M6) or AgeI/BspEI and BspEI/NotI (4D5) digestion, respectively.

2.3.4 Cloning of scFv-EHD2 and scFv-Fc

ScFv-EHD2 and scFv-Fc fusion proteins were constructed by generation of vectors enabling the subsequent insertion of scFv sequences (Figure 2.1). PSecTagAL1 vectors containing appropriate restriction sites, linkers, and the respective dimerization modules were constructed by PCR, restriction digestion, and ligation steps. ScFv-EHD2 and scFv-Fc molecules were generated via transfer of the corresponding scFv as AgeI/NotI fragment into pSecTagAL1-linker-EHD2-His and pSecTagAL1-linker-Fc, respectively.

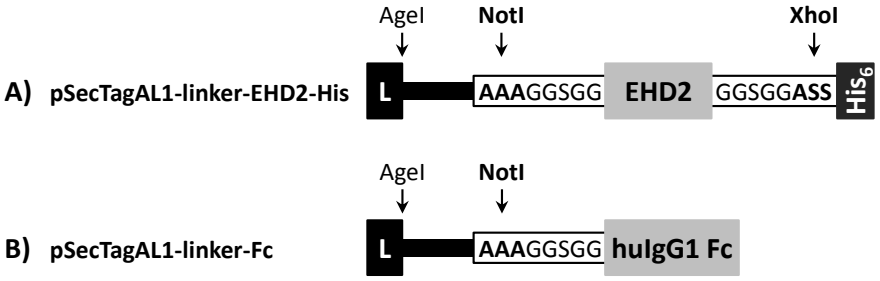

Figure 2.1: Schematic representation of relevant vector parts for cloning of scFv-EHD2 and scFv-Fc molecules. A) pSecTagAL1-linker-EHD2-His was constructed for generation of scFv-EHD2 fusion proteins. B) pSecTagAL1-linker-Fc allows generation of scFv-Fc molecules. Amino acid sequences of linkers are shown. Residues originating from restriction sites used for cloning are highlighted, and respective restriction enzymes are indicated. L, Igκ chain leader sequence.

2.3.5 Cloning of Db-scTRAIL and dsDb-scTRAIL

All scTRAIL molecules generated in this study contain a single-chain version of TRAIL consisting of amino acids 118 to 281 with linkers of a single glycine connecting the TRAIL subunits ($scTRAIL_{281\text{-}G\text{-}118}$). ScTRAIL was expressed using a pIRESpuro vector that was already available, while all other scTRAIL molecules were cloned into pSecTagAL1. For the generation of Db-scTRAIL and dsDb-scTRAIL fusion proteins, the vector pSecTagFLAG-linker-scTRAIL was

constructed allowing insertion of Db or dsDb modules (Figure 2.2). The vector was developed based on pSecTagFLAG-linker-EHD2-linker (Figure 2.3A) via NotI/EcoRI digestion and ligation with PCR amplified NotI-linker-scTRAIL$_{281\text{-}G\text{-}118}$-EcoRI (pIRESpuro-L-F-scTRAIL$_{281\text{-}G\text{-}118}$ as template, primers #1015/1016, Table 2.2). Diabodies and disulfide-stabilized diabodies were inserted into pSecTagFLAG-linker-scTRAIL as KpnI/NotI fragments generated by PCR (primers #944/91 for hu225, #945/91 for 4D5, #947/91 for 3M6, #1213/91 for 323/A3hu3, #1249/91 for 3-43, Table 2.2).

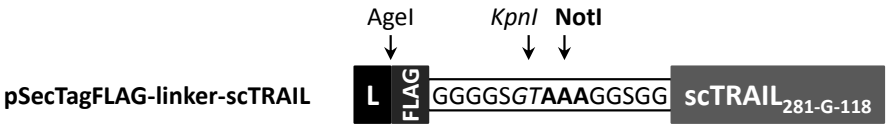

Figure 2.2: Schematic representation of the relevant vector part for cloning of Db- and dsDb-scTRAIL molecules. Amino acid sequences of the linkers of pSecTagFLAG-linker-scTRAIL are shown. Residues generated by restriction sites used for cloning and the respective restriction enzymes are indicated. L, Igκ chain leader sequence.

2.3.6 Cloning of EHD2- and Fc-containing scTRAIL fusion proteins

Modular vector systems for sequential insertion of scFv and scTRAIL moieties were generated for cloning of scFv-EHD2-scTRAIL and scFv-Fc-scTRAIL molecules and their corresponding non-targeted variants.

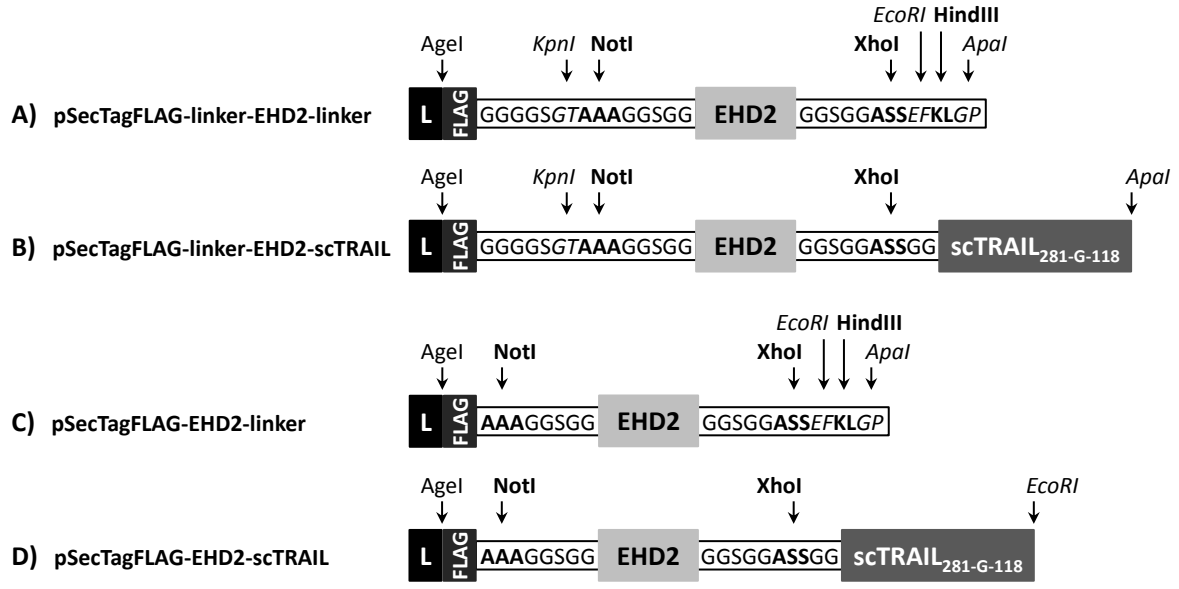

Figure 2.3: Schematic representation of relevant vector parts for cloning of EHD2-containing scTRAIL fusion proteins. A) pSecTagFLAG-linker-EHD2-linker was used to generate pSecTagFLAG-linker-EHD2-scTRAIL (B) allowing the construction of scFv-EHD2-scTRAIL fusion proteins. C) pSecTagFLAG-EHD2-linker was created for cloning of pSecTagFLAG-EHD2-scTRAIL (D) to express non-targeting EHD2-scTRAIL. Amino acid sequences of linkers are shown. Restriction enzymes and amino acids generated by their corresponding restriction sites are highlighted. L, Igκ chain leader sequence.

In order to generate scFv-EHD2-scTRAIL fusion proteins, the vector pSecTagFLAG-linker-EHD2-scTRAIL was constructed based on pSecTagFLAG-linker-EHD2-linker (Figure 2.3B and A) by insertion of the PCR fragment XhoI-scTRAIL$_{281\text{-}G\text{-}118}$-ApaI (pIRESpuro-L-F-scTRAIL$_{281\text{-}G\text{-}118}$ as template, primers #987/986, Table 2.2) after digestion with XhoI and partial digestion with ApaI. KpnI-scFv-NotI fragments generated by PCR (primers #944/91 for hu225, #945/91 for 4D5, #947/91 for 3M6, #1213/61 for 323/A3hu3, Table 2.2) were cloned into pSecTagFLAG-linker-EHD2-scTRAIL. Non-targeted EHD2-scTRAIL was expressed using pSecTagFLAG-EHD2-scTRAIL that was developed from pSecTagFLAG-EHD2-linker (Figure 2.2D and C) by ligation with the PCR-amplified XhoI/EcoRI fragment of scTRAIL$_{281\text{-}G\text{-}118}$ (pIRESpuro-L-F-scTRAIL$_{281\text{-}G\text{-}118}$ as template, primers #1019/1016, Table 2.2).

The Fc part used in scTRAIL fusion proteins was derived from human IgG1. Several versions of Fc-containing scTRAIL molecules were analyzed before developing the final format. PSecTagAL1-linker-Fc-linker (Figure 2.4A) was constructed for insertion of scTRAIL as XhoI/ApaI PCR fragment (pIRESpuro-L-F-scTRAIL$_{281\text{-}G\text{-}118}$ as template, primers #987/986, Table 2.2) after digestion with XhoI and partial digestion with ApaI. First versions of scFv-Fc-scTRAIL were expressed without a FLAG-tag using pSecTagAL1-linker-Fc-scTRAIL-v1 (Figure 2.4B) after ligation with AgeI-scFv-NotI fragments. Characterization of these fusion proteins, however, revealed cleavage products. An analysis of potential protease cleavage sites identified several candidates in the sequence connecting the Fc part and scTRAIL. Therefore, the sequence was optimized by mutation of K447 of the Fc part (EU numbering scheme) to Q and A in the XhoI restriction site to G, which removed all potential protease cleavage sites in this sequence part (Figure 2.4C). Mutations were introduced by PCR (primers #89/1081, Table 2.2) and replacement of the old with the new Fc-linker version by NotI/XhoI digestion. Since neutralization of scFv-Fc-scTRAIL fusion proteins after acidic elution from protein A beads led to strong precipitation of the protein, the final versions were expressed containing a FLAG-tag. These FLAG-tagged scFv-Fc-scTRAIL molecules were generated by transferring FLAG-scFv fragments of previously generated pSecTagFLAG-scFv-EHD2-scTRAIL sequences to pSecTagAL1-linker-Fc-scTRAIL by AgeI/NotI digestion. The final version of non-targeted Fc-scTRAIL containing a FLAG-tag and the K to Q and A to G mutations (Figure 2.4D) was constructed based on pSecTagFLAG-scFv4D5-Fc-scTRAIL by PCR (primers #1210/91, Table 2.2) and replacing of scFv4D5-Fc with KpnI-Fc by KpnI/PspXI digestion.

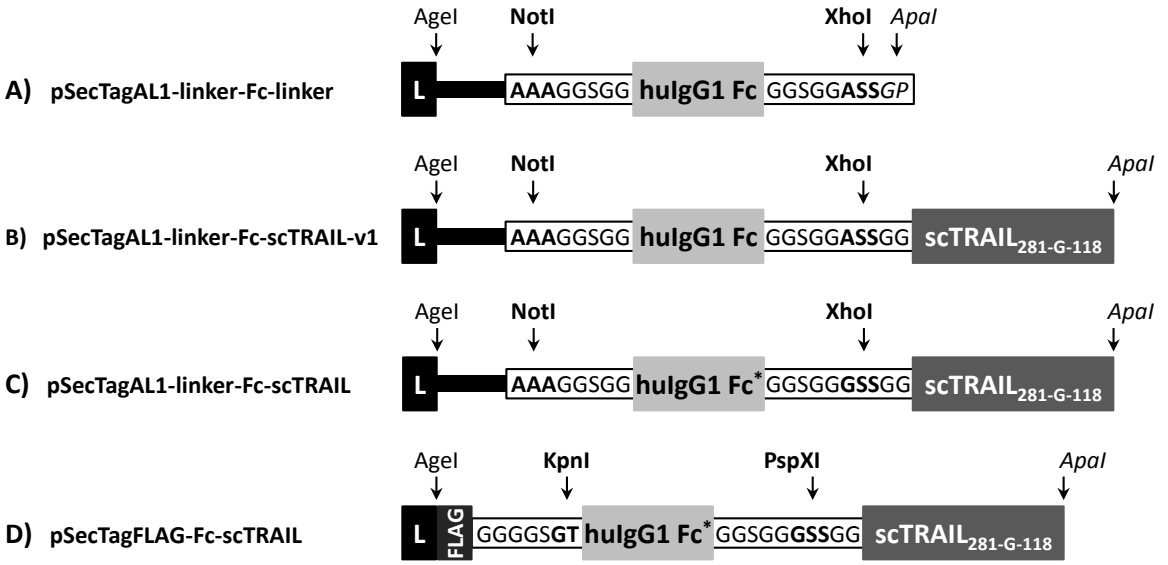

Figure 2.4: Schematic representation of relevant vector parts for cloning of Fc-containing scTRAIL molecules. A) pSecTagAL1-linker-Fc-linker was generated to develop pSecTagAL1-linker-Fc-scTRAIL-v1 (B). C) pSecTagAL1-linker-Fc-scTRAIL contains mutations (K to Q and A to G) to remove potential protease cleavage sites. D) pSecTagFLAG-Fc-scTRAIL was used to express non-targeted Fc-scTRAIL. Amino acid sequences of linkers are represented, and residues generated by restriction sites and their respective enzymes are highlighted. L, Igκ chain leader sequence. *, mutation of K447 (EU numbering scheme) of the Fc part to Q.

2.3.7 Cloning of scDb-EHD2-scTRAIL

Single-chain diabodies (scDbs) combining the selected targeting moieties were generated based on existing scDbs by replacing unrequired domains with the desired ones. PSecTagAHis-scDbhu225x3M6 was constructed using pSecTagAHis-scDbhu225xCD3 by exchanging the anti-CD3 domains with XhoI-linker-V_L3M6-linker-SgsI and SgsI-linker-V_H3M6-linker-BamHI (pSecTagAL1-Db3M6 as template, primers #1214/1215 and #1216/1217, respectively, Table 2.2). PSecTagAHis-scDb4D5xhu225 was already available and furthermore used to generate pSecTagAHis-scDb4D5x3M6 by replacing the hu225 moieties with the 3M6 PCR fragments described above. Sfi/XhoI and BamHI/NotI digestions were used to exchange V_H and V_L MocB domains of pSecTagAHis-scDbMocBxhu225 with the domains derived from pAB1-scFv323/A3hu3 to construct pSecTagAHis-scDb323/A3hu3xhu225. Single-chain diabodies were transferred from pSecTagAHis to pSecTagFLAG-linker-EHD2-scTRAIL (Figure 2.3B) as KpnI/NotI fragments adding the KpnI restriction site by PCR (primers #944/91 for hu225x3M6, #945/91 for 4D5xhu225 and 4D5x3M6, #1213/91 for 323/A3hu3xhu225, Table 2.2).

2.4 Prokaryotic protein production

ScFvs were expressed in the periplasm of *E. coli* TG1. 20 ml 2xTY medium containing 1 % (w/v) glucose and 100 µg/ml ampicillin were inoculated with pAB1-scFv transformed bacteria and

incubated shaking at 37 °C. The next day, 10 ml of the overnight culture were added to 1 l 2xTY supplemented with 0.1 % (w/v) glucose and 100 µg/ml ampicillin and incubated shaking at 37 °C until the optical density measured at 600 nm reached 0.8 to 1.0 (exponential growth phase). After addition of IPTG to a final concentration of 1 mM to induce periplasmic protein expression, incubation was continued shaking at room temperature for 3 h. Cells were harvested by centrifugation (6,200 g, 10 min) and resuspended in 50 ml PPB. Lysozyme (50 µg/ml) was used to hydrolyze the bacterial cell wall. The cell suspension was incubated on ice for 30 min, followed by addition of $MgSO_4$ (10 mM) to stabilize the spheroblasts and another centrifugation step (9,820 g, 10 min). The protein-containing supernatant was dialyzed against 5 l 1xPBS at 4 °C overnight. After centrifugation (9,820 g, 10 min), proteins were purified from the dialyzed supernatant via IMAC (see 2.6.1).

2.5 Cell culture

2.5.1 General cultivation techniques

All cells were cultivated in a humidified atmosphere containing 5 % CO_2 at 37 °C. HEK293T cells were grown in RPMI 1640 medium (+ L-glutamine) with 5 % FBS, while all other cell lines were cultivated in RPMI 1640 medium (+L-glutamine) supplemented with 10 % FBS. Cell passaging was typically performed every two to three days depending on the confluence. Prior to detachment of the cells by addition of 1x Trypsin-EDTA (37 °C, up to 5 min depending on the cell line), cells were washed with DPBS. Detached cells were resuspended in medium and harvested by centrifugation (500 g, 5 min). In order to count the cells using a Neubauer chamber, the cell suspension was mixed 1:2 with eosin staining solution to discriminate viable and dead cells. Cells were stored in FBS containing 10 % (v/v) dimethyl sulfoxide at -80 °C after gentle cooling in an isopropanol-filled cryobox. Frozen cells were thawed at 37 °C, resuspended in medium, centrifuged (500 g, 5 min), and cultivated in appropriate medium.

2.5.2 Transfection and selection of stably transfected clones

Eukaryotic protein expression with transfected HEK293T cells was used for production of all recombinant antibodies and fusion proteins, except for scFvs. $1 \cdot 10^6$ cells per well were seeded into 6-well plates in 2 ml culture medium. The next day, medium was replaced by 1.7 ml Opti-MEM®. Transfection solutions A (6.7 µl Lipofectamine® 2000, 166 µl Opti-MEM®) and B (2.7 µg DNA, 166 µl Opti-MEM®) were prepared, mixed, incubated for 20 min at room temperature,

and added drop by drop to the cells. After cultivation for 6 h up to overnight, transfection medium was removed and cells were transferred to 25 cm^2 cell culture flasks containing culture medium. Before adding Zeocin™ (300 µg/ml) or Puromycin (10 µg/ml) to select for stably transfected clones, cells were cultivated for at least 6 h. Medium was regularly replaced until untransfected cells had died and transfected cells started to grow. Cells were stepwise expanded for protein production and storage of a fraction of the cells at -80 °C. Cell pools expressing EGFR-targeting scTRAIL fusion proteins, EHD2-scTRAIL, and Fc-scTRAIL were furthermore subjected to limiting dilution cloning. Suspensions of the cell pools were serially diluted to concentrations of 25 cells/ml and 50 cells/ml. Cell suspensions of each concentration were seeded into 96-well plates (200 µl/well, 1 plate/concentration). Cells were cultivated until clones started to grow. Supernatants of grown clones were analyzed for protein expression in ELISA (see 2.8) and clones were stepwise expanded. Up to 8 clones per protein were selected for further analysis. $1 \cdot 10^6$ cells of each clone were seeded per well into 6-well plates. After 24 h, culture medium was replaced by production medium and cells were cultivated for another 24 h. Supernatants were analyzed in ELISA for the amount of expressed protein. The two most promising clones of each construct were selected and expanded to one TripleFlask™ for protein production, purification and determination of the protein yield. Final protein production was performed with the clone showing best production properties.

2.5.3 Eukaryotic protein production

Stably transfected HEK293T cells were expanded to a number of 175 cm^2 cell culture flasks or TripleFlasks™ depending on the required protein amount (at least six 175 cm^2 cell culture flasks or two TripleFlasks™). During expansion, concentrations of 50 µg/ml Zeocin™ and 10 µg/ml Puromycin were used. After reaching approximately 80 % confluence, medium was removed, cells were washed with DPBS, and production medium was added (30 ml per 175 cm^2 cell culture flask, 100 ml per TripleFlask™). Opti-MEM® was used for production of recombinant antibodies. Expression of scTRAIL fusion proteins required Opti-MEM® supplemented with 50 µM $ZnCl_2$. Production medium was replaced every two to four days up to five times. Collected supernatant was cleared from cells by centrifugation (500 g, 5 min) and stored at 4 °C. Depending on their amount, detached cells were transferred back to the cell culture flasks. To reduce the volume of the collected supernatant, ammonium sulfate (390 g/l) was added stepwise to the filtered supernatant to precipitate the proteins, while

stirring at 4 °C. Precipitated proteins were pelleted by centrifugation (11,250 g, 1 h, 4 °C), resuspended in at least 10 ml DPBS (depending on the supernatant volume), and optionally dialyzed against 5 l PBS overnight at 4 °C. Proteins were then purified via IMAC, protein A or FLAG affinity chromatography (see 2.6.1, 2.6.2, and 2.6.3, respectively).

2.6 Purification of recombinant proteins

2.6.1 Immobilized metal ion affinity chromatography

His-tagged proteins were purified from dialyzed periplasmic preparations or resuspended precipitates of cell culture supernatants via immobilized metal ion affinity chromatography (IMAC). 0.5 ml of equilibrated Ni-NTA agarose was added to the protein solution and incubated rolling for at least 3 h at 4 °C. The suspension was then transferred to a chromatography column to separate protein-loaded Ni-NTA agarose from the flow-through. Unspecifically bound proteins were removed using IMAC wash buffer, and washing progress was monitored qualitatively by Bradford assay (10 µl sample, 90 µl 1x Bradford solution). Ni-NTA agarose-bound protein was eluted in 500 µl fractions with IMAC elution buffer. The protein concentration of the eluted fractions was analyzed by Bradford assay as described above. Protein-containing fractions were pooled and dialyzed against 5 l PBS overnight at 4 °C.

2.6.2 Protein A affinity chromatography

Antibody- and receptor-Fc fusion proteins were purified via protein A affinity chromatography. 0.25 ml protein A affinity resin were added to the resuspended precipitate of a cell culture supernatant and incubated rolling overnight at 4 C. The resin was collected in chromatography columns and washed with protein A wash buffer to remove unbound proteins. Qualitative Bradford assay was used to determine the protein amount in wash and elution fractions as described above (see 2.6.1). Elution was performed in 500 µl fractions using protein A elution buffer. Protein-rich fractions were pooled and dialyzed against 5 l PBS overnight at 4 °C.

2.6.3 FLAG affinity chromatography

All scTRAIL molecules were purified via FLAG affinity chromatography. Depending on the volume of collected cell culture supernatant, 1.5 ml to 4 ml anti-FLAG® M2 affinity resin were used. Prior to addition to the resuspended cell culture supernatant precipitate, the affinity gel

was equilibrated by three sequential washing steps with 100 mM glycin HCl, pH 3.5 and another five washing rounds with DPBS. To capture the target protein, protein solution and affinity resin were incubated rolling at 4 °C for at least 2 h up to overnight. The resin was collected by centrifugation (1,000 g, 5 min) and subsequent transfer to a chromatography column. Washing was performed using DPBS as wash buffer. Wash and elution steps were analyzed by qualitative Bradford assay as described above (see 2.6.1). Resin-bound protein was eluted with DPBS containing 100 µg/ml FLAG peptide. The elution progress was continuously monitored to collect the complete protein-containing eluate, which was dialyzed against 5 l PBS overnight at 4 °C. To recycle the affinity gel, equilibration was repeated, and resin was stored in 50 % (v/v) glycerol in PBS containing 0.02 % sodium azide at 4 °C.

2.6.4 Preparative size exclusion chromatography

Purified proteins were analyzed by size exclusion HPLC (see 2.7.3). Protein eluates containing considerable amounts of aggregates, fractions with wrong oligomerization status, or cleavage products were further purified by size exclusion FPLC. Concentrated protein was applied on a Superdex 200 10/300 GL column using PBS as mobile phase and a flow rate of 0.5 ml/min. Protein was collected in 100 µl to 250 µl fractions. Fractions containing the desired protein configuration were pooled. Preparative size exclusion chromatography was performed by Doris Göttsch (Institute of Cell Biology and Immunology, University of Stuttgart, Germany).

2.7 Biochemical characterization of recombinant proteins

2.7.1 Protein concentration

Protein concentration (c in mg/ml) was determined by measuring the absorption at 280 nm (A) with a NanoDrop™ ND-1000 spectrophotometer and using the molecular mass (M in mg/µmol) and extinction coefficient (ε in ml/(µmol·cm)) of the respective protein in the Beer-Lambert equation ($c = \frac{A \cdot M}{\varepsilon \cdot d}$ with d being the path length in cm). The molecular weight and the extinction coefficient were calculated with the ExPASy ProtParam tool. Optionally, protein solutions were concentrated using Vivaspin 500, 30,000 MWCO PES centrifugal filters.

2.7.2 SDS polyacrylamide gel electrophoresis

Protein purity and integrity was analyzed by SDS polyacrylamide gel electrophoresis (SDS-PAGE). Depending on the expected molecular weight of the protein, 8 %, 10 %, or 12 %

polyacrylamide (PAA)-containing gels were prepared (Table 2.3). Protein samples (2 µg protein) were mixed with Laemmli loading buffer (reducing or non-reducing, final concentration 1x) and incubated for 5 min at 95 °C, prior to loading on the gel together with PageRuler™ prestained protein ladder. Electrophoresis was performed with SDS-PAGE running buffer and a constant current of 40 mA/gel. After three rounds of boiling in demineralized water, gels were incubated in Coomassie staining solution for at least 1 h at room temperature. Excess staining was removed by incubation in demineralized water.

Table 2.3: Composition of SDS polyacrylamide gels. Described volumes are sufficient for two gels.

Component	Stacking gel	Separating gel		
	5 % PAA	8 % PAA	10 % PAA	12 % PAA
ddH_2O	4.1 ml	6.9	5.9 ml	4.9 ml
30 % acrylamide mix	1.0 ml	4 ml	5.0 ml	6.0 ml
1.5 M Tris-HCl pH 8.0	–	3.8 ml	3.8 ml	3.8 ml
1 M Tris-HCl pH 6.8	0.75 ml	–	–	–
10 % SDS	0.06 ml	0.15 ml	0.15 ml	0.15 ml
10 % APS	0.06 ml	0.15 ml	0.15 ml	0.15 ml
TEMED	0.006 ml	0.009 ml	0.006 ml	0.006 ml

2.7.3 Analytical size exclusion chromatography

Measuring the hydrodynamic radius by size exclusion HPLC, protein purity, integrity, and the oligomerization status were analyzed under native conditions. 20 µl protein sample (0.1 mg/ml to 0.5 mg/ml) were injected onto a Yarra™ 3 µm SEC-2000 or -3000 HPLC column using a Waters 2695 Separations Module and a Waters 2489 UV/Visible Detector. Size exclusion HPLC was performed with 0.1 M Na_2HPO_4/NaH_2PO_4, 0.1 M Na_2SO_4, pH 6.7 as mobile phase at a flow rate of 0.5 ml/min. Thyroglobulin (669 kDa, 8.5 nm), β-amylase (200 kDa, 5.4 nM), bovine serum albumin (67 kDa, 3.55 nm), carbonic anhydrase (29 kDa, 2.35 nm), and FLAG peptide (1 kDa) were used as reference molecules. Alternatively, a mixture of thyroglobulin (669 kDa, 8.5 nm), apoferritin (443 kDa, 6.1 nM), alcohol dehydrogenase (150 kDa), bovine serum albumin (67 kDa, 3.55 nm), carbonic anhydrase (29 kDa, 2.35 nm), and FLAG peptide (1 kDa) was applied.

2.7.4 Thermal stability

Thermal stability of the proteins was analyzed by dynamic light scattering using a Zetasizer Nano ZS. 100 µg protein in 1 ml PBS were sterile filtered into a glass cuvette before measuring the particle size in a temperature range of 35 °C to 90 °C in 1 °C intervals. Measurements were

performed twice at each temperature after equilibration of the sample for 2 min. The melting point was defined as the temperature showing a clear increase in the detected mean count rate.

2.8 Enzyme-linked immunosorbent assay

Enzyme-linked immunosorbent assay (ELISA) was used to analyze binding of recombinant antibodies and fusions proteins to their respective antigens and target receptors. Furthermore, protein concentrations in cell culture supernatants, in plasma and in serum samples were measured by ELISA to determine high-producer clones, plasma stability and pharmacokinetics, respectively. Soluble antigen or receptor-Fc fusion proteins (200 ng/well or 300 ng/well in 100 µl, as indicated) were coated overnight at 4 °C. After washing with PBS, remaining binding sites were blocked with 2 % MPBS (200 µl/well) for at least 1 h at room temperature. After another washing step with PBS, samples diluted in 2 % MPBS were added in duplicates (100 µl/well) and incubated for at least 1 h at room temperature. Depending on the analyzed protein, anti-His-HRP, anti-scDbCEAxCD3-PEG and anti-rabbit-POD, protein L-HRP, or anti-FLAG-HRP were used for detection (for dilutions, see Table 2.1). Two washing steps with PBST (0.005 % TWEEN 20) and one with PBS were performed before adding detection antibody diluted in 2 % MPBS (100 µl/well, incubation for at least 1 h at room temperature). The before-mentioned washing procedure with PBST (0.005 % TWEEN 20) and PBS was repeated and 100 µl/well substrate solution (100 mM sodium acetate pH 6.0, 0.1 mg/ml TMB, 0.006 % (v/v) H_2O_2) were added. Using anti-scDbCEAxCD3-PEG and anti-rabbit-POD as detection system, another washing and incubation step were performed prior to detection. Reaction was stopped with 50 µl/well 1 M H_2SO_4. Optical density at 450 nm was measured using an Infinite M200 microplate reader.

2.9 Flow cytometry

2.9.1 Determination of expression levels

Relative expression levels were determined by flow cytometry. 250,000 cells/well were seeded in 96-well U-bottom plates and incubated with 100 µl detection antibody diluted in PBA for 1 h at 4 °C. Detection of TAAs and TRAIL receptors was done either with directly labeled antibodies or using unlabeled primary antibodies, followed by a washing step and incubation with a labeled secondary antibody (for dilutions, see Table 2.1). Respective controls

were included, and all samples were investigated in duplicates. Washing was performed by centrifugation (500 g, 5 min) and resuspension of the cell pellet in 150 µl PBA two times. Finally, washed and pelleted cells were analyzed in 150 µl PBA using MACSQuant® Analyzer 10 (approximately 15,000 cells/gate).

2.9.2 Binding studies

Binding of recombinant antibodies and fusion proteins to antigen- and TRAIL receptor-expressing cells was evaluated by flow cytometry. 250,000 cells/well were seeded in 96-well U-bottom plates. Dilutions of the proteins in PBA were titrated on the cells in duplicates and incubated for 1 h at 4 °C. Prior to addition of detection antibody diluted in PBA (100 µl/well), washing was performed as described above (see 2.9.1). Depending on the analyzed protein, anti-His-PE, anti-human IgG γ-chain specific-PE, or anti-FLAG-PE were used for detection of bound proteins and respective controls (for dilutions, see Table 2.1). After another washing step, cells were analyzed in 150 µl PBA using MACSQuant® Analyzer 10 or MACSQuant® VYB (approximately 15,000 cells/gate). ScTRAIL molecules were furthermore investigated, while binding of the antibody part was blocked. Before adding 25 µl of the scTRAIL molecule (20 nM scTRAIL units final concentration, 1 h, 4 °C), cells were preincubated with 75 µl of blocking antibody (200-fold molar excess final concentration) or PBA for comparison with unblocked binding (30 min, 4 °C). Bound scTRAIL molecules were detected via their FLAG-tag. Relative median fluorescence intensities ($relative\ MFI$) were calculated based on the MFI of cells incubated with analyzed protein and detection system (MFI_{sample}), the MFI of cells treated only with detection system ($MFI_{detection\ system}$), and the MFI of cells alone (MFI_{cells}):

$$relative\ MFI = \frac{MFI_{sample} - (MFI_{detection\ system} - MFI_{cells})}{MFI_{cells}}$$

2.10 Cell death induction analysis

Effects of recombinant antibodies and scTRAIL molecules on Colo205 and HCT116 cells were analyzed by crystal violet staining. 50,000 Colo205 cells/well or 15,000 HCT116 cells/well were seeded in 100 µl medium (RPMI 1640, 10 % FBS, P/S) in 96-well F-bottom plates and incubated for 24 h at 37 °C, 5 % CO_2. After preincubation of the cells with 50 µl/well of medium or bortezomib (250 ng/ml final concentration corresponding to 650 nM) for 30 min at 37 °C, 5 % CO_2, serial dilutions of the proteins in medium (50 µl/well) were added in duplicates or

triplicates. Control wells were treated with 50 µl Triton X-100 (0.25 % final concentration). Cells were incubated for 16 h at 37 °C, 5 % CO_2, prior to detection of viable cells with crystal violet staining solution (50 µl/well, 20 min, room temperature). Excess staining was removed by washing with demineralized water. Dried staining was dissolved in 50 µl/well methanol by shaking for 30 min at room temperature. Viable cells were quantified by measuring the optical density at 550 nm and normalization to medium- or bortezomib-treated controls. Recombinant antibodies were only investigated on Colo205 cells in the absence of bortezomib. In order to examine the targeting effects of the antibody moiety, the scTRAIL molecules were furthermore analyzed in the presence of a blocking antibody. Cells were preincubated with a 200-fold molar excess of blocking antibody (final concentration) in medium or medium additionally containing bortezomib (250 ng/ml final conectration, 50 µl/well, 30 min, 37 °C, 5 % CO_2). Subsequent treatment with scTRAIL constructs and determination of viable cells was done as described above. Experiments performed with varying incubation times and bortezomib concentrations are indicated.

2.11 Caspase activity assay

15,000 Colo205 cells/well were seeded in 100 µl medium (RPMI 1640, 10 % FBS, P/S) in white-walled 96-well F-bottom plates and cultivated for 24 h at 37 °C, 5 % CO_2. Medium was removed and cells were preincubated with 60 µl medium or bortezomib (250 ng/ml final concentration) for 30 min at 37 °C, 5 % CO_2, prior to addition of scTRAIL molecules (20 µl) in duplicates. After varying incubation times, caspase-8 and -3/7 activities were determined using Caspase-Glo® 8 Assay and Caspase-Glo® 3/7 Assay according to the manufacturer's instructions. The measured luminescence signal is proportional to the amount of caspase activity. Luminescence signals detected 60 min and 30 min after addition of the reagent were used for data evaluation of caspase-8 and -3/7 activity, respectively.

2.12 Protein stability

2.12.1 *In vitro* plasma stability

Stability in human plasma was analyzed for EGFR-targeting and non-targeted scTRAIL molecules. Proteins were diluted to a final concentration of 100 nM scTRAIL units in 50 % human plasma and either directly stored at -20 °C (0 d value) or incubated at 37 °C for 1 d, 3 d, and 7 d prior to storage at -20 °C. Levels of intact protein were determined by binding of the

C-terminal scTRAIL moiety to TRAIL-R2 and detection via the N-terminal FLAG-tag in ELISA. 200 ng TRAIL-R2-Fc were coated per well and ELISA was performed as already described (see 2.8). Different dilutions of the construct-containing plasma samples were analyzed simultaneously to a serial dilution of the purified protein. Protein concentrations in the plasma samples were determined by interpolation from the standard curve and under consideration of the dilution factor. For final evaluation, concentrations were normalized to the 0 d value.

2.12.2 *In vivo* pharmacokinetics

Animal care and all pharmacokinetic experiments were in accordance with federal and European guidelines and have been approved by university and state authorities. *In vivo* pharmacokinetics were analyzed for EGFR-targeting and non-targeted scTRAIL molecules, as well as scFvhu225-Fc and cetuximab. 25 µg or 50 µg protein (in 150 µl PBS) were injected into the tail vein of female CD-1® mice (8 to16 weeks old, 25 g to 35 g, 3 or 6 mice per molecule). Blood samples (50 µl) were taken from the tail (3 min, 30 min, 1 h, 2 h, 6 h, 1 d, 3 d, and 7 d after injection or alternatively after 3 min, 30 min, 2 h, 6 h, 12 h, 1 d, 3 d, 7 d) and incubated on ice for 30 min, prior to centrifugation (13,000 g, 30 min, 4 °C). Serum samples were stored at -20 °C. Serum concentrations of scTRAIL constructs were determined using BD OptEIA™ human TRAIL ELISA Set as recommended by the manufacturer. Serum samples of scFvhu225-Fc and cetuximab were analyzed by binding to EGFR-Fc (300 ng/well) in ELISA as already described (see 2.8). ScFvhu225-Fc was detected with anti-scDbCEAxCD3-PEG serum and anti-rabbit IgG-POD, while detection of cetuximab was performed using HRP-conjugated protein L (for dilutions, see Table 2.1). Serum concentrations of all proteins were interpolated from a standard curve of the purified protein and normalized to the 3 min value. Initial and terminal half-lives ($t_{1/2}\alpha$, $t_{1/2}\beta$) and AUC were calculated with Microsoft Excel. Initial half-lives were calculated over the time interval of 3 min to 2 h. Terminal half-lives were calculated starting with the serum concentration at 6 h.

2.13 Pharmacodynamics and toxicity

Animal care and all pharmacodynamic experiments were in accordance with federal and European guidelines and have been approved by university and state authorities.

2.13.1 Colo205 xenograft model

A Colo205 xenograft model was used in all experimental settings to analyze the *in vivo* therapeutic activity of the scTRAIL fusion proteins. $3 \cdot 10^6$ Colo205 cells (in 100 µl DPBS) were injected subcutaneously into the left and right flank of female NMRI nude mice. Tumor growth was monitored by measuring the length (a) and width (b) of the tumors with a caliper to calculate the tumor volume ($V = a \cdot b^2/2$). Upon reaching a size of approximately 100 cm^3, treatment was started. Bortezomib (in 150 µl DPBS) was injected intraperitoneally, whereas injections of fusion proteins (in 150 µl DPBS) were done intravenously. Control animals received respective injections of 150 µl DPBS.

A first experiment was performed to analyze the anti-tumor activity of bortezomib. Mice (8 weeks old, 4 mice for PBS, 5 mice for bortezomib) received six injections of either DPBS or 5 µg bortezomib every other day starting at day 12 (days 12, 14, 16, 18, 20, 22). In a second experiment, different formats of EGFR-targeting scTRAIL fusion proteins and Fc-scTRAIL were compared under simultaneous application of bortezomib. Mice (10 weeks old, 6 mice per group) received six treatments with 5 µg bortezomib and 0.5 nmol protein (1 nmol scTRAIL units). After three treatments every other day (starting at day 13), treatment intervals were gradually increased by one day (days 13, 15, 17, 20, 24, 29). Blood samples were taken 3 min, 4 h, 24 h, and 48 h after the first and last treatment, and serum levels of the proteins were determined as already described (see 2.12.2). Blood samples taken 4 h and 24 h after the first and the last treatment were furthermore analyzed for alanine transaminase (ALT) and amylase activity (see 2.13.2 and 2.13.3, respectively). A third experiment was performed to further compare scFvhu225-Fc-scTRAIL and Fc-scTRAIL, both in co-treatment with bortezomib. Treatment of the mice (10 weeks old, 6 mice per group) with 5 µg bortezomib and 0.3 nmol or 0.1 nmol protein (0.6 nmol or 0.2 nmol scTRAIL units) started at day 14 and was repeated twice a week (corresponding to every fourth and third day, respectively) for three weeks (days 14, 18, 21, 25, 28, 32). Blood samples were collected 3 min, 4 h, and 24 h after the first treatment to determine the serum concentrations of the proteins (see 2.12.2). In a final experiment, several formats of EGFR-targeting scTRAIL fusion proteins, scFv-Fc-scTRAIL molecules with different targeting moieties, and Fc-scTRAIL were compared without simultaneous application of bortezomib. Mice (9 or 11 weeks old, 6 mice per group) were treated with 0.2 nmol protein (0.4 nmol scTRAIL units) twice a week for three weeks (days 14,

18, 21, 25, 28, 32). Blood samples were taken 4 h and 24 h after the last treatment to analyze protein and ALT levels (see 2.12.2 and 2.13.2, respectively).

2.13.2 Alanine transaminase activity assay

Serum levels of alanine transaminase (ALT) were analyzed to detect potential liver toxicity. Blood samples taken during the pharmacodynamic experiments (see 2.13.1) were incubated on ice for 30 min prior to centrifugation (13,000 g, 30 min, 4 °C) and storage of the serum at 4 °C. ALT levels were determined using Alanine Transaminase Activity Assay kit according to the manufacturer's instructions. 5 µl or 10 µl of serum were applied.

2.13.3 Amylase activity assay

Potential induction of pancreatic and renal toxicity was evaluated by determination of amylase levels in the serum. Blood samples were collected and treated as already described (see 2.13.2). Amylase activity in the serum was detected using Amylase Assay kit as recommended by the manufacturer. 5 µl of serum were analyzed.

2.14 Statistics

Data are represented as mean ± standard deviation of at least three independent experiments, except for tumor volumes that are shown as mean ± 95 % confidence interval. Pairwise and multiple comparisons were performed by GraphPad Prism® implemented unpaired t test (two-tailed) and One-Way ANOVA, followed by Tukey's post hoc test, respectively. A P value of <0.05 was considered statistically significant (*P<0.05; **P<0.01; ***P<0.001; ns, P>0.05).

Block shift was only applied when compensation of variabilities, e.g. in optical densities due to differences in ELISA developing times, was necessary and is clearly indicated. The corrected value of the experiment n (X'_n) was calculated from the measured value of experiment n (X_n), the duplicate average of experiment n (Y_n), and the average of all measured values of all experiments ($\bar{Y}$) using the equation $X'_n = X_n - (Y_n - \bar{Y})$.

3 Results

3.1 Generation and characterization of dimeric recombinant antibody formats

As outlined before, previous studies have shown that antibody-targeted scTRAIL fusion proteins (Schneider *et al.*, 2010) and especially dimeric formats (Siegemund *et al.*, 2012; Seifert *et al.*, 2014a) possess a considerably higher activity than untargeted monomeric scTRAIL versions. Thus, the first part of this study was subjected to the generation and characterization of different recombinant antibody formats suitable as fusion partner for scTRAIL. Based on the monomeric scFv, two concepts for the formation of dimeric antibodies were used. On the one hand, an scFv can be forced into a non-covalent assembly of two chains by reducing the linker length from 15 to 5 amino acid residues ($(GGGGS)_3$ to GGGGS) generating a diabody (Db; Holliger *et al.*, 1993). On the other hand, dimeric assembly can be achieved by fusion of an scFv to a dimerization module (Figure 3.1). Further stabilization of the non-covalently associated chains in the diabody can be achieved by mutation of the amino acid residues at position 44 in the V_H and position 100 in the V_L (Kabat numbering scheme) to cysteines (reviewed by Reiter *et al.*, 1996). Located at these positions, the cysteine residues have an appropriate distance and orientation enabling the formation of interchain disulfide bonds to covalently connect the two chains creating a disulfide-stabilized diabody (dsDb). As dimerization modules, the domain 2 of the heavy chain of IgE (EHD2) and a human IgG1 Fc part were used. Fusion of an scFv to the N-terminus of these modules generated scFv-EHD2 and scFv-Fc fusion proteins. Characterization of the different antibody formats, i.e. scFv, Db, dsDb, scFv-EHD2, and scFv-Fc, was performed for several targeting moieties including variants directed against EGFR, HER2, HER3, and EpCAM. The scFv molecules were analyzed as monomeric reference and produced in the periplasm of *E. coli* TG1, while all other formats were produced with stably transfected HEK293T cells and secreted into the supernatant. All proteins were expressed comprising a C-terminal His-tag for purification via immobilized metal ion affinity chromatography (IMAC), except for the scFv-Fc molecules that were expressed tagless and purified by protein A affinity chromatography.

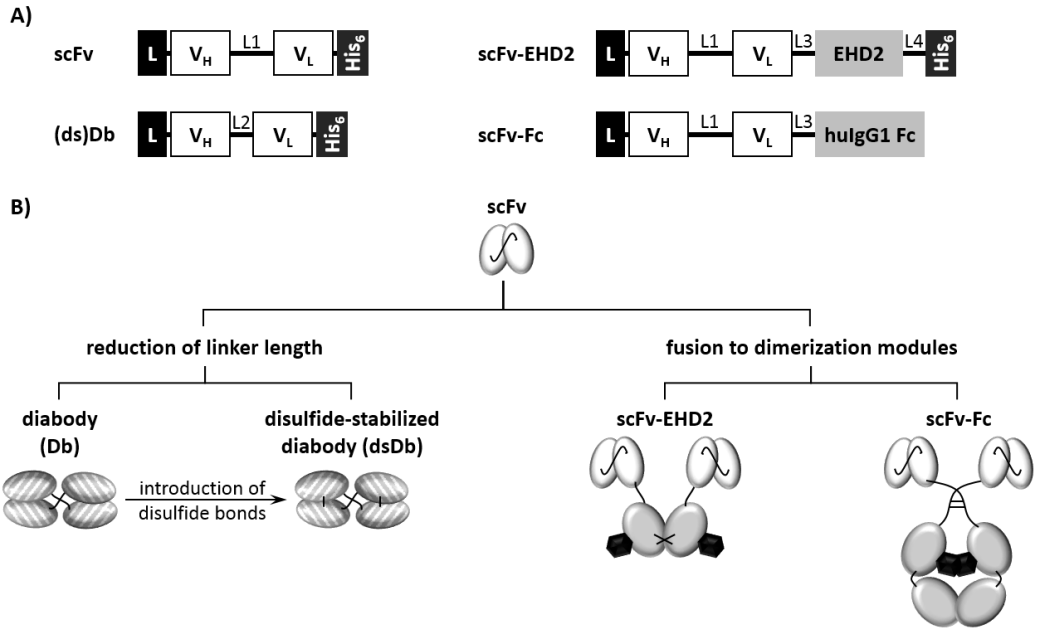

Figure 3.1: Overview of different recombinant antibody formats. A) Composition and B) schematic assembly of scFv, Db, dsDb, scFv-EHD2, and scFv-Fc. The concepts for the generation of dimeric antibody formats based on the monomeric scFv are illustrated. L, pelB leader sequence (scFv) or Igκ chain leader sequence (Db, dsDb, scFv-EHD2, scFv-Fc). L1, $(GGGGS)_3$ linker. L2, GGGGS linker. L3, AAAGGSGG linker. L4, GGSGGASS linker.

3.1.1 EGFR-targeting recombinant antibodies

The targeting moiety hu225 used to generate antibodies directed against EGFR was derived from cetuximab (antibody C225, Goldstein *et al.*, 1995) and humanized by CDR grafting (Seifert *et al.*, 2012). The different formats of EGFR-targeting antibodies were produced with yields of 1.4 (scFvhu225, dsDbhu225) up to 6.5 mg protein (scFvhu225-Fc) per liter bacterial culture or cell culture supernatant, respectively (Table 3.1). Purity and integrity of the molecules was verified by SDS-PAGE. Under reducing conditions, all proteins migrated according to their monomeric molecular masses as single bands, except for scFvhu225-EHD2 that showed two bands of similar size (Figure 3.2A). As demonstrated by previous studies, these differences arise from variations in the glycosylation status (Seifert, 2014). Under non-reducing conditions, the expected disulfide-linked dimers were observed for the dsDb, scFv-EHD2, and scFv-Fc formats (Figure 3.2B). Additionally, some high molecular weight species were found for dsDbhu225, and a small amount of the monomeric form was seen for scFvhu225-EHD2 that was even lower for scFvhu225-Fc. The thermal stability of the different formats was analyzed by dynamic light scattering revealing a melting point of 64 °C for scFvhu225 (Figure 3.2C, Table 3.1), whereas the diabody exhibited decreased stability (57 °C) that was improved by disulfide-stabilization (61 °C). A melting point of 64 °C was detected for scFvhu225-EHD2, while fusion to the Fc part further stabilized the protein (66 °C).

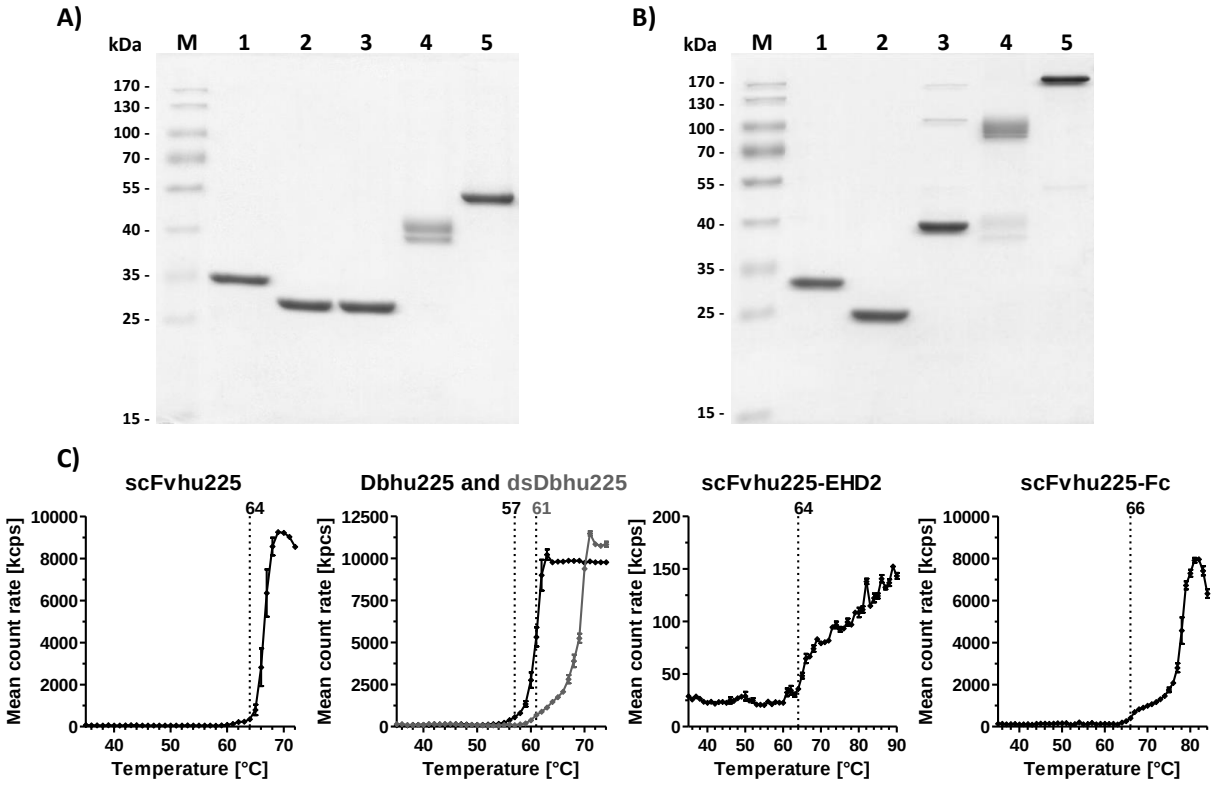

Figure 3.2: Biochemical characterization of EGFR-targeting recombinant antibodies. SDS-PAGE analysis (12 % PAA) of scFvhu225 (1), Dbhu225 (2), dsDbhu225 (3), scFvhu225-EHD2 (4), and scFvhu225-Fc (5) was performed under reducing (A) and non-reducing conditions (B). 2 µg of each protein were analyzed per lane and stained with Coomassie Brilliant Blue. M, protein marker. C) Thermal stability was determined by dynamic light scattering. Melting points [°C] are indicated with dotted lines. Measurements were performed once for each protein. Melting curves of Dbhu225 (black) and dsDbhu225 (gray) are shown in one graph.

Evaluation of the binding properties of the different formats was done by ELISA (Figure 3.3A). All molecules showed concentration-dependent binding to EGFR with EC_{50} values in the subnanomolar range (Table 3.1). EC_{50} values refer to the concentration of functional binding sites. Further investigations of binding were performed with EGFR-expressing A-431 cells via flow cytometry (Figure 3.3B). Comparable binding curves were determined for all formats revealing half-maximal binding at concentrations of 0.9 nM to 1.9 nM (Table 3.1). Since Colo205 cells were used for *in vitro* and *in vivo* characterization of the corresponding antibody-scTRAIL fusion proteins, effects of the recombinant antibodies on this cell line were examined. In a concentration range of 1 pM to 10 nM, no influence on cell viability was seen (Figure 3.3C). In summary, these data confirm the suitability of all formats for targeting of EGFR.

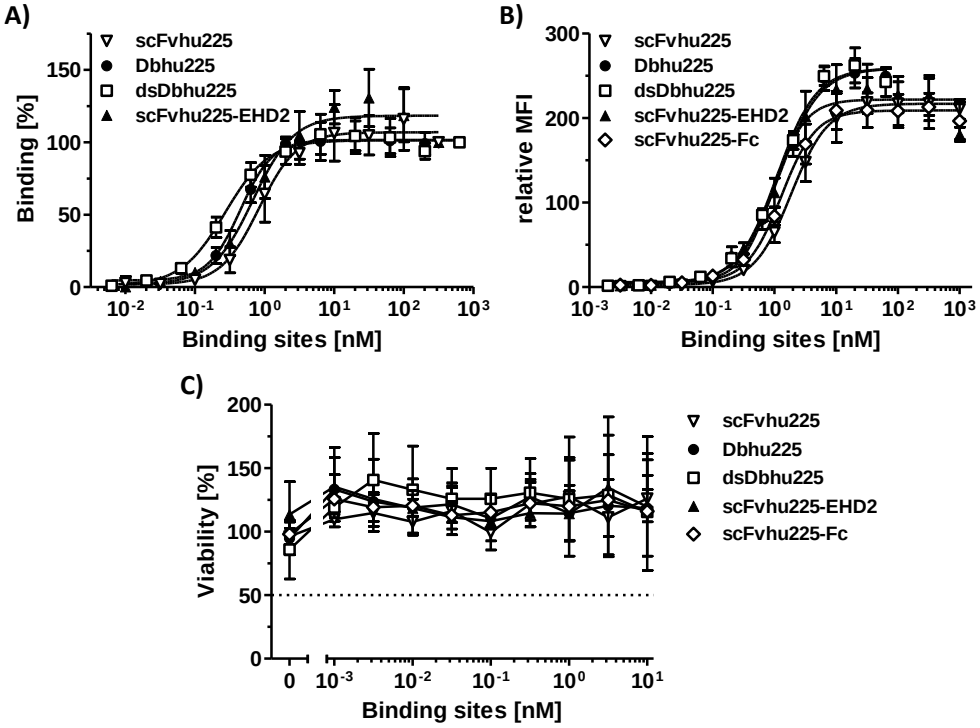

Figure 3.3: Binding analysis of EGFR-targeting recombinant antibodies and effects on Colo205 cells. A) Binding to EGFR-Fc (200 ng/well) was investigated by ELISA. Bound molecules were detected via anti-His-HRP. Optical densities (at 450 nm) were normalized to the value determined for the highest concentration. B) Binding to EGFR-expressing A-431 cells was analyzed by flow cytometry, detecting cell-bound proteins with an anti-His-PE or anti-human IgG (γ-chain specific)-PE. C) Colo205 cells (50,000/well) were treated with serial dilutions of the proteins for 16 h. Viable cells were stained with crystal violet. Concentrations refer to functional binding sites.

Table 3.1: Biochemical and binding properties of EGFR-targeting recombinant antibodies. The molecular masses (M) were calculated based on the amino acid sequences. Yields are expressed as mg protein per l bacterial culture or cell culture supernatant. Binding to EGFR-Fc and A-431 cells was determined by ELISA and flow cytometry, respectively. EC_{50} values refer to concentrations of functional binding sites.

Protein	M [kDa]	Yield [mg/l]	T_M [°C]	EC_{50} EGFR [nM]	EC_{50} A-431 [nM]
scFvhu225	28	1.4	64	0.8 ± 0.2	1.9 ± 0.2
Dbhu225	52	1.7	57	0.5 ± 0.1	1.1 ± 0.1
dsDbhu225	53	1.4	61	0.3 ± 0.05	1.0 ± 0.04
scFvhu225-EHD2	79	2.3	64	0.7 ± 0.1	0.9 ± 0.1
scFvhu225-Fc	104	6.5	66	n.d.	1.3 ± 0.1

n.d., not determined.

3.1.2 HER2-targeting recombinant antibodies

Recombinant antibodies directed against HER2 were generated using the trastuzumab-derived targeting moiety 4D5 (Carter *et al.*, 1992). The different HER2-targeting antibody formats were produced with yields ranging from 0.7 (scFv4D5) to 9.3 mg protein (scFv4D5-EHD2) per liter bacterial culture or cell culture supernatant (Table 3.2). Purity and integrity analysis was performed by SDS-PAGE. Under reducing (Figure 3.4A) as well as under non-reducing conditions (Figure 3.4B), the sizes of the detected protein bands were in good agreement with the molecular masses calculated based on the amino acid sequences. Under

non-reducing conditions, formation of disulfide-linked dimers was confirmed for dsDb4D5, scFv4D5-EHD2, and scFv4D5-Fc. High molecular weight species were additionally identified for dsDb4D5 in the absence of a reducing agent, while scFv4D5-EHD2 was found in the monomeric beside the major dimeric form. As outlined before, the appearance of scFv4D5-EHD2 as double band is caused by differential glycosylation of the EHD2 (Seifert, 2014). Good thermal stability with a melting point of 69 °C was determined for scFv4D5 (Figure 3.4C, Table 3.2). As already observed for the EGFR-targeting antibodies, converting the scFv into the diabody format led to a decrease in thermal stability (64 °C) that was again improved for the disulfide-stabilized diabody (67 °C). Melting points of 67 °C and 69 °C were measured for scFv4D5-EHD2 and scFv4D5-Fc, respectively.

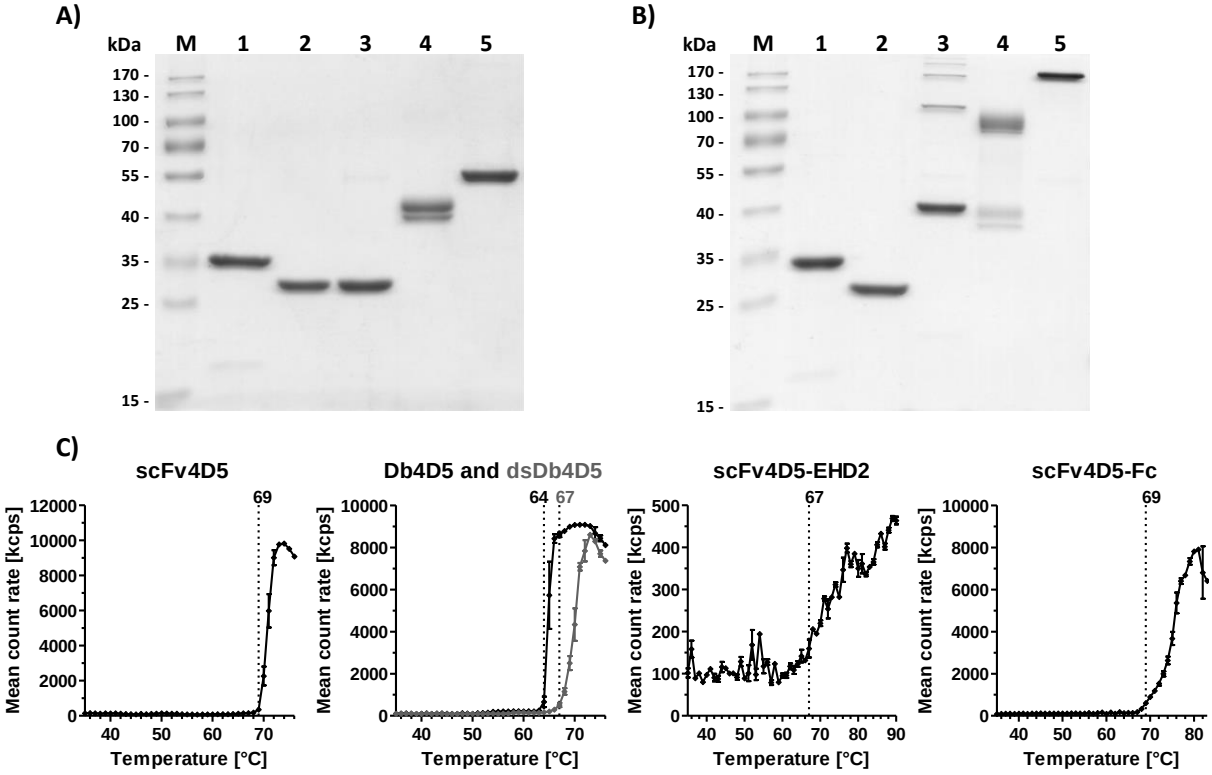

Figure 3.4: Biochemical characterization of recombinant antibodies directed against HER2. ScFv4D5 (1), Db4D5 (2), dsDb4D5 (3), scFv4D5-EHD2 (4), and scFv4D5-Fc (5) were analyzed by SDS-PAGE (12 % PAA) under reducing (A) and non-reducing conditions (B). 2 µg protein were loaded per lane and stained with Coomassie Brilliant Blue. M, protein marker. C) Dynamic light scattering was performed to determine the thermal stability. Melting points [°C] are indicated with dotted lines. Melting curves of Db4D5 (black) and dsDb4D5 (gray) are represented in one graph. Thermal stability was analyzed once for each protein.

The binding properties of the HER2-targeting recombinant antibodies were evaluated by ELISA (Figure 3.5A) and flow cytometry (Figure 3.5B) using a HER2-Fc fusion protein and HER2-expressing SKBR3 cells, respectively. The EC_{50} values determined in ELISA were in the range of 2.7 nM to 3.6 nM (concentrations referring to functional binding sites), except for the diabody that showed weaker binding (Table 3.2). Flow cytometric studies revealed half-maximal

binding at concentrations of 4.8 nM to 8.7 nM for scFv4D5, scFv4D5-EHD2, and scFv4D5-Fc. Higher EC_{50} values of 16.4 nM and 19.5 nM were detected for the diabody formats. Treatment of Colo205 cells with the recombinant antibodies was performed to assess potential effects that might be exerted by the antibody parts of the respective scTRAIL fusion proteins (Figure 3.5C). Incubation of the cells with the different formats of HER2-targeting antibodies did not identify an influence on cell viability in the analyzed concentration range. Similar to the results obtained for the EGFR-targeting recombinant antibodies, no clear differences were found for the investigated formats, apart from weaker binding of the diabody constructs.

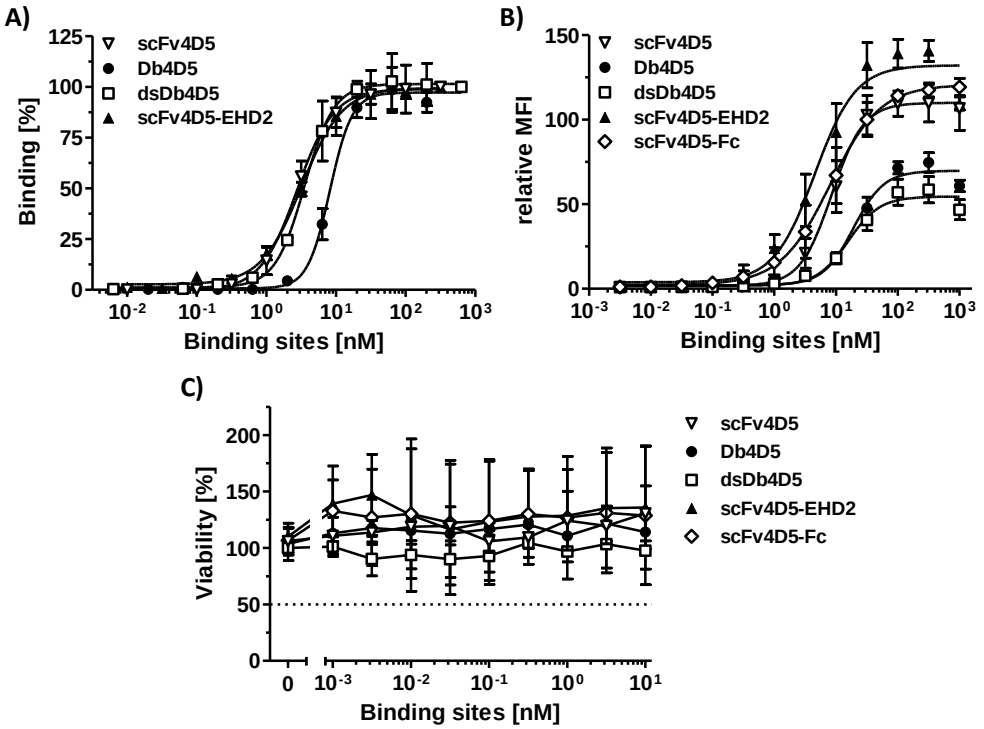

Figure 3.5: Binding analysis of HER2-targeting recombinant antibodies and effects on Colo205 cells. A) Binding to HER2-Fc (200 ng/well) was investigated in ELISA by detection of bound proteins using an HRP-conjugated anti-His-tag antibody. Optical density measured at 450 nm was normalized to the value determined for the highest concentration analyzed. B) Binding to HER2-expressing SKBR3 cells was evaluated by flow cytometry detecting bound molecules with a PE-conjugated anti-His-tag antibody or anti-human IgG (γ-chain specific)-PE. C) Effects on Colo205 cells (50,000 cells/well) were determined after treatment with serial dilutions of the proteins for 16 h. Viable cells were visualized with crystal violet. Concentrations refer to functional binding sites.

Table 3.2: Biochemical and binding properties of HER2-targeting recombinant antibodies. Molecular masses (M) were calculated based on the amino acid sequence. Yields are expressed as mg protein per liter bacterial culture or cell culture supernatant. EC_{50} values [nM of functional binding sites] for binding to HER2-Fc and SKBR3 cells were determined by ELISA and flow cytometry, respectively.

Protein	M [kDa]	Yield [mg/l]	T_M [°C]	EC_{50} HER2 [nM]	EC_{50} SKBR3 [nM]
scFv4D5	28	0.7	69	2.7 ± 0.6	8.7 ± 1.7
Db4D5	53	7.2	64	8.2 ± 0.8	19.5 ± 2.7
dsDb4D5	53	6.6	67	3.6 ± 0.4	16.4 ± 4.3
scFv4D5-EHD2	79	9.3	67	3.3 ± 0.3	4.8 ± 1.3
scFv4D5-Fc	104	5.4	69	n.d.	8.5 ± 3.2

n.d., not determined.

3.1.3 HER3-targeting recombinant antibodies

Recombinant antibodies directed against HER3 were based on the targeting moiety 3M6. 3M6 was developed as a modified version of MM-6 (MM-121, Ab #6, Schoeberl *et al.*, 2009). Since the MM-6 binding moiety contained a cysteine residue at position 89 (Kabat numbering scheme) in the CDR-L3 loop that might lead to uncontrolled formation of disulfide-linked dimers, 3M6 was generated by mutating this cysteine to serine (**3M6**, **m**utated **MM**-**6**).

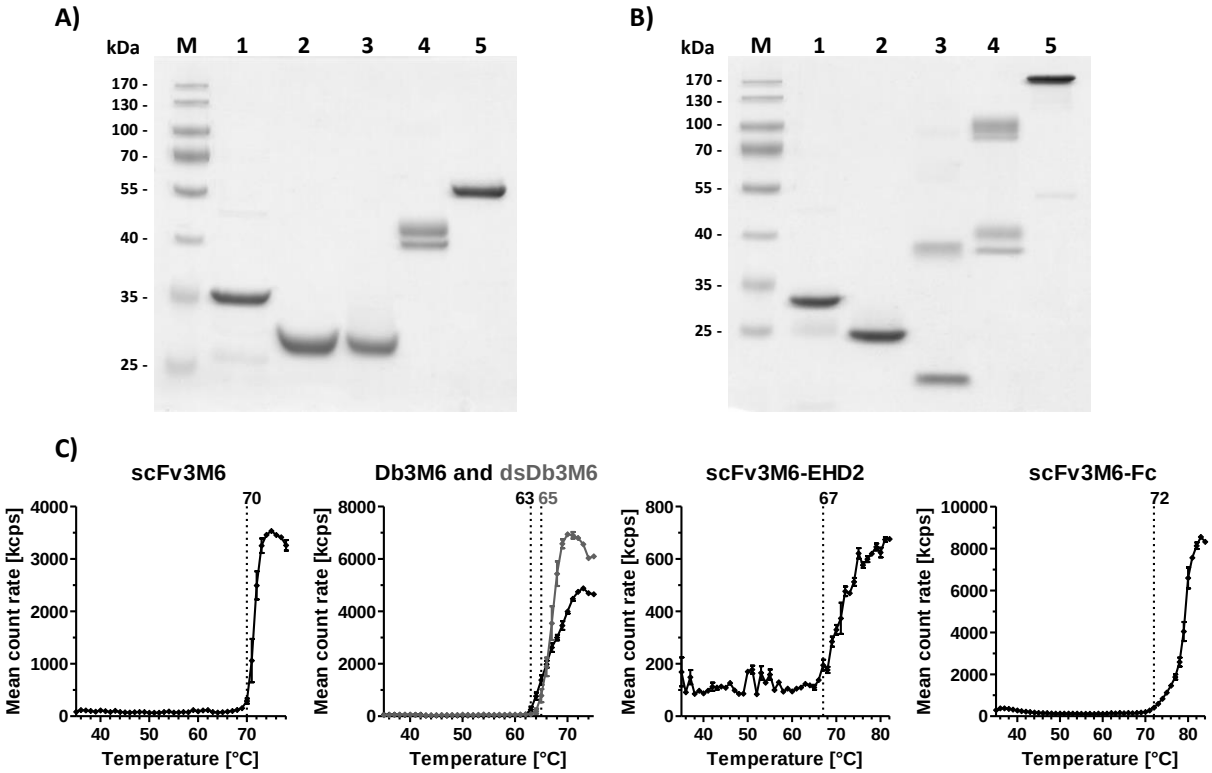

Figure 3.6: Biochemical characterization of 3M6-based recombinant antibodies. SDS-PAGE (12 % PAA) of scFv3M6 (1), Db3M6 (2), dsDb3M6 (3), scFv3M6-EHD2 (4), and scFv3M6-Fc (5) was performed under reducing (A) and non-reducing conditions (B). 2 µg protein were analyzed per lane and stained with Coomassie Brilliant Blue. M, protein marker. C) Thermal stability was determined by dynamic light scattering. Melting points [°C] are indicated with dotted lines. Measurement was performed once for each protein. Melting curves of Db3M6 (black) and dsDb3M6 (gray) are shown in one graph.

The 3M6-based antibody formats were produced with yields of 0.4 (scFv3M6) to 6.9 mg protein (Db3M6) per liter bacterial culture or cell culture supernatant (Table 3.3). SDS-PAGE analysis of the constructs confirmed their purity, while integrity was not observed for all proteins (Figure 3.6A,B). About half of the dsDb3M6 molecule migrated as a band of smaller size that was only visible under non-reducing conditions. Disulfide-linked dimers were detected for dsDb3M6, scFv3M6-EHD2, and scFv3M6-Fc under non-reducing conditions, but approximately half of scFv3M6-EHD2 remained in its monomeric form. As already seen for the EGFR- and HER2-targeting proteins, scFv3M6-EHD2 appeared as two bands of similar size due

to differences in glycosylation (Seifert, 2014). Thermal stability of the different formats was analyzed by dynamic light scattering (Figure 3.6C). ScFv3M6 showed a melting point of 70 °C that was reduced to 63°C for the diabody format and again somewhat improved to 65 °C for the disulfide-stabilized form (Table 3.3). This resembles the data of the corresponding anti-EGFR and anti-HER2 formats. Melting points of 67 °C and 72 °C were measured for scFv3M6-EHD2 and -Fc, respectively.

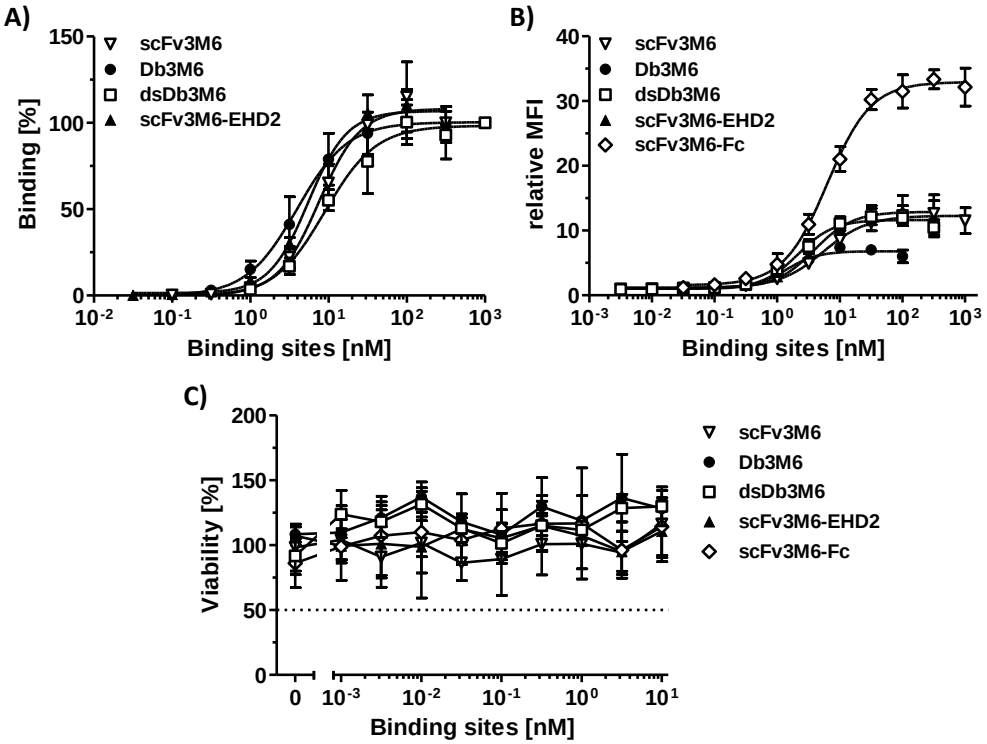

Figure 3.7: Binding analysis of 3M6-based recombinant antibodies and effects on Colo205 cells. A) Binding to HER3-Fc (200 ng/well) was investigated by ELISA. Bound molecules were detected with an anti-His-HRP. Optical density measured at 450 nm was normalized to the value determined for the highest concentration. B) Binding to HER3-expressing MCF7 cells was analyzed by flow cytometry. Detection of bound proteins was performed using a PE-conjugated anti-His-tag antibody or anti-human IgG (γ-chain specific)-PE. Binding curve of scFv3M6-Fc is represented from two independent experiments. C) Colo205 cells (50,000/well) were incubated overnight and treated with serial dilutions of the proteins for 16 h. Cell viability was determined by crystal violet staining. Concentrations refer to functional binding units.

Further characterization of the different 3M6-based formats was done by ELISA and flow cytometry (Figure 3.7A,B). All molecules showed concentration-dependent binding to HER3 with EC_{50} values of 5.5 nM to 9.5 nM (Table 3.3). Binding to cell surface-expressed HER3 was confirmed using MCF7 cells. Half-maximal binding was detected at concentrations ranging from 1.1 nM (dsDb3M6) to 7.4 nM (scFv3M6-Fc). Effects of the different recombinant antibody formats on Colo205 cells were analyzed to evaluate the contribution of the antibody part of the corresponding antibody-scTRAIL fusion proteins (Figure 3.7C). In a concentration range of 1 pM to 10 nM, none of the 3M6-based molecules had an impact on the cell viability.

Table 3.3: Biochemical and binding properties of recombinant antibodies directed against HER3. Molecular masses (M) were calculated based on the amino acid sequence. Yields are expressed as mg protein per liter bacterial culture or cell culture supernatant. Binding to HER3-Fc and $HER3^+$ cells (MCF7 for 3M6, Colo205 for 3-43) was analyzed by ELISA and flow cytometry, respectively. EC_{50} values refer to functional binding sites.

Protein	M [kDa]	Yield [mg/l]	T_M [°C]	EC_{50} HER3 [nM]	EC_{50} cells [nM]
scFv3M6	28	0.4	70	8.0 ± 1.1	5.4 ± 1.2
Db3M6	52	6.9	63	4.3 ± 1.2	1.1 ± 0.1
dsDb3M6	52	1.9	65	9.5 ± 1.4	1.9 ± 0.4
scFv3M6-EHD2	78	4.1	67	5.5 ± 0.3	3.6 ± 1.0
scFv3M6-Fc	103	6.6	72	n.d.	7.4 ± 1.6
scFv3-43-Fc	104	13.5	58	n.d.	0.2 ± 0.001

n.d., not determined.

Summing up the presented data of EGFR-, HER2-, and HER3-targeting recombinant antibodies, all formats were functional in terms of binding to the respective antigen in ELISA and flow cytometry. Thus, characterization of further antibody moieties was done only for the scFv-Fc fusion protein.

The above represented data confirmed full functionality of the 3M6-based recombinant antibodies concerning HER3 targeting, albeit with medium binding activity. Thus, another HER3 binding moiety (3-43) was analyzed in addition to the 3M6 constructs. ScFv3-43 was selected from a human scFv phage display library and was shown to exhibit considerably stronger binding to HER3 as well as a different binding site compared to scFv3M6. While 3M6 binds to domain I of HER3, parts of domains III and IV are involved in binding of 3-43 (Schmitt *et al.*, in preparation). The scFv3-43-Fc molecule was expressed with a yield of 13.5 mg protein per liter cell culture supernatant (Table 3.3). SDS-PAGE analysis revealed pure and intact protein migrating according to its calculated molecular mass and dimer formation under non-reducing conditions (Figure 3.8A). Thermal stability was measured by dynamic light scattering detecting a melting point of 58 °C (Figure 3.8B, Table 3.3). Considering the results of the 3M6-based molecules, binding of scFv3-43-Fc to cell-surface expressed HER3 was clearly stronger reaching half-maximal binding at a concentration of 0.2 nM (Figure 3.8C, Table 3.3). In contrast to all other investigated recombinant antibodies, scFv-3-43-Fc seemed to exert inhibitory effects on Colo205 cells leading to a concentration-dependent reduction of the amount of viable cells. Thus, 3-43 was included as alternative HER3-targeting scTRAIL fusion partner additionally to 3M6.

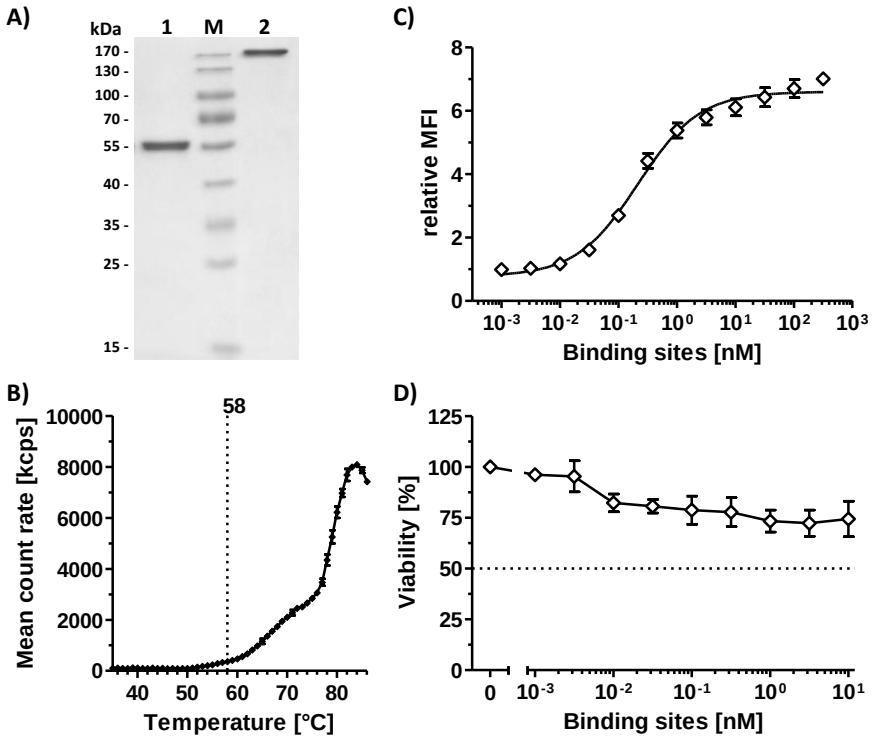

Figure 3.8: Characterization of scFv3-43-Fc. A) SDS-PAGE (12 % PAA) of scFv3-43-Fc was performed under reducing (1) and non-reducing (2) conditions. 2 µg protein were loaded per lane and stained with Coomassie Brilliant Blue. M, protein marker. B) Thermal stability was determined by dynamic light scattering. The melting point [°C] is indicated with a dotted line. Measurement was performed once. C) Binding to HER3-expressing Colo205 cells was analyzed by flow cytometry. Bound protein was detected with an anti-human IgG (γ-chain specific)-PE. D) Effects on Colo205 cells (50,000/well) were determined after treatment for 16 h. Viable cells were stained with crystal violet. Concentrations refer to functional binding sites.

3.1.4 EpCAM-targeting recombinant antibody

The scFv-Fc fusion protein directed against EpCAM was generated based on a humanized version (Fellermeier *et al.*, 2016) of the mouse antibody 323/A3 (Edwards *et al.*, 1986; Roovers *et al.*, 1998). The scFv323/A3hu3-Fc fusion protein was produced with a yield 9.7 mg protein per liter cell culture supernatant (Table 3.4). Purity and integrity of the molecule were confirmed by SDS-PAGE detecting bands of sizes corresponding to the calculated molecular masses of the monomer and dimer under reducing and non-reducing conditions, respectively (Figure 3.8A). A melting point of 54 °C was determined by dynamic light scattering (Figure 3.8B, Table 3.4). Flow cytometry was performed to investigate the binding properties (Figure 3.8C). Half-maximal binding to EpCAM-expressing Colo205 cells was observed at a concentration of 3.4 nM (Table 3.4). Similar to the recombinant antibodies based on hu225, 4D5, and 3M6, scFv323/A3hu3-Fc did not influence viability of Colo205 cells after treatment with a serial dilution for 16 h (Figure 3.8D).

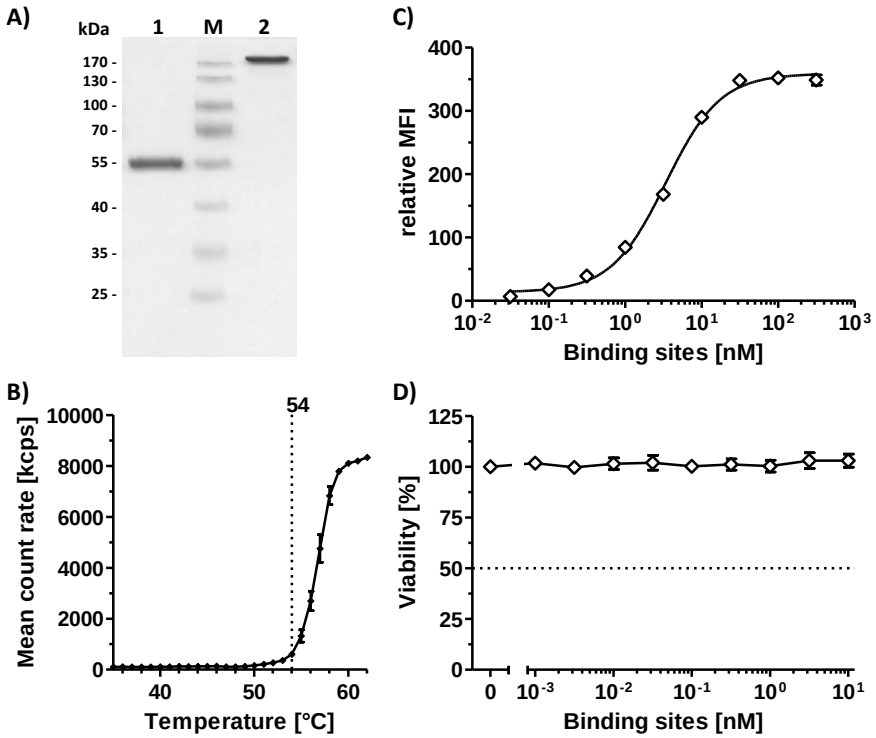

Figure 3.9: Characterization of scFv323/A3hu3-Fc. A) ScFv323/A3hu3-Fc was analyzed by SDS-PAGE (12 % PAA) under reducing (1) and non-reducing conditions (2). 2 µg protein were loaded per lane and stained with Coomassie Brilliant Blue. M, protein marker. B) Dynamic light scattering was performed to investigate thermal stability. The melting point [°C] is indicated with a dotted line. Thermal stability was measured once. C) Binding to EpCAM-expressing Colo205 cells was determined by flow cytometry. Detection of bound protein was performed using an anti-human IgG (γ-chain specific)-PE. D) Colo205 cells (50,000/well) were incubated overnight and treated for 16 h. Viable cells were stained with crystal violet. Concentrations refer to functional binding sites.

Table 3.4: Biochemical and binding properties of scFv323/A3hu3-Fc. Molecular mass (M) was calculated based on the amino acid sequence. Yield is expressed as mg protein per liter cell culture supernatant. EC_{50} value (concentration referring to functional binding sites) for binding to Colo205 cells was determined by flow cytometry.

Protein	M [kDa]	Yield [mg/l]	T_M [°C]	EC_{50} Colo205 [nM]
scFv323/A3hu3-Fc	105	9.7	54	3.4 ± 0.1

In conclusion, all analyzed antibody formats and all targeting moieties exhibited full functionality concerning binding to their respective target structure. This allows generation of the corresponding set of different formats of dimeric antibody-scTRAIL fusion proteins with specificities for EGFR, HER2, HER3, and EpCAM using the hu225, 4D5, 3M6 and 3-43, and 323/A3hu3 targeting moieties, respectively.

3.2 Comparison of different formats of scTRAIL fusion proteins

As outlined above, the concept of generating improved TRAIL therapeutics was built on previous studies demonstrating considerably higher activity of dimeric and targeted dimeric versions of scTRAIL compared to its monomeric form (Gieffers *et al.*, 2013; Seifert *et al.*, 2014a; Siegemund *et al.*, 2012). The first level of improvements consisted in the development of new single-chain variants of human TRAIL optimized for production, stability, and activity (Siegemund *et al.*, 2016). The scTRAIL version used in this study comprises the amino acid residues 118 to 281 and linkers of a single glycine to connect the subunits. Fusion of scTRAIL to the C-terminus of the dimerization modules EHD2 and the human IgG1 Fc part allowed generation of two non-targeted dimeric formats (Figure 3.10A,C). The resulting EHD2-scTRAIL and Fc-scTRAIL molecules possess six TRAIL receptor binding sites, while the monomeric scTRAIL is able to bind to three TRAIL receptors. Employing the dimeric recombinant antibody formats described above (see 3.1), a set of four different targeted dimeric scTRAIL fusion proteins was furthermore developed. According to the non-targeted versions, scTRAIL was fused to the C-terminus of the recombinant antibodies creating Db-scTRAIL, dsDb-scTRAIL, scFv-EHD2-scTRAIL, and scFv-Fc-scTRAIL. Additionally to six TRAIL receptor binding sites, all these molecules exhibit two antigen binding sites. Despite this common composition, variations in activity may arise due to differences in e.g. flexibility or pharmacokinetics. Depending on the degree of flexibility (Tatzel *et al.*, 2016), the molecules are thought to be able to simultaneously bind to antigens and TRAIL receptors either expressed on different tumor cells or also on the same cell (Figure 3.10B). Based on the already described targeting moieties, the different formats of targeted dimeric scTRAIL fusion proteins were developed with specificities for EGFR, HER2, HER3, and EpCAM. All molecules were expressed in stably transfected HEK293T cells comprising a FLAG-tag at the N-terminus for purification of the secreted protein from the supernatant via FLAG affinity chromatography. Since preparations of the initial versions of scFv-Fc-scTRAIL and Fc-scTRAIL contained considerable amounts of cleavage products, an analysis on potential protease cleavage sites was performed and identified several candidates in the sequence connecting the Fc part and scTRAIL. In order to improve the product quality of those fusion proteins, K447 (EU numbering scheme) of the Fc part was mutated to a glutamine residue and an alanine of the linker sequence was replaced by a glycine to remove all predicted protease cleavage sites in this sequence part.

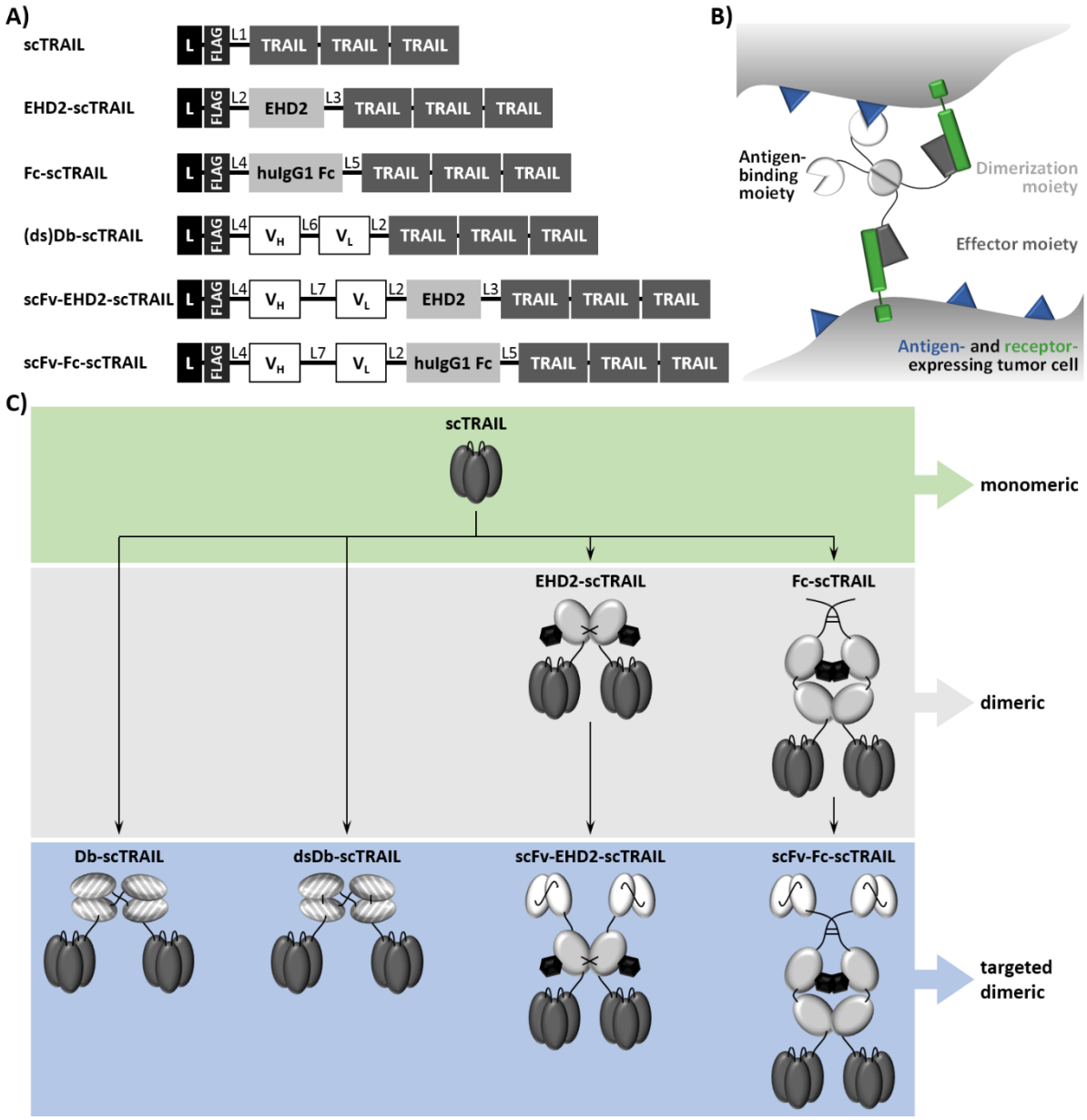

Figure 3.10: Overview of scTRAIL molecules of different formats. A) Composition of targeted and non-targeted scTRAIL versions. L, V_H (scTRAIL) or Igκ chain leader sequence (EHD2-, Fc-scTRAIL, and all targeted formats). L1, EFGG linker. L2, AAAGGSGG linker. L3, GGSGGASSGG linker. L4, GGGGSGT linker. L5, GGSGGGSSGG linker. L6, GGGGS linker. L7, $(GGGGS)_3$ linker. TRAIL subunits consist of aa 118-281 and are connected by a glycine residue. B) Concept of a targeted dimeric scTRAIL fusion protein binding to antigen- and receptor-expressing tumor cells. C) Schematic assembly of scTRAIL molecules. Different categories are highlighted.

3.2.1 EGFR-targeting and non-targeted scTRAIL fusion proteins

3.2.1.1 Biochemical characterization

Antibody-scTRAIL fusion proteins directed against EGFR comprise the above analyzed targeting moiety hu225 (see 3.1.1) and were directly compared to monomeric scTRAIL and its non-targeted dimeric variants EHD2-scTRAIL and Fc-scTRAIL. The product yields ranged from 0.7 mg protein per liter supernatant for scTRAIL to 10.4 mg protein per liter supernatant for

scFvhu225-Fc-scTRAIL (Table 3.5). In general, higher yields were achieved for all fusion proteins than for scTRAIL itself with the Fc-containing molecules showing best production properties. SDS-PAGE revealed pure and intact proteins migrating according to their calculated molecular masses (Figure 3.11A, Table 3.5). Under non-reducing conditions, the expected disulfide-linked dimers were observed. However, a fraction of scFvhu225-EHD2-scTRAIL remained in its monomeric form and high molecular weight species were found for all other molecules.

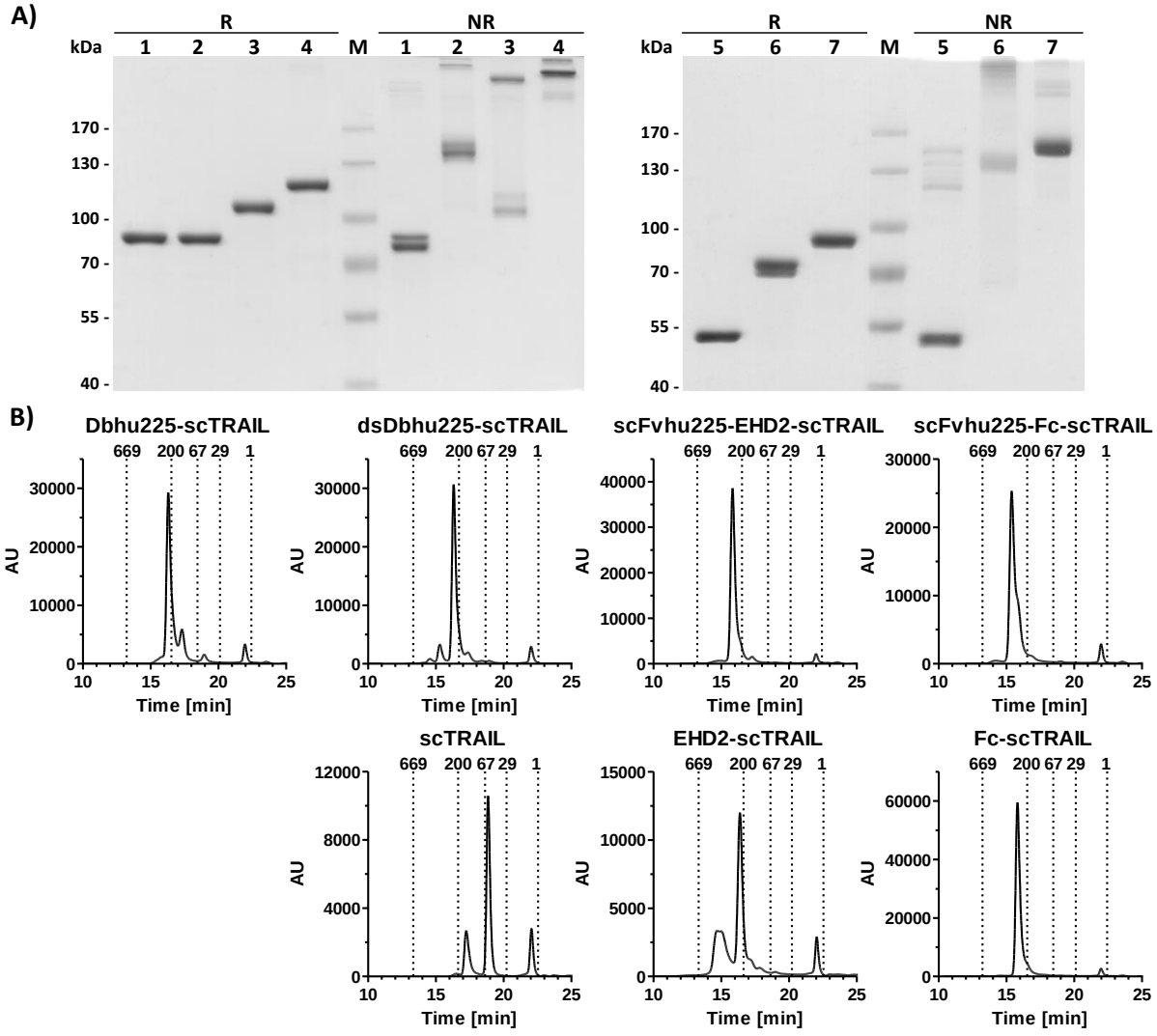

Figure 3.11: Biochemical characterization of EGFR- and non-targeted scTRAIL molecules. A) SDS-PAGE (8 % PAA) of Dbhu225-scTRAIL (1), dsDbhu225-scTRAIL (2), scFvhu225-EHD2-scTRAIL (3), scFvhu225-Fc-scTRAIL (4), scTRAIL (5), EHD2-scTRAIL (6), and Fc-scTRAIL (7) was performed under reducing (R) and non-reducing conditions (NR). 2 µg protein were analyzed per lane and proteins were stained with Coomassie Brilliant Blue. M, protein marker. B) Size exclusion HPLC was used to investigate the proteins under native conditions. Elution times of standard proteins and their corresponding molecular masses [kDa] are indicated.

In size exclusion chromatography, all proteins eluted as one major peak corresponding to the expected protein form (Figure 3.11B). A Stokes radius of 3.4 nm was determined for scTRAIL and increased sizes of 5.5 nm to 6.4 nm were measured for its fusion proteins (Table 3.5). The

elution profile of Dbhu225-scTRAIL additionally showed a minor fraction of smaller size, whereas a peak of high molecular weight species was observed for dsDbhu225-scTRAIL, scTRAIL, and EHD2-scTRAIL. This is of importance for the further evaluation of these proteins, as such multimers have been demonstrated to possess increased activity (reviewed by Koschny *et al.*, 2007b). First studies on stability were performed by dynamic light scattering detecting a melting point of 52 °C for scTRAIL and even increased temperatures for all other molecules (Table 3.5). This indicates stabilization of the proteins by fusion to an antibody and dimerization moiety. With melting points of 58 °C, the EHD2 and Fc part conferred best thermal stability on the respective fusion proteins.

Table 3.5: Biochemical properties of EGFR- and non-targeted scTRAIL molecules. Molecular masses (M) were calculated based on the amino acid sequence. Yields are expressed as mg protein per l cell culture supernatant. Stokes radii (S_r) and melting points (T_M) were determined by size exclusion HPLC and dynamic light scattering, respectively.

Protein	M [kDa]	Yield [mg/l]	S_r [nm]	T_M [°C]
Dbhu225-scTRAIL	168	3.3	5.5	55
dsDbhu225-scTRAIL	168	1.0	5.7	55
scFvhu225-EHD2-scTRAIL	194	3.8	6.0	58
scFvhu225-Fc-scTRAIL	222	10.4	6.4	58
scTRAIL	58	0.7	3.4	52
EHD2-scTRAIL	141	2.3	5.6	58
Fc-scTRAIL	169	6.9	6.0	58

3.2.1.2 Evaluation of binding properties

Since targeted scTRAIL molecules are multifunctional proteins, binding properties of the antibody as well as the scTRAIL moieties were examined. In ELISA, all formats of EGFR-targeting scTRAIL fusion proteins efficiently bound to EGFR with EC_{50} values in the sub- to low nanomolar range (Figure 3.12A, Table 3.6) similar to those identified for the respective recombinant antibodies (Table 3.1). This confirms that binding of the antibody part is not affected by fusion to scTRAIL. Half-maximal binding of targeted and non-targeted scTRAIL molecules to TRAIL receptors was exemplarily determined for human and mouse TRAIL-R2 revealing concentrations in the range of 0.8 nM to 2.5 nM for huTRAIL-R2 and slightly higher values for the mouse receptor (Figure 3.12A, Table 3.6). For direct comparison of dimeric scTRAIL constructs with monomeric scTRAIL, all protein concentrations refer to scTRAIL units.

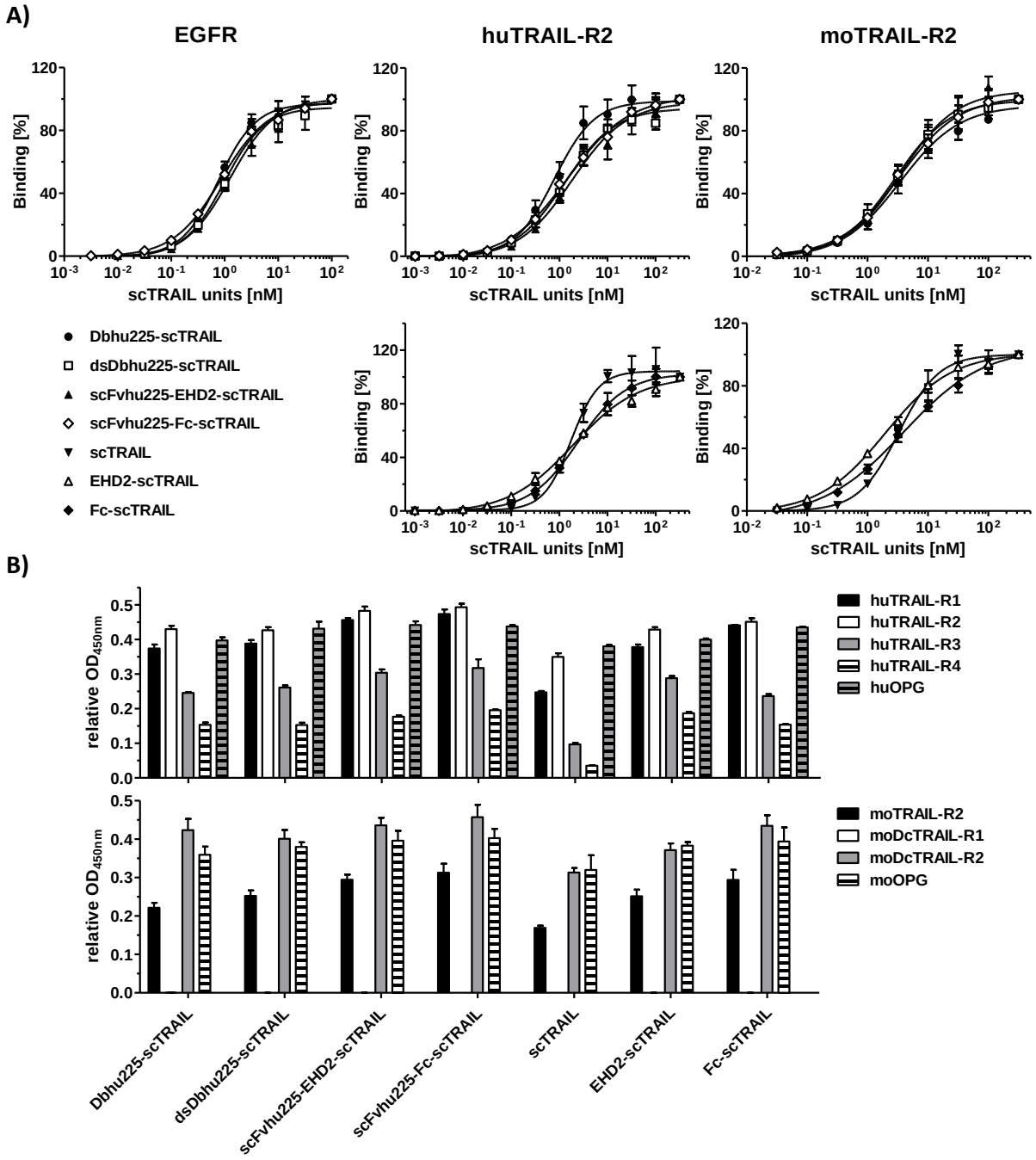

Figure 3.12: Binding of EGFR- and non-targeted scTRAIL molecules to target proteins in ELISA. Proteins were analyzed in serial dilutions (A) or at a concentration of 40 nM scTRAIL units (B). Receptor-Fc fusion proteins (300 ng/well EGFR-Fc, 200 ng/well TRAIL-R-Fc) were coated. Bound molecules were detected with an anti-FLAG-HRP. Concentrations refer to scTRAIL units. OD_{450nm} was normalized to the value of the highest concentration (A) or expressed as relative OD_{450nm} (B; OD of investigated protein divided by OD of coating control detected via anti-huIgG (Fc spec.)-POD). Block shift was performed for analysis of 40 nM scTRAIL units on human TRAIL receptors.

To further investigate TRAIL receptor binding properties, binding of the molecules to all human and mouse TRAIL receptors was analyzed at a concentration of 40 nM scTRAIL units (Figure 3.12B). All proteins were capable of binding to all human TRAIL receptors. However, only low binding to huTRAIL-R3 and huTRAIL-R4 was detected for scTRAIL. In contrast to the results obtained for the human receptors, the scTRAIL molecules were not able to bind to all

mouse TRAIL-R. No binding was observed for moDcTRAIL-R1, which is consistent with data previously published by Bossen *et al.* (2006) already revealing the incapability of human TRAIL to bind to this mouse receptor. These data confirm the designated target specificities of EGFR-targeting and non-targeted scTRAIL molecules.

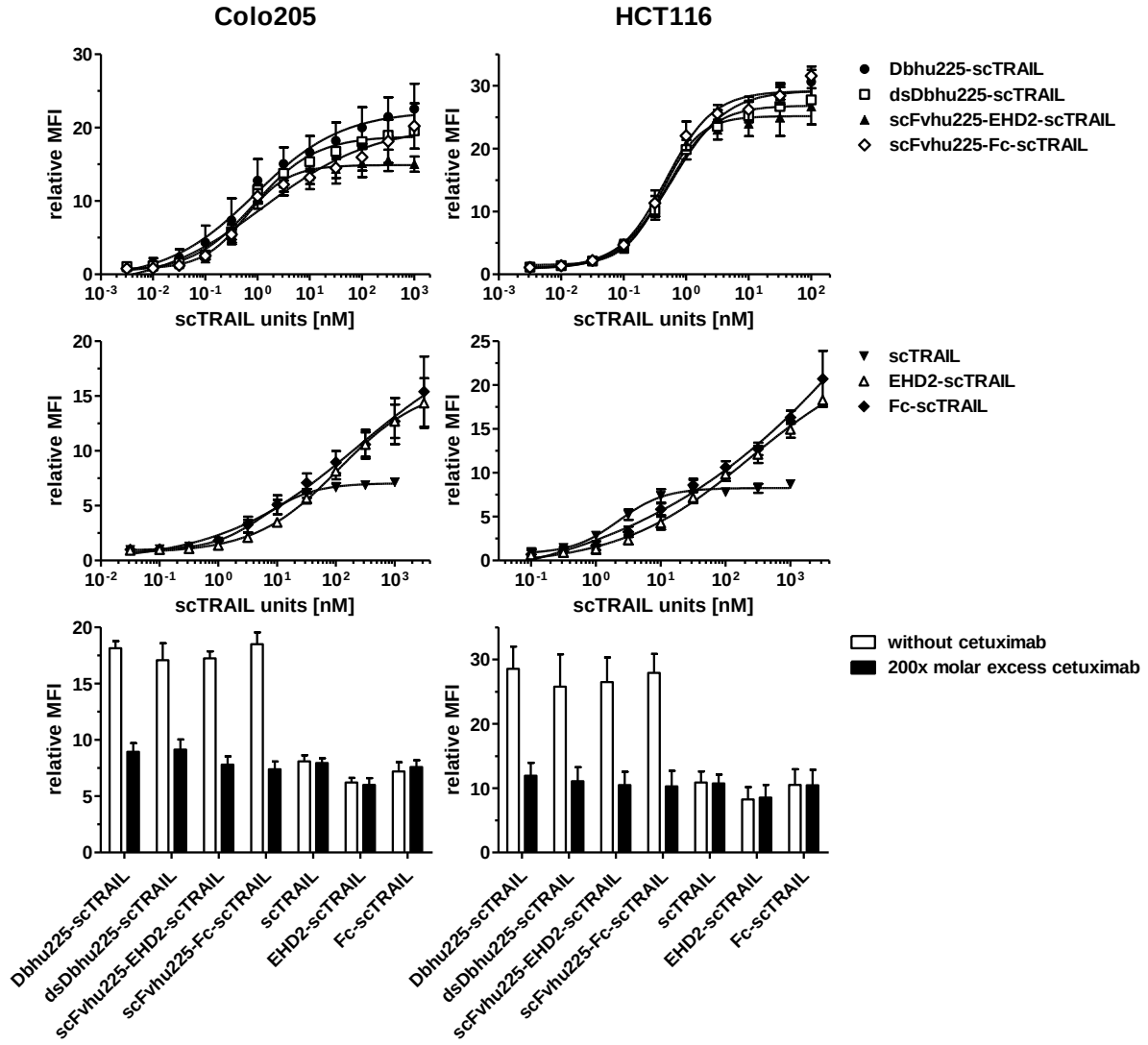

Figure 3.13: Binding of EGFR- and non-targeted scTRAIL molecules to cell surface-expressed receptors. Flow cytometry was performed to determine binding to Colo205 and HCT116 cells. Either serial dilutions or a concentration of 20 nM scTRAIL units were analyzed and bound proteins were detected using a PE-conjugated anti-FLAG antibody. To block binding of the antibody moiety to EGFR, cells were preincubated with a 200-fold molar excess of cetuximab, prior to addition of the scTRAIL molecules. Concentrations refer to scTRAIL units.

Binding was further analyzed on the cell lines that were also used to investigate cell death induction. Targeted as well as non-targeted scTRAIL constructs bound to Colo205 and HCT116 cells in a concentration-dependent manner (Figure 3.13). While strong binding with EC_{50} values of 0.4 nm to 1.7 nm (Table 3.6) was detected for the targeted fusion proteins, EHD2-scTRAIL and Fc-scTRAIL did not reach saturation levels for concentrations up to 3 µM. To analyze the contribution of the antibody and scTRAIL moieties on binding, blocking studies

were performed by incubating Colo205 and HCT116 cells with a 200-fold molar excess of cetuximab, prior to addition of the molecules (20 nM scTRAIL units). In the presence of cetuximab, binding of all targeted fusion proteins was reduced to the level observed for the non-targeted variants that was completely unaffected by blocking of EGFR. This demonstrates that binding of antibody-targeted scTRAIL molecules to Colo205 and HCT116 cells is mediated via both EGFR and TRAIL receptors. Statistical analysis of the EC_{50} values of the ELISA and flow cytometry studies revealed significantly reduced EGFR binding of scFvhu225-EHD2-scTRAIL compared to e.g. Dbhu225-scTRAIL in ELISA ($P<0.001$), while no significant differences were observed for binding to Colo205 cells ($P>0.05$) and even significantly increased binding of scFvhu225-EHD2-scTRAIL compared to Dbhu225-scTRAIL was seen for HCT116 cells ($P<0.05$). This illustrates that there are no consistent differences in the binding activity due to the format. Summing up the results of the binding studies, all molecules showed the expected behavior, i.e. comparable binding properties of targeted and non-targeted proteins for TRAIL receptors and improved cell binding of the targeted constructs mediated by the EGFR-binding antibody moiety. Furthermore, no consistent differences were identified for the different formats of EGFR-targeting scTRAIL fusion proteins.

Table 3.6: Binding properties of EGFR- and non-targeted scTRAIL molecules. EC_{50} values are represented as nM scTRAIL units and were determined by ELISA (EGFR-, huTRAIL-R2-, moTRAIL-R2-Fc) and flow cytometry (Colo205, HCT116 cells).

Protein	EGFR	huTRAIL-R2	moTRAIL-R2	Colo205	HCT116
Dbhu225-scTRAIL	0.8 ± 0.1	0.8 ± 0.1	3.9 ± 1.2	0.9 ± 0.3	0.6 ± 0.03
dsDbhu225-scTRAIL	0.9 ± 0.03	1.3 ± 0.4	3.0 ± 0.6	0.9 ± 0.1	0.5 ± 0.1
scFvhu225-EHD2-scTRAIL	1.2 ± 0.1	2.1 ± 0.7	3.8 ± 0.8	0.6 ± 0.1	0.4 ± 0.02
scFvhu225-Fc-scTRAIL	0.9 ± 0.01	1.6 ± 0.4	3.5 ± 0.7	1.7 ± 1.1	0.5 ± 0.1
scTRAIL	n.d.	1.8 ± 0.4	3.3 ± 0.2	6.7 ± 1.4	2.2 ± 0.2
EHD2-scTRAIL	n.d.	2.0 ± 0.2	2.0 ± 0.3	(>100)‡	(>100)‡
Fc-scTRAIL	n.d.	2.5 ± 0.3	4.1 ± 1.0	(>100)‡	(>100)‡

n.d., not determined. ‡, no saturation reached.

3.2.1.3 Induction of cell death and caspase activity *in vitro*

The mechanism of anti-tumoral activity of the investigated molecules consists in the induction of apoptosis leading to cell death. Thus, the proteins were evaluated for their capability to induce cell death on the colorectal carcinoma cell lines Colo205 and HCT116 either alone or in combination with the proteasome inhibitor bortezomib (BZB) that is able to sensitize cells for TRAIL-induced apoptosis (reviewed by de Wilt *et al.*, 2013). All EGFR- and non-targeting molecules induced concentration-dependent cell death on Colo205 cells in the absence as well

as in the presence of bortezomib after treatment for 16 h (Figure 3.14). Without sensitizer, the different targeted formats exhibited EC_{50} values ranging from 12.6 pM to 40.9 pM scTRAIL units (Table 3.7), whereas the non-targeted versions scTRAIL and Fc-scTRAIL required significantly higher concentrations ($P<0.01$) to induce 50 % cell death indicating beneficial effects of EGFR targeting. Furthermore, the 5-fold lower EC_{50} value of Fc-scTRAIL compared to scTRAIL ($P<0.01$) and the remaining level of approximately 40 % living cells for scTRAIL highlight the superiority of the dimeric over the monomeric scTRAIL form, which is in accordance with previous studies (Siegemund *et al.*, 2012; Seifert *et al.*, 2014a). Referring to the results of the SEC analysis, the considerable amount of high molecular weight species may explain the high activity of EHD2-scTRAIL. After preincubation with bortezomib, 5- to 20-fold lower EC_{50} values ($P<0.01$) were detected confirming the sensitizing effect. Similar to the results obtained without bortezomib, all EGFR-targeting fusion proteins exerted significantly better activity than Fc-scTRAIL ($P<0.001$) that in turn was superior to scTRAIL ($P<0.001$; Figure 3.14, Table 3.7).

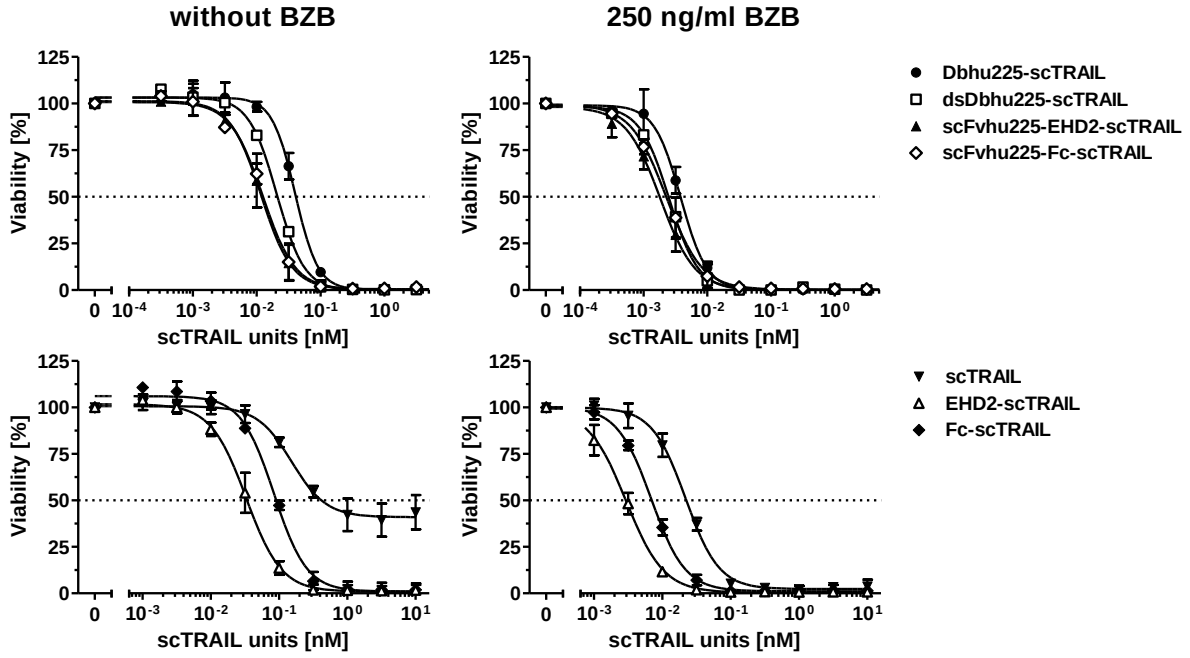

Figure 3.14: Cell death induction of EGFR- and non-targeted scTRAIL molecules on Colo205 cells. 50,000 cells per well were incubated overnight and treated with serial dilutions of the proteins for 16 h after preincubation with medium or bortezomib (BZB, 250 ng/ml) for 30 min. Viable cells were stained with crystal violet. Concentrations refer to scTRAIL units.

The data of EGFR- and non-targeting scTRAIL molecules described above already indicate a beneficial impact of EGFR targeting of the fusion proteins, although no influence was found for the recombinant antibodies alone (Figure 3.3C). To further analyze the contribution of the antibody moieties in the fusion proteins to cell death induction, binding to EGFR was blocked

by preincubation of Colo205 cells with a 200-fold molar excess of cetuximab (Figure 3.15). In the presence of cetuximab, all targeted and non-targeted constructs were still able to induce cell death treating the cells with protein alone as well as in combination with bortezomib. However, a shift in the activity profile was observed. Blocking of EGFR binding significantly increased the EC_{50} values of the targeted molecules by factors of 2 to 6 in the absence of bortezomib ($P<0.01$) and 3 to 4 in the presence of bortezomib ($P<0.05$; Table 3.7). Interestingly, also the non-targeted variants showed decreased effects after preincubation of the cells with cetuximab, although with increases of the EC_{50} values of 1.3-fold without bortezomib and 2-fold when combined with bortezomib to a lesser extent. These data further confirm a contribution of targeting EGFR to cell death induction.

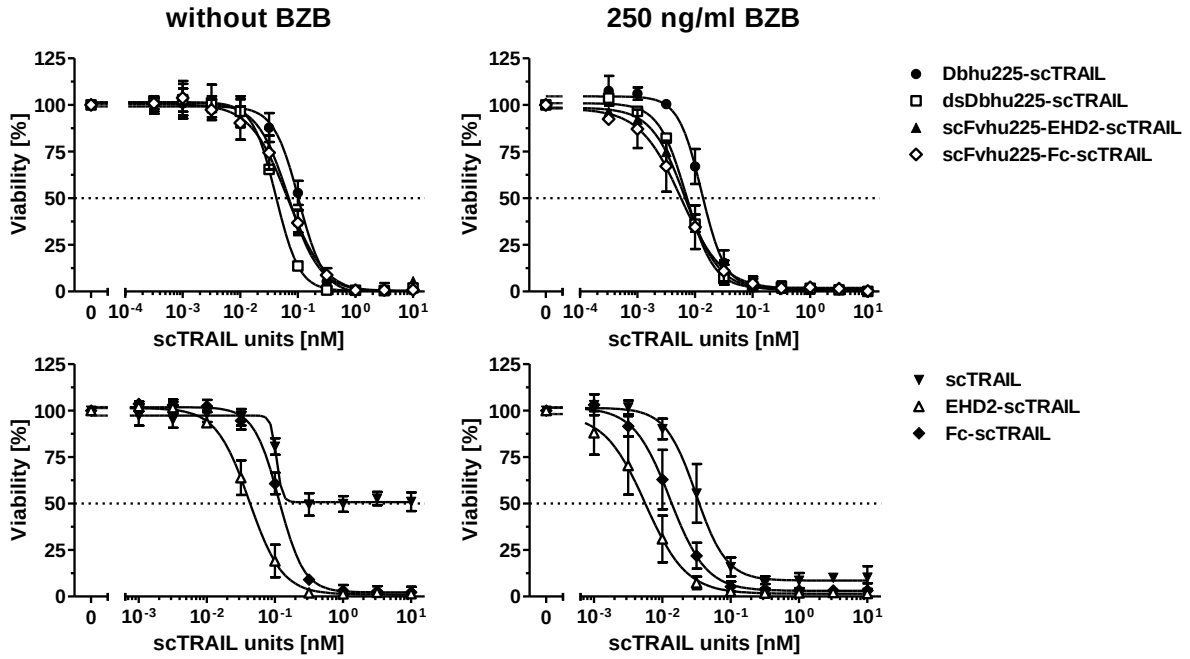

Figure 3.15: Cell death induction of EGFR- and non-targeted scTRAIL molecules on Colo205 cells in the presence of cetuximab. 50,000 cells per well were incubated overnight. To block binding of the molecules to EGFR, cells were preincubated with a 200-fold molar excess of cetuximab in medium or medium containing BZB (250 ng/ml) for 30 min. After treatment of the cells with the proteins for 16 h, viable cells were stained with crystal violet. Concentrations refer to scTRAIL units.

In order to validate the cell death-inducing effects demonstrated for Colo205 cells, further studies were performed using HCT116 cells, a colorectal carcinoma cell line like Colo205, but with activating mutations in KRAS and PIK3CA instead of BRAF. Confirming their activity on Colo205 cells, all EGFR- and non-targeting molecules induced cell death on HCT116 cells (Figure 3.16). In the absence of bortezomib, EC_{50} values of 11.3 pM to 34.9 pM scTRAIL units were determined for the targeted proteins, while 165.7 pM and 1122.7 pM were necessary to kill 50 % of the cells by Fc-scTRAIL and scTRAIL, respectively (Table 3.7). This corresponds to a

significant increase in the EC_{50} values of these non-targeted compared to the EGFR-targeted constructs ($P<0.01$). With EC_{50} values decreased by factors of 16 to 136 ($P<0.01$), bortezomib exhibited an even more intense sensitizing effect on HCT116 cells than that observed for Colo205 cells. In agreement with the data obtained for Colo205 cells, strongest cell death induction was identified for the targeted scTRAIL fusion proteins, followed by Fc-scTRAIL, and finally scTRAIL alone as well as in combination with bortezomib. Again, EHD2-scTRAIL was more active than Fc-scTRAIL ($P<0.05$), which is supposed to result from the presence of multimeric forms exerting higher activity.

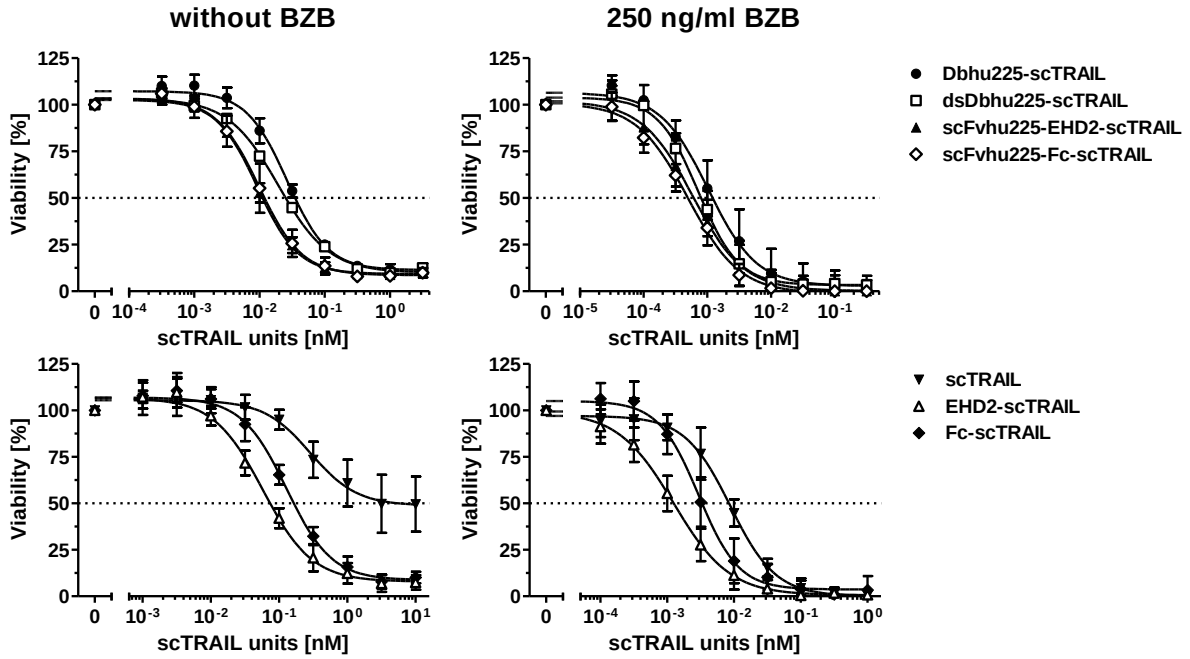

Figure 3.16: Cell death induction of EGFR- and non-targeted scTRAIL molecules on HCT116 cells. 15,000 cells were seeded per well. After preincubation with medium or bortezomib (250 ng/ml) for 30 min, cells were treated with the proteins for 16 h. Cell viability was analyzed by crystal violet staining. Concentrations refer to scTRAIL units.

Statistical analysis of all possible comparisons is beyond the scope of this study. However, major differences are illustrated. Attempting to make a conclusion about possible variations in the cell death-inducing activity of the different EGFR-targeted formats, comparison of the EC_{50} values on Colo205 or HCT116 cells in the absence or presence of bortezomib only revealed significantly lower activity for Dbhu225-scTRAIL under all conditions ($P<0.05$). With respect to the presence of protein fractions with smaller size (Figure 3.11B), this decreased activity may be related to heterogeneity of the protein preparation rather than to lower activity of the format itself.

Table 3.7: EC_{50} values of cell death induction of EGFR- and non-targeted scTRAIL molecules. EC_{50} values [pM scTRAIL units] were determined for Colo205 and HCT116 cells treated for 16 h with protein after preincubation with medium or BZB (250 ng/ml). To block binding to EGFR, cells were preincubated with cetuximab (200-fold molar excess) in medium or medium containing BZB (250 ng/ml).

Protein	Colo205				HCT116	
	without cetuximab		with cetuximab		without cetuximab	
	without BZB	with BZB	without BZB	with BZB	without BZB	with BZB
Dbhu225-scTRAIL	40.9 ± 3.0	3.7 ± 0.4	100.6 ± 12.0	14.1 ± 2.1	34.9 ± 2.4	1.7 ± 0.8
dsDbhu225-scTRAIL	21.5 ± 3.4	2.4 ± 0.5	41.9 ± 4.1	7.3 ± 0.7	25.2 ± 4.0	0.8 ± 0.2
scFvhu225-EHD2-scTRAIL	12.6 ± 2.6	1.8 ± 0.4	69.3 ± 11.6	6.8 ± 0.9	11.3 ± 1.7	0.7 ± 0.3
scFvhu225-Fc-scTRAIL	12.8 ± 1.6	2.3 ± 0.5	66.0 ± 12.2	6.0 ± 2.1	12.5 ± 4.7	0.5 ± 0.1
scTRAIL	474.7 ± 139.3	22.4 ± 2.3	–	36.0 ± 9.6	1122.7 ± 353.1	8.2 ± 1.5
EHD2-scTRAIL	34.5 ± 6.8	2.9 ± 0.4	44.6 ± 8.4	6.0 ± 2.2	75.0 ± 13.5	1.3 ± 0.4
Fc-scTRAIL	90.7 ± 3.5	7.0 ± 0.2	118.1 ± 8.7	14.1 ± 4.0	165.7 ± 25.6	3.6 ± 1.5

–, less than 50 % of cells dead.

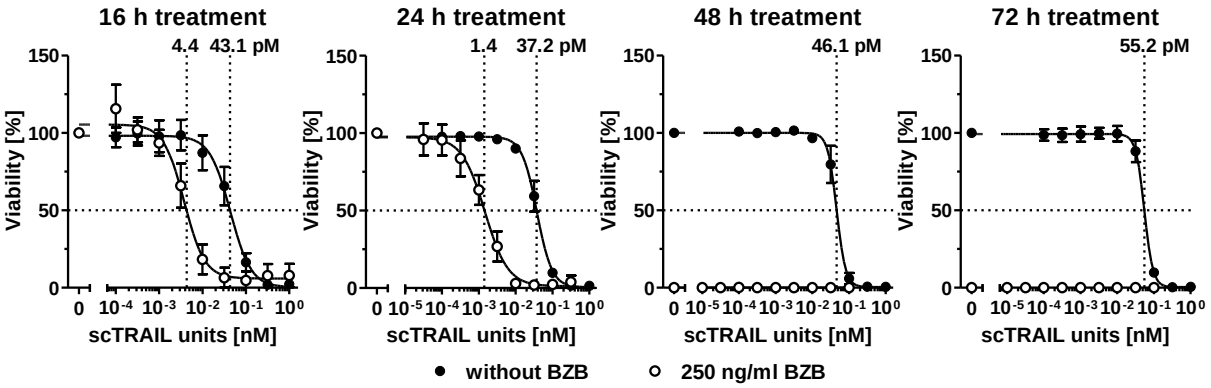

Figure 3.17: Effects of treatment length on cell death induction of Dbhu225-scTRAIL on Colo205 cells. After preincubation with medium or bortezomib (250 ng/ml), Colo205 cells (50,000/well) were treated with serial dilutions of Dbhu225-scTRAIL for 16 h, 24 h, 48 h, and 72 h. Viable cells were stained with crystal violet and quantified by measuring the OD at 550 nm. EC_{50} values [pM scTRAIL units] are indicated with dotted lines.

Besides analyzing cell death induction on different cell lines and the impact of combination with bortezomib or blocking of EGFR binding, further studies were performed to evaluate the influence of the treatment length. Effects of Dbhu225-scTRAIL on Colo205 cells were investigated in the absence and presence of bortezomib for treatment intervals of 16 h, 24 h, 48 h, and 72 h (Figure 3.17). In accordance with the data described above (Table 3.7), 50 % cell death was detected at concentrations of 43.1 (± 10.8) pM and 4.4 (± 1.1) pM scTRAIL units after treatment for 16 h without and with bortezomib, respectively. With EC_{50} values of 37.2 (± 5.2) pM and 1.4 (± 0.5) pM, an increase in the treatment length to 24 h induced a significant difference ($P<0.05$) only in combination with bortezomib. Further extending the treatments to 48 h and 72 h killed all cells treated with bortezomib, while similar EC_{50} values

were observed for cells treated with protein alone. Thus, extension of the treatment length did not alter the activity of Dbhu225-scTRAIL, but led to a more distinct switch between concentrations inducing cell death or not.

Since previous studies and the above represented data already describe a considerable difference in the capability of monomeric, dimeric, and targeted dimeric scTRAIL versions to induce cell death, further experiments were performed to investigate these variabilities on the level of caspase-8 and -3/7 activity. To especially gain insight into variations in the kinetics of cell death induction, time-dependent activation of caspases by scFvhu225-Fc-scTRAIL, Fc-scTRAIL, and scTRAIL was analyzed in Colo205 cells either alone or in combination with bortezomib. In a first experiment, levels of active caspase-8 induced by 10 pM of the proteins (corresponding to scTRAIL units) in combination with bortezomib were determined. Treatment with bortezomib alone, but also together with scTRAIL or Fc-scTRAIL did not or only marginally increase caspase-8 activity compared to cells incubated in medium. Only scFvhu225-Fc-scTRAIL was able to trigger activation of caspase-8 at the examined treatment interval of 8 h (Figure 3.18).

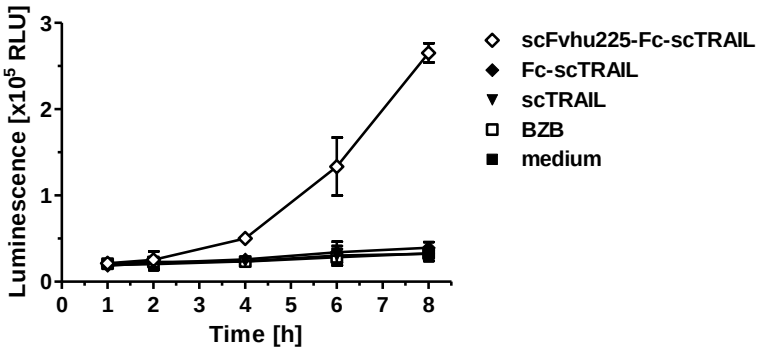

Figure 3.18: Induction of caspase-8 activity in Colo205 cells. Colo205 cells (15,000/well) were preincubated with BZB (250 ng/ml) for 30 min and treated with 10 pM protein (scTRAIL units) for different intervals. Caspase-8 activity was determined using Caspase-Glo® 8 Assay and measuring the luminescence signal (proportional to the amount of caspase-8 activity). RLU, relative light units.

Since the investigated concentration of 10 pM corresponds to the EC_{50} value of scFvhu225-Fc-scTRAIL that is clearly lower than those of the other proteins (Table 3.7), additional studies were performed with increased protein concentrations and extended treatment lengths. Besides the initiator caspase (Figure 3.19A), also executioner caspases-3/7 (Figure 3.19B) were analyzed in these settings. Similar to the results obtained for an incubation time of 8 h, treatment with bortezomib for 20 h did not or only marginally increase caspase-8 and -3/7 activity. At a concentration of 100 pM scTRAIL units in combination with bortezomib, scTRAIL was able to induce caspase-8 and -3/7 activation, albeit requiring a treatment interval of 20 h.

In contrast, activation triggered by Fc-scTRAIL was clearly accelerated with marked caspase-8 and -3/7 activity already seen after 8 h. The targeted dimeric scFvhu225-Fc-scTRAIL showed an even faster and stronger activation that was already detectable after 2 h and reached clearly higher levels than the other proteins. Further increasing the protein concentration to 1 nM scTRAIL units in the presence of bortezomib accelerated the kinetics of activating initiator as well as executioner caspases of all molecules. Similar activation profiles were determined for both Fc fusion proteins inducing comparable levels of active caspases, though slightly delayed for the non-targeted construct. Despite a clearly faster activation kinetic with maximum activity measured already after 8 h, scTRAIL was not capable of reaching levels as high as those induced by the dimeric molecules. Application of the proteins at a concentration of 1 nM in the absence of bortezomib did not alter their activation profiles, but led to a slight reduction in the overall activity levels, especially for caspase-3/7 as compared to the combination with bortezomib. This is in agreement with data reporting that bortezomib treatment can also affect the level of XIAP that exerts inhibitory effects on caspase-3/7 (reviewed by de Wilt *et al.*, 2013). With reference to these results of caspase activities and those obtained for induction of cell death, all EGFR-targeting formats possess superior properties compared to those of Fc-scTRAIL that outperformed the monomeric scTRAIL.

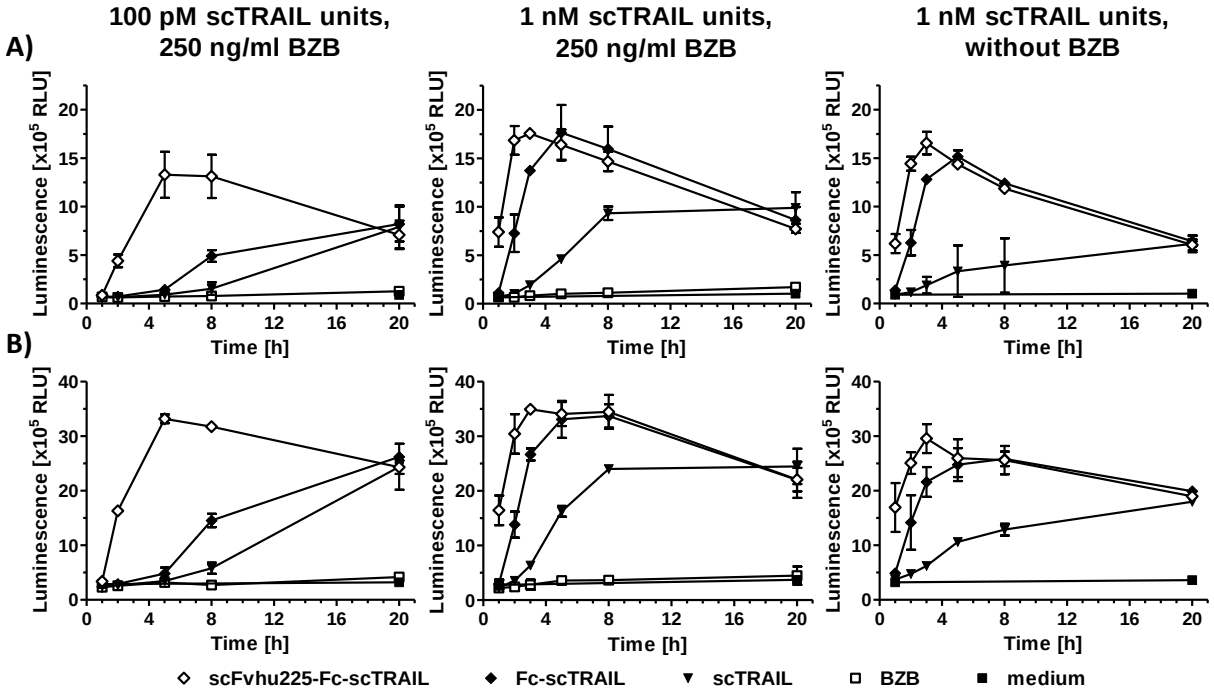

Figure 3.19: Induction of caspase-8 and -3/7 activity in Colo205 cells. Colo205 cells (15,000/well) were treated with the indicated concentrations of protein for different treatment intervals after preincubation with either BZB (250 ng/ml) or medium. Caspase-8 (A) and -3/7 (B) activities were determined using Caspase-Glo® 8 Assay and Caspase-Glo® 3/7 Assay, respectively. Measured luminescence signal is proportional to the amount of caspase activity. Data are represented as mean ± SD of two independent experiments. RLU, relative light units.

3.2.1.4 Plasma stability and *in vivo* pharmacokinetics

Stability and serum half-lives of proteins are of great importance for therapeutic applications, as they determine their bioavailability and are thus factors limiting their potential to induce therapeutic effects.

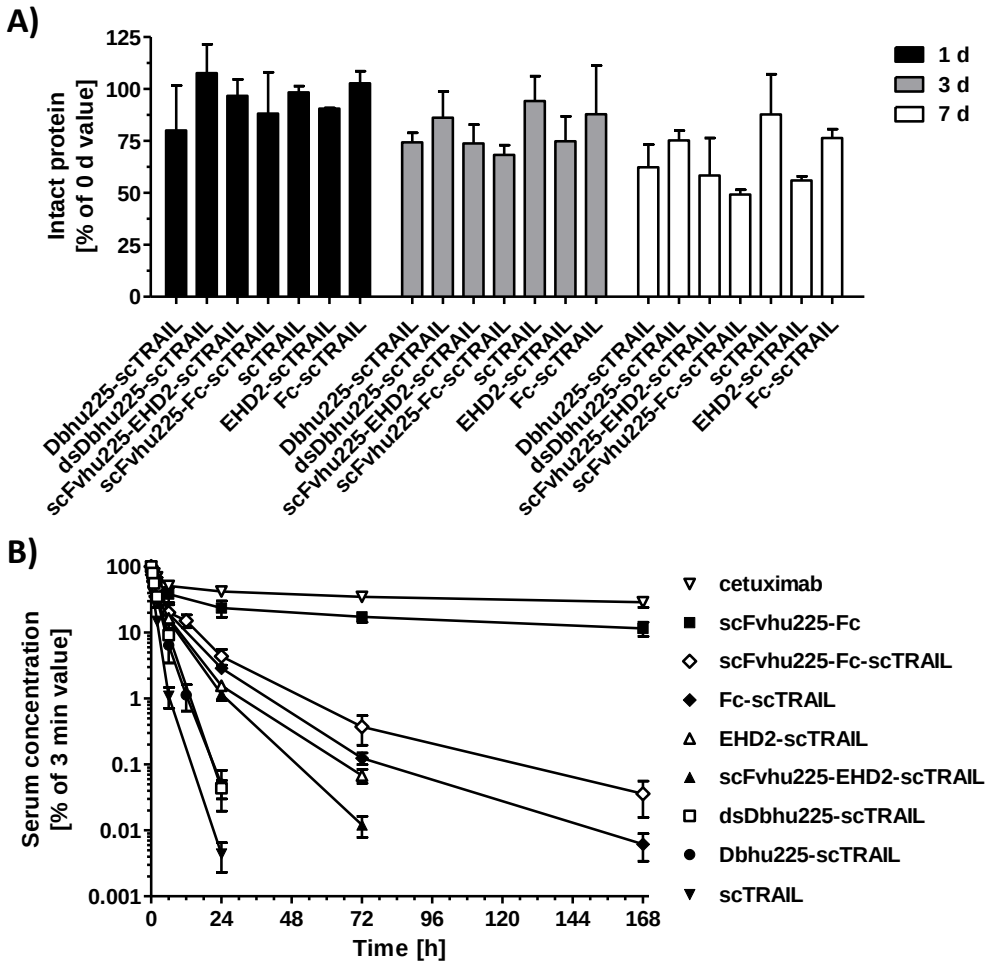

Figure 3.20: Plasma stability and *in vivo* pharmacokinetics of EGFR- and non-targeted scTRAIL molecules. A) 100 nM scTRAIL units were incubated in 50 % human plasma at 37 °C for 1 d, 3 d, and 7 d or directly frozen. Levels of intact protein were measured in ELISA by binding to human TRAIL-R2-Fc and detection with an anti-FLAG-HRP. Data were normalized to the concentration of the sample directly frozen. B) Pharmacokinetic profiles were determined in female CD-1® mice (3 or 6 mice per molecule) after injection of 25 µg or 50 µg protein into the tail vein. Blood samples were collected after the indicated time intervals. Serum concentrations were analyzed by ELISA and normalized to the level detected after 3 min.

First, the stability of all EGFR- and non-targeting fusion proteins was evaluated in human plasma (Figure 3.20A). The molecules were diluted in 50 % plasma and either directly frozen or incubated at 37 °C for 1 d, 3 d, and 7 d. Levels of intact protein were analyzed in ELISA by binding of the C-terminal scTRAIL to human TRAIL-R2 and detection via the N-terminal FLAG-tag. All molecules showed a time-dependent decrease in the measured protein concentration reaching approximately 50 % or higher levels after 7 d. Deviations between different experiments were rather large for some proteins and thus do not allow clear conclusions

about differences in the stabilities of the proteins. Despite these variabilities, scTRAIL, Fc-scTRAIL, and dsDbhu225-scTRAIL still seem to be slightly more stable. The increased stability of dsDbhu225-scTRAIL may indicate a positive influence of the introduction of disulfide bonds for the diabody construct.

In vivo half-lives of the proteins were determined in tumor-free CD-1® mice after i.v. injection of 25 µg or 50 µg protein (Figure 3.20B). Blood samples were collected after different time intervals and serum concentrations of the molecules were analyzed by ELISA. With the shortest initial and terminal half-lives (Table 3.8), scTRAIL was only detectable for 24 h after injection. Similar pharmacokinetic properties were obtained for Dbhu225-scTRAIL and its disulfide-stabilized form revealing only a marginal improvement compared to scTRAIL. In contrast to that, the EHD2-containing fusion proteins showed with 6.5 h (scFvhu225-EHD2-scTRAIL) and 8.7 h (EHD2-scTRAIL) significantly prolonged terminal half-lives ($P<0.01$ and $P<0.001$, respectively). As expected, best pharmacokinetic properties were observed for scFvhu225-Fc-scTRAIL and Fc-scTRAIL exhibiting terminal half-lives of 17.8 h and 14.5 h that represent a significant increase compared to the EHD2 constructs ($P<0.001$). These differences also translated into the corresponding areas under the curve (AUC). With an AUC of 603 %·h, scFvhu225-Fc-scTRAIL possessed a more than 2-fold higher systemic exposure than the diabody molecules. Despite these superior properties, comparison with scFvhu225-Fc and cetuximab demonstrated 6- to 15-fold reduced half-lives of the Fc-containing scTRAIL fusion proteins ($P<0.001$) indicating a role of additional processes in the elimination of scTRAIL molecules.

Table 3.8: Pharmacokinetic properties. PK was evaluated in female CD-1® mice (3 or 6 mice per molecule) injecting 25 µg or 50 µg protein into the tail vein. Initial half-lives ($t_{1/2}\alpha$) were calculated for the time interval of 3 min to 2 h. The terminal half-life ($t_{1/2}\beta$) was determined starting with the serum concentration at 6 h.

Protein	$t_{1/2}\alpha$ [h]	$t_{1/2}\beta$ [h]	AUC [%·h]
Dbhu225-scTRAIL	1.2 ± 0.3	2.6 ± 0.2	235 ± 48
dsDbhu225-scTRAIL	1.3 ± 0.2	2.3 ±0.1	292 ± 21
scFvhu225-EHD2-scTRAIL	1.5 ± 0.1	6.5 ± 0.2	402 ± 51
scFvhu225-Fc-scTRAIL	1.9 ± 0.3	17.8 ± 2.3	603 ± 101
scTRAIL	0.7 ± 0.03	2.2 ± 0.1	118 ± 12
EHD2-scTRAIL	1.4 ± 0.04	8.7 ± 0.4	422 ± 22
Fc-scTRAIL	3.1 ± 0.1	14.5 ± 0.8	592 ± 23
scFvhu225-Fc	2.7 ± 0.8	111.9 ± 23.3	3257 ± 562
Cetuximab	4.8 ± 1.9	218.4 ± 27.0	6129 ± 682

3.2.1.5 *In vivo* activity of different formats of scTRAIL fusion proteins

Final studies on the functionality and differences of the alternative formats of scTRAIL molecules were performed by investigating the *in vivo* therapeutic activity. In all experimental settings, a Colo205 xenograft model was established in NMRI nude mice by subcutaneous injections of $3 \cdot 10^6$ cells into the left and right flank. Treatment was started after tumors reached a volume of approximately 100 mm^3. A first experiment was arranged to evaluate the effects of bortezomib treatment alone (Figure 3.21). Mice received six intraperitoneal injections of bortezomib (5 µg) or PBS every other day. After an observation time of 27 d, no differences in tumor growth were induced by treatment with bortezomib. Based on these data, experiments analyzing combinations of protein and bortezomib only included a control group treated with bortezomib.

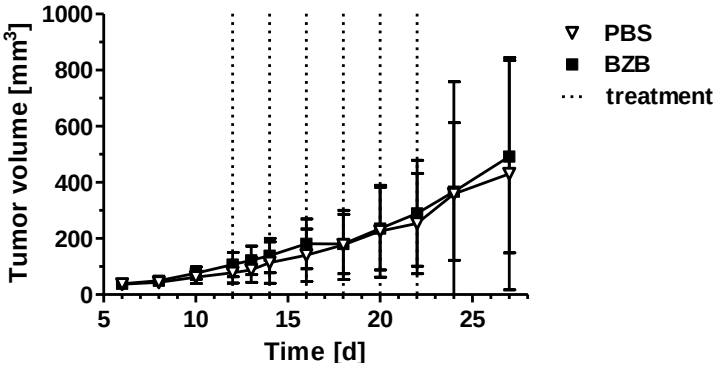

Figure 3.21: Effects of bortezomib *in vivo*. A Colo205 xenograft model was established in NMRI nude mice (4 mice for PBS, 5 mice for BZB). Upon reaching a tumor size of approximately 100 mm^3, mice received six i.p. injections of bortezomib (5 µg) or PBS as control (days 12, 14, 16, 18, 20, 22). Treatments are indicated with a dotted line.

In a second experiment, the therapeutic activities of the different EGFR-targeting scTRAIL formats and the non-targeted Fc-scTRAIL were compared in combination with bortezomib (Figure 3.22). Since *in vitro* and PK studies did not identify relevant differences in the properties of Dbhu225-scTRAIL and dsDbhu225-scTRAIL and high molecular weight species were found for the disulfide-stabilized form, only the unmodified diabody construct was analyzed resulting in five groups, i.e. BZB alone and combined with either Dbhu225-scTRAIL, scFvhu225-EHD2-scTRAIL, scFvhu225-Fc-scTRAIL, or Fc-scTRAIL. Mice received six combinatorial treatments of 5 µg bortezomib (i.p.) and 0.5 nmol protein (corresponding to 1 nmol scTRAIL units; i.v.). After three treatments every other day, treatment intervals were gradually increased by one day. Already a single treatment with protein and bortezomib induced extensive tumor regression that continued until almost complete and persistent tumor remission was observed (Figure 3.22A).

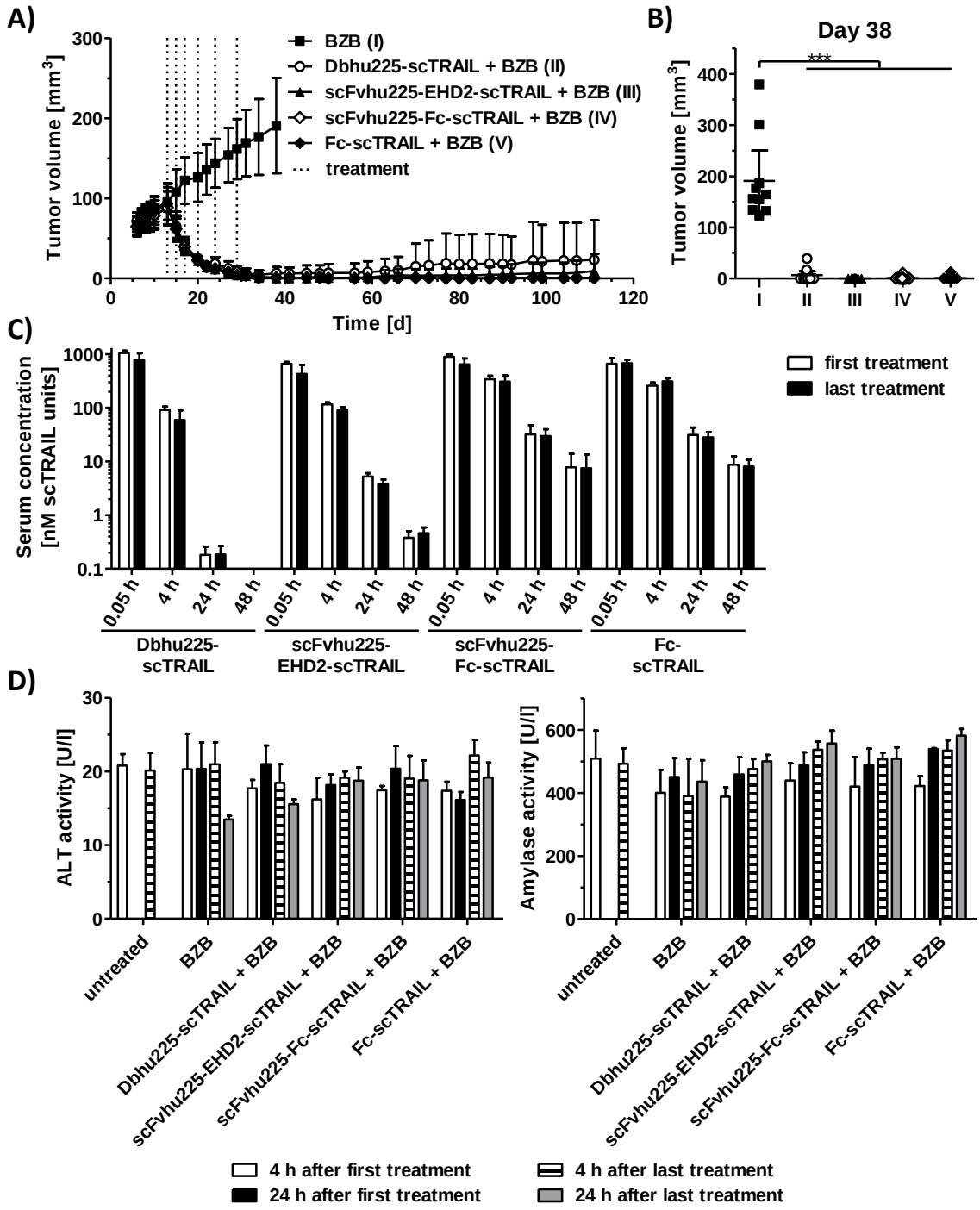

Figure 3.22: *In vivo* activity and PK of different EGFR-targeting scTRAIL formats and Fc-scTRAIL in combination with bortezomib. A) NMRI nude mice (6 mice per group) bearing Colo205 tumors with a size of approximately 100 mm^3 received six combinatorial treatments of bortezomib (5 µg; i.p.) and protein (0.5 nmol protein corresponding to 1 nmol scTRAIL units; i.v.). Dotted lines indicate days of treatment (days 13, 15, 17, 20, 24, 29). B) Tumor volumes of groups I to V at day 38 are represented (numbering of groups according to A). Statistical analysis was performed by One-Way ANOVA, followed by Tukey's post hoc test (*P<0.05; **P<0.01; ***P<0.001; ns, P>0.05). C) Serum concentrations of samples taken 3 min, 4 h, 24 h, and 48 h after the first (day 13) and last treatment (day 29) were determined by ELISA. D) Potential toxicity of the treatments was evaluated by measuring ALT and amylase activity in serum samples collected 4 h and 24 h after the first and the last treatment.

Even after more than 100 d, only single tumors in the groups treated with Dbhu225-scTRAIL and scFvhu225-EHD2-scTRAIL slowly started to regrow. Except for these observations, no differences in the effects exerted by the different proteins were seen. Statistical analysis of

the tumor volumes at day 38 revealed a significant reduction in all protein-treated groups compared to mice only receiving bortezomib injections (Figure 3.22B). In order to confirm the PK data already described in tumor-free mice (see 3.2.1.4), serum concentrations of the proteins were examined after the first and last treatment (Figure 3.22C). Since the detected PK profiles of all proteins were in perfect accordance with those measured in CD-1® mice, the presence of Colo205 tumors and the application of clearly higher doses (84 µg to 111 µg protein instead of 25 µg or 50 µg) did not affect the *in vivo* half-lives of the proteins. Furthermore, no accumulation of the proteins due to multiple injections was observed as demonstrated by comparable serum concentrations determined after the first and last treatment. The potential induction of toxicity by the treatments was examined 4 h and 24 h after the first and the last injections (Figure 3.22D). Effects on the liver were assessed by measuring levels of alanine transaminase (ALT) in the serum, whereas pancreatic and renal toxicity was evaluated by determination of amylase activity. Compared to untreated mice, neither bortezomib alone nor combinations with any protein induced elevated levels of ALT or amylase at any analyzed point confirming safety of the treatments.

In contrast to the *in vitro* data, no beneficial impact of targeting EGFR was observed *in vivo* in the above represented experiment. Since all proteins induced complete tumor regression, another study was performed using lower doses of scFvhu225-Fc-scTRAIL and Fc-scTRAIL to investigate potential targeting effects in more detail. The treatment comprised six administrations of 5 µg bortezomib (i.p.) and 0.3 nmol or 0.1 nmol protein (corresponding to 0.6 nmol and 0.2 nmol scTRAIL units; i.v.) twice a week. Application of the higher doses again induced almost complete and persisting tumor remission for both proteins (Figure 3.23A), but only partial remission and regrowth were observed for treatment with a dose of 0.1 nmol. After 67 days, tumor volumes of mice treated with 0.1 nmol scFvhu225-Fc-scTRAIL were higher than those of mice receiving 0.1 nmol Fc-scTRAIL, but significant differences were only detected between treatment with 0.1 nmol scFvhu225-Fc-scTRAIL and the higher dose of both proteins (Figure 3.23B). The analyzed serum concentrations of the constructs were consistent with the previously described data and reflected the respective doses (Figure 3.23C).

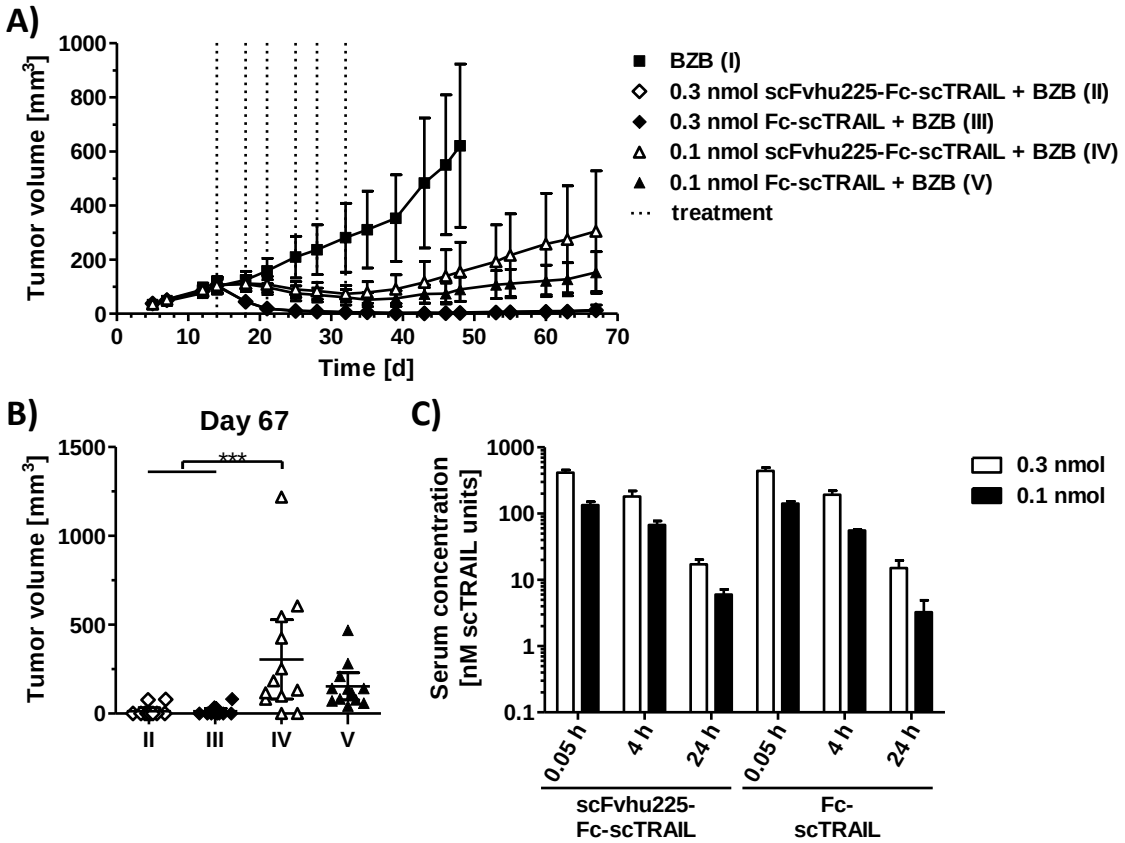

Figure 3.23: Anti-tumor effects and PK of scFvhu225-Fc-scTRAIL and Fc-scTRAIL in combination with bortezomib. A) NMRI nude mice (6 mice per group) with established Colo205 tumors were treated with BZB (5 µg; i.p.) and protein (0.3 nmol or 0.1 nmol protein corresponding to 0.6 nmol or 0.2 nmol scTRAIL units, respectively; i.v.) twice a week for three weeks (days 14, 18, 21, 25, 28, 32). Treatments are indicated with dotted lines. B) Tumor volumes of groups II to V at day 67 are shown (numbering of groups according to A). Statistical analysis was performed by One-Way ANOVA, followed by Tukey's post hoc test (*P<0.05; **P<0.01; ***P<0.001; ns, P>0.05). C) PK was analyzed by determination of the serum concentrations 3 min, 4 h, and 24 h after the first treatment (day 14) by ELISA.

Since no favorable effects of targeting EGFR, but also no variations due to differences in the PK of the molecules were observed in the previous experiments, a final study was performed investigating Dbhu225-scTRAIL, scFvhu225-EHD2-scTRAIL, scFvhu225-Fc-scTRAIL, and Fc-scTRAIL in the absence of bortezomib. Mice received six i.v. injections of 0.2 nmol protein (corresponding to 0.4 nmol scTRAIL units) twice a week. While treatment with both Fc constructs resulted in almost complete tumor remission, only a retardation of tumor growth was seen for Dbhu225- and scFvhu225-EHD2-scTRAIL (Figure 3.24A). Compared to control mice, tumor volumes of all protein-treated groups were significantly reduced at day 47 (Figure 3.24B). Yet, significant differences between the different proteins were only obtained for Fc-scTRAIL versus Dbhu225-scTRAIL and scFvhu225-EHD2-scTRAIL. Serum concentrations of the molecules fitted the PK data determined before (Figure 3.24C). Again, no liver toxicity was induced as examined by measuring ALT levels (Figure 3.24D). Thus, this final PD experiment

demonstrated higher activity of the longer-circulating Fc constructs, but no favorable influence of fusion to an antibody moiety was found.

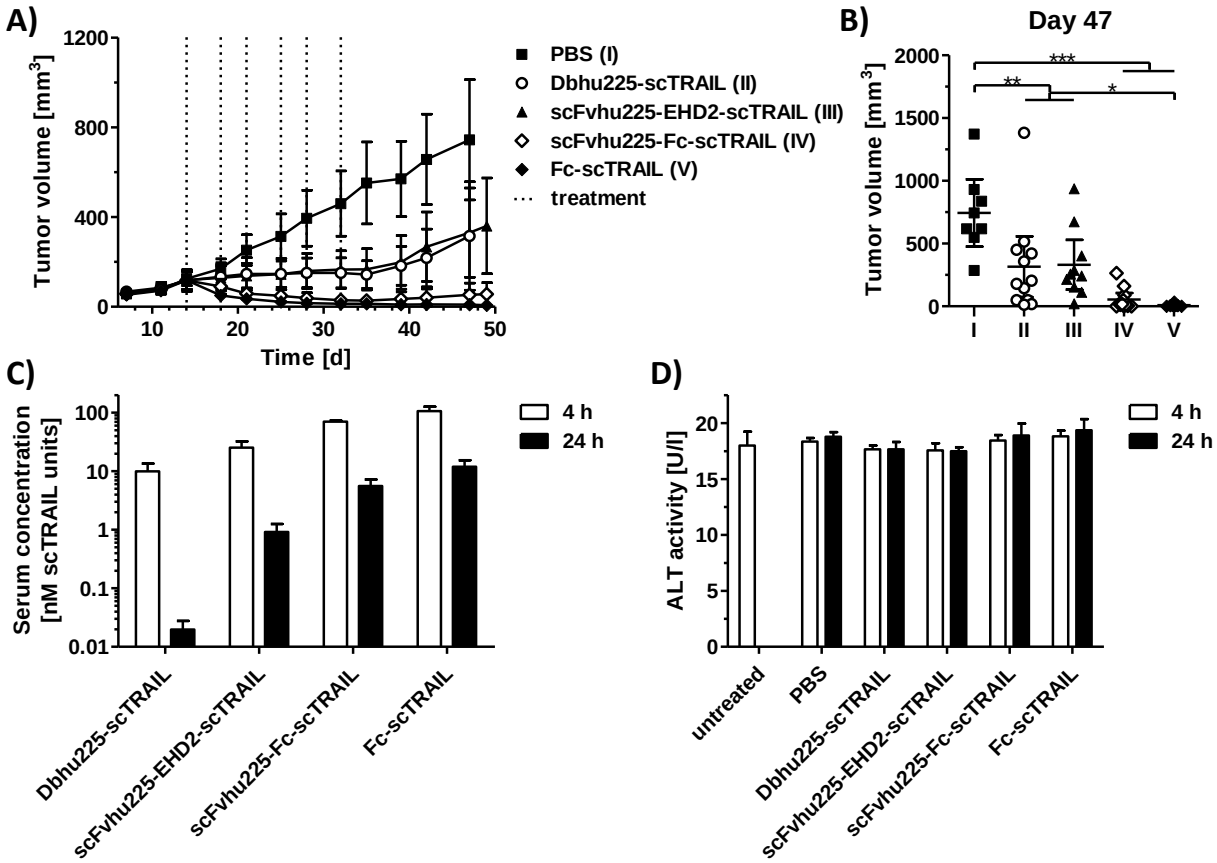

Figure 3.24: *In vivo* effects and PK of different formats of EGFR-targeting scTRAIL fusion proteins and Fc-scTRAIL in the absence of bortezomib. A) NMRI nude mice bearing Colo205 tumors (6 mice per group) received six i.v. treatments with 0.2 nmol protein (corresponding to 0.4 nmol scTRAIL units) or PBS as control. Dotted lines indicate the days of treatment (days 14, 18, 21, 25, 28, 32). B) Statistical analysis of tumor volumes of groups I to IV (numbering of groups according to A) at day 47 was done by One-Way ANOVA, followed by Tukey's post hoc test (*P<0.05; **P<0.01; ***P<0.001; ns, P>0.05). C) Serum concentrations 4 h and 24 h after the last treatment (day 32) were determined by ELISA. D) To measure potential toxic effects, ALT activity was analyzed 4 h and 24 h after the last treatment.

Summing up all data generated for the EGFR- and non-targeting scTRAIL fusion proteins, all targeted formats exerted better *in vitro* effects than the non-targeted dimeric molecule that in turn was superior to scTRAIL. Furthermore, highest yields were achieved for the Fc fusion proteins. *In vivo* PK studies revealed longest half-lives for the Fc constructs that probably translated into enhanced therapeutic activity at a dose of 0.2 nmol protein in the absence of bortezomib. However, the analyzed settings failed to confirm the beneficial impact of targeting *in vivo*.

3.2.2 HER2-targeting scTRAIL fusion proteins

3.2.2.1 Biochemical characterization

As outlined before, further validation of the different targeted dimeric scTRAIL formats, i.e. Db-scTRAIL, dsDb-scTRAIL, scFv-EHD2-scTRAIL, and scFv-Fc-scTRAIL, was done by exchanging the targeting moieties. Fusion proteins directed against HER2 were based on recombinant antibodies containing the 4D5 targeting moiety (see 3.1.2). All molecules were produced with yields in the range of 1.8 to 12.7 mg protein per liter cell culture supernatant (Table 3.9) confirming considerably better production properties of the Fc construct. SDS-PAGE verified purity and integrity of all proteins, but also identified bands of higher molecular masses under non-reducing conditions (Figure 3.25A). Size exclusion HPLC was performed to investigate the proteins under native conditions. All molecules eluted as one predominant peak of the expected size (Figure 3.25B) with a small amount of high molecular weight species detected for scFv4D5-Fc-scTRAIL, and even higher amounts observed for scFv4D5-EHD2-scTRAIL and dsDb4D5-scTRAIL. Hydrodynamic radii ranged from 5.3 nm to 6.7 nm (Table 3.9) and were thus comparable to those of the corresponding EGFR-targeting formats (Table 3.5). Dynamic light scattering revealed melting points of 54 °C to 63 C again indicating better thermal stability of the EHD2 and Fc constructs than of the diabody molecules (Table 3.9).

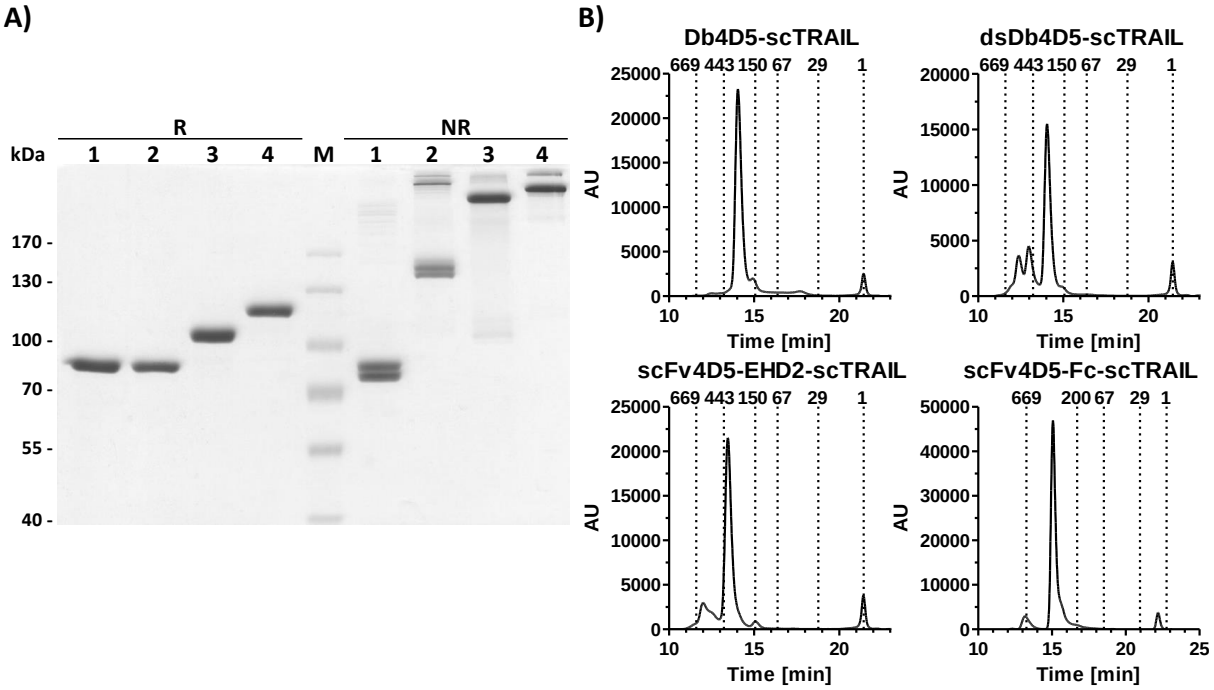

Figure 3.25: Biochemical characterization of HER2-targeting scTRAIL fusion proteins. A) Db4D5-scTRAIL (1), dsDb4D5-scTRAIL (2), scFv4D5-EHD2-scTRAIL (3), and scFv4D5-Fc-scTRAIL (4) were analyzed in SDS-PAGE (8 % PAA) under reducing (R) and non-reducing conditions (NR). 2 µg of protein were loaded per lane and stained with Coomassie Brilliant Blue. M, protein marker. B) Proteins were separated depending on their sizes by HPLC. Elution points of standard proteins and their respective molecular masses [kDa] are indicated with dotted lines.

3.2.2.2 Evaluation of binding properties

The binding capacities provided by the antibody and scTRAIL moieties were validated by investigating binding to HER2 as well as to human TRAIL-R2 in ELISA (Figure 3.26). All proteins bound in a concentration-dependent manner to both target proteins. HER2 binding properties were with EC_{50} values of 4.3 nM to 9.3 nM scTRAIL units (Table 3.9) similar to those of the respective recombinant antibodies (Table 3.2), and binding to huTRAIL-R2 was comparable to that detected for the EGFR- and non-targeting molecules (Table 3.6). Further binding studies were performed by flow cytometry (Figure 3.26) measuring half-maximal binding to Colo205 cells at concentrations of 14.9 nM to 28.2 nM scTRAIL units (Table 3.9). Statistical analysis of the EC_{50} values of the ELISA and flow cytometry studies identified significantly reduced binding of Db4D5-scTRAIL to HER2 ($P<0.05$), whereas significantly increased binding of this molecule compared to scFv4D5-Fc-scTRAIL was detected on Colo205 cells ($P<0.05$), and no significant differences were observed for human TRAIL-R2 binding ($P>0.05$). Hence, there are no consistent differences in the binding properties of the HER2-targeting scTRAIL formats.

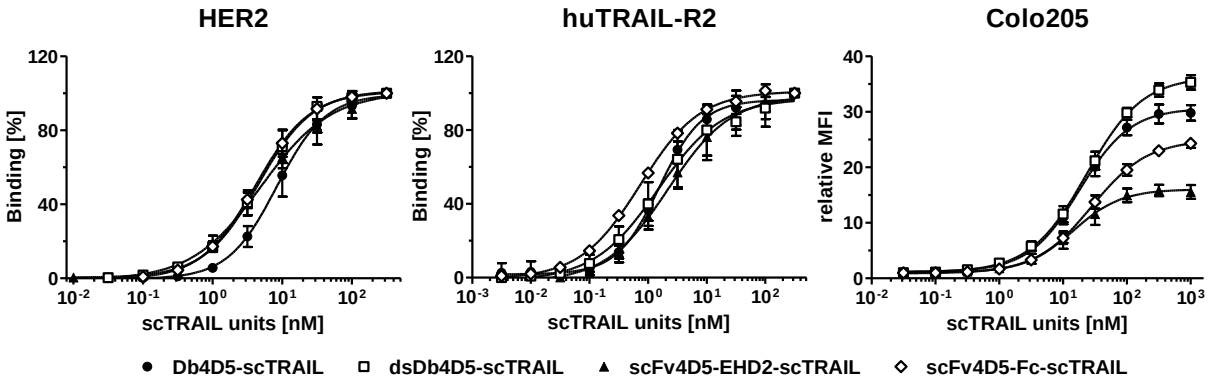

Figure 3.26: Binding studies of HER2-targeting scTRAIL molecules. Binding to receptor-Fc fusion proteins was evaluated by ELISA. 300 ng HER2-Fc or 200 ng huTRAIL-R2-Fc were coated per well. Bound proteins were detected with an anti-FLAG-HRP conjugate. Optical densities measured at 450 nm were normalized to the value determined for the highest concentration analyzed. Binding to Colo205 cells was investigated by flow cytometry detecting bound proteins using a PE-conjugated anti-FLAG antibody. Concentrations refer to scTRAIL units.

Table 3.9: Biochemical and binding properties of HER2-targeting scTRAIL fusion proteins. Molecular masses (M) were calculated based on the amino acid sequence. Yields are expressed as mg protein per liter cell culture supernatant. Stokes radii (S_r) and melting points (T_M) were determined by size exclusion HPLC and dynamic light scattering, respectively. Half-maximal binding was analyzed by ELISA (HER2-, huTRAIL-R2-Fc) and flow cytometry (Colo205 cells) and is represented as nM of scTRAIL units.

Protein	M [kDa]	Yield [mg/l]	S_r [nm]	T_M [°C]	EC_{50} HER2 [nM]	EC_{50} huTRAIL-R2 [nM]	EC_{50} Colo205 [nM]
Db4D5-scTRAIL	168	1.8	5.3	54	9.3 ± 2.9	1.5 ± 0.2	18.3 ± 3.1
dsDb4D5-scTRAIL	168	2.3	5.3	56	4.7 ± 1.0	2.2 ± 1.6	23.3 ± 3.7
scFv4D5-EHD2-scTRAIL	194	2.1	5.9	57	5.1 ± 1.3	2.4 ± 0.7	14.9 ± 3.7
scFv4D5-Fc-scTRAIL	222	12.7	6.7	63	4.3 ± 0.6	0.7 ± 0.04	28.2 ± 3.0

3.2.2.3 Induction of cell death *in vitro*

Bioactivity of the molecules was determined by investigating their potential to induce cell death on two colorectal carcinoma cell lines. All proteins were capable of inducing cell death on Colo205 cells alone or in combination with bortezomib (Figure 3.27A). Compared to dsDb4D5-scTRAIL and scFv4D5-Fc-scTRAIL that elicited 50 % cell death at concentrations of 40.5 pM and 58.6 pM in the absence of bortezomib, lower activity was observed for Db4D5-scTRAIL and scFv4D5-EHD2-scTRAIL ($P<0.001$; Table 3.10). Since high molecular weight species were not only detected for dsDb4D5-scTRAIL and scFv4D5-Fc-scTRAIL, but also for scFv4D5-EHD2-scTRAIL (Figure 3.25), the SEC results are only partially able to explain the differences in cell death induction. Preincubation with bortezomib showed the desired sensitization (significant decrease in EC_{50} values with $P<0.001$) with similar variations in the activity profiles of the different formats.

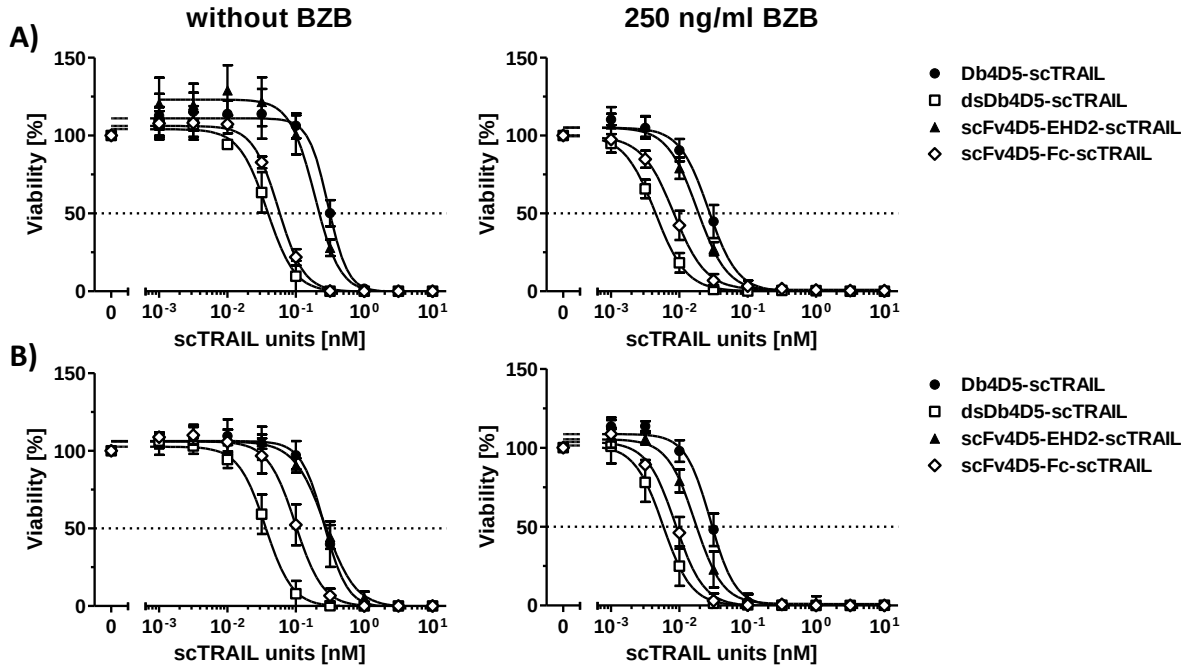

Figure 3.27: Cell death induction of HER2-targeting scTRAIL molecules on Colo205 cells. A) Colo205 cells (50,000/well) were cultivated overnight. After preincubation with medium or BZB (250 ng/ml) for 30 min, cells were treated with serial dilutions of the proteins for 16 h. Viable cells were stained with crystal violet. B) In order to analyze the effects of targeting HER2, cells were pretreated with a 200-fold molar excess of trastuzumab in medium or medium containing BZB (250 ng/ml). All other steps were performed as described in A. Concentrations refer to scTRAIL units.

Although the HER2-targeting recombinant antibodies alone did not exert any effects on Colo205 cells (Figure 3.5C), further studies were performed after pretreatment with a 200-fold molar excess of trastuzumab to analyze the potential contribution of targeting HER2 of the scTRAIL molecules (Figure 3.27B). In contrast to the results of the EGFR-targeting fusion

proteins, no significant alterations in cell death induction (P>0.05) were measured for the scTRAIL constructs directed against HER2 under blocking conditions, except for scFv4D5-Fc-scTRAIL in the absence of bortezomib (P<0.05). This indicates that the HER2-targeting 4D5 antibody moieties have no effect on cell death induction of the respective fusion proteins (Table 3.10).

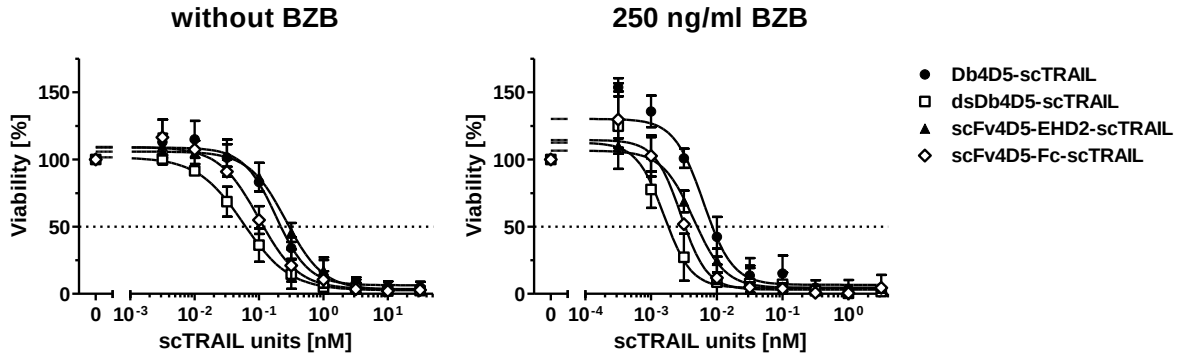

Figure 3.28: Cell death induction of HER2-targeting scTRAIL molecules on HCT116 cells. Prior to treatment of HCT116 cells (15,000/well) with serial dilutions of the proteins for 16 h, cells were preincubated with medium or BZB (250 ng/ml) for 30 min. Viable cells were visualized by crystal violet staining. Concentrations refer to scTRAIL units.

The activity of the HER2-targeting scTRAIL molecules demonstrated for Colo205 cells was confirmed using HCT116 cells (Figure 3.28). Similar to the results obtained for Colo205 cells, dsDb4D5-scTRAIL and scFv4D5-Fc-scTRAIL showed with EC_{50} values of 66.4 pM and 125.1 pM in the absence of bortezomib better effects than the other two formats (P<0.05; Table 3.10). Preincubation with bortezomib strongly sensitized the cells for treatment with the HER2-targeting scTRAIL molecules as illustrated by 25- to 57-fold lower EC_{50} values (P<0.01).

Table 3.10: EC_{50} values of cell death induction of HER2-targeting scTRAIL molecules. Effects on Colo205 and HCT116 cells were analyzed after preincubation with medium or BZB (250 ng/ml) and treatment with the proteins for 16 h. Additional studies were performed in the presence of a 200-fold molar excess of trastuzumab to block binding of the molecules to HER2. EC_{50} values are represented as pM scTRAIL units.

Protein	Colo205				HCT116	
	without trastuzumab		with trastuzumab		without trastuzumab	
	without BZB	with BZB	without BZB	with BZB	without BZB	with BZB
Db4D5-scTRAIL	319.9 ± 27.4	27.9 ± 4.9	270.1 ± 51.4	30.3 ± 4.6	227.8 ± 33.1	9.1 ± 1.6
dsDb4D5-scTRAIL	40.5 ± 7.9	4.5 ± 0.6	37.6 ± 7.8	6.0 ± 1.5	66.4 ± 18.2	2.0 ± 0.6
scFv4D5-EHD2-scTRAIL	224.0 ± 22.1	19.1 ± 1.9	281.7 ± 37.5	18.2 ± 2.9	297.1 ± 42.7	5.2 ± 1.2
scFv4D5-Fc-scTRAIL	58.6 ± 5.3	8.4 ± 1.2	103.1 ± 21.2	9.1 ± 1.2	125.1 ±31.6	3.3 ± 0.2

In summary, comparable binding properties were determined for all HER2-targeting formats, while the highest production yield and best thermal stability was found for the Fc construct. Further differences were detected in cell death induction, but are supposed to be caused by heterogeneities of the protein preparations.

3.2.3 HER3-targeting scTRAIL fusion proteins

3.2.3.1 Biochemical characterization

The third set of targeted dimeric scTRAIL formats was generated using the HER3-targeting moiety 3M6. Additionally, the Db-scTRAIL and scFv-Fc-scTRAIL formats were constructed comprising the 3-43 targeting moiety that already showed better binding properties than the corresponding 3M6-based recombinant antibody (see 3.1.3).

Yields ranged from 1.7 to 8.8 mg protein per liter cell culture supernatant and again confirmed best production properties of the Fc constructs for both targeting moieties (Table 3.11). Purity and integrity of the proteins was verified by SDS-PAGE analysis, however identifying considerable amounts of the monomeric form of dsDb3M6-scTRAIL and scFv3M6-EHD2-scTRAIL under non-reducing conditions (Figure 3.29A). Investigation of the proteins under native conditions by size exclusion HPLC revealed major peaks of the expected size only for the Fc constructs (Figure 3.29B). While approximately half of the protein of Db3-43-scTRAIL remained in its monomeric form, even higher amounts of monomer were detected for scFv3M6-EHD2-scTRAIL and the 3M6-based diabody molecules that were almost completely found as monomers. The hydrodynamic radii determined for the dimeric forms of 5.4 nm to 6.7 nm (Table 3.11) reflected the sizes of the EGFR- and HER2-targeting molecules (Table 3.5, Table 3.9). Dynamic light scattering identified melting points of 57 °C and 61 °C for scFv3M6-Fc-scTRAIL and scFv3-43-Fc-scTRAIL confirming better stability compared to the other formats (Table 3.11).

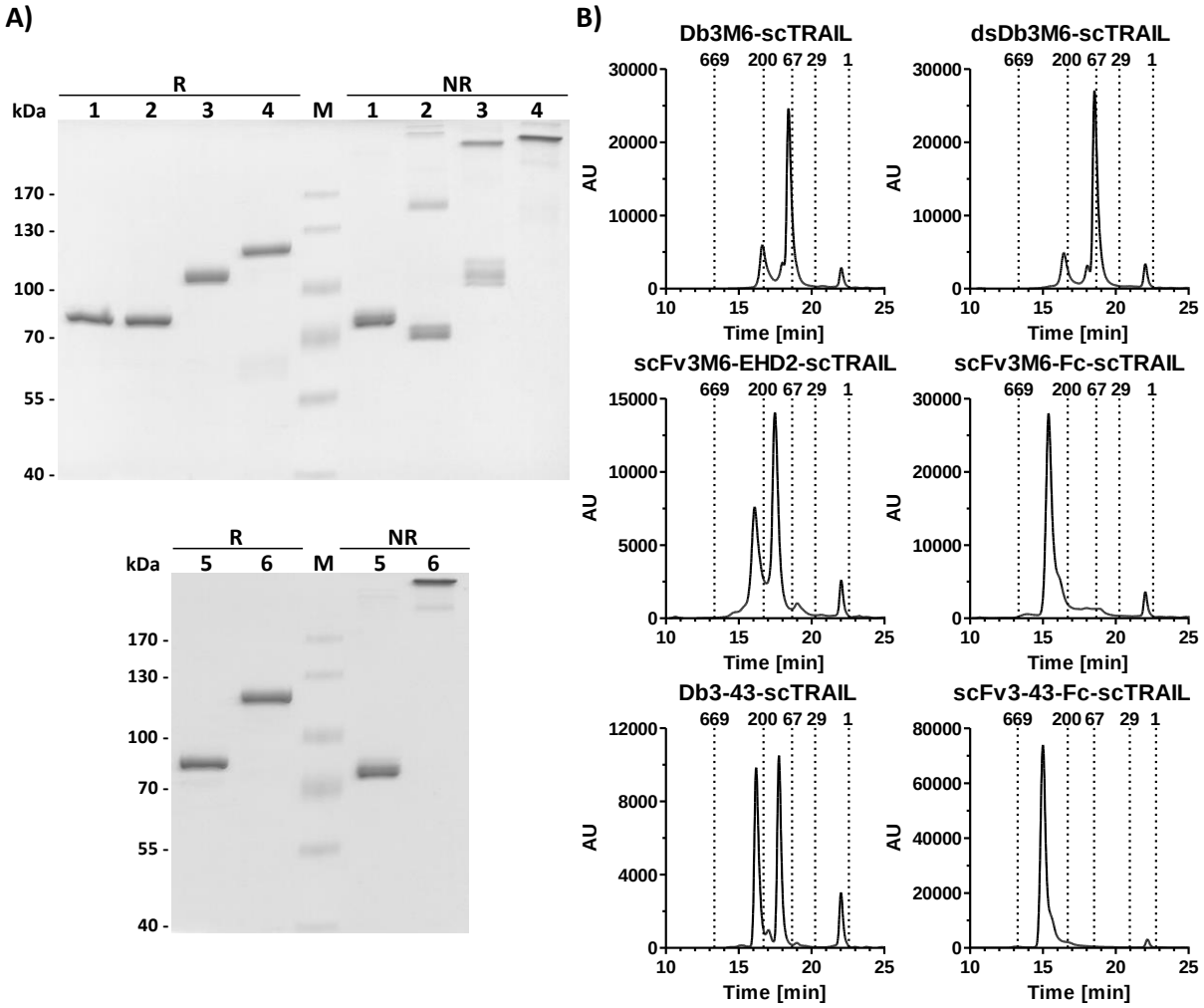

Figure 3.29: Biochemical characterization of HER3-targeting scTRAIL fusion proteins. A) SDS-PAGE (8 % PAA) of Db3M6-scTRAIL (1), dsDb3M6-scTRAIL (2), scFv3M6-EHD2-scTRAIL (3), scFv3M6-Fc-scTRAIL (4), Db3-43-scTRAIL (5), and scFv3-43-Fc-scTRAIL (6) was performed under reducing (R) and non-reducing conditions (NR). 2 µg protein were analyzed per lane. Proteins were stained with Coomassie Brilliant Blue. M, protein marker. B) Size exclusion HPLC was used to investigate proteins under native conditions. Elution times of standard proteins and the corresponding molecular masses [kDa] are indicated.

3.2.3.2 Evaluation of binding properties

Binding studies were performed by ELISA and flow cytometry analyzing binding to HER3, human TRAIL-R2, and Colo205 cells (Figure 3.30). In agreement with the data obtained for the corresponding recombinant antibodies (Table 3.3), the 3M6-based scTRAIL molecules bound to HER3 with EC_{50} values of 3.3 nM to 6.6 nM, whereas half-maximal binding of Db3-43-scTRAIL and scFv3-43-Fc-scTRAIL was detected at significantly lower concentrations of 0.6 nM and 0.3 nM ($P<0.01$), respectively (Table 3.11). Binding to huTRAIL-R2 reflected with EC_{50} values ranging from 2.1 nM to 3.4 nM that determined for the EGFR-, HER2- and non-targeted scTRAIL constructs (Table 3.6, Table 3.9). At low concentrations, both 3-43 molecules

exhibited stronger binding to Colo205 cells than the 3M6-based formats, though no saturation was reached for the Fc constructs for concentrations up to 1 µM.

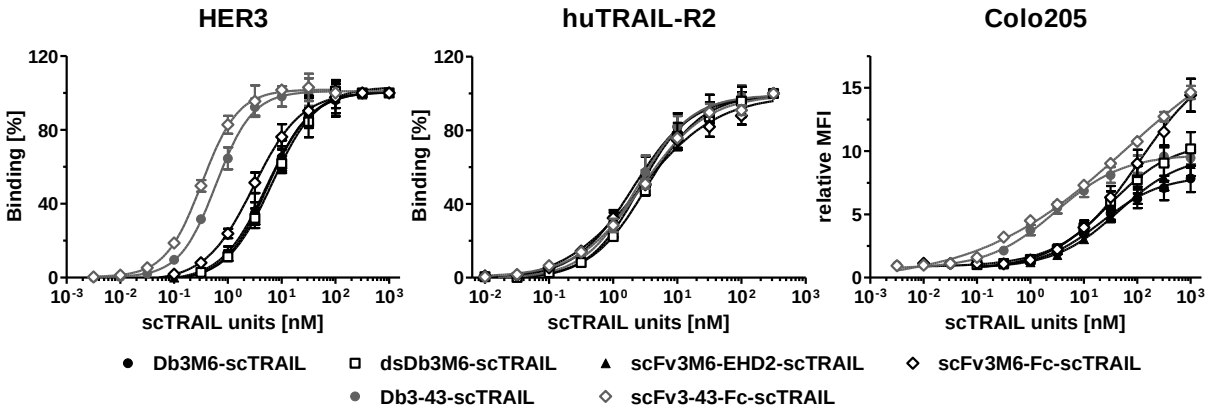

Figure 3.30: Binding studies of HER3-targeting scTRAIL molecules. Binding to receptor-Fc fusion proteins (200 ng/well) was analyzed by ELISA detecting bound proteins with an anti-FLAG-HRP. Optical densities measured at 450 nm were normalized to the value determined for the highest concentration. Binding to Colo205 cells was investigated by flow cytometry. A PE-conjugated anti-FLAG antibody was used for detection of bound proteins. Concentrations refer to scTRAIL units.

Table 3.11: Biochemical and binding properties of HER3-targeting scTRAIL molecules. Molecular masses (M) were calculated based on the amino acid sequence. Yields are expressed as mg protein per liter cell culture supernatant. Size exclusion HPLC and dynamic light scattering were performed to determine Stokes radii (S_r) and melting points (T_M), respectively. Half-maximal binding was analyzed by ELISA (HER3-, huTRAIL-R2-Fc) and flow cytometry (Colo205 cells). Concentrations refer to scTRAIL units.

Protein	M [kDa]	Yield [mg/l]	S_r [nm]	T_M [°C]	EC_{50} HER3 [nM]	EC_{50} huTRAIL-R2 [nM]	EC_{50} Colo205 [nM]
Db3M6-scTRAIL	167	1.9	5.4	52	5.6 ± 1.0	2.7 ± 0.4	20.4 ± 1.8
dsDb3M6-scTRAIL	167	1.7	5.6	52	6.6 ± 0.9	3.4 ± 0.3	29.1 ± 1.6
scFv3M6-EHD2-scTRAIL	193	1.9	5.9	55	5.7 ± 1.3	2.1 ± 0.2	44.4 ± 0.7
scFv3M6-Fc-scTRAIL	221	3.8	6.6	57	3.3 ± 0.3	2.6 ± 0.1	(112.0 ± 17.9)‡
Db3-43-scTRAIL	169	1.9	5.8	52	0.6 ± 0.03	2.5 ± 0.7	3.1 ±0.5
scFv3-43-Fc-scTRAIL	222	8.8	6.7	61	0.3 ± 0.01	2.9 ± 0.3	(68.0 ± 9.4)‡

‡, no saturation reached.

3.2.3.3 Induction of cell death *in vitro*

Bioactivity of the molecules was assessed by investigation of their potential to induce cell death on Colo205 and HCT116 cells. All HER3-targeting fusion proteins showed concentration-dependent induction of cell death on Colo205 cells in the absence and presence of bortezomib (Figure 3.31A). Significant differences in the activities of different formats comprising the same antibody moieties were found, but are supposed to result from the substantial heterogeneities of the protein preparations (Figure 3.29B). Comparison of the homogeneously formed scFv3M6-Fc-scTRAIL and scFv3-43-Fc-scTRAIL molecules revealed significantly stronger effects of the 3-43-based fusion protein ($P<0.001$). These differences were found for

pretreatment with medium as well as with bortezomib that sensitized the cells as indicated by significantly lower EC_{50} values (P<0.001; Table 3.12).

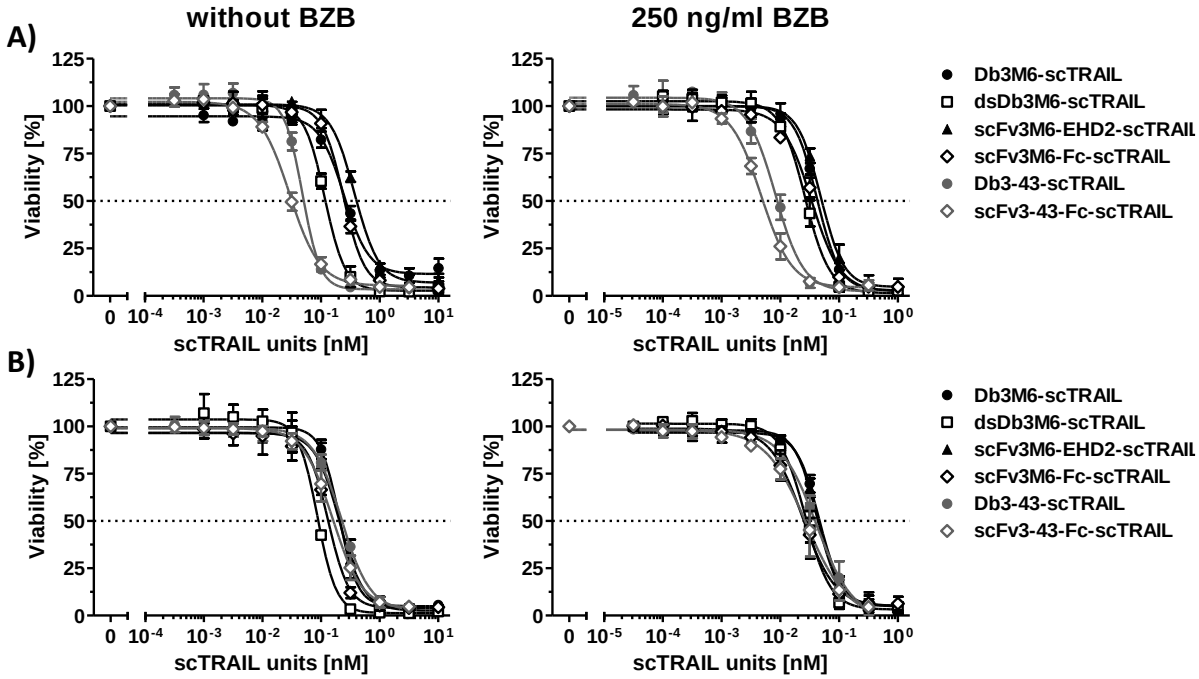

Figure 3.31: Cell death induction of HER3-targeting scTRAIL molecules on Colo205 cells. A) Colo205 cells (50,000/well) were preincubated with medium or BZB (250 ng/ml) for 30 min and treated with serial dilutions of the proteins. After 16 h, viable cells were stained with crystal violet. B) Binding of the molecules to HER3 was blocked by pretreatment of the cells with a 200-fold molar excess of scFv3M6-Fc or scFv3-43-Fc in medium or medium containing BZB (250 ng/ml). Remaining experimental set-up is described in A. Concentrations refer to scTRAIL units.

Further studies were performed to analyze the impact of HER3 targeting by the different targeting moieties (Figure 3.31B). Experiments with the recombinant antibodies already demonstrated no influence for the 3M6 molecules, while scFv3-43-Fc seemed to exert inhibitory effects on Colo205 cells (Figure 3.7C, Figure 3.8D). The EC_{50} values obtained for the 3M6-based fusion proteins after pretreatment with a 200-fold molar excess of scFv3M6-Fc did either not differ significantly from those observed in the absence of the blocking antibody or were even significantly reduced (P<0.05) instead of increased. However, preincubation with excess amounts of scFv3-43-Fc led to a 4- to 5-fold increase in the EC_{50} values of Db3-43-scTRAIL and scFv3-43-Fc-scTRAIL in the absence and presence of bortezomib (P<0.01) corresponding to activity levels similar to those of the 3M6 constructs (Table 3.12). This indicates that targeting HER3 via the 3M6 moiety is not able to improve the properties of the respective scTRAIL fusion proteins. In contrast, the 3-43-based molecules that exhibit better binding to HER3 show clearly enhanced induction of cell death.

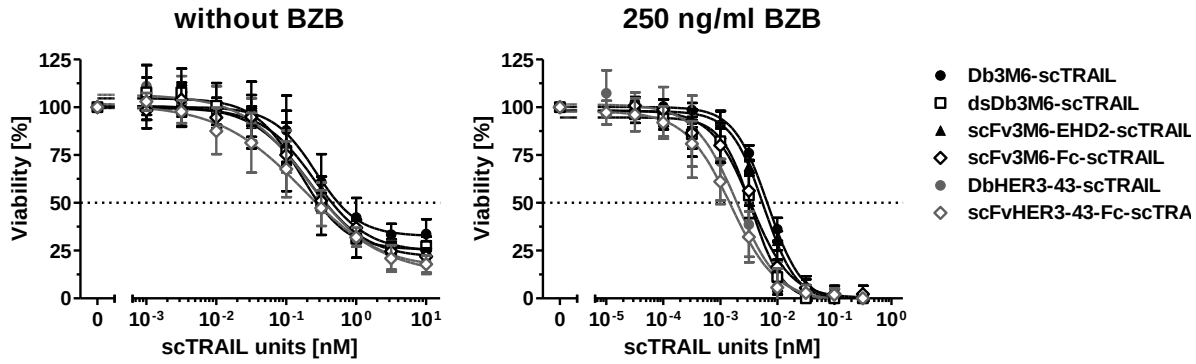

Figure 3.32: Cell death induction of HER3-targeting scTRAIL molecules on HCT116 cells. After preincubation with medium or BZB (250 ng/well) for 30 min, cells (15,000/well) were treated with serial dilutions of the proteins for 16 h. Cell viability was determined by crystal violet staining. Concentrations refer to scTRAIL units.

The activities of the HER3-targeting molecules were further validated on HCT116 cells (Figure 3.32). All fusion proteins were able to induce cell death in the absence and presence of bortezomib. Differing from the data obtained for Colo205 cells, similar effects were observed for all 3M6- and 3-43-based molecules with EC_{50} values ranging from 272.8 pM to 593.2 pM in the absence of bortezomib ($P>0.05$). Preincubation with bortezomib strongly sensitized the cells reducing the EC_{50} values by factors of 81 to 168 ($P<0.05$; Table 3.12).

Table 3.12: EC_{50} values of cell death induction of HER3-targeting scTRAIL molecules. After preincubation with medium or BZB (250 ng/ml), Colo205 or HCT116 cells were treated with the proteins for 16 h. Further studies were performed adding a 200-fold molar excess of scFv3M6-Fc or scFv3-43-Fc to the preincubation medium. EC_{50} values are represented as pM scTRAIL units.

Protein	Colo205				HCT116	
	without blocking antibody		with blocking antibody		without blocking antibody	
	without BZB	with BZB	without BZB	with BZB	without BZB	with BZB
Db3M6-scTRAIL	264.1 ± 21.1	43.0 ± 2.2	209.5 ± 6.0	46.6 ± 3.4	593.2 ± 289.6	6.7 ± 0.8
dsDb3M6-scTRAIL	119.8 ± 9.5	27.3 ± 2.9	88.7 ± 4.4	28.0 ± 3.2	319.8 ± 173.4	3.4 ± 0.9
scFv3M6-EHD2-scTRAIL	402.0 ± 16.8	51.1 ±5.3	204.1 ± 49.0	44.0 ± 4.7	446.2 ± 100.1	5.5 ± 0.6
scFv3M6-Fc-scTRAIL	251.3 ± 12.2	34.1 ± 3.0	132.3 ± 6.3	25.8 ± 6.4	370.2 ± 83.0	3.5 ± 1.4
Db3-43-scTRAIL	50.6 ± 1.6	8.9 ± 1.1	226.7 ± 11.4	40.1 ± 6.1	348.1 ± 99.9	2.2 ± 1.1
scFv3-43-Fc-scTRAIL	32.1 ± 3.2	5.1 ± 0.6	163.9 ± 31.2	27.8 ± 8.4	272.8 ± 144.3	1.6 ± 0.8

In conclusion, the 3-43 scTRAIL molecules showed improved HER3-binding activity compared to the 3M6-based fusion proteins. Furthermore, superior properties were identified for both Fc constructs with respect to production yield, stability, and reliable formation of the dimer. Variations in the capability of different formats comprising the same targeting moiety to induce cell death were attributed to heterogeneities of the protein preparations, but

beneficial effects of the 3-43-based fusion proteins were found, yet only on Colo205 cells, indicating a role of binding strength on cell death induction.

3.2.4 EpCAM-targeting scTRAIL fusion proteins

3.2.4.1 Biochemical characterization

To finally validate the different formats of targeted dimeric scTRAIL molecules, Db-scTRAIL, scFv-EHD2-scTRAIL, and scFv-Fc-scTRAIL fusion proteins were generated containing the EpCAM-targeting moiety 323/A3hu3 (see 3.1.4). With 5.2 mg protein per liter cell culture supernatant, a 6- to 7-fold higher yield was achieved for scFv323/A3hu3-Fc-scTRAIL compared to the other formats (Table 3.13). SDS-PAGE analysis confirmed purity and integrity of all proteins under denaturing reducing and non-reducing conditions (Figure 3.33A).

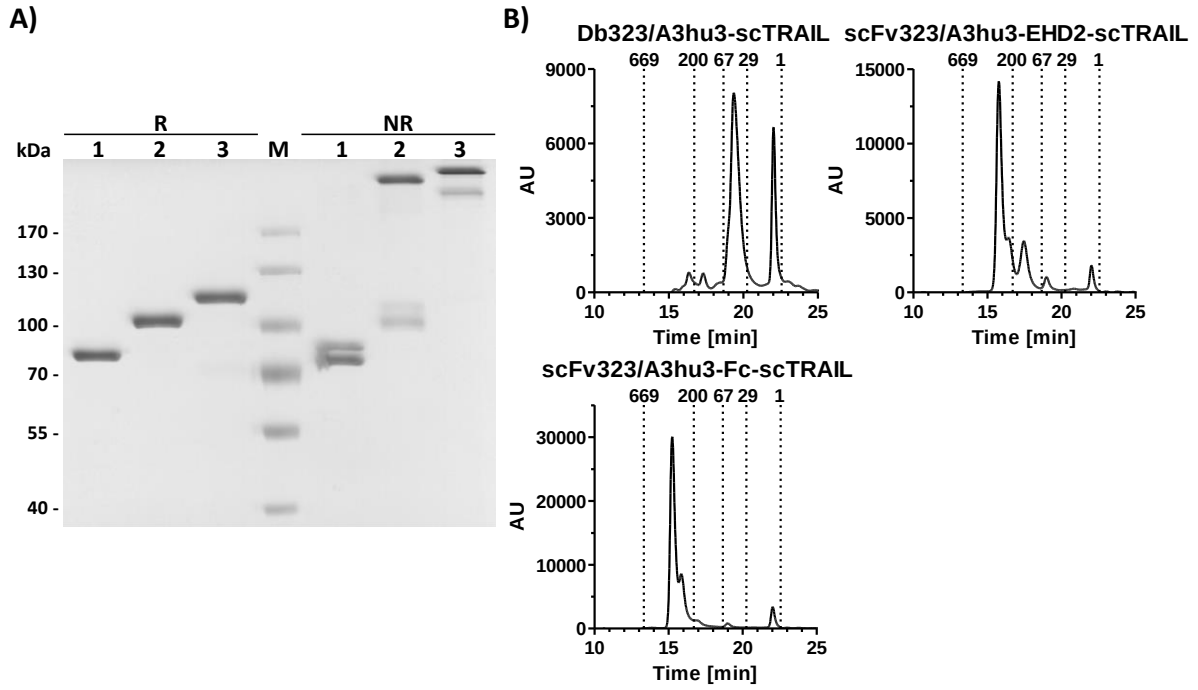

Figure 3.33: Biochemical characterization of EpCAM-targeting scTRAIL fusion proteins. A) Db323/A3hu3-scTRAIL (1), scFv323/A3hu3-EHD2-scTRAIL (2), and scFv323/A3hu3-Fc-scTRAIL (3) were analyzed in SDS-PAGE (8 % PAA) under reducing (R) and non-reducing conditions (NR). 2 µg protein were loaded per lane and proteins were stained with Coomassie Brilliant Blue. M, protein marker. B) Size exclusion HPLC was performed to investigate proteins under native conditions. Elution times of standard proteins and their respective molecular masses [kDa] are indicated with dotted lines.

Under native conditions examined by size exclusion HPLC, scFv323/A3hu3-EHD2-scTRAIL and scFv323/A3hu3-Fc-scTRAIL eluted as one major peak corresponding to the expected size (Figure 3.33B), whereas only a small amount of the correctly assembled dimer was detected for the diabody fusion protein. The considerable peak of FLAG peptide seen for the latter molecule becomes apparent due to the low concentration of the fusion protein itself. Protein

fractions of smaller size were additionally found for the EHD2 and Fc constructs. The hydrodynamic radii were determined for the dimeric forms of the proteins and ranged from 5.7 nm to 6.7 nm (Table 3.13), which resembles the above described data. Thermal stability was measured by dynamic light scattering identifying a melting point of 60 °C for the Fc molecule that is 7 °C and 4 °C higher than those of Db323/A3hu3-scTRAIL and scFv323/A3hu3-EHD2-scTRAIL, respectively (Table 3.13).

3.2.4.2 Evaluation of binding properties

Binding properties of the EpCAM-targeting scTRAIL molecules were evaluated by ELISA and flow cytometry by determination of binding to EpCAM, human TRAIL-R2, and Colo205 cells (Figure 3.34). ScFv323/A3hu3-EHD2-scTRAIL and scFv323/A3hu3-Fc-scTRAIL bound to EpCAM with similar EC_{50} values of 2.7 nM and 2.5 nM ($P>0.05$; Table 3.13), while the diabody construct exhibited significantly weaker binding ($P<0.001$) and did not reach saturation levels for concentrations up to 300 nM. Similarly, half-maximal binding of the EHD2 and Fc molecules to human TRAIL-R2 was detected at a concentration of 1.5 nM, whereas Db323/A3hu3-scTRAIL required a significantly higher concentration of 2.7 nM ($P<0.01$; Table 3.13). This indicates that antigen and TRAIL-R2 binding are affected by the insufficient dimer formation of Db323/A3hu3-scTRAIL (Figure 3.33B). With an EC_{50} value of 85.6 nM for binding to Colo205 cells, the diabody construct again showed lower binding activity ($P<0.001$) compared to 15.1 nM and 9.8 nM measured for scFv323/A3hu3-EHD2-scTRAIL and scFv323/A3hu3-Fc-scTRAIL, respectively (Table 3.13).

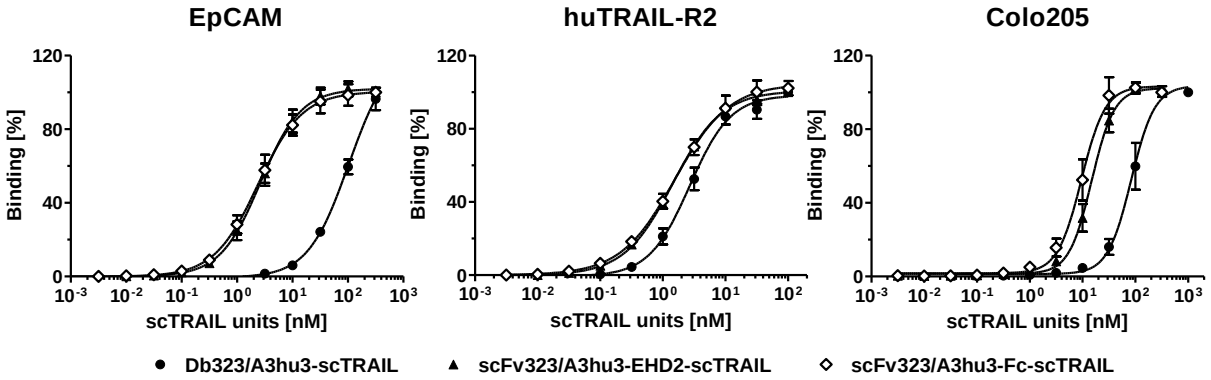

Figure 3.34: Binding studies of EpCAM-targeting scTRAIL molecules. Binding to sEpCAM and huTRAIL-R2-Fc (each 200 ng/well) was analyzed by ELISA detecting bound proteins with an anti-FLAG-HRP. OD was measured at 450 nm. Flow cytometry was performed to investigate binding to Colo205 cells. A PE-conjugated anti-FLAG antibody was used for detection. Data were normalized to the value determined for the highest concentration. Concentrations refer to scTRAIL units.

Table 3.13: Biochemical and binding properties of EpCAM-targeting scTRAIL molecules. Molecular masses (M) were calculated based on the amino acid sequence. Yields are expressed as mg protein per liter cell culture supernatant. Stokes radii (S_r) and melting points (T_M) were determined by size exclusion HPLC and dynamic light scattering, respectively. EC_{50} values of binding to sEpCAM and huTRAIL-R2-Fc (ELISA), as well as to Colo205 cells (flow cytometry) are represented as nM scTRAIL units.

Protein	M [kDa]	Yield [mg/l]	S_r [nm]	T_M [°C]	EC_{50} EpCAM [nM]	EC_{50} huTRAIL-R2 [nM]	EC_{50} Colo205 [nM]
Db323/A3hu3-scTRAIL	169	0.7	5.7	53	(118.0 ± 33.7)‡	2.7 ± 0.4	85.6 ± 17.7
scFv323/A3hu3-EHD2-scTRAIL	195	0.9	6.2	56	2.7 ± 0.4	1.5 ± 0.1	15.1 ± 2.3
scFv323/A3hu3-Fc-scTRAIL	223	5.2	6.7	60	2.5 ± 0.5	1.5 ± 0.2	9.8 ± 1.9

‡, no saturation reached.

3.2.4.3 Induction of cell death *in vitro*

As already described above, bioactivity of the molecules was investigated by analyzing cell death induction on Colo205 and HCT116 cells. In the absence and presence of bortezomib, all EpCAM-targeting molecules were capable of inducing cell death on Colo205 cells (Figure 3.35A). Resembling the Colo205 binding data (Table 3.13), the EHD2 and Fc constructs exerted with EC_{50} values of 85.5 pM und 57.2 pM in the absence of bortezomib similar effects ($P>0.05$) that were 7- to 10-fold stronger than the activity observed for Db323/A3hu3-scTRAIL ($P<0.05$; Table 3.14). Comparable differences between the formats were found in the presence of bortezomib that significantly increased cell death induction ($P<0.05$).

Experiments with scFv323/A3hu3-Fc did not reveal an influence of the recombinant antibody alone on Colo205 cells (Figure 3.9D). Evaluation of a potential contribution of the EpCAM-targeting antibody moiety on cell death induction of the scTRAIL molecules was performed by preincubation of the cells with a 200-fold molar excess of scFv323/A3hu3-Fc (Figure 3.35B). This induced an increase in the EC_{50} values of Db323/A3hu3-scTRAIL by factors of 4 and 2 in the absence ($P<0.05$) and presence of bortezomib ($P<0.01$), respectively. Interestingly, similar ($P>0.05$) or even significantly lower values ($P<0.05$) were detected for the EHD2 and Fc constructs under blocking conditions (Table 3.14).

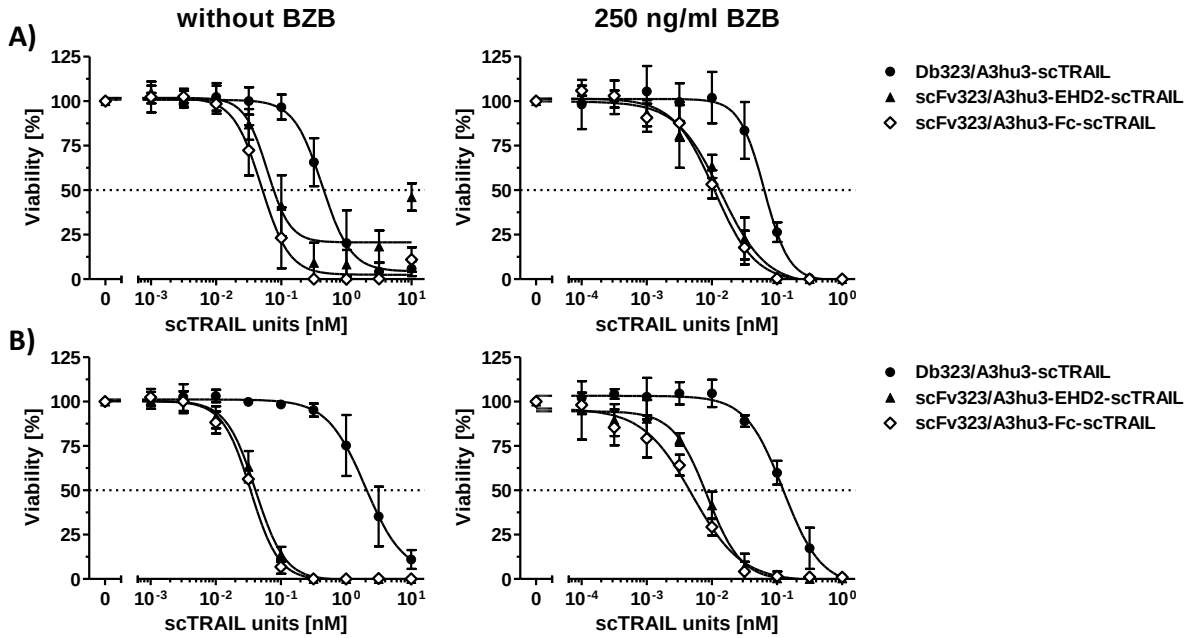

Figure 3.35: Cell death induction of EpCAM-targeting scTRAIL molecules on Colo205 cells. A) Cells (50,000/well) were treated with serial dilutions of the proteins for 16 h after preincubation with medium or BZB (250 ng/ml) for 30 min. Viable cells were stained with crystal violet. B) A 200-fold molar excess of scFv323/A3hu3-Fc was added during preincubation, while all other steps were performed as described in A. Concentrations refer to scTRAIL units.

Experiments using HCT116 cells confirmed the capability of the EpCAM-targeting scTRAIL fusion proteins to induce cell death (Figure 3.36). Reflecting the results obtained for Colo205 cells, the EHD2 and Fc molecules elicited similar ($P>0.05$) and considerably stronger effects compared to Db323/A3hu3-scTRAIL ($P<0.05$) in the absence as well as in presence of bortezomib (Table 3.14).

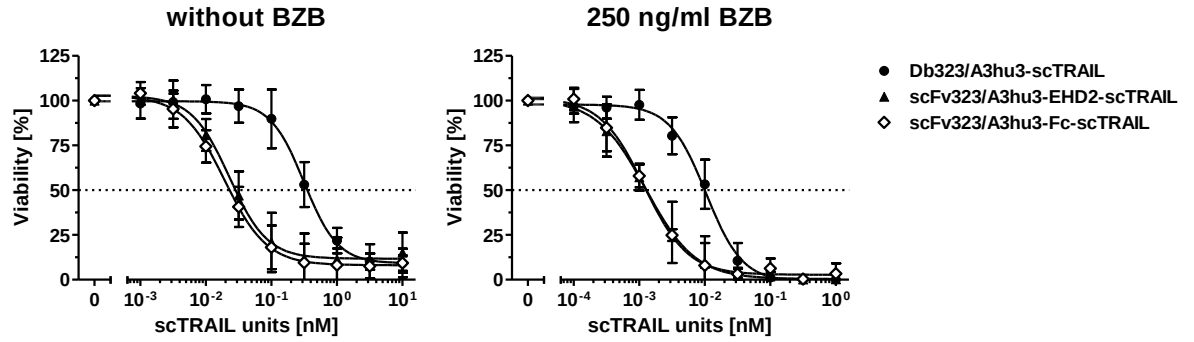

Figure 3.36: Cell death induction of EpCAM-targeting scTRAIL molecules on HCT116 cells. HCT116 cells (15,000/well) were preincubated with medium or BZB (250 ng/ml) for 30 min and treated with serial dilutions of the proteins for 16 h. Viable cells were visualized by crystal violet staining. Concentrations refer to scTRAIL units.

Table 3.14: EC_{50} values of cell death induction of EpCAM-targeting scTRAIL molecules. Half-maximal effective concentrations are represented as pM scTRAIL units for Colo205 and HCT116 cells preincubated with medium or BZB (250 ng/ml). Additional experiments were performed in the presence of a 200-fold molar excess of scFv323/A3hu3-Fc during the preincubation step.

Protein	Colo205				HCT116	
	without scFv323/A3hu3-Fc		with scFv323/A3hu3-Fc		without scFv323/A3hu3-Fc	
	without BZB	with BZB	without BZB	with BZB	without BZB	with BZB
Db323/A3hu3-scTRAIL	569.7 ± 275.7	63.3 ± 8.9	2294.5 ± 838.3	127.8 ± 15.2	410.8 ± 190.5	11.7 ± 5.2
scFv323/A3hu3-EHD2-scTRAIL	85.5 ± 22.6	13.3 ± 4.4	40.9 ± 6.2	7.7 ± 1.0	32.5 ± 14.4	1.4 ± 0.6
scFv323/A3hu3-Fc-scTRAIL	57.2 ± 21.5	11.2 ± 2.7	34.0 ± 0.7	4.4 ± 0.8	24.8 ± 8.5	1.3 ± 0.2

Consequently, the data of the EpCAM-targeting scTRAIL fusion proteins confirm the observations already described for the other targeted scTRAIL molecules. In summary, the results of all these sets of targeted dimeric scTRAIL fusion proteins allow several conclusions about the different formats: i) The format has no consistent influence on the binding activity. ii) Differences in the capability to induce cell death *in vitro* are supposed to solely result from heterogeneities of the protein preparations. iii) Superior properties were detected for the Fc constructs with respect to production yield, thermal stability, reliable dimer formation, pharmacokinetics, and *in vivo* therapeutic activity. iv) Targeting effects were only identified *in vitro* and only for molecules comprising the hu225 and 3-43 moieties, thus requiring further analysis of scTRAIL constructs of different targeting moieties to unravel the determinants of *in vitro* targeting effects and also to provide a deeper understanding of *in vivo* activities. Concerning the non-targeted formats, better activity was observed for the dimeric compared to the monomeric form.

3.3 Comparison of scTRAIL fusion proteins with different targeting moieties

Based on the above mentioned results that demonstrate superior properties of scFv-Fc-scTRAIL compared to the other targeted dimeric formats, further studies of scFv-Fc-scTRAIL molecules and Fc-scTRAIL were performed to evaluate variations due to different targeting moieties. Attention was in particular focused on gaining insight into factors influencing targeting effects *in vitro* as well as *in vivo*. To allow reliable comparison, several experiments were repeated analyzing the scFv-Fc-scTRAIL molecules of different targeting moieties simultaneously in the same experimental setting. Referring to the biochemical properties described above, the targeting moiety seems to have an influence of on the production yields ranging from 3.8 (3M6) to 12.7 mg (4D5) protein per liter cell culture supernatant as well as on the thermal stability with melting points differing by 6 °C.

3.3.1 Binding properties

Binding to target proteins and tumor cell lines was investigated as the first level to determine differences in the activities of the scFv-Fc-scTRAIL molecules. Evaluation of binding to the respective antigens in ELISA revealed strong binding of the hu225- and 3-43-based fusion proteins with EC_{50} values of 0.9 nM and 0.3 nM that were 3- to 14-fold lower ($P<0.01$) than the concentrations detected for the other constructs (Table 3.15). Consistent with the above represented data, EC_{50} values of binding to human TRAIL-R2 were in the low nanomolar range for all molecules. Further ELISA studies were performed to verify antigen specificities (Figure 3.37A) and binding to human and mouse TRAIL receptors (Figure 3.37B,C). All molecules bound to their designated target antigens, and no binding to EGFR, HER2, HER3, or EpCAM was identified for Fc-scTRAIL. In accordance with the data obtained for the different formats of EGFR-targeting scTRAIL fusion proteins (Figure 3.12), all scFv-Fc-scTRAIL constructs and Fc-scTRAIL were capable of binding to all human and mouse TRAIL receptors, except for mouse DcTRAIL-R1.

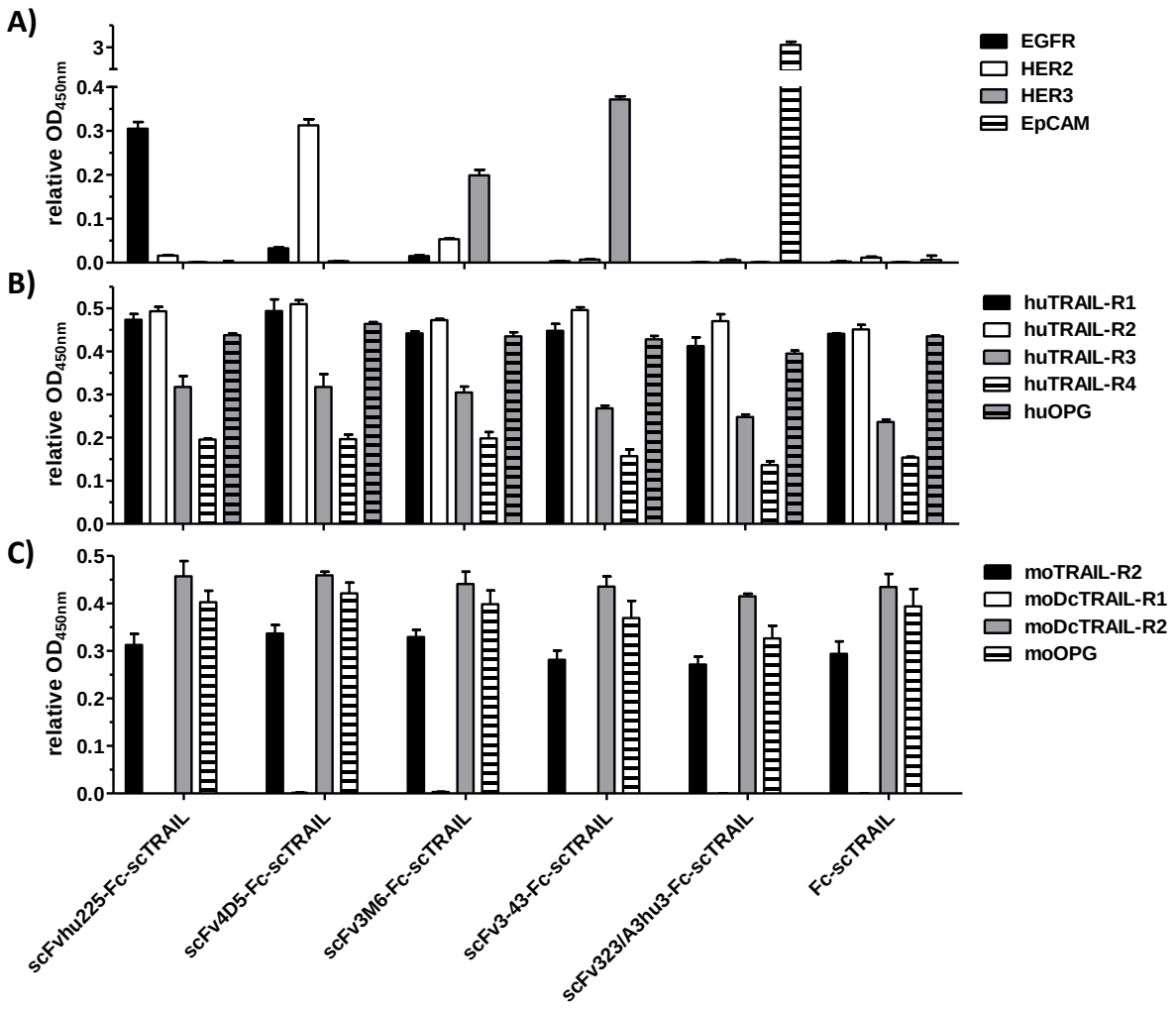

Figure 3.37: Binding of scFv-Fc-scTRAIL molecules and Fc-scTRAIL to target proteins in ELISA. A) 20 nM protein (scTRAIL units) were analyzed for binding to receptor-Fc fusion proteins or sEpCAM (300 ng/well). Bound molecules were detected with an anti-FLAG-HRP or anti-human IgG (Fc specific)-POD. B) Binding of the molecules to Fc fusion proteins of human and C) mouse TRAIL receptors (200 ng/well) was investigated at a concentration of 40 nM scTRAIL units. Bound molecules were detected with an anti-FLAG-HRP. relative OD_{450nm}, OD of sample measured at 450 nm divided by OD of coating control (detection of coated protein via anti-human IgG (Fc specific)-POD or anti-FLAG-HRP). Block shift was performed for binding to human TRAIL receptors.

To further characterize the two colorectal carcinoma cell lines Colo205 and HCT116, relative expression levels of EGFR, HER2, HER3, HER4, EpCAM, and all TRAIL receptors were determined by flow cytometry (Figure 3.38A). While HER2 and HER3 were expressed in higher levels on Colo205 compared to HCT116 cells, no differences in the expression levels of EGFR and EpCAM were observed between the two cell lines. Likewise, TRAIL receptor expression levels were comparable for both cell lines, except for TRAIL-R1 that was more strongly expressed on HCT116 cells. Binding studies of the scFv-Fc-scTRAIL molecules and Fc-scTRAIL on Colo205 cells confirmed the data already obtained (see 3.1) and were further verified on HCT116 cells (Figure 3.38B). Differing from the ELISA data, strongest binding to both cell lines was identified for the construct comprising the hu225 targeting moiety, followed by

323/A3hu3, 4D5, and the HER3-targeting molecules that did not reach saturation levels for concentrations up to 1 µM (Table 3.15). Of note, binding levels of the 4D5 and especially 3-43 constructs on Colo205 cells were higher than those of Fc-scTRAIL already for low protein concentrations. In contrast, on HCT116 cells, increased binding of these proteins compared to Fc-scTRAIL was only observed for high concentrations indicating an impact of receptor expression levels on binding activities.

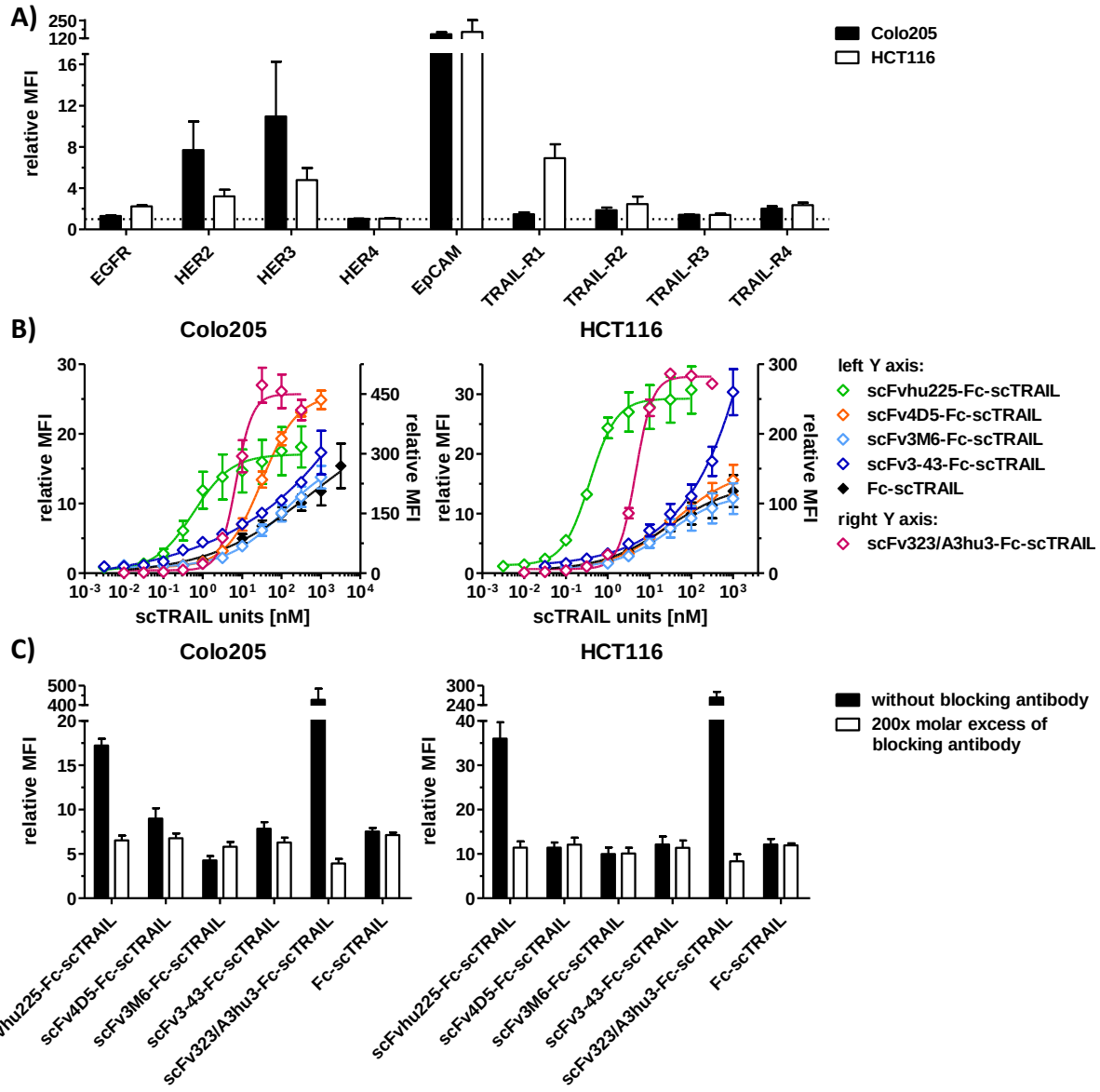

Figure 3.38: Flow cytometry studies of scFv-Fc-scTRAIL molecules and Fc-scTRAIL on Colo205 and HCT116 cells. A) Relative EGFR, HER2, HER3, HER4, EpCAM, and TRAIL-R expression levels were investigated. B) Serial dilutions of the molecules were analyzed. Concentrations refer to scTRAIL units. C) Binding of 20 nM scTRAIL units to Colo205 and HCT116 cells was determined after preincubation with PBA or a 200-fold molar excess of the respective blocking antibody. Binding of Fc-scTRAIL was measured in the presence of all blocking antibodies separately and is here represented as the mean of blocking with all different antibodies. Bound molecules were detected via anti-FLAG-PE.

The contribution of the antibody moieties to cell binding was further investigated by blocking experiments (Figure 3.38C). After preincubation of Colo205 cells with a 200-fold molar excess of the respective blocking antibody, binding of the hu225, 4D5, 3-43, and 323/A3hu3 constructs was reduced to a level similar to that of the non-targeted Fc-scTRAIL that was not influenced by the presence of blocking antibodies. In constrast, binding of scFv3M6-Fc-scTRAIL was not decreased by excess amounts of scFv3M6-Fc, but rather increased binding levels were detected. On HCT116 cells, only binding of scFvhu225-Fc-scTRAIL and scFv323/A3hu3-Fc-scTRAIL was affected by blocking with the respective antibody, whereas all other targeted scTRAIL molecules already showed binding levels similar to Fc-scTRAIL without blocking. Consequently, comparison of the binding properties revealed strongest antigen binding for scFvhu225-Fc-scTRAIL and scFv3-43-Fc-scTRAIL in ELISA. Enhanced binding to Colo205 cells was confirmed for molecules comprising the hu225, 4D5, 3-43, and 323/A3hu3 moieties. However, only the hu225 and 323/A3hu3 antibody units improved binding of the respective scTRAIL molecules on HCT116 cells.

Table 3.15: Binding properties of scFv-Fc-scTRAIL molecules and Fc-scTRAIL. EC_{50} values are expressed as nM scTRAIL units and were determined by ELISA (EGFR-, HER2-, HER3-, huTRAIL-R2-Fc, sEpCAM) and flow cytometry (Colo205, HCT116 cells).

Protein	Antigen	huTRAIL-R2	Colo205	HCT116
scFvhu225-Fc-scTRAIL	0.9 ± 0.01	1.0 ± 0.02	1.4 ± 1.1	0.4 ± 0.1
scFv4D5-Fc-scTRAIL	4.3 ± 0.6	1.2 ± 0.1	32.5 ± 7.9	(34.8 ± 6.8)‡
scFv3M6-Fc-scTRAIL	3.3 ± 0.3	1.6 ± 0.2	(>100)‡	(26.3 ± 0.9)‡
scFv3-43-Fc-scTRAIL	0.3 ± 0.01	1.2 ± 0.1	(>100)‡	(>100)‡
scFv323/A3hu3-Fc-scTRAIL	2.5 ± 0.5	1.4 ± 0.1	7.2 ± 0.4	4.8 ± 0.3
Fc-scTRAIL	n.d.	1.4 ± 0.1	(>100)‡	(20.9 ± 2.1)‡

n.d., not determined. ‡, no saturation reached.

3.3.2 Induction of cell death *in vitro*

To reliably compare induction of cell death by the different scFv-Fc-scTRAIL molecules and Fc-scTRAIL, experiments analyzing Colo205 and HCT116 cells in the absence and presence of bortezomib were repeated. In addition to Colo205 cells, blocking studies were furthermore performed using HCT116 cells. Overall, these data were in good agreement with the results already described (Table 3.16). In the absence of bortezomib, strongest effects on Colo205 cells were observed for scFvhu225-Fc-scTRAIL and scFv3-43-Fc-scTRAIL (significantly reduced EC_{50} values compared to 4D5, 3M6, 323/A3hu3, and non-targeted constructs with $P<0.05$), followed by the EpCAM-targeting molecule (significantly reduced EC_{50} value compared to 4D5, 3M6, and non-targeted constructs with $P<0.01$), while the remaining fusion proteins exhibited

similar or even decreased activity compared to Fc-scTRAIL. In the presence of bortezomib, only the hu225 and 3-43 constructs showed significantly improved properties in comparison to the non-targeted fusion protein (P<0.01). HCT116 cells were most effectively killed by the EGFR- and EpCAM-targeting scTRAIL molecules without and with bortezomib (P<0.05), and no beneficial contribution was identified for the other targeting moieties. Preincubation with the respective blocking antibody increased the EC_{50} values of the hu225 and 3-43 constructs on Colo205 cells in the absence and presence of bortezomib (P<0.01) to the level of the non-targeted fusion protein or even higher. However, blocking of EpCAM binding did not reduce cell death induction of scFv323/A3hu3-Fc-scTRAIL. On HCT116 cells, blocking significantly increased the EC_{50} values of the hu225 molecule (P<0.01), while the activity of scFv323/A3hu3-Fc-scTRAIL was not influenced to a similar extent.

Table 3.16: EC_{50} values of cell death induction of scFv-Fc-scTRAIL molecules and Fc-scTRAIL. EC_{50} values [pM scTRAIL units] were determined after 16 h of treatment of Colo205 and HCT116 cells in the absence or presence of BZB (250 ng/ml). To analyze potential targeting effects, cells were preincubated with a 200-fold molar excess of the respective blocking antibody (Ab) in medium or medium containing BZB (250 ng/ml). Fc-scTRAIL was investigated in the presence of a mixture of all blocking antibodies.

Protein	Colo205				HCT116			
	without blocking Ab		with blocking Ab		without blocking Ab		with blocking Ab	
	without BZB	with BZB	without BZB	with BZB	without BZB	with BZB	without BZB	with BZB
scFvhu225-Fc-scTRAIL	22.6 ± 3.4	7.9 ± 1.7	106.9 ± 9.0	18.5 ± 3.6	12.9 ± 3.9	1.3 ± 0.2	103.2 ± 22.7	4.0 ± 0.6
scFv4D5-Fc-scTRAIL	104.4 ± 6.0	29.7 ± 3.5	163.3 ± 9.4	35.6 ± 3.1	109.5 ± 10.7	5.0 ± 1.4	79.2 ± 17.7	4.9 ± 1.6
scFv3M6-Fc-scTRAIL	247.8 ± 8.8	39.5 ± 5.7	143.8 ± 10.1	26.4 ± 2.9	173.1 ± 27.2	5.7 ± 0.4	125.0 ± 15.3	5.4 ± 1.5
scFv3-43-Fc-scTRAIL	31.1 ± 3.5	6.8 ± 0.9	217.3 ± 6.5	33.1 ± 5.7	131.1 ± 7.1	3.0 ± 0.8	148.4 ± 31.2	7.1 ± 1.1
scFv323/A3hu3-Fc-scTRAIL	58.0 ± 12.1	17.7 ± 2.9	31.5 ± 5.7	9.7 ± 1.9	13.5 ± 0.8	1.3 ± 0.3	31.1 ± 6.9	1.0 ± 0.1
Fc-scTRAIL	96.4 ± 11.5	21.7 ± 3.5	130.0 ± 10.6	35.7 ± 9.7	98.9 ± 22.0	3.2 ± 0.3	75.1 ± 17.3	4.9 ± 0.7

Since a 200-fold molar excess of blocking antibody did not reduce the activity of scFv323/A3hu3-Fc-scTRAIL to the level of Fc-scTRAIL, additional blocking experiments were performed investigating the effects of the EpCAM-targeting fusion protein and the non-targeted construct after increasing the molar excess of scFv323/A3hu3-Fc to 500-fold (Figure 3.39). Even in the presence of these considerable amounts of blocking antibody, scFv323/A3hu3-Fc-scTRAIL induced cell death 2- to 3.4-fold more strongly than Fc-scTRAIL (P<0.05) on Colo205 and HCT116 cells in the absence as well as in presence of bortezomib. Thus, the beneficial properties of scFv323/A3hu3-Fc-scTRAIL were not impaired by blocking of

EpCAM binding and require further studies to elucidate the factors provoking this superior activity. With respect to the more than 16- and 9-fold higher relative MFIs of the EpCAM-targeting molecule on Colo205 and HCT116 cells compared to all other fusion proteins (Figure 3.38B), the lacking effects of blocking EpCAM binding on cell death induction may be related to high EpCAM expression levels.

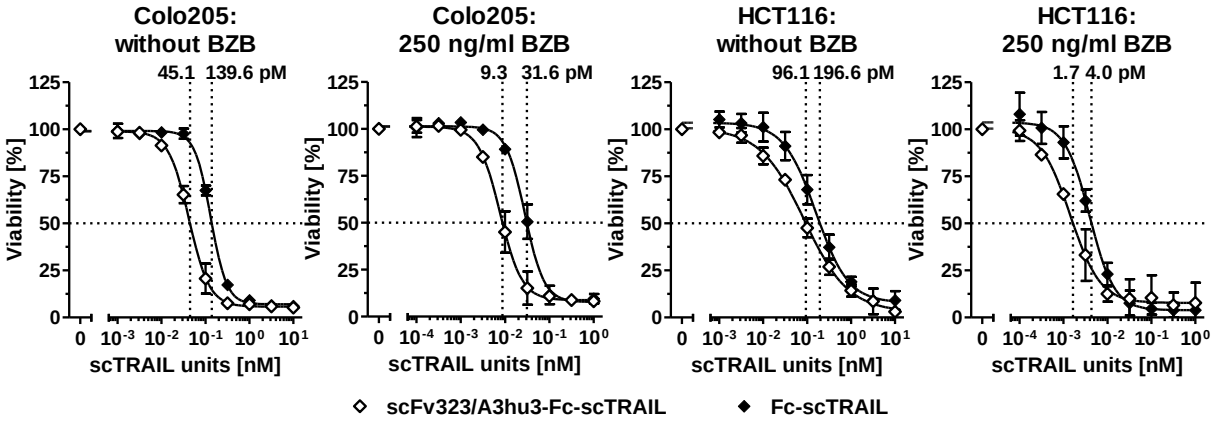

Figure 3.39: Blocking studies of scFv323/A3hu3-Fc-scTRAIL-induced cell death. Colo205 (50,000/well) and HCT116 cells (15,000/well) were treated with serial dilutions of scFv323/A3hu3-Fc-scTRAIL and Fc-scTRAIL for 16 h after preincubation with a 500-fold molar excess of scFv323/A3hu3-Fc in medium or medium containing BZB (250 ng/ml). Viable cells were stained with crystal violet. Concentrations refer to scTRAIL units. EC_{50} values [pM scTRAIL units] are indicated with dotted lines.

Additional studies of cell death induction were designed to analyze a potential influence of bortezomib on targeting. The hu225 and 3-43 constructs that exhibited strong targeting effects on Colo205 cells were compared to Fc-scTRAIL after preincubation of Colo205 cells with increasing concentrations of bortezomib (Figure 3.40). Investigations of the differences in the EC_{50} values of scFvhu225-Fc-scTRAIL and Fc-scTRAIL revealed a decrease from factor 9.7 (± 1.4) over 5.0 (± 1.7) and 4.6 (± 0.6) to 4.1 (± 0.7) in the presence of medium, 250 ng/ml, 750 ng/ml, and 1250 ng/ml bortezomib, respectively. This corresponds to a significant reduction ($P<0.01$) of targeting effects with each increase in the bortezomib concentration. Differing from these data, the impact of augmented bortezomib concentrations on targeting effects of scFv3-43-Fc-scTRAIL was with differences of factors 6.5 (± 0.5), 5.6 (± 0.8), 5.9 (± 0.8), and 6.0 (± 0.6) compared to Fc-scTRAIL not significant ($P>0.05$). Hence, there is no distinct influence of bortezomib on targeting and impacts seem to be construct-dependent.

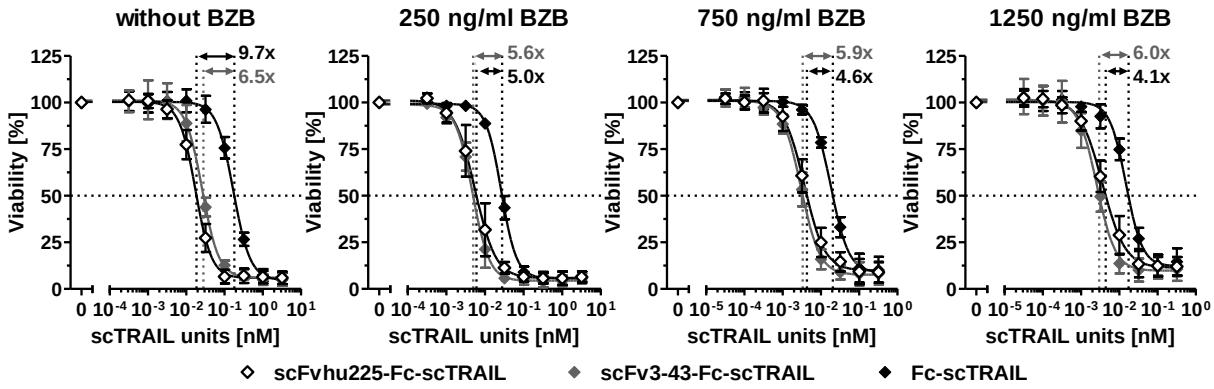

Figure 3.40: Effects of varying bortezomib concentrations on cell death induction on Colo205 cells. After preincubation with medium or increasing concentrations of BZB (250 ng/ml, 750 ng/ml, 1250 ng/ml) for 30 min, Colo205 cells (50,000/well) were treated with serial dilutions of the molecules for 16 h. Cell viability was determined by crystal violet staining. Concentrations refer to scTRAIL units. Differences between the EC_{50} values of the targeted molecules and Fc-scTRAIL are indicated.

As an attempt to unravel potential determinants of targeting effects *in vitro*, EC_{50} values of cell death induction in the absence and presence of blocking antibody were correlated with the EC_{50} values of antigen binding in ELISA. The results obtained for Colo205 cells demonstrated that the two molecules (hu225, 3-43) showing strong cell death induction that can be reduced to the level of Fc-scTRAIL by the respective blocking antibodies possess strong binding to their corresponding antigen (Figure 3.41A). Here, the EC_{50} values of antigen binding were lower than those of binding to TRAIL-R2. These relationships were found in the absence and presence of bortezomib. This indicates that binding of the antibody part to the antigen needs to be stronger than binding of the scTRAIL moiety to the receptors to obtain targeting effects *in vitro*. However, the results determined for HCT116 cells are not able to confirm this correlation (Figure 3.41B). In accordance with the data observed on Colo205 cells, the hu225 construct showed strong antigen binding and cell death induction that is reduced by cetuximab. In contrast to Colo205 cells, scFv3-43-Fc-scTRAIL did not exert higher activity than Fc-scTRAIL on HCT116 cells. Again, the observations were similar in the absence and presence of bortezomib. Additionally considering the binding properties for Colo205 and HCT116 cells (Figure 3.38) allows further explanation of these results. While the hu225 and 3-43 molecules both exhibit better binding than Fc-scTRAIL on Colo205 cells, superior binding on HCT116 cells was only seen for scFvhu225-Fc-scTRAIL, especially at the low concentrations applied for cell death induction. Consistent with these observations, scFv323/A3hu3-Fc-scTRAIL shows improved binding and cell death induction compared to Fc-scTRAIL on both cell lines. Thus, strong binding of the antibody part to the purified antigen seems to be necessary, but also

needs to translate into effective binding to the respective cells, which may be influenced by receptor expression levels.

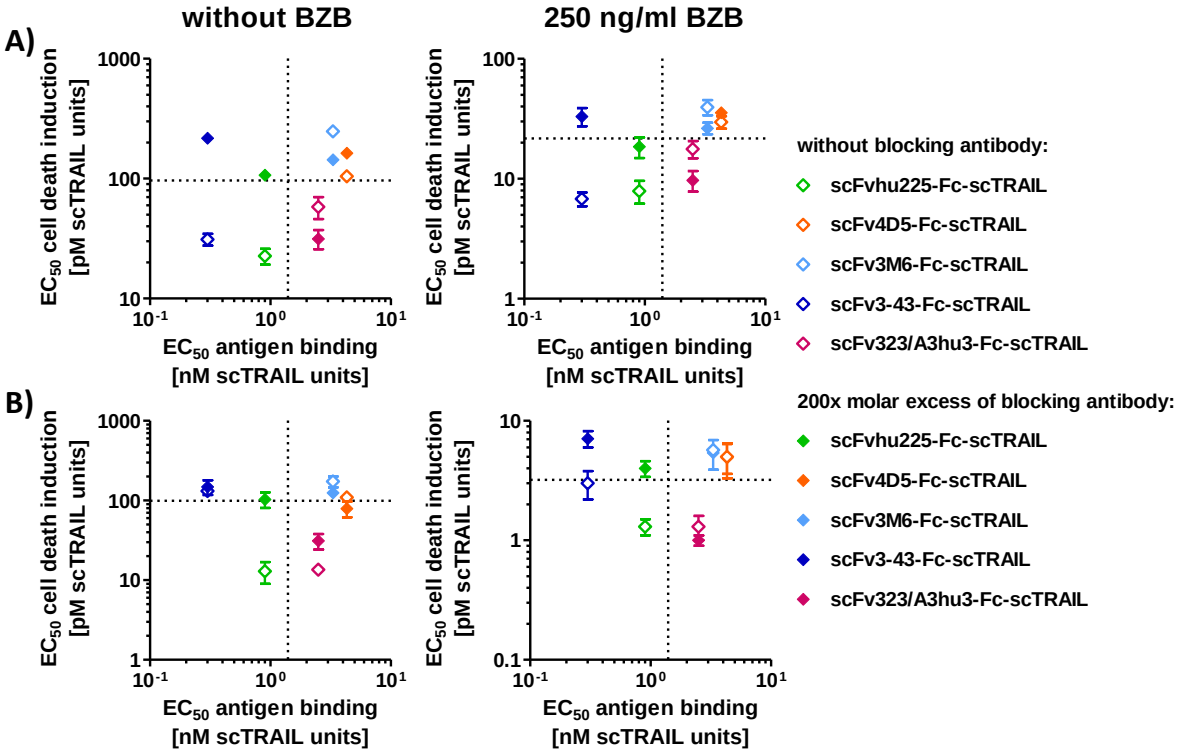

Figure 3.41: Analysis of potential correlation of cell death induction and antigen binding. EC_{50} values of cell death induction in the absence and presence of excess amounts of the respective blocking antibody (Table 3.16) were plotted against the EC_{50} value of binding to the corresponding antigen (Table 3.15). Plots were prepared for data determined in the absence and presence of BZB (250 ng/ml) for Colo205 (A) and HCT116 cells (B). EC_{50} values of Fc-scTRAIL for binding to huTRAIL-R2 and cell death induction are indicated with dotted lines.

In summary, these data identified superior cell death induction of the hu225, 3-43, and 323/A3hu3 constructs on Colo205 cells, and of hu225 and 323/A3hu3 fusion proteins on HCT116 cells. Blocking of antigen binding of the hu225 and 3-43 moieties led to a reduction of this increased activity that was not obtained for scFv323/A3hu3-Fc-scTRAIL. Correlation with the binding properties indicated an importance of strong antigen and cell binding (better than Fc-scTRAIL in particular at low protein concentrations) for targeting effects *in vitro*.

3.3.3 *In vivo* activity of scTRAIL fusion proteins with different targeting moieties

The *in vivo* studies of EGFR-targeting scTRAIL formats and Fc-scTRAIL (see 3.2.1.5) were not able to confirm the beneficial impact of targeting observed *in vitro*. Thus, another *in vivo* experiment was performed evaluating scFv-Fc-scTRAIL molecules comprising the 3-43 and 323/A3hu3 targeting moieties in addition to scFvhu225-Fc-scTRAIL and Fc-scTRAIL in the absence of bortezomib. NMRI nude mice with established Colo205 tumors received i.v.

injections of 0.2 nmol protein (corresponding to 0.4 nmol scTRAIL units) twice a week for three weeks. Treatments with the EGFR-, HER3-, and non-targeted molecules resulted in almost complete tumor remission, whereas only limited tumor regression and fast regrowth were observed for scFv323/A3hu3-Fc-scTRAIL (Figure 3.42A). Stable tumor remission over the monitoring period of almost 100 d was seen for scFv3-43-Fc-scTRAIL and only marginal regrowth was detected for Fc-scTRAIL at the end of the experiment. Differing from these data, considerably stronger regrowth of tumors treated with scFvhu225-Fc-scTRAIL was measured. Statistical analysis of the tumor volumes at day 69 revealed significant differences only between scFv323/A3hu3-Fc-scTRAIL compared to the HER3- and non-targeted molecules (Figure 3.42B).

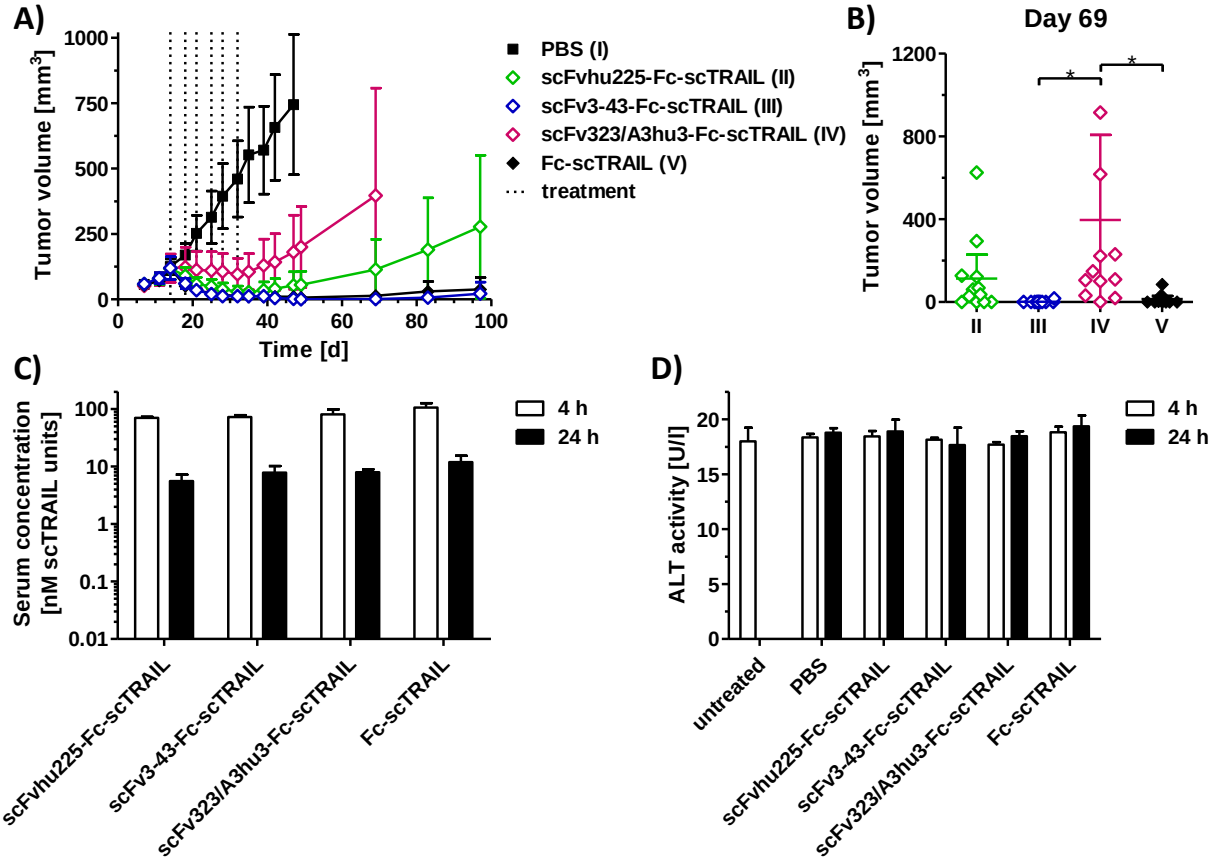

Figure 3.42: *In vivo* activity and PK of scFv-Fc-scTRAIL molecules and Fc-scTRAIL. A) NMRI nude mice (6 mice per group) with established Colo205 tumors were treated with 0.2 nmol protein (corresponding to 0.4 nmol scTRAIL units; i.v.) or PBS twice a week for three weeks (days 14, 18, 21, 25, 28, 32). Treatments are indicated with dotted lines. B) Statistical analysis of tumor volumes of groups II to V (numbering according to A) at day 69 was performed by One-Way ANOVA, followed by Tukey's post hoc test (*P<0.05; **P<0.01; ***P<0.001; ns, P>0.05). C) Serum concentrations of the molecules and D) ALT were determined 4 h and 24 h after the last treatment (day 32).

Serum concentrations of the proteins were determined 4 h and 24 h after the last treatment (Figure 3.42C) and resembled the PK data of scFvhu225-Fc-scTRAIL and Fc-scTRAIL described previously. Since serum levels of all molecules were comparable, no differences in *in vivo* half-lives were induced by the different targeting moieties, although cross-reactivity with the corresponding mouse receptor was demonstrated for 3-43 (Schmitt *et al.*, in preparation). Similar to the data generated before, none of the molecules induced toxic effects on the liver as measured by ALT levels in the serum 4 h and 24 h after the last treatment (Figure 3.42D).

Consequently, major differences in the binding properties and cell death induction capabilities of the scFv-Fc-scTRAIL fusion proteins due to the different targeting moieties were detected. The hu225, 3-43, and 323/A3hu3 constructs were identified as superior candidates on Colo205 cells, while highest activity on HCT116 cells was shown for the EGFR- and EpCAM-targeting proteins. Analyzing a potential correlation of cell death induction and binding properties indicated improved cell binding of the targeted compared to the non-targeted molecule, particularly at low concentrations, as relevant factor for targeting effects *in vitro*. However, a beneficial impact of the antibody moiety on the *in vivo* therapeutic activity remains to be confirmed.

3.4 Generation and analysis of dual-targeting scTRAIL fusion proteins

As a strategy to further improve scTRAIL-based therapeutics, a format was developed that allows dimeric assembly combined with simultaneous targeting of two different tumor-associated antigens in one molecule. Using a bispecific single-chain diabody (scDb) that is built up of the variable domains of the heavy and light chain of two antibodies of different specificity, scDb-EHD2-scTRAIL molecules were generated by replacing the scFv of the scFv-EHD2-scTRAIL fusion protein by a scDb (Figure 3.43). Based on the targeting moieties described before, four different scDb-EHD2-scTRAIL fusion proteins directed against EGFRxHER3, EpCAMxEGFR, HER2xEGFR, and HER2xHER3 were produced by combining hu225x3M6, 323/A3hu3xhu225, 4D5xhu225, and 4D5x3M6, respectively. According to the other scTRAIL constructs, scDb-EHD2-scTRAIL fusion proteins were expressed in stably transfected HEK293T cells comprising a FLAG-tag at the N-terminus for purification via FLAG affinity chromatography from the cell culture supernatant.

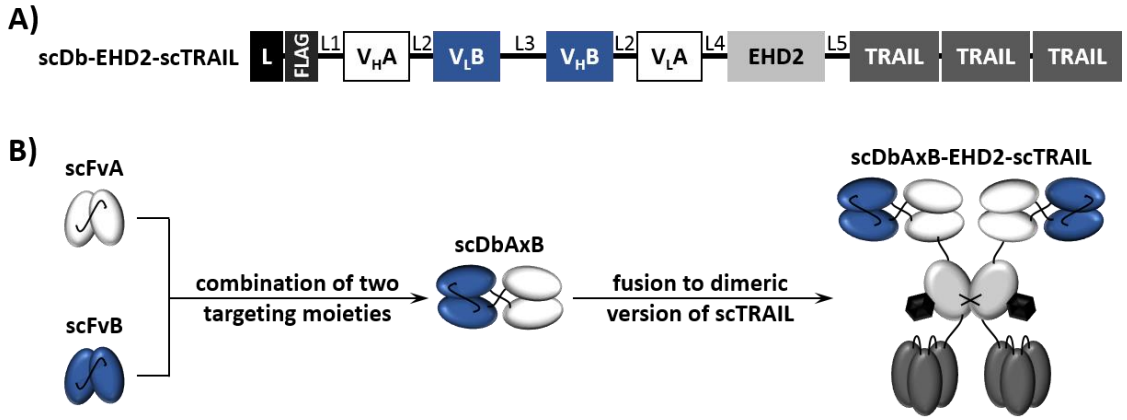

Figure 3.43: Schematic representation and generation of scDb-EHD2-scTRAIL molecules. A) Composition and B) schematic assembly of scDb-EHD2-scTRAIL molecules targeting two tumor-associated antigens A and B. L, Igκ chain leader sequence. L1, GGGGSGT linker. L2, GGGGS linker. L3, GGGGSGGRASGGGGS linker. L4, AAAGGSGG linker. L5, GGSGGASSGG linker. TRAIL subunits consist of aa 118-281 and are connected by a glycine residue.

3.4.1 Biochemical characterization

The scDb-EHD2-scTRAIL molecules were produced with yields ranging from 1.2 to 3.3 mg protein per liter cell culture supernatant (Table 3.17). Purity and integrity of the proteins was verified in SDS-PAGE, but revealed considerable amounts of the monomeric form of scDbhu225x3M6-EHD2-scTRAIL, scDb323/A3hu3xhu225-EHD2-scTRAIL, and scDb4D5x3M6-EHD2-scTRAIL under non-reducing conditions (Figure 3.44A). Size exclusion HPLC identified inhomogeneous preparations for all proteins under native conditions (Figure 3.44B) confirming large fractions of the monomeric form for the hu225x3M6, 323/A3hu3xhu225, and

4D5x3M6 constructs. In contrast, high molecular weight species were detected for scDb4D5xhu225-EHD2-scTRAIL. The hydrodynamic radii of the desired dimeric form of the molecules varied from 6.2 nm to 7.0 nm (Table 3.17). Analysis of the thermal stability by dynamic light scattering demonstrated similar melting points for all proteins of 56 °C and 57 °C (Table 3.17).

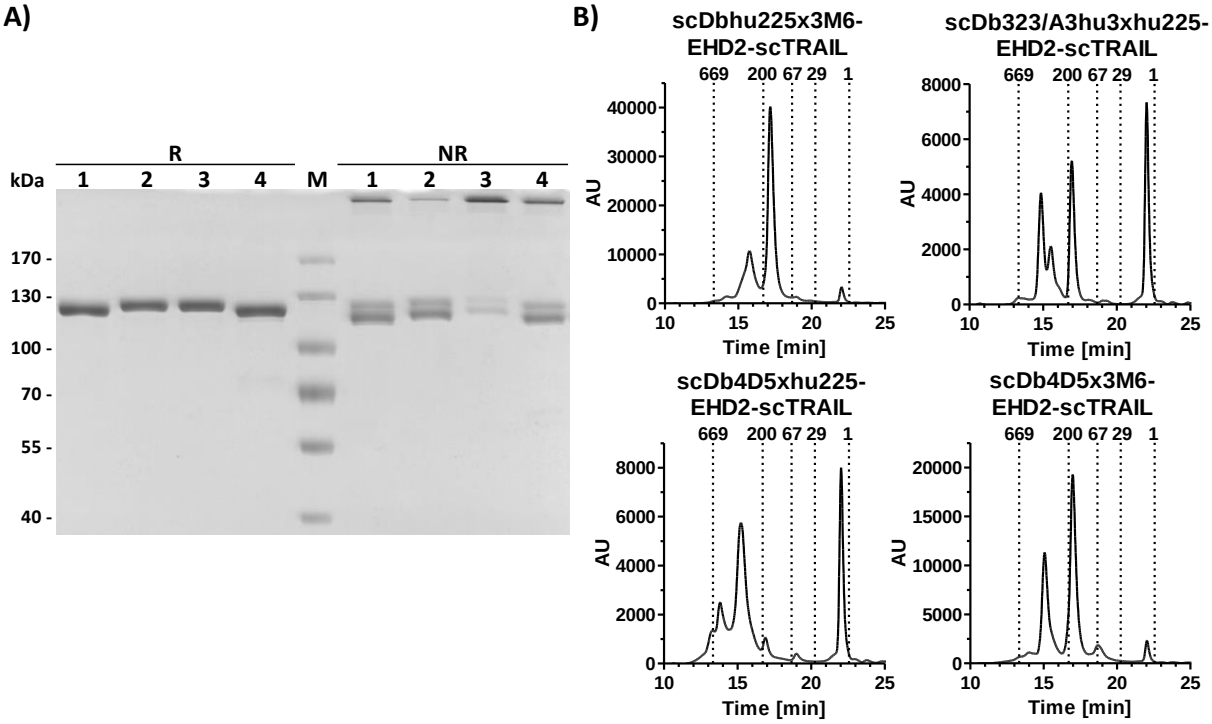

Figure 3.44: Biochemical characterization of scDb-EHD2-scTRAIL molecules. A) SDS-PAGE (8 % PAA) of scDb-EHD2-scTRAIL fusion proteins comprising the targeting moieties hu225x3M6 (1), 323/A3hu3xhu225 (2), 4D5xhu225 (3), and 4D5x3M6 (4) was performed under reducing (R) and non-reducing conditions (NR). 2 µg protein were loaded per lane and proteins were stained with Coomassie Brilliant Blue. M, protein marker. B) Proteins were analyzed by size exclusion HPLC. Elution times of standard proteins and their respective molecular masses [kDa] are indicated.

3.4.2 Evaluation of binding properties

To fully characterize the binding properties of the scDb-EHD2-scTRAIL molecules, binding to both antigens, human TRAIL-R2, and Colo205 cells was investigated (Figure 3.45). Consistent with the binding properties of the hu225 targeting moiety (Table 3.1), the hu225x3M6 and 323/A3hu3xhu225 constructs showed strong binding to EGFR with EC_{50} values in the subnanomolar range (Table 3.17), whereas a significantly higher concentration of 5.1 nM ($P<0.001$) was necessary to reach half-maximal binding of scDb4D5xhu225-EHD2-scTRAIL. Binding of scDb4D5x3M6-EHD2-scTRAIL to HER2 was similar to that detected for the 4D5 targeting moiety (Table 3.2). Again, the 4D5xhu225 molecule exhibited reduced binding ($P<0.001$) indicating an impaired binding activity of both targeting moieties of this protein.

Binding analysis to HER3 revealed an EC_{50} value of 2.3 nM for scDbhu225x3M6-EHD2-scTRAIL, which resembles values determined for 3M6 fusion proteins before (Table 3.11), and weaker binding for the 4D5x3M6 molecule (P<0.001). Half-maximal binding of scDb323/A3hu3xhu225-EHD2-scTRAIL to EpCAM reflected the binding properties of the 323/A3hu3 targeting moiety (Table 3.4). In agreement with the data of the other scTRAIL fusion proteins, all molecules bound to human TRAIL-R2 with similar EC_{50} values of 2.3 nM to 4.4 nM (P>0.05). Although strong antigen binding of both targeting moieties of the hu225x3M6 and 323/A3hu3xhu225 constructs was detected in ELISA, these properties only translated into effective binding to Colo205 cells for scDbhu225x3M6-EHD2-scTRAIL, while all other proteins showed similar (P>0.05) and significantly weaker binding activities than the hu225x3M6 construct (P<0.001). Thus, all molecules bound to their designated target proteins, albeit in some cases with a lower binding strength than the respective recombinant antibody. Superior binding to Colo205 cells was identified for the hu225x3M6 construct and only marginal differences were found for the other proteins.

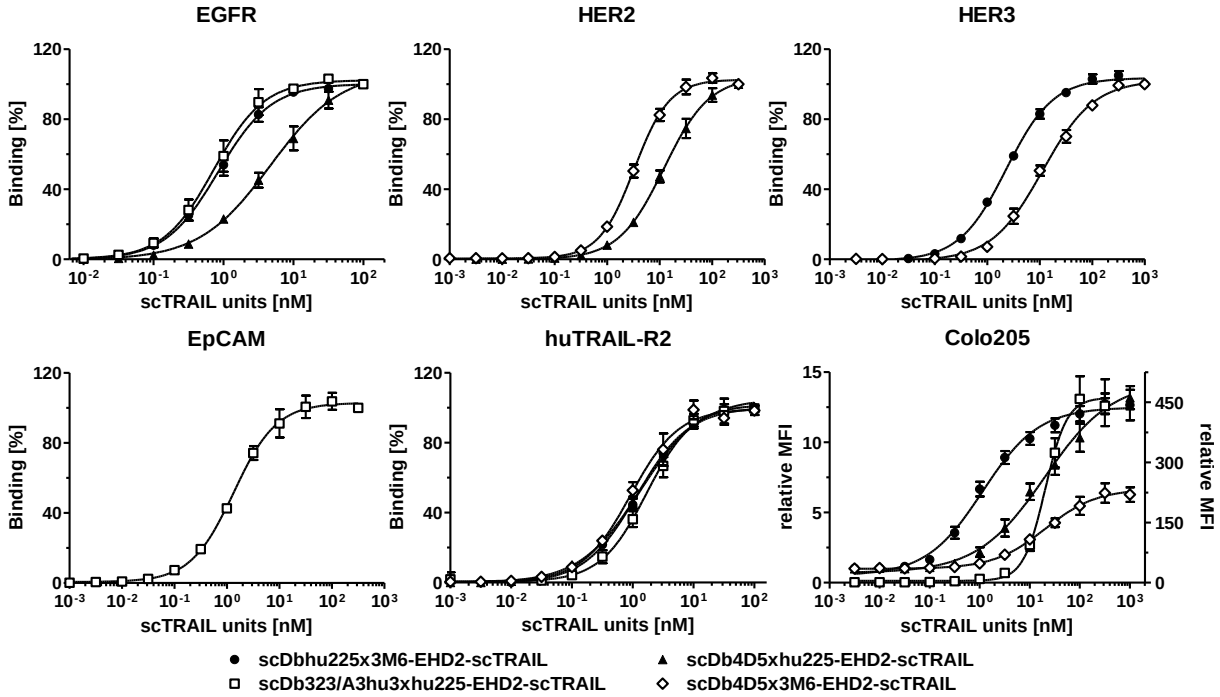

Figure 3.45: Binding studies of scDb-EHD2-scTRAIL molecules. Binding to EGFR-Fc (300 ng/well), HER2-Fc (300 ng/well), HER3-Fc (300 ng/well), sEpCAM (200 ng/well), and huTRAIL-R2-Fc (200 ng/well) was analyzed by ELISA. Bound proteins were detected with an anti-FLAG-HRP or anti-human IgG (Fc specific)-POD. OD measured at 450 nm was normalized to the value determined for the highest concentration. Flow cytometry was performed to investigate binding to Colo205 cells detecting bound molecules using a PE-conjugated anti-FLAG antibody. Binding of scDb323/A3hu3xhu225-EHD2-scTRAIL to Colo205 cells is plotted on the right Y axis. Concentrations refer to scTRAIL units.

Table 3.17: Biochemical and binding properties of scDb-EHD2-scTRAIL molecules. Molecular masses (M) were calculated based on the amino acid sequence. Yields are expressed as mg protein per liter cell culture supernatant. Stokes radii (S_r) and melting points (T_M) were determined by size exclusion HPLC and dynamic light scattering, respectively. Half-maximal binding was analyzed by ELISA (AgA, AgB, huTRAIL-R2-Fc) and flow cytometry (Colo205 cells) and is represented as nM scTRAIL units. AgA and AgB refer to antigens (Ag) of scDbAxB.

Protein	M [kDa]	Yield [mg/l]	S_r [nm]	T_M [°C]	EC_{50} AgA [nM]	EC_{50} AgB [nM]	EC_{50} huTRAIL-R2 [nM]	EC_{50} Colo205 [nM]
scDbhu225x3M6-EHD2-scTRAIL	244	3.3	6.2	57	0.9 ± 0.1	2.3 ± 0.2	2.8 ± 1.2	1.1 ± 0.1
scDb323/A3hu3xhu225-EHD2-scTRAIL	246	1.2	7.0	56	1.4 ± 0.03	0.8 ± 0.2	4.4 ± 2.2	20.7 ± 1.2
scDb4D5xhu225-EHD2-scTRAIL	245	1.6	6.7	56	12.5 ± 1.8	5.1 ± 1.2	3.1 ± 1.4	26.5 ± 4.4
scDb4D5x3M6-EHD2-scTRAIL	244	2.8	6.8	57	3.3 ± 0.3	11.4 ± 1.5	2.3 ± 1.0	23.7 ± 3.4

3.4.3 Induction of cell death *in vitro*

Cell death induction of the dual-targeting scTRAIL fusion proteins was investigated on Colo205 (Figure 3.46A) and HCT116 cells (Figure 3.46B) in the absence and presence of bortezomib. All proteins showed concentration-dependent induction of cell death on both cells lines. On Colo205 cells in the absence and presence of bortezomib, lowest EC_{50} values were determined for the construct comprising the 4D5xhu225 targeting moieties, followed by hu225x3M6, 4D5x3M6, and 323/A3hu3xhu225 (Table 3.18). Differing effects were found on HCT116 cells identifying highest activity for the hu225x3M6 protein, followed by 323/A3hu3xhu225, 4D5xhu225, and 4D5x3M6. Although the heterogeneities detected in the protein preparations do not allow clear conclusions about the activities of the different molecules, comparison of the results of Colo205 and HCT116 cells highlights cell line-specific differences and common properties. On the one hand, the construct directed against HER2 and EGFR exerted despite the large amount of high molecular weight species (Figure 3.44B) strongest effects only on Colo205 cells, whereas lower activity was measured on HCT116 cells. On the other hand, scDbhu225x3M6-EHD2-scTRAIL exhibiting the highest fraction of monomer strongly induced cell death on both cell lines, which indicates a favorable impact of combining these targeting moieties. To further evaluate the characteristics of combined targeting of two antigens in one scTRAIL fusion protein, the activity of scDb4D5xhu225-EHD2-scTRAIL on Colo205 cells in the presence of bortezomib was assessed simultaneously to Dbhu225-scTRAIL and Db4D5-scTRAIL alone or in combination. Regarding equimolar concentrations of scTRAIL units, the scDb-EHD2-scTRAIL molecule induced cell death more potently than Db4D5-scTRAIL, but less effectively as compared to Dbhu225-scTRAIL, while similar activity was observed for the

respective combination of the two Db-scTRAIL molecules (Figure 3.46C). Comparable results were obtained on HCT116 cells (Figure 3.46D).

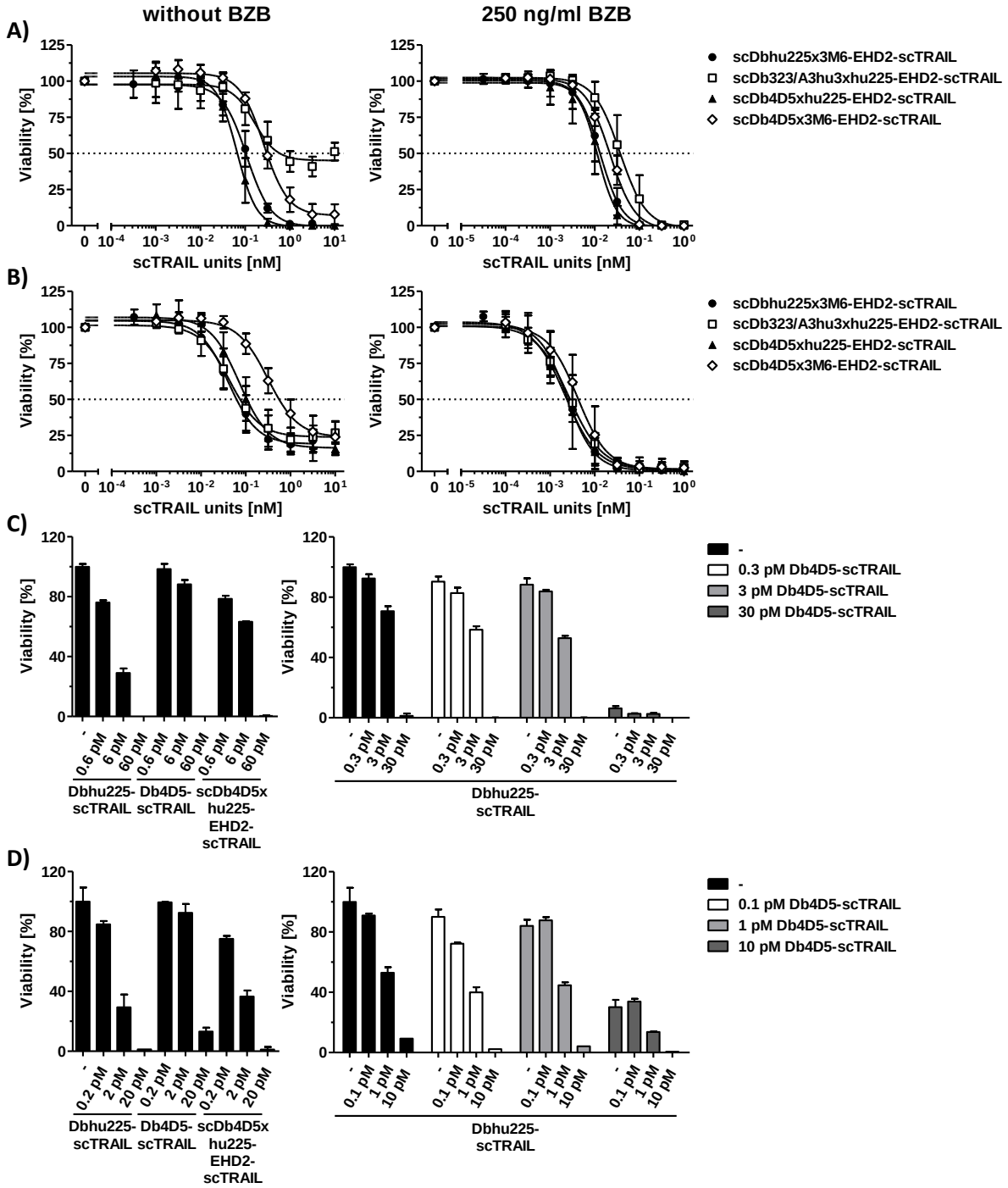

Figure 3.46: Cell death induction of scDb-EHD2-scTRAIL molecules. A) Colo205 (50,000/well) and B) HCT116 cells (15,000/well) were treated with serial dilutions of the molecules for 16 h after preincubation with medium or BZB (250 ng/ml) for 30 min. Viable cells were stained with crystal violet. C) Effects of scDb4D5xhu225-EHD2-scTRAIL were compared to Dbhu225-scTRAIL and Db4D5-scTRAIL alone or in combination after pretreatment with BZB (250 ng/ml) for Colo205 and D) HCT116 cells. Experiments of C and D were performed once. Concentrations refer to scTRAIL units.

In summary, these data confirm that using a bispecific scDb as antibody moiety fused to a dimeric scTRAIL molecule allows targeting of two different antigens. However, size exclusion chromatography data revealed either large fractions of high molecular weight species or monomers. Based on the data obtained for the different formats of targeted dimeric scTRAIL molecules, these problems in product quality may be improved by using the human IgG1 Fc part as dimerization module instead of the EHD2. The binding studies verified binding to the corresponding target proteins, although in some cases with decreased activity. Hence, generation of dual-targeting dimeric scTRAIL fusion proteins requires further optimization steps, i.e. ideal orientation of the variable domains in the scDb and possibly adjustments of linker lengths. Despite the heterogeneities of the protein preparations, cell death induction analysis on Colo205 and HCT116 cells indicated a cell line-dependent relevance of the different combinations of targets and beneficial effects of the hu225x3M6 construct, which are probably related to its superior cell binding activity.

Table 3.18: EC_{50} values of cell death induction of scDb-EHD2-scTRAIL molecules. EC_{50} values [pM scTRAIL units] were determined for Colo205 and HCT116 cells after pretreatment with medium or BZB (250 ng/ml).

Protein	Colo205		HCT116	
	without BZB	with BZB	without BZB	with BZB
scDbhu225x3M6-EHD2-scTRAIL	104.2 ± 25.7	13.5 ± 4.2	68.0 ± 21.9	2.4 ± 0.4
scDb323/A3hu3xhu225-EHD2-scTRAIL	775.3 ± 525.0	41.5 ± 17.2	87.9 ± 39.6	3.0 ± 1.1
scDb4D5xhu225-EHD2-scTRAIL	69.1 ± 20.1	11.2 ± 4.1	114.7 ± 49.5	2.9 ± 1.2
scDb4D5x3M6-EHD2-scTRAIL	314.1 ± 50.8	22.0 ± 3.9	597.7 ± 172.0	4.8 ± 2.3

4 Discussion

Considering the diversity and large number of second generation TRAIL-based therapeutics, the need of systematic comparison arises to further guide optimization and therapeutic development of those molecules. In this study, four different formats of dimeric antibody-scTRAIL fusion proteins comprising five distinct targeting moieties have been generated. Comprehensive analysis of biochemical and functional properties confirmed the suitability of all formats to combine targeting and defined oligomerization of scTRAIL in general and revealed the superiority of Fc-based constructs in terms of production, stability, pharmacokinetics, and pharmacodynamics. Major differences in the *in vitro* bioactivity were found depending on the incorporated antibody moiety. The factors underlying these differences remain to be fully elucidated, but seem to be linked to properties of both the antibody and the targeted antigen. While beneficial effects of targeting were confirmed for certain antibody moieties *in vitro*, further improvement of the highly potent activity of non-targeted Fc-scTRAIL was not observed *in vivo*.

4.1 Dimeric recombinant antibody formats as fusion partners of scTRAIL

In order to create a set of different formats of targeted dimeric scTRAIL molecules, the first part of this study was dedicated to generating and characterizing dimeric recombinant antibodies as potential fusion partners of scTRAIL. In recent decades, a diverse set of dimeric recombinant antibody formats has been developed in an attempt to improve e.g. binding properties compared to monomeric scFvs (reviewed by Kontermann, 2010; Nuñez-Prado *et al.*, 2015). A well-established format is the diabody that has already been successfully used to equip various fusion partners, like scTRAIL (Siegemund *et al.*, 2012), IL-2 (Frey *et al.*, 2010), IL-15 and GM-CSF (Kaspar *et al.*, 2007), or B7.2 (Hornig *et al.*, 2012), with tumor-targeting properties. Regarding the non-covalent assembly of the diabody, dissociation of the two chains might be possible. In fact, Huang *et al.* (2005) demonstrated dissociation of a diabody into an inactive monomeric form at dilute concentrations. In order to address this possible stability issue, structural analysis has been performed and identified positions in the variable domains suitable for introduction of cysteine residues to form interchain disulfide bonds (reviewed by Reiter *et al.*, 1996). In accordance with previous reports, disulfide-stabilization increased the thermal stability of all diabodies analyzed in this study, although with increases of 2 °C to 4 °C to a lesser extent than that described for an anti-CEA diabody, showing a melting

point improved by 10 °C (FitzGerald *et al.*, 1997). This less pronounced stabilizing effect might be related to the already considerably higher melting points of the unmodified diabodies investigated in this study. Since diabodies possess a rather compact structure (Holliger *et al.*, 1993), additional strategies have been developed in order to generate bivalent molecules that show an organization and flexibility similar to that of natural immunoglobulins. This has been achieved using separate modules for targeting, e.g. scFvs, and dimerization, e.g. the heavy chain domain 2 of IgE or the Fc part of human IgG1. The EHD2 has already been applied not only to generate bivalent recombinant antibodies, but also scTRAIL fusion proteins, and lacks additional effector functions (Seifert *et al.*, 2014a). The Fc part of human IgG1 is an established fusion partner of various proteins mediating, besides dimeric assembly, effector functions, like recycling via the FcRn (reviewed by Beck and Reichert, 2011; Kontermann, 2010). Employing these extensively investigated antibody formats of different structural organization, flexibility, size, and effector functions, all targeting moieties were successfully converted into diverse types of dimeric recombinant antibodies without loss of binding activity.

Based on these recombinant antibody formats, the respective scTRAIL molecules were generated by fusion of scTRAIL to their C-terminus. In its natural configuration, TRAIL is expressed as a type II transmembrane protein, thus anchored to the cell membrane via its N-terminus (Wiley *et al.*, 1995). Linking a fusion partner N-terminally to scTRAIL therefore reflects the physiological structure, and most TRAIL fusion proteins utilize this concept (Table 1.1), although fusion partners have also been attached to the C-terminus of TRAIL yielding active proteins (Gieffers *et al.*, 2013; Liu *et al.*, 2014). In terms of production properties, the different formats of dimeric antibody-scTRAIL molecules showed major variations. In accordance with literature (reviewed by Levin *et al.*, 2015), incorporating the Fc part greatly enhanced the product yield. Extensive development and characterization of various kinds of Fc fusion proteins have moreover demonstrated its beneficial effects on stability and solubility (reviewed by Levin *et al.*, 2015). This is consistent with the results obtained for the scFv-Fc-scTRAIL molecules of all five antibody moieties exhibiting better thermal stability than the other formats. Investigations of the fusion proteins after incubation in human plasma at physiological temperatures, however, did not confirm superior stability of the Fc construct. Thus, plasma stability may be limited rather by the susceptibility (especially of the linker sequences) to proteolytic cleavage than by thermal stability of the dimerization modules, although introduction of disulfide bonds into the diabody appeared to have a positive impact.

While all formats of the EGFR- and HER2-targeting molecules reliably formed the desired dimers, only the Fc part was capable of converting the HER3- and EpCAM-specific proteins completely into the dimeric form. Hence, dimer formation seems to be influenced by the antibody moiety. Stable association of the diabody chains has been described to depend on the interfaces formed by the variable domains and therefore on the antibody sequence (reviewed by Todorovska *et al.*, 2001). In contrast, dimer formation via the EHD2 is supposed to be unaffected by the respective antibody (Seifert *et al.*, 2014a). Here, the differences in dimeric assembly may additionally be caused by protein batch-specific variations. With respect to functional properties, all formats of all antibody moieties retained antigen as well as TRAIL receptor binding activity, which is in agreement with previous studies, using particularly the hu225 targeting moiety in similar scTRAIL molecules (Seifert *et al.*, 2014a; Siegemund *et al.*, 2012; Siegemund *et al.*, 2016). Likewise, 323/A3hu3 has recently been demonstrated to confer EpCAM-binding properties to (sc)TNFSF members in scFv-TNFSF and scFv-scTNFSF molecules (Fellermeier *et al.*, 2016). While proteins combining (sc)TRAIL with distinct antibody moieties directed against EGFR, HER2, and EpCAM have already been described (Table 1.1), no HER3-targeting scTRAIL fusion protein has been available yet. Since in recent years, HER3 has become an attractive target for tumor therapy (reviewed by Hsieh and Moasser, 2007; Kol *et al.*, 2014), HER3-targeting scTRAIL molecules might be especially promising. Referring to TRAIL receptor binding properties, half-maximal binding of all analyzed constructs to human TRAIL-R2 was with values in the sub- to low nanomolar range in line with previous studies reporting affinities of 0.76 nM to 2 nM (Lang *et al.*, 2016). Consistent with the described specificities of human TRAIL for human and mouse TRAIL receptors (Bossen *et al.*, 2006), the scTRAIL fusion proteins were capable of binding to all human and mouse TRAIL-R, except for moDcTRAIL-R1. Highlighting differences between the human and mouse TRAIL – TRAIL receptor system, modeling studies have revealed the molecular reasons for the lacking interaction of moDcTRAIL-R1 and human TRAIL. Binding of moTRAIL to this receptor crucially involves a salt bridge that cannot be formed with the human ligand due to an uncharged serine at the corresponding position (Schneider *et al.*, 2003). These differences have to be considered for the translation of data obtained in mouse models. In addition to the lacking interaction with moDcTRAIL-R1, the lower binding activity of human TRAIL for moTRAIL-R2 compared to huTRAIL-R2 may contribute to differential activities in mice and humans, e.g. altering the risk for toxic effects.

The investigated targeted dimeric scTRAIL fusion proteins are supposed to act in trans, i.e. to bind simultaneously to target antigens and TRAIL receptors on distinct cells, as well as in cis with concomitant binding to both kinds of target structures on the same cell. Recent studies by Tatzel *et al.* (2016) demonstrated the crucial dependence on a long flexible linker incorporated between an scFv and a single-chain version of TRAIL for the capability to bend over and act in cis. By analyzing the cell population surviving treatment with an scFv-scTRAIL variant lacking a spacer sequence, they could show that this format exclusively acted in trans. In contrast, the respective spacer-containing version was able to exert effects in cis. Accordingly, further experiments are required to reveal whether the investigated targeted dimeric scTRAIL fusion proteins act in cis or in trans or both. Especially scFv-EHD2-scTRAIL and scFv-Fc-scTRAIL molecules with their central dimerization moiety and flexible linkers on both ends connecting the antibody and scTRAIL units are supposed to possess greater flexibility. With respect to therapeutic application, there might even be sound scientific rationale to use a mixture of trans- and cis-acting formats to effectively target solid tumors (which might profit from a bystander effect) and circulating tumor cells, respectively.

4.2 TRAIL valency and active tumor cell targeting as factors influencing *in vitro* bioactivity of scTRAIL fusion proteins

Previous studies of EHD2-scTRAIL, scTRAIL-RBD-Fc, and hexameric isoleucine zipper-fused TRAIL have demonstrated the superior activity obtained by assembly of two (sc)TRAIL units in one molecule thereby generating six TRAIL receptor binding sites. The markedly improved effects of these molecules rely on the increased TRAIL valency that allows efficient clustering and thus activation of death receptors (Gieffers *et al.*, 2013; Han *et al.*, 2016; Seifert *et al.*, 2014a). In line with these data, dimeric assembly of two scTRAIL units via the EHD2 and an Fc part significantly enhanced the cytotoxic activity compared to monomeric scTRAIL. Further studies on caspase activities confirmed faster and more pronounced activation of initiator and executioner caspases by Fc-scTRAIL compared to scTRAIL. Similarly, increased caspase activities have already been observed for tetra- and pentavalent forms of a TRAIL-R2-directed nanobody (Huet *et al.*, 2014). Analysis of these and other TRAIL-R2-agonistic scaffold proteins and antibody fragments that allow successive extension of single binding sites confirmed the requirement of an at least tetravalent format to improve the exerted effects compared to homotrimeric TRAIL (Huet *et al.*, 2014; Liu *et al.*, 2015; Swers *et al.*, 2013; Wang *et al.*, 2013).

Recent data of Beyrath *et al.* (2016), however, demonstrated that the required degree of oligomerization is cell line-dependent. Even dimeric TRAIL-R2-specific peptides were described to be sufficient to induce apoptosis on some cell lines, while having antagonistic effects on others. They furthermore showed that the valency of the analyzed peptides is not the sole determinant for efficient apoptosis induction. Additionally, an appropriate spatial distribution is essential to avoid sterical hindrance of multivalent receptor binding (Beyrath *et al.*, 2016). Using a single-chain version of the natural homotrimeric ligand circumvents this problem, and obviously, the flexibility provided by the homodimerization modules and linkers employed in this study is sufficient to also allow more than trivalent receptor binding.

In accordance with previous reports of scFvhu225-EHD2-scTRAIL and EHD2-scTRAIL fusion proteins (Seifert *et al.*, 2014a), all formats of EGFR-targeted dimeric scTRAIL molecules showed significantly improved induction of cell death *in vitro* compared to non-targeted dimeric Fc-scTRAIL. Initially, the sets of different dimeric antibody-scTRAIL formats comprising several targeting moieties were generated to validate both the suitability of the distinct formats and the concept of improving the bioactivity of dimeric scTRAIL fusion proteins by combination with an antibody part. However, cell death induction assays did not confirm targeting effects for all antibody moieties. Attempting to understand the factors underlying these differences, the EC_{50} values of cell death induction were correlated with the binding properties of the respective molecules. A first analysis indicated potent antigen binding by the antibody moiety (stronger than binding to TRAIL-R2) as requirement for targeting effects. Despite the effective binding activity of the HER3-specific antibody moiety 3-43 to its isolated antigen, increased bioactivity of the corresponding scFv-Fc-scTRAIL fusion protein compared to Fc-scTRAIL was only obtained for Colo205 cells. Examination of the binding properties for the relevant cell lines revealed that scFv-Fc-scTRAIL molecules showing targeting effects in cytotoxicity assays exhibited improved binding to the respective cell line compared to Fc-scTRAIL. While increased binding of scFv3-43-Fc-scTRAIL was seen on Colo205 cells, no differences to Fc-scTRAIL were found on HCT116 cells that displayed lower HER3 expression levels. These differential HER3 expression profiles were confirmed by a recent quantitative study reporting 2,850 receptor molecules on Colo205 cells and 1,520 on HCT116 cells (Schmitt *et al.*, in preparation). Thus, active targeting of dimeric scTRAIL molecules seemed to depend on enhanced binding properties for the respective cell line that in turn appeared to be determined by the antibody affinity and sufficient antigen expression levels. Unlike this

observation, active targeting has been demonstrated for all reported scFv-(sc)TRAIL molecules (Table 1.1), although K_D values of the antibody part as high as 142 nM have been described (Stieglmaier *et al.*, 2008). In contrast to scFv-(sc)TRAIL fusion proteins that show an activity comparable to soluble TRAIL in the absence of target antigen expression (Wajant *et al.*, 2001), dimeric versions of scTRAIL *per se* exert considerably stronger effects. While scFv-(sc)TRAIL molecules require membrane-attachment to signal via TRAIL-R2, dimeric forms intrinsically possess this capacity. This explains why dimeric scTRAIL molecules have higher requirements to improve their activity by active targeting than non-oligomerized forms of TRAIL.

Consistent with previous studies (Seifert *et al.*, 2014a), inhibition of EGFR or HER3 binding with excess amounts of blocking antibodies reduced the cell death-inducing activity of scFvhu225-Fc-scTRAIL (on Colo205 and HCT116 cells) and scFv3-43-Fc-scTRAIL (on Colo205 cells) to a level comparable to that of Fc-scTRAIL. This confirms active targeting by these antibody moieties and additionally demonstrates that the beneficial effects observed in these short-term *in vitro* experiments are induced due to mechanistic binding to the receptor, not because of inhibition of receptor signaling, which would also occur in the presence of blocking antibody. Especially for the analyzed cell lines that both have activating mutations in BRAF (Colo205) or KRAS and PIK3CA (HCT116), blocking of the receptors is not supposed to prevent downstream signaling. Since the hu225 targeting moiety is derived from cetuximab, it is in general capable of blocking EGFR activation and signaling in wild-type KRAS-expressing cells. Indeed, investigations of Dbhu225-scTRAIL on Caco-2 cells that exhibit a wild-type status for MAPK and PI3K pathways confirmed the ability of this molecule to reduce basal and ligand-induced proliferation. In addition, Caco-2 cells surviving treatment with Dbhu225-scTRAIL have been characterized by very low EGFR expression levels, further indicating an importance of targeting EGFR for efficient elimination of the cells (Möller *et al.*, 2014). Referring to the data of Tatzel *et al.* (2016) that demonstrated an enrichment of target-positive cells for trans-acting molecules, survival of cells expressing very low levels of EGFR might indicate that Dbhu225-scTRAIL exerts effects in cis. Although KRAS mutation has been associated with a switch of apoptotic to oncogenic TRAIL signaling (Hoogwater *et al.*, 2010; von Karstedt *et al.*, 2015), the analyzed scTRAIL molecules efficiently induced cell death in both cell lines. In the context of non-apoptotic signaling, low concentrations of the soluble form of the death ligand FasL have been reported to induce migration and proliferation, whereas membrane-attached or soluble oligomerized variants trigger apoptosis (reviewed by Wajant, 2015). In the case of TRAIL,

evidence that also oligomeric forms are generally able to induce non-apoptotic signaling is provided by a study reporting activation of proinflammatory pathways in melanoma cell lines by cross-linked FLAG-TNC-TRAIL (Berg *et al.*, 2009). Further rationale for the combination of TRAIL with anti-EGFR or also anti-HER2 therapeutics is related to this complex non-apoptotic signaling that can be induced by TRAIL. In colorectal cancer cells, cross-talk with EGFR and HER2 signaling via SRC family kinases and ADAM-17 has been described, leading to proteolytic release of TGF-α that in turn induces autocrine and paracrine EGFR/HER2 pro-survival signaling (reviewed by Azijli *et al.*, 2013). Therefore, combining TRAIL and anti-EGFR/HER2 therapy can overcome this pro-survival signaling loop that might be induced by TRAIL therapy alone. In fact, synergistic effects of combinatorial treatment with an anti-HER2 and an anti-TRAIL-R2 antibody have been confirmed in a mouse model of breast cancer (Stagg *et al.*, 2008). Together with the results of this study, depending on cell line- and antibody-specific properties, incorporation of a receptor-blocking antibody moiety in dimeric scTRAIL molecules can have beneficial effects in terms of targeting the therapeutic to tumor cells and modulating signaling pathways to synergize with TRAIL activity. Similarly, targeting of EpCAM with an antagonistic antibody additionally provides a means of selectively killing cancer stem cells and inhibiting its mitogenic signaling activity (reviewed by Munz *et al.*, 2009). Despite significantly improved cell death induction of scFv323/A3hu3-Fc-scTRAIL compared to Fc-scTRAIL, addition of the respective blocking antibody did not or only partially reduce or even increase this favorable activity. Although scFv323/A3hu3-Fc alone did not show any effects on Colo205 cells for concentrations up to 10 nM, further experiments are required to determine whether higher doses used for blocking may exert inhibitory activity. In conclusion, selection of an appropriate antibody moiety with respect to binding strength, specificity for a sufficiently expressed antigen, and interference with a relevant signaling pathway has the potential to improve the *in vitro* bioactivity of the respective dimeric scTRAIL fusion proteins.

4.3 Protein format as factor influencing *in vivo* pharmacokinetics of scTRAIL fusion proteins

Investigations of the pharmacokinetic properties of the different formats of scTRAIL molecules revealed significant differences. According to the expectations, the Fc fusion proteins exhibited longest terminal half-lives. Furthermore, both scFvhu225-EHD2-scTRAIL and EHD2-scTRAIL showed a significantly extended PK profile compared to the diabody constructs and

scTRAIL, which is consistent with previous PK analysis of these protein formats (Seifert *et al.*, 2014a). Since only the targeted, but not the non-targeted EHD2 fusion protein has an increased molecular mass and hydrodynamic radius compared to Dbhu225-scTRAIL and dsDbhu225-scTRAIL, the prolonged half-lives cannot simply be explained by increases in size. Another factor potentially influencing these differences is thermal stability, which was demonstrated to be improved for the EHD2-comprising molecules. However, the higher melting points did not translate into enhanced stability in human plasma at 37 °C. Therefore, it remains unclear, if thermal stability contributes to the differences in half-lives observed for diabody and EHD2 constructs or which other factors might be involved.

The half-lives of the Fc fusion proteins of 17.8 h and 14.5 h were in a similar range to that reported for a scTRAIL-RBD-Fc construct (Gieffers *et al.*, 2013). Yet these half-lives were dramatically shorter than those observed for other Fc fusion proteins (Unverdorben *et al.*, 2016), and a significant reduction compared to scFvhu225-Fc was found. Similarly, conjugation and fusion of TRAIL to HSA have been described to improve its half-life to 6.2 h and 15 h (Byeon *et al.*, 2014; Müller *et al.*, 2010), which is again considerably lower than those reported for other HSA fusion proteins, reaching values up to almost 50 h (Müller *et al.*, 2007). Consistent with these data, fusion of TRAIL to an albumin-binding domain (Li *et al.*, 2016) was not as effective as described for e.g. a single-chain diabody (Stork *et al.*, 2007). An even shorter half-life of only 100 min has been estimated for a fusion protein of the human IgG1 Fc part and homotrimeric TRAIL (Wang *et al.*, 2014), which highlights the importance of incorporating a single-chain version of TRAIL. Interestingly, a reduced PK profile has also been demonstrated for scFvhu225-EHD2-scTRAIL compared to the respective recombinant antibody scFvhu225-EHD2, despite the considerable increase in size for the scTRAIL molecule (Seifert *et al.*, 2014a). Based on the presence of an additional linker and effector moiety in scFvhu225-Fc-scTRAIL compared to scFvhu225-Fc, the serum half-life may be reduced due to decreased stability and increased susceptibility for cleavage by proteases. Indeed, the thermal stability of the corresponding scTRAIL molecule is 8 °C lower than that of the recombinant antibody. Analysis of the stability in human plasma at physiological temperatures revealed that at least 50 % of the scTRAIL fusion proteins remain intact after seven days. This level is clearly higher than that detected after seven days *in vivo*, indicating that decreased stability is unlikely the limiting factor.

Another aspect influencing pharmacokinetic properties is target-mediated clearance (reviewed by Wang *et al.*, 2008). Since the investigated scTRAIL molecules were capable of binding to all mouse TRAIL receptors, except for moDcTRAIL-R1, TRAIL receptor-mediated processes may lead to reduced levels of scTRAIL fusion proteins in the serum. An indicator of such target-mediated clearance is the observation of dose-dependent differences in elimination leading to increased half-lives for higher doses (reviewed by Wang *et al.*, 2008). A prominent example is cetuximab, for which short serum half-lives have been found and attributed to receptor-mediated clearance. Consistent with the described observation, prolonged half-lives and accumulation have been demonstrated for increased doses and multiple application of high doses of cetuximab, respectively (Tan *et al.*, 2006). However, application of increased and/or multiple doses of scTRAIL molecules during the pharmacodynamic experiments did not lead to saturation effects as indicated by comparable PK profiles determined for all settings. Generation and analysis of fusion proteins comprising a receptor-dead variant of scTRAIL may provide deeper insight into the role of target-mediated clearance. Mutations selectively disrupting TRAIL receptor binding sites have been described previously (Hymowitz *et al.*, 2000) and can be used to develop a scTRAIL variant that lacks the ability to bind to TRAIL receptors. Increased serum half-lives of fusion proteins thereof would indicate the relevance of target-mediated processes. A strategy restoring improved PK properties of antibodies eliminated due to target binding has been developed and successfully applied for an anti-PCSK9 and an anti-IL-6R antibody. Engineering antigen binding to occur in a pH-sensitive manner, i.e. binding at physiological pH and dissociation at acidic endosomal pH, allowed exploitation of neonatal Fc receptor (FcRn)-mediated recycling after antibody release in the endosome (Chaparro-Riggers *et al.*, 2012; Igawa *et al.*, 2010b). A corresponding engineering approach might confer prolonged serum half-lives on Fc-containing scTRAIL fusion proteins, if in fact limited due to target-mediated clearance. Recent studies of a scTRAIL molecule largely incapable of binding to TRAIL receptors, though, revealed PK properties similar to those of the respective fusion protein comprising fully active scTRAIL (Marquardt and Seifert, unpublished data). Therefore, TRAIL receptor-mediated clearance does not seem to be the main cause of the significantly reduced serum half-lives of Fc-containing scTRAIL constructs.

Further factors that may influence the pharmacokinetic behavior of the analyzed fusion proteins are FcRn-mediated recycling and non-specific clearance. The exceptionally long half-

lives of IgGs are linked to their ability to bind to the neonatal Fc receptor in a pH-dependent manner (reviewed by Kontermann, 2009). In order to evaluate whether the fusion of scTRAIL to the Fc part impairs FcRn-mediated recycling, binding studies of scFvhu225-Fc-scTRAIL, Fc-scTRAIL, and scFvhu225-Fc to the FcRn similar to those described by Unverdorben *et al.* (2016) are required. By performing quartz crystal microbalance measurements, FcRn binding kinetics at pH 6.0 and pH 7.4, as well as the dissociation behavior due to changes of pH from 6.0 to 7.4 can be determined to unravel potential differences. Modification of the linker connecting the Fc part and scTRAIL as well as incorporation of mutations in the Fc part shown to enhance FcRn interaction (Datta-Mannan *et al.*, 2012) might provide a strategy to overcome potential limitations. Since a reduced pharmacokinetic profile has also been reported for scFvhu225-EHD2-scTRAIL compared to scFvhu225-EHD2 (Seifert *et al.*, 2014a), other factors seem to affect the PK of the analyzed scTRAIL molecules independent of a potential contribution of altered FcRn-mediated recycling. Regarding non-specific clearance of antibodies, binding to negatively charged structures has been proposed as the main reason underlying this process. Previous studies demonstrated a correlation between basic isoelectric points (pI) and atypical rapid clearance of monoclonal antibodies. Reducing the pI by at least one unit was shown to restore improved PK properties, decreasing the clearance by factors of 2 to 4 (Igawa *et al.*, 2010a; Li *et al.*, 2014). In order to analyze a potential influence of scTRAIL on the pI of the respective fusion protein, isoelectric points were calculated based on the amino acid sequences, revealing values of 8.2, 8.0, 8.1, and 8.1 for scFvhu225-Fc-scTRAIL, Fc-scTRAIL, scTRAIL, and scFvhu225-Fc, respectively. Thus, the recombinant antibody, scTRAIL, and the fusion proteins thereof have similar calculated isoelectric points, thereby indicating the importance of other factors in provoking the differences in half-lives. Recent studies investigating non-specific clearance based on binding to negatively charged heparin or cell membranes demonstrated that instead of the isoelectric point, fast clearance is rather mediated by positively charged patches within the protein (Datta-Mannan *et al.*, 2015a; Datta-Mannan *et al.*, 2015b). Visualization of positively charged amino acids in the crystal structure of TRAIL indeed confirmed the existence of positively charged areas (Figure 4.1A). Hence, non-specific clearance due to binding of positively charged patches of scTRAIL to negatively charged structures might at least contribute to the reduced serum half-lives of Fc-containing scTRAIL molecules compared to scFvhu225-Fc.

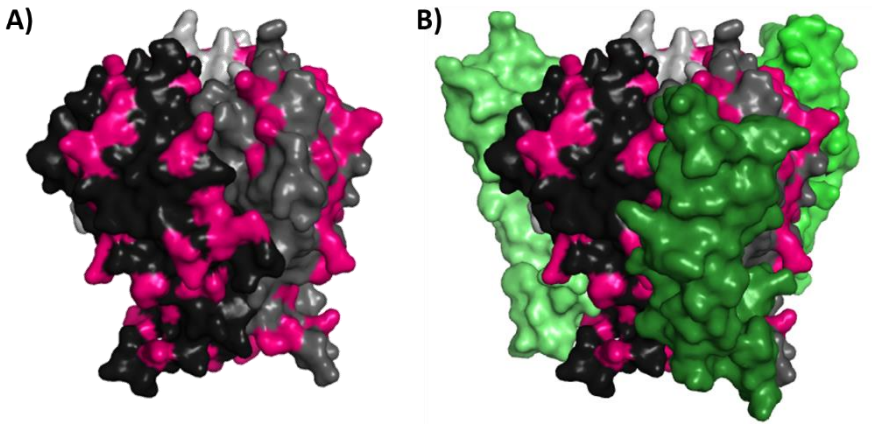

Figure 4.1: Visualization of positively charged patches at the surface of TRAIL. Surfaces of the THD of homotrimeric TRAIL alone (A) and in complex with three TRAIL-R2 chains (B) are represented. Visualization of PDB 1DU3 (Cha *et al.*, 2000) was performed using PyMOL. TRAIL monomers are shown in light gray, gray, and dark gray. TRAIL-R2 chains are colored in different shades of green. Positively charged amino acids are highlighted in magenta.

Datta-Mannan *et al.* (2015a) used molecular surface modeling to identify amino acid substitutions that disrupt positively charged regions and successfully demonstrated enhanced pharmacokinetic properties of the respectively modified antibodies compared to the parental forms without affecting the pI. Accordingly, balancing the positively charged areas in scTRAIL might provide a strategy to generate fusion proteins with improved half-lives. Since positively charged amino acids are partly located at the interface formed by two TRAIL monomers (Figure 4.1), disruption of these patches might influence binding to TRAIL receptors and therefore activity. Besides careful selection of amino acid substitutions and investigations of potential immunogenicity, validation of the activity of the generated variant will be required for the development of a potentially PK-optimized scTRAIL version.

4.4 Protein format and targeting as factors influencing pharmacodynamics of scTRAIL fusion proteins

In vivo studies confirmed potent activity of all analyzed formats of EGFR-targeting scTRAIL fusion proteins. This is consistent with previous investigations, reporting significantly reduced tumor volumes by treatment with Dbhu225-scTRAIL and scFvhu225-EHD2-scTRAIL (Seifert *et al.*, 2014; Siegemund *et al.*, 2012; Siegemund *et al.*, 2016). Although direct comparison of doses used in those experiments and in the present study might be complicated by tumor heterogeneities, the scTRAIL variant and linkers employed here seem to generate proteins that are even more active. The single-chain version of TRAIL used in the present study comprised the amino acids 118 to 281 and linkers of a single glycine residue. This variant was

derived from a previous optimization study and was chosen due to favorable properties regarding product quality, thermal stability, and activity. This optimization study additionally identified other promising scTRAIL versions containing reduced and modified sequences and evaluated one variant as Dbhu225-scTRAIL fusion protein in a Colo205 xenograft model. However, application of 0.3 nmol of that Dbhu225-scTRAIL variant in combination with 5 µg bortezomib on eight consecutive days induced only marginal effects (Siegemund *et al.*, 2016), while six treatments with 0.2 nmol of the Dbhu225-scTRAIL version used in the present study significantly reduced tumor growth in the absence of bortezomib. These data clearly illustrate the influence of the scTRAIL version and linkers on efficacy. The *in vivo* experiments were not only performed to confirm activity, but also to compare the PD effects induced by the already described diabody and EHD2 formats, and the newly established scFv-Fc-scTRAIL. In general, pharmacodynamic properties of a therapeutic are driven by a specific pharmacokinetic parameter, such as peak concentration (C_{max}) or systemic exposure (AUC; reviewed by Tuntland *et al.*, 2014). Applying six injections of 0.5 nmol protein in combination with bortezomib, the first PD experiment did not reveal any differences between the analyzed formats. Initial peak concentrations determined 3 min after injection were similar for all molecules, which might suggest a C_{max}-driven effect. Since the treatment regimen of this experiment induced almost complete tumor remission, another PD study was conducted, injecting 0.2 nmol of the EGFR-targeting formats without bortezomib to identify potential differences that might have been masked by the high doses applied before. Similar anti-tumor activity was determined for Dbhu225-scTRAIL and scFvhu225-EHD2-scTRAIL, whereas scFvhu225-Fc-scTRAIL induced considerably stronger effects, indicating that the AUC has an influence on the *in vivo* activity. However, it should be noted that the PD studies were not designed to elucidate the pharmacokinetic parameter driving the effects, which would require extensive studies, systematically comparing the effect of varying dosing schedules (reviewed by Tuntland *et al.*, 2014). The observation that a prolonged serum half-life translates into improved anti-tumor activity is in accordance with previous reports of an HSA-TNC-TRAIL and an ABD-TRAIL fusion protein that have been shown to exhibit a dramatically improved serum half-life and *in vivo* activity compared to TNC-TRAIL and TRAIL, respectively (Li *et al.*, 2016; Müller *et al.*, 2010).

Consistent with data described for a scTRAIL-RBD-Fc construct (Gieffers *et al.*, 2013), also non-targeted Fc-scTRAIL potently induced tumor regression. In contrast to the *in vitro* bioactivities

and a previous *in vivo* study of targeted and non-targeted EHD2-scTRAIL molecules, targeting did not improve the efficacy of hu225- and 3-43-based scFv-Fc-scTRAIL fusion proteins compared to Fc-scTRAIL *in vivo* and even significantly reduced the anti-tumor activity of scFv323/A3hu3-Fc-scTRAIL. Seifert *et al.* (2014a) reported significantly improved anti-tumor activity of scFvhu225-EHD2-scTRAIL in a Colo205 xenograft model compared to non-targeted EHD2-scTRAIL. While EHD2-scTRAIL (0.35 nmol protein in combination with bortezomib, 4 applications) only marginally influenced tumor growth (Seifert *et al.*, 2014a), Fc-scTRAIL induced almost complete tumor regression already after four applications of 0.2 nmol protein without bortezomib. In line with the observation of increased *in vivo* activity of scFvhu225-Fc-scTRAIL compared to scFvhu225-EHD2-scTRAIL, the different effects of EHD2-scTRAIL and Fc-scTRAIL seem to be related to the significant differences in PK properties. Thus, due to its improved serum half-life, Fc-scTRAIL might reach sufficient levels at the tumor site, even without targeting. Interestingly, no targeting effects have also been observed for a fusion protein of scTRAIL and scFvhu225 in a Colo205 xenograft model, despite of improved activity *in vitro* (Siegemund *et al.*, 2012). The superior *in vivo* effects of Dbhu225-scTRAIL observed in the same study might therefore be mediated rather by dimeric assembly of scTRAIL than by targeting. While several *in vivo* studies of targeted non-oligomerized (sc)TRAIL lacked a respective control of untargeted TRAIL (Aronin *et al.*, 2013; de Bruyn *et al.*, 2010; de Bruyn *et al.*, 2011; Spitzer *et al.*, 2010), thereby not allowing conclusions about targeting effects, other investigations clearly demonstrated improved activity of the targeted versions in mouse models (Cao *et al.*, 2008; Kim *et al.*, 2012; Liu *et al.*, 2014; Schneider *et al.*, 2010; Stieglmaier *et al.*, 2008). In order to evaluate the reasons for the discrepancy between *in vitro* and *in vivo* data obtained in this study, further experiments are required. Several hypotheses arise that might explain the lack of beneficial targeting effects *in vivo*: i) Long-circulating dimeric scTRAIL fusion proteins already exert maximum anti-tumor effects and cannot be improved by targeting. ii) The improved activity of scFv-Fc-scTRAIL compared to Fc-scTRAIL is compensated by reduced extravasation and tumor penetration due to increased size. iii) Instead of specifically targeting tumor cells, the antibody moiety directs the construct additionally to other healthy tissues. iv) The characteristics of the analyzed tumor model are not adequate to reveal the full potential of the targeted molecules. A strategy to investigate the influence of incorporating an antibody moiety in general is the generation of an scFv-Fc-scTRAIL molecule of irrelevant specificity. However, variations in the *in vivo* effects of this construct compared

to Fc-scTRAIL cannot be explicitly attributed to the increase in size, but might also involve non-specific clearance processes. Addressing especially the observation of decreased activity of scFv323/A3hu3-Fc-scTRAIL, experiments treating mice with excess amounts of the respective blocking antibody prior to application of the scTRAIL molecule might reveal a potential impact of targeting the scTRAIL fusion protein to a specific antigen. To ultimately elucidate differences of scFv-Fc-scTRAIL and Fc-scTRAIL molecules in terms of tumor localization and penetration as well as uptake in healthy tissues, biodistribution analysis is crucially required. According to imaging studies of labeled TRAIL receptor-targeting antibodies (Ciprotti *et al.*, 2015; Oldenhuis *et al.*, 2009), such data will help to reveal the differential ability of the constructs to localize to tumors. Despite of employing an antibody moiety with high specificity to the respective antigen, a fusion partner may strongly influence tumor localization. For example, a fusion protein of murine TRAIL and an scFv directed against the alternatively-spliced EDA domain of fibronectin showed specific tumor uptake, while molecules comprising most other members of the murine TNFSF instead of TRAIL were additionally found in high levels in certain healthy tissues (Hemmerle *et al.*, 2014). Likewise, incorporation of different antibody moieties might dramatically influence the localization of the molecules. Biodistribution studies of a transferrin-PEG-TRAIL conjugate furthermore indicate that tumor uptake is not necessarily impaired for large-sized therapeutics. Even though transferrin with a molecular mass of 80 kDa considerably increased the size of the respective conjugate, transferrin-PEG-TRAIL exhibited significantly higher tumor uptake compared to PEG-TRAIL (Kim *et al.*, 2012). Accordingly, biodistribution analysis of scFv-Fc-scTRAIL and Fc-scTRAIL molecules will have to reveal potential differences in tumor localization. Addressing the last hypothesis mentioned above, which refers to characteristics of the tumor model, the *in vitro* experiments already demonstrated that targeting effects depend on properties not only of the antibody moieties, but also of the analyzed cell lines. Investigation of the antigen and TRAIL receptor expression levels on Colo205 tumors is therefore required to determine potential alterations between the *in vivo* and *in vitro* situation. Since *in vitro* studies indicated an importance of sufficient antigen expression levels (probably relative to TRAIL receptor levels), tumor models using cell lines known to express higher antigen levels are necessary to exclude insufficient antigen expression as reason for lacking targeting effects. However, by analyzing different cell lines, besides antigen expression levels, also other factors, like mutations in relevant signaling pathways, might influence the outcome. Modification of a TRAIL-sensitive cell line to stably

express various, but defined levels of the antigen is needed in order to circumvent an impact of other aspects and to support antigen expression levels as factor important for targeting effects *in vitro* and potentially *in vivo*. Thus, further studies are required to understand the role of targeting *in vivo*.

Referring to the *in vitro* data discussed above (see 4.2), selection of an appropriate antibody moiety with respect to tumor characteristics is able to provide additional effects synergizing with TRAIL activity. As already outlined, the hu225 targeting moiety is able to inhibit EGFR-induced proliferation in tumor cells exhibiting a wild-type status for MAPK and PI3K pathways (Möller *et al.*, 2014). Since EGFR signaling has been described to contribute to TRAIL resistance (reviewed by Azijli *et al.*, 2013), blocking of EGFR is moreover able to sensitize tumor cells for TRAIL treatment, and even direct induction of apoptosis by cetuximab has been reported (reviewed by Galizia *et al.*, 2007). Furthermore, only scFv3-43-Fc seemed to exert inhibitory effects on Colo205 cells *in vitro*, and the respective scTRAIL fusion protein (together with Fc-scTRAIL) showed most promising efficacy *in vivo*. Therefore, antibody moieties offer a great potential to equip scTRAIL fusion proteins with additional anti-tumor activity. Further rational for the incorporation of targeting moieties is provided by toxicity analysis. Monitoring of body weight and determination of ALT and amylase serum levels did not indicate any signs of toxicity induced by the investigated scTRAIL molecules. This is consistent with data reported for Dbhu225-scTRAIL and scFvhu225-EHD2-scTRAIL, where even doses of 1 nmol protein in combination with bortezomib did not induce adverse effects (Seifert *et al.*, 2014a; Siegemund *et al.*, 2016). In previous studies, histological and caspase-3 activity analysis of liver tissue of treated mice further demonstrated good tolerability of Dbhu225-scTRAIL, which was additionally verified treating primary human hepatocytes in the absence as well as in presence of bortezomib (Siegemund *et al.*, 2012). More extensive investigations of human liver cells and intact liver tissue have been performed for scFvhu225-scTRAIL. These studies confirmed safety and revealed a superior toxicity profile of targeted compared to non-targeted scTRAIL on inflamed liver tissue (Wahl *et al.*, 2013), indicating favorable effects of targeting with respect to safety. Further validation of tolerability of hexavalent TRAIL-R agonists is provided by toxicology studies of scTRAIL-RBD-Fc in mice and cynomolgus monkeys (Gieffers *et al.*, 2013). These results illustrate promising safety properties of the investigated molecules. Recently, Papadopoulos *et al.* (2015), however, reported partly significant hepatotoxicity of a tetravalent TRAIL-R2-agonistic nanobody in a phase I study, despite lacking toxicity in

cynomolgus monkeys and on human hepatocytes. The authors suppose a correlation between hepatotoxicity and the presence of preexisting anti-drug antibodies, but also indicate that the improved activity of multivalent TRAIL-R agonists may limit the maximum tolerated dose due to hepatotoxicity (Papadopoulos *et al.*, 2015). Supporting the assumption that hepatotoxicity is mediated by anti-drug antibodies, safety studies of recombinant human TRAIL in cynomolgus monkeys demonstrated that the observation of hepatotoxic effects is related to the formation of anti-drug antibodies that are able to cross-link TRAIL and therefore induce increased clustering of TRAIL receptors and apoptosis activation (Zuch de Zafra *et al.*, 2016). Hence, further development of the investigated scTRAIL molecules requires careful assessment of potential toxicities.

4.5 Combined targeting of two TAAs as improvement strategy for dimeric antibody-scTRAIL fusion proteins

Based on the results of the *in vivo* experiments that failed to show beneficial effects of targeting, the concept of improving dimeric scTRAIL molecules by incorporation of targeting moieties is in question. Assuming that the therapeutic potential of the fusion proteins can be enhanced by antibody moieties (e.g. by signaling inhibition or increased tolerability, see 4.4), further optimization of the developed scDb-EHD2-scTRAIL format is necessary. Regarding the EHD2 as dimerization module, the generated data revealed improved performance of the Fc part in terms of production, stability, dimer formation, PK, and PD. Especially, the strong heterogeneity and low amount of dimer of all scDb-EHD2-scTRAIL preparations suggests the replacement of the EHD2 by an Fc part. With respect to the scDb, binding studies demonstrated significantly reduced activity of several antibody moieties in certain combinations. Since a dramatic influence of the domain order of bispecific diabodies on functional properties, like binding and T cell retargeting, has been reported by previous studies (Asano *et al.*, 2013; Lu *et al.*, 2004), further development of these molecules requires systematic generation and characterization of scDb versions of different orientation. Final optimization of the format may be achieved by variation of linkers within the scDb as well as linkers connecting scDb, dimerization module, and scTRAIL according to Siegemund *et al.* (2016). By increasing the linker length of Dbhu225 from five to ten amino acids and modification of the linker connecting Dbhu225 and scTRAIL, a considerably improved product quality has been obtained (Siegemund *et al.*, 2016). Another strategy for further optimization

might be provided by the use of alternative bispecific antibody formats as fusion partner of scTRAIL, including small molecules, like tandem scFvs, and IgG-like formats, such as dual variable domain immunoglobulins or CrossMabs (reviewed by Kontermann and Brinkmann, 2015). Concerning the specificities, for example, combination of antagonistic anti-HER2 and -HER3 antibody moieties has been demonstrated to efficiently inhibit proliferation of HER2-amplified tumor cells (McDonagh *et al.*, 2012). Therefore, selection of targeting moieties fitting the characteristics of the respective tumor allows generation of highly selective therapeutics as well as modulation of relevant receptor signaling.

4.6 Conclusions and Outlook

By generating and comprehensively characterizing four different targeted dimeric scTRAIL formats comprising five distinct antibody moieties, this study is the first to comparatively analyze the impact of format and targeting on biochemical and functional properties to further guide the development of potent scTRAIL-based therapeutics. *In vitro* experiments identified scFv-Fc-scTRAIL as superior format in terms of production, dimer formation, and stability and furthermore indicated factors relevant to improve cell death induction by targeting. Namely, these targeting effects seemed to be related to enhanced cell binding of scFv-Fc-scTRAIL compared to non-targeted Fc-scTRAIL, which appeared to be determined by a potent binding activity of the antibody (relative to scTRAIL) and sufficient antigen expression levels (relative to TRAIL receptors). *In vivo* studies confirmed significantly prolonged serum half-lives of Fc fusion proteins that translated into improved anti-tumor activity. Surprisingly, no beneficial effects of targeting were observed in the investigated Colo205 xenograft model.

Referring to the lack of targeting effects *in vivo*, further experiments already suggested above (see 4.4) are required to determine the underlying reasons. Assuming that the size increase hampers the activity of the targeted molecules, employing smaller ligands, such as single domain antibodies (reviewed by Kontermann, 2010), antigen-binding scaffold proteins (reviewed by Gebauer and Skerra, 2009) or peptides (Ferrieu-Weisbuch *et al.*, 2006; Liu *et al.*, 2014), might provide a strategy to incorporate a targeting moiety leading to a more limited increase in size. Most likely, targeting and other effects exerted by antibody moieties highly depend on tumor properties. Therefore, analysis of biomarkers (Wagner *et al*., 2007; Soria *et al.*, 2011) and gene or protein expression profiles (Chen *et al.*, 2012; O'Reilly *et al.*, 2014; Passante *et al.*, 2013; Weyhenmeyer *et al.*, 2016) seems to be crucial to predict TRAIL

sensitivity of a certain tumor and to suggest i) an appropriate antibody moiety or alternative fusion partner, ii) the incorporation of a receptor-specific TRAIL variant, and iii) a suitable sensitizer. Considering the long list of established TRAIL fusion proteins (see Table 1.1), there is a large diversity of antibodies and ligands that can be selected as fusion partners explicitly fitting the requirements for treatment of a specific tumor. Likewise, tumor cell line-dependent incorporation of a TRAIL-R1- or TRAIL-R2-specific TRAIL version might provide a strategy to improve cell death induction (reviewed by de Miguel *et al.*, 2016). With respect to selection of an optimal sensitizer, significantly improved bioactivity by co-treatment with bortezomib was observed for both cell lines *in vitro*. However, a previous *in vivo* experiment revealed only slightly enhanced efficacy of Dbhu225-scTRAIL in the presence of bortezomib (Siegemund *et al.*, 2012). In accordance with the strong sensitizing effect of the SMAC mimetic SM83 reported e.g. for oncogenic KRAS-expressing cell lines (Möller *et al.*, 2014), significantly improved activity of Dbhu225-scTRAIL in combination with SM83 compared to bortezomib was found in a Colo205 xenograft model (Hutt, unpublished data), highlighting the influence of an appropriately selected sensitizer. Apart from SMAC mimetics, the meanwhile broad variety of highly potent sensitizers offers the possibility to adjust the sensitization strategy depending on specific tumor characteristics, e.g. inhibiting anti-apoptotic BCL-2 family members, histone deacetylases, cyclin-dependent kinase 9, and the molecular chaperone Hsp90, as well as inducing ER stress (reviewed by Lemke *et al.*, 2014; Stolfi *et al.*, 2012). As an alternative to separate treatments with TRAIL and sensitizer, a concept has been established integrating both in one molecule. Fusion of a SMAC-derived peptide to TRAIL via a linker including protease cleavage sites and a membrane-penetrating domain has demonstrated considerably increased activity on various cell lines (Pieczykolan *et al.*, 2014). Besides analysis of the fusion proteins in less artificial systems, like patient-derived xenografts (reviewed by Hidalgo *et al.*, 2014), additional experiments might be performed to determine their potential in non-cancerous diseases. Positive effects of TRAIL administration have been shown for example for certain autoimmune diseases and infections (reviewed by Amarante-Mendes and Griffith, 2015). Further development of the molecules for therapeutic application will additionally require generation of high producer cell lines, a strategy for purification of tagless versions, as well as extensive toxicity analysis.

In conclusion, this study identified scFv-Fc-scTRAIL as superior dimeric antibody-scTRAIL format and hu225, 3-43, and 323/A3hu3 as favorable targeting moieties *in vitro*, whereas *in*

vivo experiments revealed the potent anti-tumor activity of Fc-scTRAIL, which even exceeded that of certain targeted counterparts. Therefore, the long-circulating dimeric Fc-scTRAIL fusion protein represents a promising version of second generation scTRAIL molecules and potentially exerts maximum activity, at least in the investigated tumor model. Allowing the combination with various fusion partners, Fc-scTRAIL provides a platform that can be readily equipped with additional properties likely to synergize with TRAIL activity in a tumor type-specific manner, thereby offering the opportunity for tumor-tailored optimization.

5 Bibliography

Allen, J. E., Ferrini, R., Dicker, D. T., Batzer, G., Chen, E., Oltean, D. I., … El-Deiry, W. S. (2012). Targeting TRAIL Death Receptor 4 with Trivalent DR4 Atrimer Complexes. *Molecular Cancer Therapeutics*, *11*(10), 2087–2095.

Almasan, A., & Ashkenazi, A. (2003). Apo2L/TRAIL: Apoptosis signaling, biology, and potential for cancer therapy. *Cytokine and Growth Factor Reviews*, *14*(3–4), 337–348.

Amarante-Mendes, G. P., & Griffith, T. S. (2015). Therapeutic applications of TRAIL receptor agonists in cancer and beyond. *Pharmacology and Therapeutics*, *155*, 117–131.

Aronin, A., Amsili, S., Prigozhina, T. B., Tzdaka, K., Rachmilewitz, J., Shani, N., … Dranitzki Elhalel, M. (2013). Fn14•Trail effectively inhibits hepatocellular carcinoma growth. *PloS One*, *8*(10), e77050.

Arteaga, C. L., & Engelman, J. A. (2014). ERBB receptors: From oncogene discovery to basic science to mechanism-based cancer therapeutics. *Cancer Cell*, *25*(3), 282–303.

Asano, R., Kumagai, T., Nagai, K., Taki, S., Shimomura, I., Arai, K., … Kumagai, I. (2013). Domain order of a bispecific diabody dramatically enhances its antitumor activity beyond structural format conversion: The case of the hEx3 diabody. *Protein Engineering, Design and Selection*, *26*(5), 359–367.

Ashkenazi, A. (2002). Targeting death and decoy receptors of the tumour-necrosis factor superfamily. *Nature Reviews. Cancer*, *2*(June), 420–430.

Ashkenazi, A. (2008). Targeting the extrinsic apoptosis pathway in cancer. *Cytokine and Growth Factor Reviews*, *19*(3–4), 325–331.

Ashkenazi, A. (2015). Targeting the extrinsic apoptotic pathway in cancer: lessons learned and future directions. *The Journal of Clinical Investigation*, *125*(2), 487–489.

Ashkenazi, A., Pai, R. C., Fong, S., Leung, S., Lawrence, D. A., Marsters, S. A., … Schwall, R. H. (1999). Safety and antitumor activity of recombinant soluble Apo2 ligand. *Journal of Clinical Investigation*, *104*(2), 155–162.

Assohou-Luty, C., Gerspach, J., Siegmund, D., Müller, N., Huard, B., Tiegs, G., … Wajant, H. (2006). A CD40-CD95L fusion protein interferes with CD40L-induced prosurvival signaling and allows membrane CD40L-restricted activation of CD95. *Journal of Molecular Medicine*, *84*(9), 785–797.

Attar, R., Sajjad, F., Qureshi, M. Z., Tahir, F., Hussain, E., Fayyaz, S., & Farooqi, A. A. (2014). TRAIL based therapy: Overview of mesenchymal stem cell based delivery and miRNA controlled expression of TRAIL. *Asian Pacific Journal of Cancer Prevention*, *15*(16), 6495–6497.

Austin, C. D., Lawrence, D. A., Peden, A. A., Varfolomeev, E. E., Totpal, K., De Mazière, A. M., … Ashkenazi, A. (2006). Death-receptor activation halts clathrin-dependent endocytosis. *Proceedings of the National Academy of Sciences of the United States of America*, *103*(27), 10283–10288.

Azijli, K., Weyhenmeyer, B., Peters, G. J., de Jong, S., & Kruyt, F. A. E. (2013). Non-canonical kinase signaling by the death ligand TRAIL in cancer cells: discord in the death receptor family. *Cell Death and Differentiation*, *20*(7), 858–868.

Baeuerle, P. A., & Gires, O. (2007). EpCAM (CD326) finding its role in cancer. *British Journal of Cancer*, *96*(3), 417–423.

Beck, A., & Reichert, J. M. (2011). Therapeutic Fc-fusion proteins and peptides as successful alternatives to antibodies. *mAbs*, *3*(5), 415–416.

Belch, A., Sharma, A., Spencer, A., Tarantolo, S., Bahlis, N. J., Doval, D., … Chanan-Khan, A. A. (2010). A Multicenter Randomized Phase II Trial of Mapatumumab, a TRAIL-R1 Agonist Monoclonal

Antibody, In Combination with Bortezomib In Patients with Relapsed/Refractory Multiple Myeloma (MM). *Blood, 116*(21), 5031.

Berg, D., Lehne, M., Müller, N., Siegmund, D., Münkel, S., Sebald, W., … Wajant, H. (2007). Enforced covalent trimerization increases the activity of the TNF ligand family members TRAIL and CD95L. *Cell Death and Differentiation*, *14*(12), 2021–2034.

Berg, D., Stühmer, T., Siegmund, D., Müller, N., Giner, T., Dittrich-Breiholz, O., … Wajant, H. (2009). Oligomerized tumor necrosis factor-related apoptosis inducing ligand strongly induces cell death in myeloma cells, but also activates proinflammatory signaling pathways. *FEBS Journal*, *276*(23), 6912–6927.

Bertsch, U., Röder, C., Kalthoff, H., & Trauzold, A. (2014). Compartmentalization of TNF-related apoptosis-inducing ligand (TRAIL) death receptor functions: emerging role of nuclear TRAIL-R2. *Cell Death & Disease*, *5*, e1390.

Beyrath, J., Chekkat, N., Smulski, C. R., Lombardo, C. M., Lechner, M., Seguin, C., … Fournel, S. (2016). Synthetic ligands of death receptor 5 display a cell-selective agonistic effect at different oligomerization levels. *Oncotarget*, *7*(40), 64942–64956.

Bodmer, J. L., Meier, P., Tschopp, J., & Schneider, P. (2000). Cysteine 230 is essential for the structure and activity of the cytotoxic ligand TRAIL. *Journal of Biological Chemistry*, *275*(27), 20632–20637.

Bodmer, J. L., Schneider, P., & Tschopp, J. (2002). The molecular architecture of the TNF superfamily. *Trends in Biochemical Sciences*, *27*(1), 19–26.

Bossen, C., Ingold, K., Tardivel, A., Bodmer, J.-L., Gaide, O., Hertig, S., … Schneider, P. (2006). Interactions of tumor necrosis factor (TNF) and TNF receptor family members in the mouse and human. *The Journal of Biological Chemistry*, *281*(20), 13964–13971.

Bremer, E., De Bruyn, M., Samplonius, D. F., Bijma, T., Ten Cate, B., De Leij, L. F. M. H., & Helfrich, W. (2008a). Targeted delivery of a designed sTRAIL mutant results in superior apoptotic activity towards EGFR-positive tumor cells. *Journal of Molecular Medicine*, *86*(8), 909–924.

Bremer, E., Kuijlen, J., Samplonius, D., Walczak, H., De Leij, L., & Helfrich, W. (2004a). Target cell-restricted and -enhanced apoptosis induction by a scFv:sTRAIL fusion protein with specificity for the pancarcinoma-associated antigen EGP2. *International Journal of Cancer*, *109*(2), 281–290.

Bremer, E., Samplonius, D. F., Peipp, M., Van Genne, L., Kroesen, B. J., Fey, G. H., … Helfrich, W. (2005b). Target cell-restricted apoptosis induction of acute leukemic T cells by a recombinant tumor necrosis factor-related apoptosis-inducing ligand fusion protein with specificity for human CD7. *Cancer Research*, *65*(8), 3380–3388.

Bremer, E., Samplonius, D. F., van Genne, L., Dijkstra, M. H., Kroesen, B. J., de Leij, L. F. M. H., & Helfrich, W. (2005a). Simultaneous Inhibition of Epidermal Growth Factor Receptor (EGFR) Signaling and Enhanced Activation of Tumor Necrosis Factor-related Apoptosis-inducing Ligand (TRAIL) Receptor-mediated Apoptosis Induction by an scFv:sTRAIL Fusion Protein with Specificity for Human EGFR. *Journal of Biological Chemistry*, *280*(11), 10025–10033.

Bremer, E., Samplonius, D., Kroesen, B.-J., van Genne, L., de Leij, L., & Helfrich, W. (2004b). Exceptionally potent anti-tumor bystander activity of an scFv:sTRAIL fusion protein with specificity for EGP2 toward target antigen-negative tumor cells. *Neoplasia (New York, N.Y.)*, *6*(5), 636–645.

Bremer, E., van Dam, G. M., de Bruyn, M., van Riezen, M., Dijkstra, M., Kamps, G., … Haisma, H. (2008b). Potent systemic anticancer activity of adenovirally expressed EGFR-selective TRAIL fusion protein. *Molecular Therapy : The Journal of the American Society of Gene Therapy*, *16*(12), 1919–1926.

Brünker, P., Wartha, K., Friess, T., Grau-Richards, S., Waldhauer, I., Koller, C. F., … Umana, P. (2016). RG7386, a Novel Tetravalent FAP-DR5 Antibody, Effectively Triggers FAP-Dependent, Avidity-

Driven DR5 Hyperclustering and Tumor Cell Apoptosis. *Molecular Cancer Therapeutics*, *15*(5), 946–957.

Byeon, H. J., Min, S. Y., Kim, I., Lee, E. S., Oh, K. T., Shin, B. S., … Youn, Y. S. (2014). Human Serum Albumin-TRAIL Conjugate for the Treatment of Rheumatoid Arthritis. *Bioconjugate Chemistry*, *25*(12), 2212–2221.

Camidge, D. R., Herbst, R. S., Gordon, M. S., Eckhardt, S. G., Kurzrock, R., Durbin, B., … Mendelson, D. (2010). A phase I safety and pharmacokinetic study of the death receptor 5 agonistic antibody PRO95780 in patients with advanced malignancies. *Clinical Cancer Research*, *16*(4), 1256–1263.

Cao, L., Du, P., Jiang, S.-H., Jin, G.-H., Huang, Q.-L., & Hua, Z.-C. (2008). Enhancement of antitumor properties of TRAIL by targeted delivery to the tumor neovasculature. *Molecular Cancer Therapeutics*, *7*(4), 851–861.

Carswell, E. A., Old, L. J., Kassel, R. L., Green, S., Fiore, N., & Williamson, B. (1975). An endotoxin-induced serum factor that causes necrosis of tumors. *Proceedings of the National Academy of Sciences of the United States of America*, *72*(9), 3666–3670.

Carter, P., Presta, L. E. N., Gormant, C. M., Ridgwayt, J. B. B., Hennert, D., Wongt, W. L. T., … Shepard, H. M. (1992). Humanization of an anti-p185HER2 antibody for human cancer therapy. *PNAS*, *89*(10), 4285–4289.

Cha, S. S., Kim, M. S., Choi, Y. H., Sung, B. J., Shin, N. K., Shin, H. C., … Oh, B. H. (1999). 2.8 Å resolution crystal structure of human TRAIL, a cytokine with selective antitumor activity. *Immunity*, *11*(2), 253–261.

Cha, S. S., Sung, B. J., Kim, Y. A., Song, Y. L., Kim, H. J., Kim, S., … Oh, B. H. (2000). Crystal structure of TRAIL-DR5 complex identifies a critical role of the unique frame insertion in conferring recognition specificity. *Journal of Biological Chemistry*, *275*(40), 31171–31177.

Chae, S. Y., Kim, T. H., Park, K., Jin, C.-H., Son, S., Lee, S., … Lee, K. C. (2010). Improved Antitumor Activity and Tumor Targeting of NH2-Terminal-Specific PEGylated Tumor Necrosis Factor-Related Apoptosis-Inducing Ligand. *Molecular Cancer Therapeutics*, *9*(6), 1719–1729.

Chang, D. W., Xing, Z., Pan, Y., Algeciras-Schimnich, A., Barnhart, B. C., Yaish-Ohad, S., … Yang, X. (2002). C-FLIPL is a dual function regulator for caspase-8 activation and CD95-mediated apoptosis. *EMBO Journal*, *21*(14), 3704–3714.

Chaparro-Riggers, J., Liang, H., DeVay, R. M., Bai, L., Sutton, J. E., Chen, W., … Rajpal, A. (2012). Increasing serum half-life and extending cholesterol lowering in vivo by engineering antibody with pH-sensitive binding to PCSK9. *Journal of Biological Chemistry*, *287*(14), 11090–11097.

Chattopadhyay, K., Ramagopal, U. a, Mukhopadhaya, A., Malashkevich, V. N., Dilorenzo, T. P., Brenowitz, M., … Almo, S. C. (2007). Assembly and structural properties of glucocorticoid-induced TNF receptor ligand: Implications for function. *Proceedings of the National Academy of Sciences of the United States of America*, *104*(49), 19452–19457.

Chen, D., Frezza, M., Schmitt, S., Kanwar, J., & P Dou, Q. (2011). Bortezomib as the first proteasome inhibitor anticancer drug: current status and future perspectives. *Current Cancer Drug Targets*, *11*(3), 239–253.

Chen, J.-J., Knudsen, S., Mazin, W., Dahlgaard, J., & Zhang, B. (2012). A 71-gene signature of TRAIL sensitivity in cancer cells. *Molecular Cancer Therapeutics*, *11*(1), 34–44.

Chipuk, J. E., Moldoveanu, T., Llambi, F., Parsons, M. J., & Green, D. R. (2010). The BCL-2 Family Reunion. *Molecular Cell*, *37*(3), 299–310.

Chuntharapai, A., Dodge, K., Grimmer, K., Schroeder, K., Marsters, S. A., Koeppen, H., … Kim, K. J. (2001). Isotype-dependent inhibition of tumor growth in vivo by monoclonal antibodies to death receptor 4. *J Immunol*, *166*(8), 4891–4898.

Ciardiello, F., & Tortora, G. (2003). Epidermal growth factor receptor (EGFR) as a target in cancer therapy: understanding the role of receptor expression and other molecular determinants that could influence the response to anti-EGFR drugs. *European Journal of Cancer*, *39*, 1348–1354.

Ciprotti, M., Tebbutt, N. C., Lee, F. T., Lee, S. T., Gan, H. K., McKee, D. C., … Scott, A. M. (2015). Phase I imaging and pharmacodynamic trial of CS-1008 in patients with metastatic colorectal cancer. *Journal of Clinical Oncology*, *33*(24), 2609–2616.

Clohessy, J. G., Zhuang, J., De Boer, J., Gil-Gómez, G., & Brady, H. J. M. (2006). Mcl-1 interacts with truncated bid and inhibits its induction of cytochrome c release and its role in receptor-mediated apoptosis. *Journal of Biological Chemistry*, *281*(9), 5750–5759.

Coley, W. B. (1891). II. Contribution to the Knowledge of Sarcoma. *Annals of Surgery*, *14*(3), 199–220.

Corti, A., Fassina, G., Marcucci, F., Barbanti, E., & Cassani, G. (1992). Oligomeric tumour necrosis factor alpha slowly converts into inactive forms at bioactive levels. *The Biochemical Journal*, *284*(Pt 3), 905–910.

Cotter, T. G. (2009). Apoptosis and cancer: the genesis of a research field. *Nature Reviews. Cancer*, *9*(7), 501–507.

Daniels, R. a, Turley, H., Kimberley, F. C., Liu, X. S., Mongkolsapaya, J., Ch'En, P., … Screaton, G. R. (2005). Expression of TRAIL and TRAIL receptors in normal and malignant tissues. *Cell Research*, *15*(6), 430–438.

Datta-Mannan, A., Chow, C. K., Dickinson, C., Driver, D., Lu, J., Witcher, D. R., & Wroblewski, V. J. (2012). FcRn affinity-pharmacokinetic relationship of five human IgG4 antibodies engineered for improved in vitro FcRn binding properties in cynomolgus monkeys. *Drug Metabolism and Disposition*, *40*(8), 1545–1555.

Datta-Mannan, A., Lu, J., Witcher, D. R., Leung, D., Tang, Y., & Wroblewski, V. J. (2015b). The interplay of non-specific binding, target-mediated clearance and FcRn interactions on the pharmacokinetics of humanized antibodies. *mAbs*, *7*(6), 1084–1093.

Datta-Mannan, A., Thangaraju, A., Leung, D., Tang, Y., Witcher, D. R., Lu, J., & Wroblewski, V. J. (2015a). Balancing charge in the complementarity-determining regions of humanized mAbs without affecting pI reduces non-specific binding and improves the pharmacokinetics. *mAbs, 7*(3), 483–493.

De Bruyn, M., Bremer, E., & Helfrich, W. (2013). Antibody-based fusion proteins to target death receptors in cancer. *Cancer Letters*, *332*(2), 175–183.

De Bruyn, M., Rybczynska, A. a, Wei, Y., Schwenkert, M., Fey, G. H., Dierckx, R. a J. O., … Bremer, E. (2010). Melanoma-associated Chondroitin Sulfate Proteoglycan (MCSP)-targeted delivery of soluble TRAIL potently inhibits melanoma outgrowth in vitro and in vivo. *Molecular Cancer*, *9*, 301.

De Bruyn, M., Wei, Y., Wiersma, V. R., Samplonius, D. F., Klip, H. G., Van Der Zee, A. G. J., … Bremer, E. (2011). Cell surface delivery of TRAIL strongly augments the tumoricidal activity of T cells. *Clinical Cancer Research*, *17*(17), 5626–5637.

De Miguel, D., Gallego-Lleyda, A., Anel, A., & Martinez-Lostao, L. (2015). Liposome-bound TRAIL induces superior DR5 clustering and enhanced DISC recruitment in histiocytic lymphoma U937 cells. *Leukemia Research*, *39*(6), 657–666.

De Miguel, D., Lemke, J., Anel, A., Walczak, H., & Martinez-Lostao, L. (2016). Onto better TRAILs for cancer treatment. *Cell Death and Differentiation Advance Online Publication*, *4*, 1–15.

De Wilt, L. H. A. M., Kroon, J., Jansen, G., de Jong, S., Peters, G. J., & Kruyt, F. A. E. (2013). Bortezomib and TRAIL: a perfect match for apoptotic elimination of tumour cells? *Critical Reviews in Oncology/hematology*, *85*(3), 363–372.

Degli-Esposti, M. a, Dougall, W. C., Smolak, P. J., Waugh, J. Y., Smith, C. a, & Goodwin, R. G. (1997b). The novel receptor TRAIL-R4 induces NF-kappaB and protects against TRAIL-mediated apoptosis, yet remains an incomplete death domain. *Immunity*, *7*(6), 813–820.

Degli-Esposti, M. A., Smolak, P. J., Walczak, H., Waugh, J., Huang, C. P., DuBose, R. F., … Smith, C. A. (1997a). Cloning and characterization of TRAIL-R3, a novel member of the emerging TRAIL receptor family. *The Journal of Experimental Medicine*, *186*(7), 1165–1170.

Den Hollander, M. W., Gietema, J. A., de Jong, S., Walenkamp, A. M. E., Reyners, A. K. L., Oldenhuis, C. N. A. M., & De Vries, E. G. E. (2013). Translating TRAIL-receptor targeting agents to the clinic. *Cancer Letters*, *332*(2), 194–201.

Deveraux, Q. L., Takahashi, R., Salvesen, G. S., & Reed, J. C. (1997). X-linked IAP is a direct inhibitor of cell-death proteases. *Nature*, *388*(6639), 300–304.

Dimberg, L. Y., Anderson, C. K., Camidge, R., Behbakht, K., Thorburn, A., & Ford, H. L. (2013). On the TRAIL to successful cancer therapy? Predicting and counteracting resistance against TRAIL-based therapeutics. *Oncogene*, *32*(11), 1341–1350.

Ecker, D. M., Jones, S. D., & Levine, H. L. (2015). The therapeutic monoclonal antibody market. *mAbs*, *7*(1), 9–14.

Edwards, D. P., Grzyb, K. T., Dressier, L. G., Mansel, R. E., Zava, D. T., Sledge, G. W., & McGuire, W. L. (1986). Monoclonal Antibody Identification and Characterization of a Mr 43,000 Membrane Glycoprotein Associated with Human Breast Cancer. *Cancer Research*, *46*(3), 1306–1317.

El-Mesery, M., Trebing, J., Schäfer, V., Weisenberger, D., Siegmund, D., & Wajant, H. (2013). CD40-directed scFv-TRAIL fusion proteins induce CD40-restricted tumor cell death and activate dendritic cells. *Cell Death & Disease*, *4*, e916.

Elmore, S. (2007). Apoptosis: a review of programmed cell death. *Toxicologic Pathology*, *35*(4), 495–516.

Emery, J. G., Mcdonnell, P., Burke, M. B., Deen, K. C., Lyn, S., Silverman, C., … Young, P. R. (1998). Osteoprotegerin Is a Receptor for the Cytotoxic Ligand TRAIL. *The Journal of Biological Chemistry*, *273*(23), 14363–14367.

Espevik, T., Brockhaus, M., Loetscher, H., Nonstad, U., & Shalaby, R. (1990). Characterization of binding and biological effects of monoclonal antibodies against a human tumor necrosis factor receptor. *J Exp Med*, *171*(2), 415–426.

Fadeel, B., Thorpe, C. J., Yonehara, S., & Chiodi, F. (1997). Anti-Fas IgG1 antibodies recognizing the same epitope of Fas/APO-1 mediate different biological effects in vitro. *International Immunology*, *9*(2), 201–209.

Fellermeier, S., Beha, N., Meyer, J.-E., Ring, S., Bader, S., Kontermann, R. E., & Müller, D. (2016). Advancing targeted costimulation with antibody-fusion proteins by introducing TNF superfamily members in a single-chain format. *OncoImmunology*.

Ferrieu-Weisbuch, C., Michel, S., Collomb-Clerc, E., Pothion, C., Deléage, G., & Jolivet-Reynaud, C. (2006). Characterization of prostate-specific antigen binding peptides selected by phage display technology. *Journal of Molecular Recognition*, *19*(1), 10–20.

FitzGerald, K., Holliger, P., & Winter, G. (1997). Improved tumour targeting by disulphide stabilized diabodies expressed in Pichia pastoris. *Protein Engineering*, *10*(10), 1221–1225.

Frey, K., Schliemann, C., Schwager, K., Giavazzi, R., Johannsen, M., & Neri, D. (2010). The immunocytokine F8-IL2 improves the therapeutic performance of sunitinib in a mouse model of renal cell carcinoma. *Journal of Urology*, *184*(6), 2540–2548.

Galizia, G., Lieto, E., De Vita, F., Orditura, M., Castellano, P., Troiani, T., … Ciardiello, F. (2007). Cetuximab, a chimeric human mouse anti-epidermal growth factor receptor monoclonal antibody, in the treatment of human colorectal cancer. *Oncogene*, *26*(25), 3654–3660.

Galligan, L., Longley, D. B., McEwan, M., Wilson, T. R., McLaughlin, K., & Johnston, P. G. (2005). Chemotherapy and TRAIL-mediated colon cancer cell death: the roles of p53, TRAIL receptors, and c-FLIP. *Molecular Cancer Therapeutics*, *4*(12), 2026–2036.

Ganten, T. M., Koschny, R., Haas, T. L., Sykora, J., Li-Weber, M., Herzer, K., & Walczak, H. (2005). Proteasome inhibition sensitizes hepatocellular carcinoma cells, but not human hepatocytes, to TRAIL. *Hepatology (Baltimore, Md.)*, *42*(3), 588–597.

Ganten, T. M., Koschny, R., Sykora, J., Schulze-Bergkamen, H., Büchler, P., Haas, T. L., … Walczak, H. (2006). Preclinical differentiation between apparently safe and potentially hepatotoxic applications of TRAIL either alone or in combination with chemotherapeutic drugs. *Clinical Cancer Research*, *12*(8), 2640–2646.

Ganten, T. M., Sykora, J., Koschny, R., Batke, E., Aulmann, S., Mansmann, U., … Walczak, H. (2009). Prognostic significance of tumour necrosis factor-related apoptosis-inducing ligand (TRAIL) receptor expression in patients with breast cancer. *Journal of Molecular Medicine (Berlin, Germany)*, *87*(10), 995–1007.

Gebauer, M., & Skerra, A. (2009). Engineered protein scaffolds as next-generation antibody therapeutics. *Current Opinion in Chemical Biology*, *13*(3), 245–255.

Gieffers, C., Kluge, M., Merz, C., Sykora, J., Thiemann, M., Schaal, R., … Hill, O. (2013). APG350 induces superior clustering of TRAIL receptors and shows therapeutic antitumor efficacy independent of cross-linking via Fcγ receptors. *Molecular Cancer Therapeutics*, *12*(12), 2735–2747.

Goldstein, N. I., Prewett, M., Zuklys, K., Rockwell, P., & Mendelsohn, J. (1995). Biological efficacy of a chimeric antibody to the epidermal growth factor receptor in a human tumor xenograft model. *Clinical Cancer Research: An Official Journal of the American Association for Cancer Research*, *1*(11), 1311–1318.

Golks, A., Brenner, D., Fritsch, C., Krammer, P. H., & Lavrik, I. N. (2005). c-FLIPR, a new regulator of death receptor-induced apoptosis. *Journal of Biological Chemistry*, *280*(15), 14507–14513.

Gonzalvez, F., Lawrence, D., Yang, B., Yee, S., Pitti, R., Marsters, S., … Ashkenazi, A. (2012). TRAF2 Sets a Threshold for Extrinsic Apoptosis by Tagging Caspase-8 with a Ubiquitin Shutoff Timer. *Molecular Cell*, *48*(6), 888–899.

Graves, J. D., Kordich, J. J., Huang, T. H., Piasecki, J., Bush, T. L., Sullivan, T., … Holland, P. M. (2014). Apo2L/TRAIL and the death receptor 5 agonist antibody AMG 655 cooperate to promote receptor clustering and antitumor activity. *Cancer Cell*, *26*(2), 177–189.

Griffith, T., & Broghammer, E. L. (2001). Suppression of Tumor Growth Following Intralesional Therapy with TRAIL Recombinant Adenovirus. *Molecular Therapy*, *4*(3), 257–266.

Guo, L., Fan, L., Pang, Z., Ren, J., Ren, Y., Li, J., … Jiang, X. (2011a). TRAIL and doxorubicin combination enhances anti-glioblastoma effect based on passive tumor targeting of liposomes. *Journal of Controlled Release*, *154*(1), 93–102.

Guo, L., Fan, L., Ren, J., Pang, Z., Ren, Y., Li, J., … Jiang, X. (2011b). A novel combination of TRAIL and doxorubicin enhances antitumor effect based on passive tumor-targeting of liposomes. *Nanotechnology*, *22*(26), 265105.

Han, J. H., Moon, A. R., Chang, J. H., Bae, J., Choi, J. M., Lee, S. H., & Kim, T.-H. (2016). Potentiation of TRAIL killing activity by multimerization through isoleucine zipper hexamerization motif. *BMB Reports*, *49*(5), 282–287.

Haynes, N. M., Hawkins, E. D., Li, M., McLaughlin, N. M., Hämmerling, G. J., Schwendener, R., … Smyth, M. J. (2010). CD11c+ dendritic cells and B cells contribute to the tumoricidal activity of anti-DR5 antibody therapy in established tumors. *Journal of Immunology (Baltimore, Md. : 1950)*, *185*(1), 532–541.

He, Y., Hendriks, D., van Ginkel, R., Samplonius, D., Bremer, E., & Helfrich, W. (2016). Melanoma-Directed Activation of Apoptosis Using a Bispecific Antibody Directed at MCSP and TRAIL Receptor-2/Death Receptor-5. *Journal of Investigative Dermatology*, *136*(2), 541–544.

Hemann, M. T., & Lowe, S. W. (2006). The p53–Bcl-2 connection. *Cell Death and Differentiation*, *13*(8), 1256–1259.

Hemmerle, T., Hess, C., Venetz, D., & Neri, D. (2014). Tumor targeting properties of antibody fusion proteins based on different members of the murine tumor necrosis superfamily. *Journal of Biotechnology*, *172*, 73–76.

Hendriks, D., He, Y., Koopmans, I., Wiersma, V. R., van Ginkel, R. J., Samplonius, D. F., … Bremer, E. (2016). Programmed Death Ligand 1 (PD-L1)-targeted TRAIL combines PD-L1-mediated checkpoint inhibition with TRAIL-mediated apoptosis induction. *OncoImmunology*, *1*(July).

Herbst, R. S., Eckhardt, S. G., Kurzrock, R., Ebbinghaus, S., O'Dwyer, P. J., Gordon, M. S., … Mendelson, D. S. (2010). Phase I dose-escalation study of recombinant human Apo2L/TRAIL, a dual proapoptotic receptor agonist, in patients with advanced cancer. *Journal of Clinical Oncology*, *28*(17), 2839–2846.

Hidalgo, M., Amant, F., Biankin, A. V., Budinská, E., Byrne, A. T., Caldas, C., … Villanueva, A. (2014). Patient-derived Xenograft models: An emerging platform for translational cancer research. *Cancer Discovery*, *4*(9), 998–1013.

Hinz, S., Trauzold, A., Boenicke, L., Sandberg, C., Beckmann, S., Bayer, E., … Ungefroren, H. (2000). Bcl-XL protects pancreatic adenocarcinoma cells against CD95- and TRAIL-receptor-mediated apoptosis. *Oncogene*, *19*(48), 5477–5486.

Holland, P. M. (2013). Targeting Apo2L/TRAIL receptors by soluble Apo2L/TRAIL. *Cancer Letters*, *332*(2), 156–162.

Holland, P. M. (2014). Death receptor agonist therapies for cancer, which is the right TRAIL? *Cytokine and Growth Factor Reviews*, *25*(2), 185–193.

Holler, N., Tardivel, A., Kovacsovics-Bankowski, M., Hertig, S., Gaide, O., Martinon, F., … Tschopp, J. (2003). Two adjacent trimeric Fas ligands are required for Fas signaling and formation of a death-inducing signaling complex. *Molecular and Cellular Biology*, *23*(4), 1428–1440.

Holliger, P., Prospero, T., & Winter, G. (1993). "Diabodies": small bivalent and bispecific antibody fragments. *Proceedings of the National Academy of Sciences of the United States of America*, *90*(14), 6444–6448.

Hoogwater, F. J. H., Nijkamp, M. W., Smakman, N., Steller, E. J. A., Emmink, B. L., Westendorp, B. F., … Kranenburg, O. (2010). Oncogenic K-Ras Turns Death Receptors Into Metastasis-Promoting Receptors in Human and Mouse Colorectal Cancer Cells. *Gastroenterology*, *138*(7), 2357–2367.

Hornig, N., Kermer, V., Frey, K., Diebolder, P., Kontermann, R. E., & Müller, D. (2012). Combination of a bispecific antibody and costimulatory antibody-ligand fusion proteins for targeted cancer immunotherapy. *Journal of Immunotherapy (Hagerstown, Md. : 1997)*, *35*(5), 418–429.

Hsieh, A., & Moasser, M. (2007). Targeting HER proteins in cancer therapy and the role of the non-target HER3. *British Journal of Cancer*, *97*, 453–457.

Huang, B.-C., Foote, L. J., Lankford, T. K., Davern, S. M., McKeown, C. K., & Kennel, S. J. (2005). A diabody that dissociates to monomer forms at low concentration: effects on binding activity and tumor targeting. *Biochemical and Biophysical Research Communications*, *327*(4), 999–1005.

Huet, H. a, Growney, J. D., Johnson, J. a, Li, J., Bilic, S., Ostrom, L., … Ettenberg, S. a. (2014). Multivalent nanobodies targeting death receptor 5 elicit superior tumor cell killing through efficient caspase induction. *mAbs*, *6*(6), 1560–1570.

Hymowitz, S. G., Christinger, H. W., Fuh, G., Ultsch, M., O'Connell, M., Kelley, R. F., … de Vos, A. M. (1999). Triggering Cell Death: The Crystal Structure of Apo2L/TRAIL in a Complex with Death Receptor 5. *Molecular Cell*, *4*(4), 563–571.

Hymowitz, S. G., Connell, M. P. O., Ultsch, M. H., Hurst, A., Totpal, K., Ashkenazi, A., … Chem, a J. B. (2000). A Unique Zinc-Binding Site Revealed by a High-Resolution X-ray Structure of Apo2L/TRAIL. *Biochemistry*, *39*, 633–640.

Hynes, N. E., & Lane, H. a. (2005). ERBB receptors and cancer: the complexity of targeted inhibitors. *Nature Reviews. Cancer*, *5*(5), 341–354.

Ichikawa, K., Liu, W., Zhao, L., Wang, Z., Liu, D., Ohtsuka, T., … Zhou, T. (2001). Tumoricidal activity of a novel anti-human DR5 monoclonal antibody without hepatocyte cytotoxicity. *Nature Medicine*, *7*(8), 954–960.

Igawa, T., Ishii, S., Tachibana, T., Maeda, A., Higuchi, Y., Shimaoka, S., … Hattori, K. (2010b). Antibody recycling by engineered pH-dependent antigen binding improves the duration of antigen neutralization. *Nature Biotechnology*, *28*(11), 1203–1207.

Igawa, T., Tsunoda, H., Tachibana, T., Maeda, A., Mimoto, F., Moriyama, C., … Hattori, K. (2010a). Reduced elimination of IgG antibodies by engineering the variable region. *Protein Engineering, Design and Selection*, *23*(5), 385–392.

Iyer, A. K., Khaled, G., Fang, J., & Maeda, H. (2006). Exploiting the enhanced permeability and retention effect for tumor targeting. *Drug Discovery Today*, *11*(17–18), 812–818.

Jin, Z., Li, Y., Pitti, R., Lawrence, D., Pham, V. C., Lill, J. R., & Ashkenazi, A. (2009). Cullin3-Based Polyubiquitination and p62-Dependent Aggregation of Caspase-8 Mediate Extrinsic Apoptosis Signaling. *Cell*, *137*(4), 721–735.

Johnstone, R. W., Ruefli, A. A., & Lowe, S. W. (2002). Apoptosis: A link between cancer genetics and chemotherapy. *Cell*, *108*(2), 153–164.

Jouan-Lanhouet, S., Arshad, M., Piquet-Pellorce, C., Martin-Chouly, C., Le Moigne-Muller, G., Herreweghe, F. Van, … Dimanche-Boitrel, M.-T. (2012). TRAIL induces necroptosis involving RIPK1/RIPK3-dependent PARP-1 activation. *Cell Death and Differentiation*, *19*(10), 2003–2014.

Kaplan-Lefko, P. J., Graves, J. D., Zoog, S. J., Pan, Y., Wall, J., Branstetter, D. G., … Gliniak, B. C. (2010). Conatumumab, a fully human agonist antibody to death receptor 5, induces apoptosis via caspase activation in multiple tumor types. *Cancer Biology and Therapy*, *9*(8), 618–631.

Kaspar, M., Trachsel, E., & Neri, D. (2007). The antibody-mediated targeted delivery of interleukin-15 and GM-CSF to the tumor neovasculature inhibits tumor growth and metastasis. *Cancer Research*, *67*(10), 4940–4948.

Kelley, R. F., Totpal, K., Lindstrom, S. H., Mathieu, M., Billeci, K., DeForge, L., … Ashkenazi, A. (2005). Receptor-selective mutants of apoptosis-inducing ligand 2/tumor necrosis factor-related apoptosis-inducing ligand reveal a greater contribution of Death Receptor (DR) 5 than DR4 to apoptosis signaling. *Journal of Biological Chemistry*, *280*(3), 2205–2212.

Kelley, S. K., Harris, L. a, Xie, D., Deforge, L., Totpal, K., Bussiere, J., & Fox, J. a. (2001). Preclinical studies to predict the disposition of Apo2L/tumor necrosis factor-related apoptosis-inducing ligand in humans: characterization of in vivo efficacy, pharmacokinetics, and safety. *The Journal of Pharmacology and Experimental Therapeutics*, *299*(1), 31–38.

Kim, H., Jeong, D., Kang, H. E., Lee, K. C., & Na, K. (2013). A sulfate polysaccharide/TNF-related apoptosis-inducing ligand (TRAIL) complex for the long-term delivery of TRAIL in poly(lactic-co-glycolic acid) (PLGA) microspheres. *Journal of Pharmacy and Pharmacology*, *65*(1), 11–21.

Kim, T. H., Jiang, H. H., Park, C. W., Youn, Y. S., Lee, S., Chen, X., & Lee, K. C. (2011b). PEGylated TNF-related apoptosis-inducing ligand (TRAIL)-loaded sustained release PLGA microspheres for enhanced stability and antitumor activity. *Journal of Controlled Release*, *150*(1), 63–69.

Kim, T. H., Jo, Y. G., Jiang, H. H., Lim, S. M., Youn, Y. S., Lee, S., … Lee, K. C. (2012). PEG-transferrin conjugated TRAIL (TNF-related apoptosis-inducing ligand) for therapeutic tumor targeting. *Journal of Controlled Release: Official Journal of the Controlled Release Society*, *162*(2), 422–428.

Kim, T. H., Youn, Y. S., Jiang, H. H., Lee, S., Chen, X., & Lee, K. C. (2011a). PEGylated TNF-related apoptosis-inducing ligand (TRAIL) analogues: Pharmacokinetics and antitumor effects. *Bioconjugate Chemistry*, *22*(8), 1631–1637.

Kimura, K., Taguchi, T., Urushizaki, I., Ohno, R., Abe, O., Furue, H., … Yamada, K. (1987). Phase I study of recombinant human tumor necrosis factor. *Cancer Chemotherapy and Pharmacology*, *20*(3), 223–229.

Kohlhaas, S. L., Craxton, A., Sun, X., Pinkoski, M. J., & Cohen, G. M. (2007). Receptor-mediated Endocytosis Is Not Required for Tumor Necrosis Factor-related Apoptosis-inducing Ligand (TRAIL)-induced Apoptosis. *The Journal of Biological Chemistry*, *282*(17), 12831–12841.

Kol, A., Terwisscha van Scheltinga, A. G. T., Timmer-Bosscha, H., Lamberts, L. E., Bensch, F., de Vries, E. G. E., & Schröder, C. P. (2014). HER3, serious partner in crime: Therapeutic approaches and potential biomarkers for effect of HER3-targeting. *Pharmacology & Therapeutics*, *143*(1), 1–11.

Kontermann, R. E. (2009). Strategies to extend plasma half-lives of recombinant antibodies. *BioDrugs*, *23*(2), 93–109.

Kontermann, R. E. (2010). Alternative antibody formats. *Current Opinion in Molecular Therapeutics*, *12*(2), 176–183.

Kontermann, R. E., & Brinkmann, U. (2015). Bispecific antibodies. *Drug Discovery Today*, *20*(7), 838–847.

Kontermann, R. E., Martineau, P., Cummings, C. E., Karpas, A., Allen, D., Derbyshire, E., & Winter, G. (1997). Enzyme immunoassays using bispecific diabodies. *Immunotechnology*, *3*, 137–144.

Koschny, R., Ganten, T. M., Sykora, J., Haas, T. L., Sprick, M. R., Kolb, A., … Walczak, H. (2007a). TRAIL/bortezomib cotreatment is potentially hepatotoxic but induces cancer-specific apoptosis within a therapeutic window. *Hepatology*, *45*(3), 649–658.

Koschny, R., Walczak, H., & Ganten, T. M. (2007b). The promise of TRAIL--potential and risks of a novel anticancer therapy. *Journal of Molecular Medicine (Berlin, Germany)*, *85*(9), 923–935.

Krieg, A., Mersch, S., Wolf, N., Stoecklein, N. H., Verde, P. E., am Esch, J. S., … Mahotka, C. (2013). Expression of TRAIL-splice variants in gastric carcinomas: identification of TRAIL-γ as a prognostic marker. *BMC Cancer*, *13*(1), 384.

Krippner-Heidenreich, A., Grunwald, I., Zimmermann, G., Kühnle, M., Gerspach, J., Sterns, T., … Scheurich, P. (2008). Single-chain TNF, a TNF derivative with enhanced stability and antitumoral activity. *Journal of Immunology*, *180*(12), 8176–8183.

Krueger, A., Schmitz, I., Baumann, S., Krammer, P. H., & Kirchhoff, S. (2001). Cellular FLICE-inhibitory Protein Splice Variants Inhibit Different Steps of Caspase-8 Activation at the CD95 Death-inducing Signaling Complex. *Journal of Biological Chemistry*, *276*(23), 20633–20640.

Lang, I., Füllsack, S., Wyzgol, A., Fick, A., Trebing, J., Arana, J. A. C., … Wajant, H. (2016). Binding studies of TNF receptor superfamily (TNFRSF) receptors on intact cells. *Journal of Biological Chemistry*, *291*(10), 5022–5037.

Lawrence, D., Shahrokh, Z., Marsters, S., Achilles, K., Shih, D., Mounho, B., … Ashkenazi, A. (2001). Differential hepatocyte toxicity of recombinant Apo2L / TRAIL versions. *Nat. Med.*, *7*(4), 383–385.

Lemke, J., Noack, A., Adam, D., Tchikov, V., Bertsch, U., Röder, C., … Trauzold, A. (2010). TRAIL signaling is mediated by DR4 in pancreatic tumor cells despite the expression of functional DR5. *Journal of Molecular Medicine*, *88*(7), 729–740.

Lemke, J., von Karstedt, S., Zinngrebe, J., & Walczak, H. (2014). Getting TRAIL back on track for cancer therapy. *Cell Death and Differentiation*, *21*(9), 1350–1364.

Levin, D., Golding, B., Strome, S. E., & Sauna, Z. E. (2015). Fc fusion as a platform technology: Potential for modulating immunogenicity. *Trends in Biotechnology*, *33*(1), 27–34.

Li, B., Tesar, D., Boswell, C. A., Cahaya, H. S., Wong, A., Zhang, J., … Kelley, R. F. (2014). Framework selection can influence pharmacokinetics of a humanized therapeutic antibody through differences in molecule charge. *mAbs*, *6*(5), 1255–1264.

Li, F., & Ravetch, J. V. (2012). Apoptotic and antitumor activity of death receptor antibodies require inhibitory Fcγ receptor engagement. *Proceedings of the National Academy of Sciences of the United States of America*, *109*(27), 10966–10971.

Li, F., & Ravetch, J. V. (2013). Antitumor activities of agonistic anti-TNFR antibodies require differential FcγRIIB coengagement in vivo. *Proceedings of the National Academy of Sciences*, *110*(48), 19501–19506.

Li, J., Knee, D. A., Wang, Y., Zhang, Q., Johnson, J. A., Cheng, J., … Stover, D. (2008). LBY135, a novel anti-DR5 agonistic antibody induces tumor cell-specific cytotoxic activity in human colon tumor cell lines and xenografts. *Drug Development Research*, *69*(2), 69–82.

Li, R., Yang, H., Jia, D., Nie, Q., Cai, H., Fan, Q., … Lu, X. (2016). Fusion to an albumin-binding domain with a high affinity for albumin extends the circulatory half-life and enhances the in vivo antitumor effects of human TRAIL. *Journal of Controlled Release*, *228*, 96–106.

Li, S., Schmitz, K. R., Jeffrey, P. D., Wiltzius, J. J. W., Kussie, P., & Ferguson, K. M. (2005). Structural basis for inhibition of the epidermal growth factor receptor by cetuximab. *Cancer Cell*, *7*(4), 301–311.

Li, Y., Jin, X., Li, J., Jin, X., Yu, J., Sun, X., … Wu, X. (2012). Expression of TRAIL, DR4, and DR5 in bladder cancer: correlation with response to adjuvant therapy and implications of prognosis. *Urology*, *79*(4), 968.e7-15.

Lim, S. M., Kim, T. H., Jiang, H. H., Park, C. W., Lee, S., Chen, X., & Lee, K. C. (2011). Improved biological half-life and anti-tumor activity of TNF-related apoptosis-inducing ligand (TRAIL) using PEG-exposed nanoparticles. *Biomaterials*, *32*(13), 3538–3546.

Liu, F., Si, Y., Liu, G., Li, S., Zhang, J., & Ma, Y. (2015). The tetravalent anti-DR5 antibody without cross-linking direct induces apoptosis of cancer cells. *Biomedicine & Pharmacotherapy*, *70*, 41–45.

Liu, R., Ma, X., Wang, H., Xi, Y., Qian, M., Yang, W., … Xi, L. (2014). The novel fusion protein sTRAIL-TMTP1 exhibits a targeted inhibition of primary tumors and metastases. *Journal of Molecular Medicine (Berlin, Germany)*, *92*(2), 165–175.

Liu, Y., Lang, F., Xie, X., Prabhu, S., Xu, J., Sampath, D., … Puduvalli, V. K. (2011). Efficacy of adenovirally expressed soluble TRAIL in human glioma organotypic slice culture and glioma xenografts. *Cell Death & Disease*, *2*, e121.

Locksley, R. M., Killeen, N., & Lenardo, M. J. (2001). The TNF and TNF receptor superfamilies: Integrating mammalian biology. *Cell*, *104*(4), 487–501.

Lu, D., Jimenez, X., Witte, L., & Zhu, Z. (2004). The effect of variable domain orientation and arrangement on the antigen-binding activity of a recombinant human bispecific diabody. *Biochemical and Biophysical Research Communications*, *318*(2), 507–513.

Maaser, K., & Borlak, J. (2008). A genome-wide expression analysis identifies a network of EpCAM-induced cell cycle regulators. *British Journal of Cancer*, *99*(10), 1635–1643.

MacFarlane, M., Inoue, S., Kohlhaas, S. L., Majid, A., Harper, N., Kennedy, D. B. J., … Cohen, G. M. (2005a). Chronic lymphocytic leukemic cells exhibit apoptotic signaling via TRAIL-R1. *Cell Death and Differentiation*, *12*, 773–782.

MacFarlane, M., Kohlhaas, S. L., Sutcliffe, M. J., Dyer, M. J. S., & Cohen, G. M. (2005b). TRAIL receptor-selective mutants signal to apoptosis via TRAIL-R1 in primary lymphoid malignancies. *Cancer Research*, *65*(24), 11265–11270.

Maduro, J. H., Noordhuis, M. G., ten Hoor, K. A., Pras, E., Arts, H. J. G., Eijsink, J. J. H., … van der Zee, A. G. J. (2009). The Prognostic Value of TRAIL and its Death Receptors in Cervical Cancer. *International Journal of Radiation Oncology Biology Physics*, *75*(1), 203–211.

Maetzel, D., Denzel, S., Mack, B., Canis, M., Went, P., Benk, M., … Gires, O. (2009). Nuclear signalling by tumour-associated antigen EpCAM. *Nature Cell Biology*, *11*(2), 162–171.

Marsters, S. A., Sheridan, J. P., Pitti, R. M., Huang, A., Skubatch, M., Baldwin, D., … Ashkenazi, A. (1997). A novel receptor for Apo2L/TRAIL contains a truncated death domain. *Current Biology: CB*, *7*(12), 1003–1006.

McDonagh, C. F., Huhalov, A., Harms, B. D., Adams, S., Paragas, V., Oyama, S., … Nielsen, U. B. (2012). Antitumor activity of a novel bispecific antibody that targets the ErbB2/ErbB3 oncogenic unit and inhibits heregulin-induced activation of ErbB3. *Molecular Cancer Therapeutics*, *11*(3), 582–593.

McLornan, D. P., Barrett, H. L., Cummins, R., McDermott, U., McDowell, C., Conlon, S. J., … Johnston, P. G. (2010). Prognostic significance of TRAIL signaling molecules in stage II and III colorectal cancer. *Clinical Cancer Research*, *16*(13), 3442–3451.

Mérino, D., Lalaoui, N., Morizot, A., Schneider, P., Solary, E., & Micheau, O. (2006). Differential inhibition of TRAIL-mediated DR5-DISC formation by decoy receptors 1 and 2. *Molecular and Cellular Biology*, *26*(19), 7046–7055.

Micheau, O., & Tschopp, J. (2003). Induction of TNF Receptor I-Mediated Apoptosis via Two Sequential Signaling Complexes. *Cell*, *114*, 181–190.

Micheau, O., Thome, M., Schneider, P., Holler, N., Tschopp, J., Nicholson, D. W., … Grütter, M. G. (2002). The long form of FLIP is an activator of caspase-8 at the Fas death-inducing signaling complex. *Journal of Biological Chemistry*, *277*(47), 45162–45171.

Milutinovic, S., Kashyap, A. K., Yanagi, T., Wimer, C., Zhou, S., O'Neil, R., … Reed, J. C. (2016). Dual Agonist Surrobody Simultaneously Activates Death Receptors DR4 and DR5 to Induce Cancer Cell Death. *Molecular Cancer Therapeutics*, *15*(1), 114–124.

Mitchell, M. J., Wayne, E., Rana, K., Schaffer, C. B., & King, M. R. (2014). TRAIL-coated leukocytes that kill cancer cells in the circulation. *Proceedings of the National Academy of Sciences of the United States of America*, *111*(3). 930-935.

Möller, Y., Siegemund, M., Beyes, S., Herr, R., Lecis, D., Delia, D., … Olayioye, M. A. (2014). EGFR-Targeted TRAIL and a Smac Mimetic Synergize to Overcome Apoptosis Resistance in KRAS Mutant Colorectal Cancer Cells. *PloS One*, *9*(9), e107165.

Mühlenbeck, F., Schneider, P., Bodmer, J. L., Schwenzer, R., Hauser, A., Schubert, G., … Wajant, H. (2000). The tumor necrosis factor-related apoptosis-inducing ligand receptors TRAIL-R1 and TRAIL-R2 have distinct cross-linking requirements for initiation of apoptosis and are non-redundant in JNK activation. *Journal of Biological Chemistry*, *275*(41), 32208–32213.

Müller, D., Karle, A., Meißburger, B., Höfig, I., Stork, R., & Kontermann, R. E. (2007). Improved pharmacokinetics of recombinant bispecific antibody molecules by fusion to human serum albumin. *Journal of Biological Chemistry*, *282*(17), 12650–12660.

Müller, N., Schneider, B., Pfizenmaier, K., & Wajant, H. (2010). Superior serum half life of albumin tagged TNF ligands. *Biochemical and Biophysical Research Communications*, *396*(4), 793–799.

Munshi, A., Pappas, G., Honda, T., McDonnell, T. J., Younes, A., Li, Y., & Meyn, R. E. (2001). TRAIL (APO-2L) induces apoptosis in human prostate cancer cells that is inhibitable by Bcl-2. *Oncogene*, *20*(29), 3757–3765.

Munz, M., Baeuerle, P. A., & Gires, O. (2009). The Emerging Role of EpCAM in Cancer and Stem Cell Signaling. *Cancer Research*, *69*(14), 5627–5629.

Nair, P. M., Flores, H., Gogineni, A., Marsters, S., Lawrence, D. A., Kelley, R. F., … Ashkenazi, A. (2015). Enhancing the antitumor efficacy of a cell-surface death ligand by covalent membrane display. *Proceedings of the National Academy of Sciences*, *112*(18), 5679–5684.

Natoni, A., MacFarlane, M., Inoue, S., Walewska, R., Majid, A., Knee, D., … Cohen, G. M. (2007). TRAIL signals to apoptosis in chronic lymphocytic leukaemia cells primarily through TRAIL-R1 whereas cross-linked agonistic TRAIL-R2 antibodies facilitate signalling via TRAIL-R2. *British Journal of Haematology*, *139*(4), 568–577.

Neumann, S., Hasenauer, J., Pollak, N., & Scheurich, P. (2014). Dominant Negative Effects of Tumor Necrosis Factor (TNF)-related Apoptosis-inducing Ligand (TRAIL) Receptor 4 on TRAIL Receptor 1 Signaling by Formation of Heteromeric Complexes. *The Journal of Biological Chemistry*, *289*(23), 16576–16587.

Newsom-Davis, T., Prieske, S., & Walczak, H. (2009). Is TRAIL the holy grail of cancer therapy? *Apoptosis*, *14*(4), 607–623.

Nuñez-Prado, N., Compte, M., Harwood, S., Álvarez-Méndez, A., Lykkemark, S., Sanz, L., & Álvarez-Vallina, L. (2015). The coming of age of engineered multivalent antibodies. *Drug Discovery Today*, *20*(5), 588–594.

O'Leary, L., van der Sloot, A. M., Reis, C. R., Deegan, S., Ryan, A. E., Dhami, S. P. S., … Szegezdi, E. (2016). Decoy receptors block TRAIL sensitivity at a supracellular level: the role of stromal cells in controlling tumour TRAIL sensitivity. *Oncogene*, *35*(10), 1261–1270.

O'Reilly, P., Ortutay, C., Gernon, G., O'Connell, E., Seoighe, C., Boyce, S., … Szegezdi, E. (2014). Co-acting gene networks predict TRAIL responsiveness of tumour cells with high accuracy. *BMC Genomics*, *15*(1), 1144.

Ogasawara, J., Watanabe-Fukunaga, R., Adachi, M., Matsuzawa, A., Kasugai, T., Kitamura, Y., … Nagata, S. (1993). Lethal effect of the anti-Fas antibody in mice. *Nature*, *364*(6440), 806–809.

Oldenhuis, C., Dijkers, E. C., Duiker, E. W., Fox, N. L., Klein, J. L., Gietema, J. A., … de Vries, E. G. (2009). Development of radiolabeled mapatumumab and imaging in solid tumor patients who are treated with gemcitabine, cisplatin, and mapatumumab. *Journal of Clinical Oncology, ASCO Annual Meeting Proceedings (Post-Meeting Edition)*, *27*(15S), e14521.

Pan, G., Ni, J., Wei, Y.-F., Yu, G., Gentz, R., & Dixit, V. M. (1997b). An Antagonist Decoy Receptor and a Death Domain-Containing Receptor for TRAIL. *Science*, *277*(5327), 815–818.

Pan, G., Ni, J., Yu, G. L., Wei, Y. F., & Dixit, V. M. (1998). TRUNDD, a new member of the TRAIL receptor family that antagonizes TRAIL signalling. *FEBS Letters*, *424*(1–2), 41–45.

Pan, G., O'Rourke, K., Chinnaiyan, A. M., Gentz, R., Ebner, R., Ni, J., & Dixit, V. M. (1997a). The receptor for the cytotoxic ligand TRAIL. *Science (New York, N.Y.)*, *276*(5309), 111–113.

Pan, L. Q., Wang, H. Bin, Lai, J., Xu, Y. C., Zhang, C., & Chen, S. Q. (2013). Site-specific PEGylation of a mutated-cysteine residue and its effect on tumor necrosis factor (TNF)-related apoptosis-inducing ligand (TRAIL). *Biomaterials*, *34*(36), 9115–9123.

Papadopoulos, K. P., Isaacs, R., Bilic, S., Kentsch, K., Huet, H. A., Hofmann, M., … Mahipal, A. (2015). Unexpected hepatotoxicity in a phase I study of TAS266, a novel tetravalent agonistic Nanobody® targeting the DR5 receptor. *Cancer Chemotherapy and Pharmacology*, *75*(5), 887–895.

Passante, E., Würstle, M. L., Hellwig, C. T., Leverkus, M., & Rehm, M. (2013). Systems analysis of apoptosis protein expression allows the case-specific prediction of cell death responsiveness of melanoma cells. *Cell Death and Differentiation*, *20*(11), 1521–1531.

Patriarca, C., Macchi, R. M., Marschner, A. K., & Mellstedt, H. (2012). Epithelial cell adhesion molecule expression (CD326) in cancer: A short review. *Cancer Treatment Reviews*, *38*(1), 68–75.

Perlstein, B., Finniss, S. A., Miller, C., Okhrimenko, H., Kazimirsky, G., Cazacu, S., … Brodie, C. (2013). TRAIL conjugated to nanoparticles exhibits increased anti-tumor activities in glioma cells and glioma stem cells in vitro and in vivo. *Neuro-Oncology*, *15*(1), 29–40.

Piao, X., Ozawa, T., Hamana, H., Shitaoka, K., Jin, A., Kishi, H., & Muraguchi, A. (2016). TRAIL-receptor 1 IgM antibodies strongly induce apoptosis in human cancer cells in vitro and in vivo. *Oncoimmunology*, *5*(5), e1131380.

Pieczykolan, J. S., Kubiński, K., Masłyk, M., Pawlak, S. D., Pieczykolan, A., Rózga, P. K., … Zieliński, R. (2014). AD-O53.2 - A novel recombinant fusion protein combining the activities of TRAIL/Apo2L and Smac/Diablo, overcomes resistance of human cancer cells to TRAIL/Apo2L. *Investigational New Drugs*, *32*(6), 1155–1166.

Ramamurthy, V., Yamniuk, A. P., Lawrence, E. J., Yong, W., Schneeweis, L. A., Cheng, L., … Sheriff, S. (2015). The structure of the death receptor 4 – TNF-related apoptosis-inducing ligand (DR4 – TRAIL) complex. *Acta Crystallographica Section F Structural Biology Communications*, *71*(10), 1273–1281.

Reiter, Y., Brinkmann, U., Lee, B., & Pastan, I. (1996). Engineering antibody Fv fragments for cancer detection and therapy: Disulfide-stabilized Fv fragments. *Nature Biotechnology*, *14*, 1239–1245.

Roovers, R. C., Henderikx, P., Helfrich, W., Van Der Linden, E., Reurs, A., De Bruine, A. P., … Hoogenboom, H. R. (1998). High-affinity recombinant phage antibodies to the pan-carcinoma marker epithelial glycoprotein-2 for tumour targeting. *British Journal of Cancer*, *78*(11), 1407–1416.

Roskoski, R. (2014). The ErbB/HER family of protein-tyrosine kinases and cancer. *Pharmacological Research*, *79*, 34–74.

Rozanov, D., Spellman, P., Savinov, A., & Strongin, A. Y. (2015). A Humanized Leucine Zipper-TRAIL Hybrid Induces Apoptosis of Tumors both In Vitro and In Vivo. *Plos One*, *10*(4), e0122980.

Sanlioglu, A. D., Korcum, A. F., Pestereli, E., Erdogan, G., Karaveli, S., Savas, B., … Sanlioglu, S. (2007). TRAIL Death Receptor-4 Expression Positively Correlates With the Tumor Grade in Breast Cancer Patients With Invasive Ductal Carcinoma. *International Journal of Radiation Oncology Biology Physics*, *69*(3), 716–723.

Schmitt, L. C., Rau, A., Seifert, S., Honer, J., Schmid, S., Hutt, M., … Kontermann, R. E. Inhibition of HER3 activation and tumor growth with a human antibody binding to a conserved epitope within domain III and IV. In preparation.

Schneider, B., Münkel, S., Krippner-Heidenreich, a, Grunwald, I., Wels, W. S., Wajant, H., … Gerspach, J. (2010). Potent antitumoral activity of TRAIL through generation of tumor-targeted single-chain fusion proteins. *Cell Death & Disease*, *1*, e68.

Schneider, P., Olson, D., Tardivel, A., Browning, B., Lugovskoy, A., Gong, D., … Zheng, T. S. (2003). Identification of a new murine tumor necrosis factor receptor locus that contains two novel murine receptors for tumor necrosis factor-related apoptosis-inducing ligand (TRAIL). *The Journal of Biological Chemistry*, *278*(7), 5444–5454.

Schoeberl, B., Faber, A. C., Li, D., Liang, M. C., Crosby, K., Onsum, M., … Wong, K. K. (2010). An ErbB3 antibody, MM-121, is active in cancers with ligand-dependent activation. *Cancer Research*, *70*(6), 2485–2494.

Schoeberl, B., Pace, E. A., Fitzgerald, J. B., Harms, B. D., Xu, L., Nie, L., … Nielsen, U. B. (2009). Therapeutically Targeting ErbB3: A Key Node in Ligand-Induced Activation of the ErbB Receptor – PI3K Axis. *Science Signaling*, *2*(77), ra31.

Seifert, O. (2014). TRAIL-based multivalent and multifunctional fusion proteins and liposomes for therapeutic applications. *Dissertation*, University of Stuttgart.

Seifert, O., Plappert, A., Fellermeier, S., Siegemund, M., Pfizenmaier, K., & Kontermann, R. E. (2014a). Tetravalent antibody-scTRAIL fusion proteins with improved properties. *Molecular Cancer Therapeutics*, *13*(1), 101–111.

Seifert, O., Plappert, A., Heidel, N., Fellermeier, S., Messerschmidt, S. K. E., Richter, F., & Kontermann, R. E. (2012). The IgM CH2 domain as covalently linked homodimerization module for the generation of fusion proteins with dual specificity. *Protein Engineering, Design & Selection: PEDS*, *25*(10), 603–612.

Seifert, O., Pollak, N., Nusser, A., Steiniger, F., Rüger, R., Pfizenmaier, K., & Kontermann, R. E. (2014b). Immuno-LipoTRAIL: Targeted delivery of TRAIL-functionalized liposomal nanoparticles. *Bioconjugate Chemistry*, *25*(5), 879–887.

Seimetz, D., Lindhofer, H., & Bokemeyer, C. (2010). Development and approval of the trifunctional antibody catumaxomab (anti-EpCAM x anti-CD3) as a targeted cancer immunotherapy. *Cancer Treatment Reviews*, *36*(6), 458–467.

Seshacharyulu, P., Ponnusamy, M. P., Haridas, D., Jain, M., Ganti, A. K., & Batra, S. K. (2012). Targeting the EGFR signaling pathway in cancer therapy. *Expert Opinion on Therapeutic Targets*, *16*(1), 15–31.

Sheridan, J. P., Marsters, S. A., Pitti, R. M., Gurney, A., Skubatch, M., Baldwin, D., … Ashkenazi, A. (1997). Control of TRAIL-Induced Apoptosis by a Family of Signaling and Decoy Receptors. *Science*, *277*(5327), 818–821.

Siegemund, M., Pollak, N., Seifert, O., Wahl, K., Hanak, K., Vogel, A., … Pfizenmaier, K. (2012). Superior antitumoral activity of dimerized targeted single-chain TRAIL fusion proteins under retention of tumor selectivity. *Cell Death & Disease*, *3*, e295.

Siegemund, M., Seifert, O., Zarani, M., Džinić, T., De Leo, V., Göttsch, D., … Kontermann, R. E. (2016). An optimized antibody-single-chain TRAIL fusion protein for cancer therapy. *mAbs*, *8*(5), 879–891.

Soria, J. C., Mark, Z., Zatloukal, P., Szima, B., Albert, I., Juhasz, E., … Blackhall, F. (2011). Randomized phase II study of dulanermin in combination with paclitaxel, carboplatin, and bevacizumab in advanced non-small-cell lung cancer. *J Clin Oncol*, *29*(33), 4442–4451.

Spierings, D. C., de Vries, E. G., Vellenga, E., van den Heuvel, F. A., Koornstra, J. J., Wesseling, J., … de Jong, S. (2004). Tissue Distribution of the Death Ligand TRAIL and Its Receptors. *Journal of Histochemistry and Cytochemistry*, *52*(6), 821–831.

Spitzer, D., McDunn, J. E., Plambeck-Suess, S., Goedegebuure, P. S., Hotchkiss, R. S., & Hawkins, W. G. (2010). A Genetically Encoded Multifunctional TRAIL Trimer Facilitates Cell-Specific Targeting and Tumor Cell Killing. *Molecular Cancer Therapeutics*, *9*(7), 2142–2151.

Stagg, J., Sharkey, J., Pommey, S., Young, R., Takeda, K., Yagita, H., … Smyth, M. J. (2008). Antibodies targeted to TRAIL receptor-2 and ErbB-2 synergize in vivo and induce an antitumor immune response. *Proceedings of the National Academy of Sciences of the United States of America*, *105*(42), 16254–16259.

Stieglmaier, J., Bremer, E., Kellner, C., Liebig, T. M., Ten Cate, B., Peipp, M., … Helfrich, W. (2008). Selective induction of apoptosis in leukemic B-lymphoid cells by a CD19-specific TRAIL fusion protein. *Cancer Immunology, Immunotherapy*, *57*(2), 233–246.

Stolfi, C., Pallone, F., & Monteleone, G. (2012). Molecular targets of TRAIL-sensitizing agents in colorectal cancer. *International Journal of Molecular Sciences*, *13*(7), 7886–7901.

Stork, R., Müller, D., & Kontermann, R. E. (2007). A novel tri-functional antibody fusion protein with improved pharmacokinetic properties generated by fusing a bispecific single-chain diabody with an albumin-binding domain from streptococcal protein G. *Protein Engineering, Design and Selection*, *20*(11), 569–576.

Sträter, J., Hinz, U., Walczak, H., Mechtersheimer, G., Koretz, K., Herfarth, C., … Lehnert, T. (2002). Expression of TRAIL and TRAIL receptors in colon carcinoma: TRAIL-R1 is an independent prognostic parameter. *Clinical Cancer Research*, *8*(12), 3734–3740.

Sun, X., Pang, Z., Ye, H., Qiu, B., Guo, L., Li, J., … Jiang, X. (2012). Co-delivery of pEGFP-hTRAIL and paclitaxel to brain glioma mediated by an angiopep-conjugated liposome. *Biomaterials*, *33*(3), 916–924.

Swers, J. S., Grinberg, L., Wang, L., Feng, H., Lekstrom, K., Carrasco, R., … Baca, M. (2013). Multivalent scaffold proteins as superagonists of TRAIL receptor 2-induced apoptosis. *Molecular Cancer Therapeutics*, *12*(7), 1235–1244.

Tai, W., Mahato, R., & Cheng, K. (2010). The role of HER2 in cancer therapy and targeted drug delivery. *Journal of Controlled Release*, *146*(3), 264–275.

Tait, S. W. G., & Green, D. R. (2010). Mitochondria and cell death: outer membrane permeabilization and beyond. *Nature Reviews. Molecular Cell Biology*, *11*(9), 621–632.

Tamada, T., Shinmi, D., Ikeda, M., Yonezawa, Y., Kataoka, S., Kuroki, R., … Motoki, K. (2015). TRAIL-R2 Superoligomerization Induced by Human Monoclonal Agonistic Antibody KMTR2. *Sci Rep*, *5*, 17936.

Tan, A. R., Moore, D. F., Hidalgo, M., Doroshow, J. H., Poplin, E. A., Goodin, S., … Rubin, E. H. (2006). Pharmacokinetics of cetuximab after administration of escalating single dosing and weekly fixed dosing in patients with solid tumors. *Clinical Cancer Research*, *12*(21), 6517–6522.

Tatzel, K., Kuroki, L., Dmitriev, I., Kashentseva, E., Curiel, D. T., Goedegebuure, S. P., … Spitzer, D. (2016). Membrane-proximal TRAIL species are incapable of inducing short circuit apoptosis signaling: Implications for drug development and basic cytokine biology. *Sci Rep*, *6*, 22661.

ten Cate, B., Bremer, E., de Bruyn, M., Bijma, T., Samplonius, D., Schwemmlein, M., … Helfrich, W. (2009). A novel AML-selective TRAIL fusion protein that is superior to Gemtuzumab Ozogamicin in terms of in vitro selectivity, activity and stability. *Leukemia*, *23*(8), 1389–1397.

Thorburn, A., Behbakht, K., & Ford, H. (2008). TRAIL receptor-targeted therapeutics: Resistance mechanisms and strategies to avoid them. *Drug Resistance Updates*, *11*(1–2), 17–24.

Todorovska, A., Roovers, R. C., Dolezal, O., Kortt, A. A., Hoogenboom, H. R., & Hudson, P. J. (2001). Design and application of diabodies, triabodies and tetrabodies for cancer targeting. *Journal of Immunological Methods*, *248*(1–2), 47–66.

Tolcher, A. W., Mita, M., Meropol, N. J., Von Mehren, M., Patnaik, A., Padavic, K., … Cohen, R. B. (2007). Phase I pharmacokinetic and biologic correlative study of mapatumumab, a fully human monoclonal antibody with agonist activity to tumor necrosis factor-related apoptosis-inducing ligand receptor-1. *Journal of Clinical Oncology*, *25*(11), 1390–1395.

Trebing, J., El-Mesery, M., Schäfer, V., Weisenberger, D., Siegmund, D., Silence, K., & Wajant, H. (2014). CD70-restricted specific activation of TRAILR1 or TRAILR2 using scFv-targeted TRAIL mutants. *Cell Death & Disease*, *5*, e1035.

Tuntland, T., Ethell, B., Kosaka, T., Blasco, F., Zang, R., Jain, M., … Hoffmaster, K. (2014). Implementation of pharmacokinetic and pharmacodynamic strategies in early research phases of drug discovery and development at novartis institute of biomedical research. *Frontiers in Pharmacology*, *5*, 174.

Tuthill, M. H., Montinaro, A., Zinngrebe, J., Prieske, K., Draber, P., Prieske, S., … Walczak, H. (2015). TRAIL-R2-specific antibodies and recombinant TRAIL can synergise to kill cancer cells. *Oncogene*, *34*(16), 2138–2144.

Uckun, F. M., Myers, D. E., Qazi, S., Ozer, Z., Rose, R., D'Cruz, O. J., & Ma, H. (2015). Recombinant human CD19L-sTRAIL effectively targets B cell precursor acute lymphoblastic leukemia. *Journal of Clinical Investigation*, *125*(3), 1006–1018.

Unverdorben, F., Richter, F., Hutt, M., Seifert, O., Malinge, P., Fischer, N., & Kontermann, R. E. (2016). Pharmacokinetic properties of IgG and various Fc fusion proteins in mice. *mAbs*, *8*(1), 120–128.

Vaseva, A. V., & Moll, U. M. (2009). The mitochondrial p53 pathway. *Biochimica et Biophysica Acta*, *1787*(5), 414–420.

Veikkolainen, V., Vaparanta, K., Halkilahti, K., Iljin, K., Sundvall, M., & Elenius, K. (2011). Function of ERBB4 is determined by alternative splicing. *Cell Cycle*, *10*(16), 2647–2657.

Velders, M. P., Rhijn, C. M. Van, Briaire, I. H., Fleuren, G. J., Warnaar, S. O., & Litvinov, S. V. (1995). Immunotherapy with Low and High Affinity Monoclonal Antibodies 17-1A and 323/A3 in a Nude Mouse Xenograft Carcinoma Model. *Cancer Research*, *55*(19), 4398–4403.

Voigt, S., Philipp, S., Davarnia, P., Winoto-Morbach, S., Röder, C., Arenz, C., … Adam, D. (2014). TRAIL-induced programmed necrosis as a novel approach to eliminate tumor cells. *BMC Cancer*, *14*, 74.

von Karstedt, S., Conti, A., Nobis, M., Montinaro, A., Hartwig, T., Lemke, J., … Walczak, H. (2015). Cancer cell-autonomous TRAIL-R signaling promotes KRAS-Driven cancer progression, invasion, and metastasis. *Cancer Cell*, *27*(4), 561–573.

Wagner, K. W., Punnoose, E. A., Januario, T., Lawrence, D. A., Pitti, R. M., Lancaster, K., … Ashkenazi, A. (2007). Death-receptor O-glycosylation controls tumor-cell sensitivity to the proapoptotic ligand Apo2L/TRAIL. *Nature Medicine*, *13*(9), 1070–1077.

Wahl, K., Siegemund, M., Lehner, F., Vondran, F., Nüssler, A., Länger, F., … Bantel, H. (2013). Increased apoptosis induction in hepatocellular carcinoma by a novel tumor-targeted TRAIL fusion protein combined with bortezomib. *Hepatology*, *57*(2), 625–636.

Wajant, H. (2015). Principles of antibody-mediated TNF receptor activation. *Cell Death and Differentiation*, *22*(11), 1727–1741.

Wajant, H., Gerspach, J., & Pfizenmaier, K. (2013). Engineering death receptor ligands for cancer therapy. *Cancer Letters*, *332*(2), 163–174.

Wajant, H., Moosmayer, D., Wüest, T., Bartke, T., Gerlach, E., Schönherr, U., … Pfizenmaier, K. (2001). Differential activation of TRAIL-R1 and -2 by soluble and membrane TRAIL allows selective surface antigen-directed activation of TRAIL-R2 by a soluble TRAIL derivative. *Oncogene*, *20*(30), 4101–4106.

Walczak, H., Miller, R. E., Ariail, K., Gliniak, B., Griffith, T. S., Kubin, M., … Lynch, D. H. (1999). Tumoricidal activity of tumor necrosis factor-related apoptosis-inducing ligand in vivo. *Nature Medicine*, *5*(2), 157–163.

Wang, H., Davis, J. S., & Wu, X. (2014). Immunoglobulin Fc domain fusion to TRAIL significantly prolongs its plasma half-life and enhances its antitumor activity. *Molecular Cancer Therapeutics*, *13*(3), 643–650.

Wang, W., He, W., Wang, L., Zhang, G., & Gao, B. (2013). Pentamerisation of a scFv directed against TRAIL receptor 2 increases its antitumour efficacy. *Immunology and Cell Biology*, *91*(5), 360–7.

Wang, W., Wang, E., & Balthasar, J. (2008). Monoclonal Antibody Pharmacokinetics and Pharmacodynamics. *Clin Pharmacol Ther.*, *84*(5), 548–558.

Wayne, E. C., Chandrasekaran, S., Mitchell, M. J., Chan, M. F., Lee, R. E., Schaffer, C. B., & King, M. R. (2016). TRAIL-coated leukocytes that prevent the bloodborne metastasis of prostate cancer. *Journal of Controlled Release*, *223*, 215–223.

Weyhenmeyer, B. C., Noonan, J., Würstle, M. L., Lincoln, F. A., Johnston, G., Rehm, M., & Murphy, B. M. (2016). Predicting the cell death responsiveness and sensitization of glioma cells to TRAIL and temozolomide. *Oncotarget*, *7*(38), 61295-61311.

Wiersma, V. R., De Bruyn, M., Shi, C., Gooden, M. J. M., Wouters, M. C. A., Samplonius, D. F., … Bremer, E. (2015). C-type lectin-like molecule-1 (CLL1)-targeted TRAIL augments the tumoricidal activity of granulocytes and potentiates therapeutic antibody-dependent cell-mediated cytotoxicity. *mAbs*, *7*(2), 321–330.

Wiersma, V. R., He, Y., Samplonius, D. F., van Ginkel, R. J., Gerssen, J., Eggleton, P., … Helfrich, W. (2014). A CD47-blocking TRAIL fusion protein with dual pro-phagocytic and pro-apoptotic anticancer activity. *British Journal of Haematology*, *164*(2), 304–307.

Wiley, S. R., Schooley, K., Smolak, P. J., Din, W. S., Huang, C. P., Nicholl, J. K., … Goodwin, R. G. (1995). Identification and characterization of a new member of the TNF family that induces apoptosis. *Immunity*, *3*(6), 673–682.

Wilson, N. S., Yang, B., Yang, A., Loeser, S., Marsters, S., Lawrence, D., … Ashkenazi, A. (2011). An Fcγ receptor-dependent mechanism drives antibody-mediated target-receptor signaling in cancer cells. *Cancer Cell*, *19*(1), 101–113.

Wyzgol, A., Müller, N., Fick, A., Munkel, S., Grigoleit, G. U., Pfizenmaier, K., & Wajant, H. (2009). Trimer stabilization, oligomerization, and antibody-mediated cell surface immobilization improve the activity of soluble trimers of CD27L, CD40L, 41BBL, and glucocorticoid-induced TNF receptor ligand. *Journal of Immunology (Baltimore, Md. : 1950)*, *183*(3), 1851–1861.

Yada, A., Yazawa, M., Ishida, S., Yoshida, H., Ichikawa, K., Kurakata, S., & Fujiwara, K. (2008). A novel humanized anti-human death receptor 5 antibody CS-1008 induces apoptosis in tumor cells without toxicity in hepatocytes. *Annals of Oncology*, *19*(6), 1060–1067.

Yan, C., Li, S., Li, Z., Peng, H., Yuan, X., Jiang, L., … Xiong, D. (2013). Human umbilical cord mesenchymal stem cells as vehicles of CD20-specific TRAIL fusion protein delivery: A double-target therapy against non-Hodgkin's lymphoma. *Molecular Pharmaceutics*, *10*(1), 142–151.

Yan, J., Wang, L., Wang, Z., Wang, Z., Wang, B., Zhu, R., … Yu, X. (2016). Engineered adenovirus fiber shaft fusion homotrimer of soluble TRAIL with enhanced stability and antitumor activity. *Cell Death and Disease*, *7*(6), e2274.

Zhang, L., & Fang, B. (2005). Mechanisms of resistance to TRAIL-induced apoptosis in cancer. *Cancer Gene Therapy*, *12*(3), 228–237.

Zhuang, L., Lee, C. S., Scolyer, R. A., McCarthy, S. W., Zhang, X. D., Thompson, J. F., … Hersey, P. (2006). Progression in melanoma is associated with decreased expression of death receptors for tumor necrosis factor-related apoptosis-inducing ligand. *Human Pathology*, *37*(10), 1286–1294.

Zuch de Zafra, C. L., Ashkenazi, A., Darbonne, W. C., Cheu, M., Totpal, K., Ortega, S., … Dybdal, N. O. (2016). Antitherapeutic antibody-mediated hepatotoxicity of recombinant human Apo2L/TRAIL in the cynomolgus monkey. *Cell Death and Disease*, *7*(8), e2338.

6 Sequences

6.1 Single-chain fragments variable

6.1.1 scFvhu225 (pAB1)

```
>pelB leader                                                                >VHhu225
|                                                                           |
ATG AAA TAC CTA TTG CCT ACG GCA GCC GCT GGA TTG TTA TTA CTC GCG GCC CAG CCG GCC ATG GCG GAA GTG CAG CTG GTT GAA AGC GGC   90
M   K   Y   L   L   P   T   A   A   A   G   L   L   L   L   A   A   Q   P   A   M   A   E   V   Q   L   V   E   S   G

GGT GGT CTG GTT CAG CCG GGT GGC AGC CTG CGT CTG AGC TGT GCG GCG AGC GGC TTT AGC CTG ACC AAC TAT GGC GTG CAT TGG GTG CGT < 180
G   G   L   V   Q   P   G   G   S   L   R   L   S   C   A   A   S   G   F   S   L   T   N   Y   G   V   H   W   V   R

CAG GCA CCG GGC AAA GGC CTG GAA TGG CTG GGC GTG ATT TGG AGC GGC GGC AAC ACC GAT TAT AAC ACC CCG TTT ACC AGC CGT TTT ACC < 270
Q   A   P   G   K   G   L   E   W   L   G   V   I   W   S   G   G   N   T   D   Y   N   T   P   F   T   S   R   F   T

ATT AGC CGT GAT AAC AGC AAA AAC ACC CTG TAT CTG CAG ATG AAC AGC CTG CGT GCG GAA GAT ACC GCG GTG TAT TAT TGC GCG CGT GCG < 360
I   S   R   D   N   S   K   N   T   L   Y   L   Q   M   N   S   L   R   A   E   D   T   A   V   Y   Y   C   A   R   A

                                                                    >linker
                                                                    |
CTG ACC TAT TAT GAT TAC GAA TTT GCG TAT TGG GGC CAG GGC ACC ACC GTT ACG GTC TCG AGC GGT GGC GGT GGT AGC GGT GGT GGC GGC < 450
L   T   Y   Y   D   Y   E   F   A   Y   W   G   Q   G   T   T   V   T   V   S   S   G   G   G   G   S   G   G   G   G

                    >VLhu225
                    |
TCT GGC GGT GGT GGA TCC GAT ATT CAG CTG ACC CAG AGC CCG AGC TTT CTG AGC GCG AGC GTG GGC GAT CGT GTT ACC ATT ACC TGT CGT < 540
S   G   G   G   G   S   D   I   Q   L   T   Q   S   P   S   F   L   S   A   S   V   G   D   R   V   T   I   T   C   R

GCA AGC CAG AGC ATT GGC ACC AAC ATT CAT TGG TAT CAG CAG AAA CCG GGC AAA GCG CCG AAA CTG CTG ATT AAA TAT GCG AGC GAA AGC < 630
A   S   Q   S   I   G   T   N   I   H   W   Y   Q   Q   K   P   G   K   A   P   K   L   L   I   K   Y   A   S   E   S

ATT AGC GGC GTG CCG AGC CGT TTT AGC GGC AGC GGT AGC GGC ACC GAA TTT ACC CTG ACC ATT AGC AGC CTG CAG CCG GAA GAT TTT GCG < 720
  I   S   G   V   P   S   R   F   S   G   S   G   S   G   T   E   F   T   L   T   I   S   S   L   Q   P   E   D   F   A

                                                                          NotI
                                                                          |
ACC TAT TAT TGC CAG CAG AAC AAC AAC TGG CCG ACC ACC TTT GGT GCG GGC ACC AAA CTG GAA ATT AAA CGT GCG GCC GCA GAA CAA AAA < 810
T   Y   Y   C   Q   Q   N   N   N   W   P   T   T   F   G   A   G   T   K   L   E   I   K   R   A   A   A   E   Q   K

                                        >His-tag
                                        |
CTC ATC TCA GAA GAG GAT CTG AAT GGG GCC GCA CAT CAC CAT CAT CAC CAT TAA
L   I   S   E   E   D   L   N   G   A   A   H   H   H   H   H   H   *
```

6.1.2 scFv4D5 (pAB1)

```
>pelB leader                                                                AgeI    >VH4D5
|                                                                           |       |
ATG AAA TAC CTA TTG CCT ACG GCA GCC GCT GGA TTG TTA TTA CTC GCG GCC CAG CCG GCC ATG GCC ACC GGT GAA GTG CAG CTC GTC GAA < 90
M   K   Y   L   L   P   T   A   A   A   G   L   L   L   L   A   A   Q   P   A   M   A   T   G   E   V   Q   L   V   E

AGT GGC GGT GGA CTT GTG CAG CCT GGC GGT TCC CTC AGA CTG TCC TGT GCC GCG TCA GGC TTC AAC ATC AAG GAC ACG TAC ATC CAC TGG < 180
S   G   G   G   L   V   Q   P   G   G   S   L   R   L   S   C   A   A   S   G   F   N   I   K   D   T   Y   I   H   W

GTG AGG CAA GCT CCT GGA AAG GGC TTG GAG TGG GTC GCT AGG ATC TAC CCG ACG AAC GGC TAC ACC AGG TAC GCT GAC TCA GTG AAG GGA < 270
V   R   Q   A   P   G   K   G   L   E   W   V   A   R   I   Y   P   T   N   G   Y   T   R   Y   A   D   S   V   K   G

AGG TTC ACG ATC AGT GCA GAC ACC AGC AAG AAC ACC GCA TAC CTC CAA ATG AAC TCC CTG AGA GCC GAG GAC ACC GCC GTG TAC TAC TGC < 360
R   F   T   I   S   A   D   T   S   K   N   T   A   Y   L   Q   M   N   S   L   R   A   E   D   T   A   V   Y   Y   C

                                                                          >linker
                                                                          |
TCT CGT TGG GGT GGA GAT GGC TTC TAC GCT ATG GAC TAC TGG GGT CAA GGC ACA CTG GTG ACC GTG TCC AGT GGT GGC GGA GGC AGT GGC < 450
S   R   W   G   G   D   G   F   Y   A   M   D   Y   W   G   Q   G   T   L   V   T   V   S   S   G   G   G   G   S   G

                                  >VL4D5
                                  |
GGA GGT GGC TCA GGA GGC GGA GGA TCC GAC ATC CAG ATG ACC CAG TCA CCC TCA AGC CTC AGT GCC AGC GTC GGA GAT AGA GTG ACC ATA < 540
G   G   G   S   G   G   G   G   S   D   I   Q   M   T   Q   S   P   S   S   L   S   A   S   V   G   D   R   V   T   I

ACG TGC CGA GCT TCT CAG GAT GTG AAC ACG GCA GTG GCT TGG TAT CAG CAA AAG CCT GGG AAA GCC CCA AAG CTG CTC ATC TAC TCC GCA < 630
T   C   R   A   S   Q   D   V   N   T   A   V   A   W   Y   Q   Q   K   P   G   K   A   P   K   L   L   I   Y   S   A

TCC TTC CTG TAT AGC GGA GTT CCA TCT AGG TTC TCA GGC TCT AGG TCT GGG ACC GAC TTC ACG CTG ACG ATC TCC TCC CTG CAA CCT GAG < 720
S   F   L   Y   S   G   V   P   S   R   F   S   G   S   R   S   G   T   D   F   T   L   T   I   S   S   L   Q   P   E

                                                                                  NotI
                                                                                  |
GAC TTC GCC ACG TAC TAC TGC CAG CAG CAC TAC ACG ACT CCT CCA ACC TTC GGT CAG GGA ACG AAG GTC GAG ATC AAG CGT GCG GCC GCA < 810
D   F   A   T   Y   Y   C   Q   Q   H   Y   T   T   P   P   T   F   G   Q   G   T   K   V   E   I   K   R   A   A   A

                                                >His-tag
                                                |
GAA CAA AAA CTC ATC TCA GAA GAG GAT CTG AAT GGG GCC GCA CAT CAC CAT CAT CAC CAT TAA
E   Q   K   L   I   S   E   E   D   L   N   G   A   A   H   H   H   H   H   H   *
```

6.1.3 scFv3M6 (pAB1)

```
>pelB leader                                                                    AgeI    >VH3M6
|                                                                               |       |
ATG AAA TAC CTA TTG CCT ACG GCA GCC GCT GGA TTG TTA TTA CTC GCG GCC CAG CCG GCC ATG GCC ACC GGT GAA GTG CAG CTG CTG GAA < 90
M   K   Y   L   L   P   T   A   A   A   G   L   L   L   L   A   A   Q   P   A   M   A   T   G   E   V   Q   L   L   E

AGC GGA GGC GGC CTG GTG CAG CCT GGC GGC TCT CTG AGA CTG AGC TGT GCC GCC AGC GGC TTC ACC TTC AGC CAC TAC GTG ATG GCC TGG < 180
S   G   G   G   L   V   Q   P   G   G   S   L   R   L   S   C   A   A   S   G   F   T   F   S   H   Y   V   M   A   W

GTC CGA CAG GCC CCT GGC AAG GGA CTG GAA TGG GTG TCC AGC ATC AGC AGC AGC GGC GGC TGG ACC CTG TAC GCC GAT AGC GTG AAG GGC < 270
V   R   Q   A   P   G   K   G   L   E   W   V   S   S   I   S   S   S   G   G   W   T   L   Y   A   D   S   V   K   G

CGG TTT ACC ATC AGC CGG GAC AAC AGC AAG AAC ACC CTG TAC CTG CAG ATG AAC AGC CTG CGG GCC GAG GAC ACC GCC GTG TAC TAC TGC < 360
R   F   T   I   S   R   D   N   S   K   N   T   L   Y   L   Q   M   N   S   L   R   A   E   D   T   A   V   Y   Y   C

                                                                                        >linker
                                                                                        |
ACC AGA GGC CTG AAG ATG GCC ACC ATC TTC GAC TAC TGG GGG CAG GGC ACC CTG GTC ACA GTC TCG AGT GGC GGG GGA GGA TCT GGG GGA < 450
T   R   G   L   K   M   A   T   I   F   D   Y   W   G   Q   G   T   L   V   T   V   S   S   G   G   G   G   S   G   G

                              >VL3M6
                              |
GGT GGA AGT GGC GGC GGT GGA TCC CAG TCT GCC CTG ACA CAG CCT GCC AGC GTG TCC GGC AGC CCT GGC CAG AGC ATC ACA ATC AGC TGC < 540
G   G   S   G   G   G   G   S   Q   S   A   L   T   Q   P   A   S   V   S   G   S   P   G   Q   S   I   T   I   S   C

ACC GGC ACC AGC AGC GAC GTG GGC AGC TAC AAC GTG GTG TCC TGG TAT CAG CAG CAC CCC GGC AAG GCC CCC AAG CTG ATC ATC TAC GAG < 630
T   G   T   S   S   D   V   G   S   Y   N   V   V   S   W   Y   Q   Q   H   P   G   K   A   P   K   L   I   I   Y   E

GTG TCC CAG CGG CCC AGC GGC GTG TCC AAC AGA TTC AGC GGC AGC AAG AGC GGC AAC ACC GCC AGC CTG ACC ATC AGC GGG CTG CAG ACC < 720
V   S   Q   R   P   S   G   V   S   N   R   F   S   G   S   K   S   G   N   T   A   S   L   T   I   S   G   L   Q   T

                                                                                                                NotI
                                                                                                                |
GAG GAC GAG GCC GAC TAC TAC TGC TCC AGC TAC GCC GGC AGC AGC ATC TTC GTG ATC TTC GGA GGT GGC ACC AAA GTG ACC GTG CTG GCG < 810
E   D   E   A   D   Y   Y   C   S   S   Y   A   G   S   S   I   F   V   I   F   G   G   G   T   K   V   T   V   L   A

                                                        >His-tag
                                                        |
GCC GCA GAA CAA AAA CTC ATC TCA GAA GAG GAT CTG AAT GGG GCC GCA CAT CAC CAT CAT CAC CAT TAA
A   A   E   Q   K   L   I   S   E   E   D   L   N   G   A   A   H   H   H   H   H   H   *
```

6.1.4 scFv3-43 (pSecTagAL1)

```
>Igk leader                                                                    AgeI    >VH3-43
|                                                                              |       |
ATG GAG ACA GAC ACA CTC CTG CTA TGG GTA CTG CTG CTC TGG GTT CCA GGT TCC ACC GGT CAA GTG CAG CTG CAG CAG TCT GGC CCT GGC < 90
M   E   T   D   T   L   L   L   W   V   L   L   L   W   V   P   G   S   T   G   Q   V   Q   L   Q   Q   S   G   P   G

CTC GTG AAG CCT AGC CAG ACC CTG AGC CTG ACC TGT GCC ATC AGC GGC GAT AGC GTG TCC AGC AAC AGA GCC GCC TGG AAC TGG ATC AGA < 180
L   V   K   P   S   Q   T   L   S   L   T   C   A   I   S   G   D   S   V   S   S   N   R   A   A   W   N   W   I   R

CAG AGC CCC AGC AGA GGC CTG GAA TGG CTG GGC CGG ACC TAC TAC CGC AGC AAG TGG TAC AAC GAC TAC GCC CAG AGC CTG AAG TCC CGG < 270
Q   S   P   S   R   G   L   E   W   L   G   R   T   Y   Y   R   S   K   W   Y   N   D   Y   A   Q   S   L   K   S   R

ATC ACC ATC AAC CCC GAC ACC CCC AAG AAC CAG TTC TCC CTG CAG CTG AAC AGC GTG ACC CCC GAG GAT ACC GCC GTG TAC TAC TGC GCC < 360
I   T   I   N   P   D   T   P   K   N   Q   F   S   L   Q   L   N   S   V   T   P   E   D   T   A   V   Y   Y   C   A

                                                                                        >linker
                                                                                        |
AGA GAT GGA CAG CTG GGC CTG GAC GCC CTG GAC ATT TGG GGC CAG GGC ACA ATG GTC ACA GTG TCC TCT GGC GGG GGA GGA TCT GGG GGA < 450
R   D   G   Q   L   G   L   D   A   L   D   I   W   G   Q   G   T   M   V   T   V   S   S   G   G   G   G   S   G   G

                              >VL3-43
                              |
GGT GGA AGT GGC GGC GGT GGA TCC CAA GCC GGA CTG ACA CAG CCT CCA GCC GTG TCT GTG GCC CCT GGA CAG ACA GCC AGC ATC ACC TGT < 540
G   G   S   G   G   G   G   S   Q   A   G   L   T   Q   P   P   A   V   S   V   A   P   G   Q   T   A   S   I   T   C

GGC CGG GAC AAC ATC GGC AGC AGA AGC GTG CAC TGG TAT CAG CAG AAA CCC GGC CAG GCC CCT GTG CTG GTG GTG TAC GAC GAC AGC GAT < 630
G   R   D   N   I   G   S   R   S   V   H   W   Y   Q   Q   K   P   G   Q   A   P   V   L   V   V   Y   D   D   S   D

AGA CCT GCC GGC ATC CCC GAG AGA TTC AGC GGC AGC AAC TAC GAG AAC ACC GCC ACC CTG ACC ATC AGC AGA GTG GAA GCC GGC GAC GAG < 720
R   P   A   G   I   P   E   R   F   S   G   S   N   Y   E   N   T   A   T   L   T   I   S   R   V   E   A   G   D   E

                                                                                                NotI        >His-tag
                                                                                                |           |
GCC GAC TAC TAC TGT CAA GTG TGG GGC ATC ACC AGC GAT CAC GTG GTG TTT GGC GGA GGC ACC AAG CTG ACA GTG CTG GCG GCC GCC CAC < 810
A   D   Y   Y   C   Q   V   W   G   I   T   S   D   H   V   V   F   G   G   G   T   K   L   T   V   L   A   A   A   H

CAT CAT CAC CAT CAC TAA
H   H   H   H   H   *
```

6.1.5 scFv323/A3hu3 (pAB1)

```
>pelB leader                                                                    AgeI    >VH323/A3hu3
|                                                                               |       |
ATG AAA TAC CTA TTG CCT ACG GCA GCC GCT GGA TTG TTA TTA CTC GCG GCC CAG CCG GCC ATG GCC ACC GGT CAA GTG CAG CTG GTG CAG < 90
M   K   Y   L   L   P   T   A   A   A   G   L   L   L   L   A   A   Q   P   A   M   A   T   G   Q   V   Q   L   V   Q

TCT GGC GCC GAA GTG AAG AAA CCA GGC GCC AGC GTG AAG GTG TCC TGC AAG GCC AGC GGC TAC ACC TTT ACC AAC TAC GGC ATG AAC TGG < 180
S   G   A   E   V   K   K   P   G   A   S   V   K   V   S   C   K   A   S   G   Y   T   F   T   N   Y   G   M   N   W

GTG CGC CAG GCC CCT GGC CAG AGA CTG GAA TGG ATG GGC TGG ATC AAC ACC TAC ACC GGC GAG CCC ACC TAC GGC GAG GAC TTC AAG GGC < 270
V   R   Q   A   P   G   Q   R   L   E   W   M   G   W   I   N   T   Y   T   G   E   P   T   Y   G   E   D   F   K   G
```

```
AGA GTG ACC ATC ACC CTG GAC ACC AGC GCC AGC ACC GCC TAC ATG GAA CTG AGC AGC CTG CGG AGC GAG GAC ACC GCC GTG TAC TAC TGC < 360
R   V   T   I   T   L   D   T   S   A   S   T   A   Y   M   E   L   S   S   L   R   S   E   D   T   A   V   Y   Y   C

                                                                                    >Linker
                                                                                    |
GCC AGA TTC GGC AAC TAC GTG GAC TAC TGG GGC CAG GGC ACC CTC GTG ACA GTC TCG AGT GGC GGC GGA GGA TCT GGC GGA GGC GGA AGT < 450
A   R   F   G   N   Y   V   D   Y   W   G   Q   G   T   L   V   T   V   S   S   G   G   G   G   S   G   G   G   G   S

                  >VL323/A3hu3
                  |
GGG GGA GGC GGA TCT GAG ATC GTG CTG ACA CAG AGC CCT GGC ACC CTG AGC CTG TCT CCA GGC GAA AGA GCC ACC CTG TCC TGC AGA AGC < 540
G   G   G   G   S   E   I   V   L   T   Q   S   P   G   T   L   S   L   S   P   G   E   R   A   T   L   S   C   R   S

AGC AAG AAC CTG CTG CAC AGC AAC GGC ATC ACC TAC CTG TAC TGG TAT CAG CAG AAG CCC GGC CAG GCC CCC AGA CTG CTG ATC TAC CAG < 630
S   K   N   L   L   H   S   N   G   I   T   Y   L   Y   W   Y   Q   Q   K   P   G   Q   A   P   R   L   L   I   Y   Q

ATG AGC AAC CTG GCC AGC GGC ATC CCC GAC AGA TTT TCT GGC AGC GGC TCC GGC ACC GAC TTC ACC CTG ACA ATC AGC AGA CTG GAA CCC < 720
M   S   N   L   A   S   G   I   P   D   R   F   S   G   S   G   S   G   T   D   F   T   L   T   I   S   R   L   E   P

                                                                                                                NotI
                                                                                                                |
GAG GAC TTC GCC GTG TAC TAC TGC GCC CAG AAC CTG GAA ATC CCC CGG ACC TTT GGC CAG GGC ACC AAG CTG GAA ATC AAG AGA GCG GCC < 810
E   D   F   A   V   Y   Y   C   A   Q   N   L   E   I   P   R   T   F   G   Q   G   T   K   L   E   I   K   R   A   A

                                                        >His-tag
                                                        |
GCA GAA CAA AAA CTC ATC TCA GAA GAG GAT CTG AAT GGG GCC GCA CAT CAC CAT CAT CAC CAT TAA
A   E   Q   K   L   I   S   E   E   D   L   N   G   A   A   H   H   H   H   H   H   *
```

6.2 Diabodies and disulfide-stabilized diabodies

6.2.1 (ds)Dbhu225 (pSecTagAL1)

Sequence of Dbhu225 is represented. Mutation of underlined codons GGC to TGT and GCG to TGC replaces G and A with cysteines, respectively, and generates sequence of dsDbhu225.

```
>Igk leader                                                                                 AgeI    VHhu225
|                                                                                           |       |
ATG GAG ACA GAC ACA CTC CTG CTA TGG GTA CTG CTG CTC TGG GTT CCA GGT TCC ACC GGT GAA GTG CAG CTG GTT GAA AGC GGC GGT GGT < 90
M   E   T   D   T   L   L   L   W   V   L   L   L   W   V   P   G   S   T   G   E   V   Q   L   V   E   S   G   G   G

CTG GTT CAG CCG GGT GGC AGC CTG CGT CTG AGC TGT GCG GCG AGC GGC TTT AGC CTG ACC AAC TAT GGC GTG CAT TGG GTG CGT CAG GCA < 180
L   V   Q   P   G   G   S   L   R   L   S   C   A   A   S   G   F   S   L   T   N   Y   G   V   H   W   V   R   Q   A

CCG GGC AAA GGC CTG GAA TGG CTG GGC GTG ATT TGG AGC GGC GGC AAC ACC GAT TAT AAC ACC CCG TTT ACC AGC CGT TTT ACC ATT AGC < 270
P   G   K   G   L   E   W   L   G   V   I   W   S   G   G   N   T   D   Y   N   T   P   F   T   S   R   F   T   I   S

CGT GAT AAC AGC AAA AAC ACC CTG TAT CTG CAG ATG AAC AGC CTG CGT GCG GAA GAT ACC GCG GTG TAT TAT TGC GCG CGT GCG CTG ACC < 360
R   D   N   S   K   N   T   L   Y   L   Q   M   N   S   L   R   A   E   D   T   A   V   Y   Y   C   A   R   A   L   T

                                                                                        >linker             >VLhu225
                                                                                        |                   |
TAT TAT GAT TAC GAA TTT GCG TAT TGG GGC CAG GGC ACC ACC GTT ACG GTC TCG AGC GGT GGC GGT GGA TCC GAT ATT CAG CTG ACC CAG < 450
Y   Y   D   Y   E   F   A   Y   W   G   Q   G   T   T   V   T   V   S   S   G   G   G   G   S   D   I   Q   L   T   Q

AGC CCG AGC TTT CTG AGC GCG AGC GTG GGC GAT CGT GTT ACC ATT ACC TGT CGT GCA AGC CAG AGC ATT GGC ACC AAC ATT CAT TGG TAT < 540
S   P   S   F   L   S   A   S   V   G   D   R   V   T   I   T   C   R   A   S   Q   S   I   G   T   N   I   H   W   Y

CAG CAG AAA CCG GGC AAA GCG CCG AAA CTG CTG ATT AAA TAT GCG AGC GAA AGC ATT AGC GGC GTG CCG AGC CGT TTT AGC GGC AGC GGT < 630
Q   Q   K   P   G   K   A   P   K   L   L   I   K   Y   A   S   E   S   I   S   G   V   P   S   R   F   S   G   S   G

AGC GGC ACC GAA TTT ACC CTG ACC ATT AGC AGC CTG CAG CCG GAA GAT TTT GCG ACC TAT TAT TGC CAG CAG AAC AAC AAC TGG CCG ACC < 720
S   G   T   E   F   T   L   T   I   S   S   L   Q   P   E   D   F   A   T   Y   Y   C   Q   Q   N   N   N   W   P   T

                                                    NotI        >His-tag
                                                    |           |
ACC TTT GGT GCG GGC ACC AAA CTG GAA ATT AAA CGT GCG GCC GCC CAC CAT CAT CAC CAT CAC TAA
T   F   G   A   G   T   K   L   E   I   K   R   A   A   A   H   H   H   H   H   H   *
```

6.2.2 (ds)Db4D5 (pSecTagAL1)

Sequence of Db4D5 is represented. Mutation of underlined codons GGC to TGT and CAG to TGC replaces G and Q with cysteines, respectively, and generates sequence of dsDb4D5.

```
>Igk leader                                                                                 AgeI    VH4D5
|                                                                                           |       |
ATG GAG ACA GAC ACA CTC CTG CTA TGG GTA CTG CTG CTC TGG GTT CCA GGT TCC ACC GGT GAA GTG CAG CTC GTC GAA AGT GGC GGT GGA < 90
M   E   T   D   T   L   L   L   W   V   L   L   L   W   V   P   G   S   T   G   E   V   Q   L   V   E   S   G   G   G

CTT GTG CAG CCT GGC GGT TCC CTC AGA CTG TCC TGT GCC GCG TCA GGC TTC AAC ATC AAG GAC ACG TAC ATC CAC TGG GTG AGG CAA GCT < 180
L   V   Q   P   G   G   S   L   R   L   S   C   A   A   S   G   F   N   I   K   D   T   Y   I   H   W   V   R   Q   A

CCT GGA AAG GGC TTG GAG TGG GTC GCT AGG ATC TAC CCG ACG AAC GGC TAC ACC AGG TAC GCT GAC TCA GTG AAG GGA AGG TTC ACG ATC < 270
P   G   K   G   L   E   W   V   A   R   I   Y   P   T   N   G   Y   T   R   Y   A   D   S   V   K   G   R   F   T   I

AGT GCA GAC ACC AGC AAG AAC ACC GCA TAC CTC CAA ATG AAC TCC CTG AGA GCC GAG GAC ACC GCC GTG TAC TAC TGC TCT CGT TGG GGT < 360
S   A   D   T   S   K   N   T   A   Y   L   Q   M   N   S   L   R   A   E   D   T   A   V   Y   Y   C   S   R   W   G
```

```
                                                                                                  >linker             >VL4D5
                                                                                                  |                   |
GGA GAT GGC TTC TAC GCT ATG GAC TAC TGG GGT CAA GGC ACA CTG GTG ACC GTC AGT TCC GGA GGA GGG GGT AGT GAC ATC CAG ATG ACC < 450
G   D   G   F   Y   A   M   D   Y   W   G   Q   G   T   L   V   T   V   S   S   G   G   G   G   S   D   I   Q   M   T

CAG TCA CCC TCA AGC CTC AGT GCC AGC GTC GGA GAT AGA GTG ACC ATA ACG TGC CGA GCT TCT CAG GAT GTG AAC ACG GCA GTG GCT TGG < 540
Q   S   P   S   S   L   S   A   S   V   G   D   R   V   T   I   T   C   R   A   S   Q   D   V   N   T   A   V   A   W

TAT CAG CAA AAG CCT GGG AAA GCC CCA AAG CTG CTC ATC TAC TCC GCA TCC TTC CTG TAT AGC GGA GTT CCA TCT AGG TTC TCA GGC TCT < 630
Y   Q   Q   K   P   G   K   A   P   K   L   L   I   Y   S   A   S   F   L   Y   S   G   V   P   S   R   F   S   G   S

AGG TCT GGG ACC GAC TTC ACG CTG ACG ATC TCC TCC CTG CAA CCT GAG GAC TTC GCC ACG TAC TAC TGC CAG CAG CAC TAC ACG ACT CCT < 720
R   S   G   T   D   F   T   L   T   I   S   S   L   Q   P   E   D   F   A   T   Y   Y   C   Q   Q   H   Y   T   T   P

                                                  NotI        >His-tag
                                                  |           |
CCA ACC TTC GGT CAG GGA ACG AAG GTC GAG ATC AAG CGT GCG GCC GCC CAC CAT CAT CAC CAT CAC TAA
P   T   F   G   Q   G   T   K   V   E   I   K   R   A   A   A   H   H   H   H   H   H   *
```

6.2.3 (ds)Db3M6 (pSecTagAL1)

Sequence of Db3M6 is represented. Mutation of underlined codons GGA to TGT and GGT to TGC replaces G and G with cysteines, respectively, and generates sequence of dsDb3M6.

```
>Igk leader                                                                                AgeI    >VH3M6
|                                                                                          |       |
ATG GAG ACA GAC ACA CTC CTG CTA TGG GTA CTG CTG CTC TGG GTT CCA GGT TCC ACC GGT GAA GTG CAG CTG CTG GAA AGC GGA GGC GGC < 90
M   E   T   D   T   L   L   L   W   V   L   L   L   W   V   P   G   S   T   G   E   V   Q   L   L   E   S   G   G   G

CTG GTG CAG CCT GGC GGC TCT CTG AGA CTG AGC TGT GCC GCC AGC GGC TTC ACC TTC AGC CAC TAC GTG ATG GCC TGG GTC CGA CAG GCC < 180
L   V   Q   P   G   G   S   L   R   L   S   C   A   A   S   G   F   T   F   S   H   Y   V   M   A   W   V   R   Q   A

CCT GGC AAG GGA CTG GAA TGG GTG TCC AGC ATC AGC AGC AGC GGC GGC TGG ACC CTG TAC GCC GAT AGC GTG AAG GGC CGG TTT ACC ATC < 270
P   G   K   G   L   E   W   V   S   S   I   S   S   S   G   G   W   T   L   Y   A   D   S   V   K   G   R   F   T   I

AGC CGG GAC AAC AGC AAG AAC ACC CTG TAC CTG CAG ATG AAC AGC CTG CGG GCC GAG GAC ACC GCC GTG TAC TAC TGC ACC AGA GGC CTG < 360
S   R   D   N   S   K   N   T   L   Y   L   Q   M   N   S   L   R   A   E   D   T   A   V   Y   Y   C   T   R   G   L

                                                                                           >linker             >VL3M6
                                                                                           |                   |
AAG ATG GCC ACC ATC TTC GAC TAC TGG GGG CAG GGC ACC CTG GTC ACA GTC TCG AGT GGG GGA GGC GGA TCC CAG TCT GCC CTG ACA CAG < 450
K   M   A   T   I   F   D   Y   W   G   Q   G   T   L   V   T   V   S   S   G   G   G   G   S   Q   S   A   L   T   Q

CCT GCC AGC GTG TCC GGC AGC CCT GGC CAG AGC ATC ACA ATC AGC TGC ACC GGC ACC AGC AGC GAC GTG GGC AGC TAC AAC GTG GTG TCC < 540
P   A   S   V   S   G   S   P   G   Q   S   I   T   I   S   C   T   G   T   S   S   D   V   G   S   Y   N   V   V   S

TGG TAT CAG CAG CAC CCC GGC AAG GCC CCC AAG CTG ATC ATC TAC GAG GTG TCC CAG CGG CCC AGC GGC GTG TCC AAC AGA TTC AGC GGC < 630
W   Y   Q   Q   H   P   G   K   A   P   K   L   I   I   Y   E   V   S   Q   R   P   S   G   V   S   N   R   F   S   G

AGC AAG AGC GGC AAC ACC GCC AGC CTG ACC ATC AGC GGG CTG CAG ACC GAG GAC GAG GCC GAC TAC TAC TGC TCC AGC TAC GCC GGC AGC < 720
S   K   S   G   N   T   A   S   L   T   I   S   G   L   Q   T   E   D   E   A   D   Y   Y   C   S   S   Y   A   G   S

                                                          NotI        >His-tag
                                                          |           |
AGC ATC TTC GTG ATC TTC GGA GGT GGC ACC AAA GTG ACC GTG CTG GCG GCC GCC CAC CAT CAT CAC CAT CAC TAA
S   I   F   V   I   F   G   G   G   T   K   V   T   V   L   A   A   A   H   H   H   H   H   H   *
```

6.2.4 Db3-43 (pSecTagAL1)

```
>Igk leader                                                                                AgeI    >VH3-43
|                                                                                          |       |
ATG GAG ACA GAC ACA CTC CTG CTA TGG GTA CTG CTG CTC TGG GTT CCA GGT TCC ACC GGT CAA GTG CAG CTG CAG CAG TCT GGC CCT GGC < 90
M   E   T   D   T   L   L   L   W   V   L   L   L   W   V   P   G   S   T   G   Q   V   Q   L   Q   Q   S   G   P   G

CTC GTG AAG CCT AGC CAG ACC CTG AGC CTG ACC TGT GCC ATC AGC GGC GAT AGC GTG TCC AGC AAC AGA GCC GCC TGG AAC TGG ATC AGA < 180
L   V   K   P   S   Q   T   L   S   L   T   C   A   I   S   G   D   S   V   S   S   N   R   A   A   W   N   W   I   R

CAG AGC CCC AGC AGA GGC CTG GAA TGG CTG GGC CGG ACC TAC TAC CGC AGC AAG TGG TAC AAC GAC TAC GCC CAG AGC CTG AAG TCC CGG < 270
Q   S   P   S   R   G   L   E   W   L   G   R   T   Y   Y   R   S   K   W   Y   N   D   Y   A   Q   S   L   K   S   R

ATC ACC ATC AAC CCC GAC ACC CCC AAG AAC CAG TTC TCC CTG CAG CTG AAC AGC GTG ACC CCC GAG GAT ACC GCC GTG TAC TAC TGC GCC < 360
I   T   I   N   P   D   T   P   K   N   Q   F   S   L   Q   L   N   S   V   T   P   E   D   T   A   V   Y   Y   C   A

                                                                                                                  >linker             >VL3-43
                                                                                                                  |                   |
AGA GAT GGA CAG CTG GGC CTG GAC GCC CTG GAC ATT TGG GGC CAG GGC ACA ATG GTC ACA GTG TCC TCT GGG GGA GGC GGA TCC CAA GCC < 450
R   D   G   Q   L   G   L   D   A   L   D   I   W   G   Q   G   T   M   V   T   V   S   S   G   G   G   G   S   Q   A

GGA CTG ACA CAG CCT CCA GCC GTG TCT GTG GCC CCT GGA CAG ACA GCC AGC ATC ACC TGT GGC CGG GAC AAC ATC GGC AGC AGA AGC GTG < 540
G   L   T   Q   P   P   A   V   S   V   A   P   G   Q   T   A   S   I   T   C   G   R   D   N   I   G   S   R   S   V

CAC TGG TAT CAG CAG AAA CCC GGC CAG GCC CCT GTG CTG GTG GTG TAC GAC GAC AGC GAT AGA CCT GCC GGC ATC CCC GAG AGA TTC AGC < 630
H   W   Y   Q   Q   K   P   G   Q   A   P   V   L   V   V   Y   D   D   S   D   R   P   A   G   I   P   E   R   F   S

GGC AGC AAC TAC GAG AAC ACC GCC ACC CTG ACC ATC AGC AGA GTG GAA GCC GGC GAC GAG GCC GAC TAC TAC TGT CAA GTG TGG GGC ATC < 720
G   S   N   Y   E   N   T   A   T   L   T   I   S   R   V   E   A   G   D   E   A   D   Y   Y   C   Q   V   W   G   I

                                                              NotI        >His-tag
                                                              |           |
ACC AGC GAT CAC GTG GTG TTT GGC GGA GGC ACC AAG CTG ACA GTG CTG GCG GCC GCC CAC CAT CAT CAC CAT CAC TAA
T   S   D   H   V   V   F   G   G   G   T   K   L   T   V   L   A   A   A   H   H   H   H   H   H   *
```

6.2.5 Db323/A3hu3 (pSecTagAL1)

```
>Igk leader                                                          AgeI    >VH323/A3hu3
|                                                                    |       |
ATG GAG ACA GAC ACA CTC CTG CTA TGG GTA CTG CTG CTC TGG GTT CCA GGT TCC ACC GGT CAA GTG CAG CTG GTG CAG TCT GGC GCC GAA < 90
  M   E   T   D   T   L   L   L   W   V   L   L   L   W   V   P   G   S   T   G   Q   V   Q   L   V   Q   S   G   A   E

GTG AAG AAA CCA GGC GCC AGC GTG AAG GTG TCC TGC AAG GCC AGC GGC TAC ACC TTT ACC AAC TAC GGC ATG AAC TGG GTG CGC CAG GCC < 180
V   K   K   P   G   A   S   V   K   V   S   C   K   A   S   G   Y   T   F   T   N   Y   G   M   N   W   V   R   Q   A

CCT GGC CAG AGA CTG GAA TGG ATG GGC TGG ATC AAC ACC TAC ACC GGC GAG CCC ACC TAC GGC GAG GAC TTC AAG GGC AGA GTG ACC ATC < 270
P   G   Q   R   L   E   W   M   G   W   I   N   T   Y   T   G   E   P   T   Y   G   E   D   F   K   G   R   V   T   I

ACC CTG GAC ACC AGC GCC AGC ACC GCC TAC ATG GAA CTG AGC AGC CTG CGG AGC GAG GAC ACC GCC GTG TAC TAC TGC GCC AGA TTC GGC < 360
T   L   D   T   S   A   S   T   A   Y   M   E   L   S   S   L   R   S   E   D   T   A   V   Y   Y   C   A   R   F   G

                                                                  >linker             >VL323/A3hu3
                                                                  |                   |
AAC TAC GTG GAC TAC TGG GGC CAG GGC ACC CTC GTG ACA GTC TCG AGC GGT GGC GGT GGA TCC GAG ATC GTG CTG ACA CAG AGC CCT GGC < 450
N   Y   V   D   Y   W   G   Q   G   T   L   V   T   V   S   S   G   G   G   G   S   E   I   V   L   T   Q   S   P   G

ACC CTG AGC CTG TCT CCA GGC GAA AGA GCC ACC CTG TCC TGC AGA AGC AGC AAG AAC CTG CTG CAC AGC AAC GGC ATC ACC TAC CTG TAC < 540
T   L   S   L   S   P   G   E   R   A   T   L   S   C   R   S   S   K   N   L   L   H   S   N   G   I   T   Y   L   Y

TGG TAT CAG CAG AAG CCC GGC CAG GCC CCC AGA CTG CTG ATC TAC CAG ATG AGC AAC CTG GCC AGC GGC ATC CCA GAC AGA TTT TCT GGC < 630
W   Y   Q   Q   K   P   G   Q   A   P   R   L   L   I   Y   Q   M   S   N   L   A   S   G   I   P   D   R   F   S   G

AGC GGC TCC GGC ACC GAC TTC ACC CTG ACA ATC AGC AGA CTG GAA CCC GAG GAC TTC GCC GTG TAC TAC TGC GCC CAG AAC CTG GAA ATC < 720
S   G   S   G   T   D   F   T   L   T   I   S   R   L   E   P   E   D   F   A   V   Y   Y   C   A   Q   N   L   E   I

                                                          NotI        >His-tag
                                                          |           |
CCC CGG ACC TTT GGC CAG GGC ACC AAG CTG GAA ATC AAG AGA GCG GCC GCC CAC CAT CAT CAC CAT CAC TAA
P   R   T   F   G   Q   G   T   K   L   E   I   K   R   A   A   A   H   H   H   H   H   H   *
```

6.3 scFv-EHD2 (pSecTagAL1)

ScFv-EHD2 constructs were generated by insertion of the respective scFv sequences (see 6.1) as AgeI-NotI fragments into the sequence represented below (after AgeI-NotI digestion).

```
>Igk leader                                                          AgeI
|                                                                    |
ATG GAG ACA GAC ACA CTC CTG CTA TGG GTA CTG CTG CTC TGG GTT CCA GGT TCC ACC GGT ... ... ... ... ... ... ... ... ... ... < 90
M   E   T   D   T   L   L   L   W   V   L   L   L   W   V   P   G   S   T   G

                  NotI>linker                    >EHD2
                  |                              |
... ... ... ... ... GCG GCC GCC GGG GGA AGC GGC GGT GAT TTC ACC CCC CCC ACA GTG AAG ATC CTC CAG AGC AGC TGT GAC GGC GGA < 180
                  A   A   A   G   G   S   G   G   D   F   T   P   P   T   V   K   I   L   Q   S   S   C   D   G   G

GGC CAC TTC CCA CCT ACC ATC CAG CTG CTG TGT CTG GTG TCC GGC TAC ACC CCC GGC ACC ATC AAC ATC ACC TGG CTG GAA GAT GGA CAA < 270
G   H   F   P   P   T   I   Q   L   L   C   L   V   S   G   Y   T   P   G   T   I   N   I   T   W   L   E   D   G   Q

GTG ATG GAC GTG GAC CTG AGC ACC GCC AGC ACC ACA CAG GAA GGC GAG CTG GCC TCT ACC CAG AGC GAG CTG ACA CTG AGC CAG AAG CAC < 360
V   M   D   V   D   L   S   T   A   S   T   T   Q   E   G   E   L   A   S   T   Q   S   E   L   T   L   S   Q   K   H

                                                                                                                  >linker
                                                                                                                  |
TGG CTG AGC GAC CGG ACC TAC ACC TGT CAA GTG ACC TAC CAG GGC CAC ACC TTC GAG GAC AGC ACC AAG AAG TGC GCC GAC AGC AAC GGA < 450
W   L   S   D   R   T   Y   T   C   Q   V   T   Y   Q   G   H   T   F   E   D   S   T   K   K   C   A   D   S   N   G

                          >His-tag
                          |
GGT TCA GGG GGC GCC TCG AGC CAC CAT CAT CAC CAT CAC TAA
G   S   G   G   A   S   S   H   H   H   H   H   H   *
```

6.4 scFv-Fc (pSecTagAL1)

ScFv-Fc constructs were generated by insertion of the respective scFv sequences (see 6.1) as AgeI-NotI fragments into the sequence represented below (after AgeI-NotI digestion).

```
>Igk leader                                                          AgeI              NotI>linker
|                                                                    |                 |
ATG GAG ACA GAC ACA CTC CTG CTA TGG GTA CTG CTG CTC TGG GTT CCA GGT TCC ACC GGT ... ... ... GCG GCC GCA GGG GGA AGC GGC < 180
M   E   T   D   T   L   L   L   W   V   L   L   L   W   V   P   G   S   T   G             A   A   A   G   G   S   G

    >hinge                                CH2
    |                                     |
GGT GAC AAA ACT CAC ACA TGC CCA CCG TGC CCA GCA CCT GAA CTC CTG GGG GGA CCG TCA GTC TTC CTC TTC CCC CCA AAA CCC AAG GAC < 270
G   D   K   T   H   T   C   P   P   C   P   A   P   E   L   L   G   G   P   S   V   F   L   F   P   P   K   P   K   D

ACC CTC ATG ATC TCC CGG ACC CCT GAG GTC ACA TGC GTG GTG GTG GAC GTG AGC CAC GAA GAC CCT GAG GTC AAG TTC AAC TGG TAC GTG < 360
T   L   M   I   S   R   T   P   E   V   T   C   V   V   V   D   V   S   H   E   D   P   E   V   K   F   N   W   Y   V

GAC GGC GTG GAG GTG CAT AAT GCC AAG ACA AAG CCG CGG GAG GAG CAG TAC AAC AGC ACG TAC CGT GTG GTC AGC GTC CTC ACC GTC CTG < 450
D   G   V   E   V   H   N   A   K   T   K   P   R   E   E   Q   Y   N   S   T   Y   R   V   V   S   V   L   T   V   L
```

```
CAC CAG GAC TGG CTG AAT GGC AAG GAG TAC AAG TGC AAG GTC TCC AAC AAA GCC CTC CCA GCC CCC ATC GAG AAA ACC ATC TCC AAA GCC < 540
H   Q   D   W   L   N   G   K   E   Y   K   C   K   V   S   N   K   A   L   P   A   P   I   E   K   T   I   S   K   A

    >CH3
    |
AAA GGG CAG CCC CGA GAA CCA CAG GTG TAC ACC CTG CCC CCA TCC CGG GAT GAG CTG ACC AAG AAC CAG GTC AGC CTG ACC TGC CTG GTC < 630
K   G   Q   P   R   E   P   Q   V   Y   T   L   P   P   S   R   D   E   L   T   K   N   Q   V   S   L   T   C   L   V

AAA GGC TTC TAT CCC AGC GAC ATC GCC GTG GAG TGG GAG AGC AAT GGG CAG CCG GAG AAC AAC TAC AAG ACC ACG CCT CCC GTG CTG GAC < 720
K   G   F   Y   P   S   D   I   A   V   E   W   E   S   N   G   Q   P   E   N   N   Y   K   T   T   P   P   V   L   D

TCC GAC GGC TCC TTC TTC CTC TAC AGC AAG CTC ACC GTG GAC AAG AGC AGG TGG CAG CAG GGG AAC GTC TTC TCA TGC TCC GTG ATG CAT < 810
S   D   G   S   F   F   L   Y   S   K   L   T   V   D   K   S   R   W   Q   Q   G   N   V   F   S   C   S   V   M   H

GAG GCT CTG CAC AAC CAC TAC ACG CAG AAG AGC CTC TCC CTG TCT CCG GGT AAA TGA
E   A   L   H   N   H   Y   T   Q   K   S   L   S   L   S   P   G   K   *
```

6.5 Bispecific single-chain diabodies

6.5.1 scDbhu225x3M6 (pSecTagAHis)

```
>Igk leader                                                                                                     >VHhu225
|                                                                                                               |
ATG GAG ACA GAC ACA CTC CTG CTA TGG GTA CTG CTG CTC TGG GTT CCA GGT TCC ACT GGT GAC GCG GCC CAG CCG GCC ATG GCG GAA GTG <90
M   E   T   D   T   L   L   L   W   V   L   L   L   W   V   P   G   S   T   G   D   A   A   Q   P   A   M   A   E   V

CAG CTG GTT GAA AGC GGC GGT GGT CTG GTT CAG CCG GGT GGC AGC CTG CGT CTG AGC TGT GCG GCG AGC GGC TTT AGC CTG ACC AAC TAT <180
Q   L   V   E   S   G   G   G   L   V   Q   P   G   G   S   L   R   L   S   C   A   A   S   G   F   S   L   T   N   Y

GGC GTG CAT TGG GTG CGT CAG GCA CCG GGC AAA GGC CTG GAA TGG CTG GGC GTG ATT TGG AGC GGC GGC AAC ACC GAT TAT AAC ACC CCG <270
G   V   H   W   V   R   Q   A   P   G   K   G   L   E   W   L   G   V   I   W   S   G   G   N   T   D   Y   N   T   P

TTT ACC AGC CGT TTT ACC ATT AGC CGT GAT AAC AGC AAA AAC ACC CTG TAT CTG CAG ATG AAC AGC CTG CGT GCG GAA GAT ACC GCG GTG <360
F   T   S   R   F   T   I   S   R   D   N   S   K   N   T   L   Y   L   Q   M   N   S   L   R   A   E   D   T   A   V

                                                                                                          >linker
                                                                                                          |
TAT TAT TGC GCG CGT GCG CTG ACC TAT TAT GAT TAC GAA TTT GCG TAT TGG GGC CAG GGC ACC ACC GTT ACG GTC TCG AGT GGC GGT GGC <450
Y   Y   C   A   R   A   L   T   Y   Y   D   Y   E   F   A   Y   W   G   Q   G   T   T   V   T   V   S   S   G   G   G

        >VL3M6
        |
GGA TCG CAG TCT GCC CTG ACA CAG CCT GCC AGC GTG TCC GGC AGC CCT GGC CAG AGC ATC ACA ATC AGC TGC ACC GGC ACC AGC AGC GAC <540
G   S   Q   S   A   L   T   Q   P   A   S   V   S   G   S   P   G   Q   S   I   T   I   S   C   T   G   T   S   S   D

GTG GGC AGC TAC AAC GTG GTG TCC TGG TAT CAG CAG CAC CCC GGC AAG GCC CCC AAG CTG ATC ATC TAC GAG GTG TCC CAG CGG CCC AGC <630
V   G   S   Y   N   V   V   S   W   Y   Q   Q   H   P   G   K   A   P   K   L   I   I   Y   E   V   S   Q   R   P   S

GGC GTG TCC AAC AGA TTC AGC GGC AGC AAG AGC GGC AAC ACC GCC AGC CTG ACC ATC AGC GGG CTG CAG ACC GAG GAC GAG GCC GAC TAC <720
G   V   S   N   R   F   S   G   S   K   S   G   N   T   A   S   L   T   I   S   G   L   Q   T   E   D   E   A   D   Y

                                                                                        >linker
                                                                                        |
TAC TGC TCC AGC TAC GCC GGC AGC AGC ATC TTC GTG ATC TTC GGA GGT GGC ACC AAA GTG ACC GTG CTG GGA GGC GGT GGC AGC GGT GGG <810
Y   C   S   S   Y   A   G   S   S   I   F   V   I   F   G   G   G   T   K   V   T   V   L   G   G   G   G   S   G   G

                            >VH3M6
                            |
CGC GCC TCG GGC GGA GGT GGC TCA GAA GTG CAG CTG CTG GAA AGC GGA GGC GGC CTG GTG CAG CCT GGC GGC TCT CTG AGA CTG AGC TGT <900
R   A   S   G   G   G   G   S   E   V   Q   L   L   E   S   G   G   G   L   V   Q   P   G   G   S   L   R   L   S   C

GCC GCC AGC GGC TTC ACC TTC AGC CAC TAC GTG ATG GCC TGG GTC CGA CAG GCC CCT GGC AAG GGA CTG GAA TGG GTG TCC AGC ATC AGC <990
A   A   S   G   F   T   F   S   H   Y   V   M   A   W   V   R   Q   A   P   G   K   G   L   E   W   V   S   S   I   S

AGC AGC GGC GGC TGG ACC CTG TAC GCC GAT AGC GTG AAG GGC CGG TTT ACC ATC AGC CGG GAC AAC AGC AAG AAC ACC CTG TAC CTG CAG <1080
S   S   G   G   W   T   L   Y   A   D   S   V   K   G   R   F   T   I   S   R   D   N   S   K   N   T   L   Y   L   Q

ATG AAC AGC CTG CGG GCC GAG GAC ACC GCC GTG TAC TAC TGC ACC AGA GGC CTG AAG ATG GCC ACC ATC TTC GAC TAC TGG GGG CAG GGC <1170
M   N   S   L   R   A   E   D   T   A   V   Y   Y   C   T   R   G   L   K   M   A   T   I   F   D   Y   W   G   Q   G

                          >linker           >VLhu225
                          |                 |
ACC CTG GTC ACA GTC TCG AGT GGA GGC GGG GGA TCC GAT ATT CAG CTG ACC CAG AGC CCG AGC TTT CTG AGC GCG AGC GTG GGC GAT CGT <1260
T   L   V   T   V   S   S   G   G   G   G   S   D   I   Q   L   T   Q   S   P   S   F   L   S   A   S   V   G   D   R

GTT ACC ATT ACC TGT CGT GCA AGC CAG AGC ATT GGC ACC AAC ATT CAT TGG TAT CAG CAG AAA CCG GGC AAA GCG CCG AAA CTG CTG ATT <1350
V   T   I   T   C   R   A   S   Q   S   I   G   T   N   I   H   W   Y   Q   Q   K   P   G   K   A   P   K   L   L   I

AAA TAT GCG AGC GAA AGC ATT AGC GGC GTG CCG AGC CGT TTT AGC GGC AGC GGT AGC GGC ACC GAA TTT ACC CTG ACC ATT AGC AGC CTG <1440
K   Y   A   S   E   S   I   S   G   V   P   S   R   F   S   G   S   G   S   G   T   E   F   T   L   T   I   S   S   L

CAG CCG GAA GAT TTT GCG ACC TAT TAT TGC CAG CAG AAC AAC AAC TGG CCG ACC ACC TTT GGT GCG GGC ACC AAA CTG GAA ATT AAA CGT <1530
Q   P   E   D   F   A   T   Y   Y   C   Q   Q   N   N   N   W   P   T   T   F   G   A   G   T   K   L   E   I   K   R

NotI        >His-tag
|           |
GCG GCC GCC CAC CAT CAT CAC CAT CAC TAA
A   A   A   H   H   H   H   H   H   *
```

6.5.2 scDb323/A3hu3xhu225 (pSecTagAHis)

```
>Igk leader
|
ATG GAG ACA GAC ACA CTC CTG CTA TGG GTA CTG CTG CTC TGG GTT CCA GGT TCC ACT GGT GAC GCG GCC CAG CCG GCC ATG GCC ACC GGT <90
M   E   T   D   T   L   L   L   W   V   L   L   L   W   V   P   G   S   T   G   D   A   A   Q   P   A   M   A   T   G
```

```
>VH323/A3hu3
|
CAA GTG CAG CTG GTG CAG TCT GGC GCC GAA GTG AAG AAA CCA GGC GCC AGC GTG AAG GTG TCC TGC AAG GCC AGC GGC TAC ACC TTT ACC <180
Q   V   Q   L   V   Q   S   G   A   E   V   K   K   P   G   A   S   V   K   V   S   C   K   A   S   G   Y   T   F   T

AAC TAC GGC ATG AAC TGG GTG CGC CAG GCC CCT GGC CAG AGA CTG GAA TGG ATG GGC TGG ATC AAC ACC TAC ACC GGC GAG CCC ACC TAC <270
N   Y   G   M   N   W   V   R   Q   A   P   G   Q   R   L   E   W   M   G   W   I   N   T   Y   T   G   E   P   T   Y

GGC GAG GAC TTC AAG GGC AGA GTG ACC ATC ACC CTG GAC ACC AGC GCC AGC ACC GCC TAC ATG GAA CTG AGC AGC CTG CGG AGC GAG GAC <360
G   E   D   F   K   G   R   V   T   I   T   L   D   T   S   A   S   T   A   Y   M   E   L   S   S   L   R   S   E   D

                                                                                                                >linker
                                                                                                                |
ACC GCC GTG TAC TAC TGC GCC AGA TTC GGC AAC TAC GTG GAC TAC TGG GGC CAG GGC ACC CTC GTG ACA GTC TCG AGT GGC GGT GGC GGA <450
T   A   V   Y   Y   C   A   R   F   G   N   Y   V   D   Y   W   G   Q   G   T   L   V   T   V   S   S   G   G   G   G

    >VLhu225
    |
TCG GAT ATT CAG CTG ACC CAG AGC CCG AGC TTT CTG AGC GCG AGC GTG GGC GAT CGT GTT ACC ATT ACC TGT CGT GCA AGC CAG AGC ATT <540
S   D   I   Q   L   T   Q   S   P   S   F   L   S   A   S   V   G   D   R   V   T   I   T   C   R   A   S   Q   S   I

GGC ACC AAC ATT CAT TGG TAT CAG CAG AAA CCG GGC AAA GCG CCG AAA CTG CTG ATT AAA TAT GCG AGC GAA AGC ATT AGC GGC GTG CCG <630
G   T   N   I   H   W   Y   Q   Q   K   P   G   K   A   P   K   L   L   I   K   Y   A   S   E   S   I   S   G   V   P

AGC CGT TTT AGC GGC AGC GGT AGC GGC ACC GAA TTT ACC CTG ACC ATT AGC AGC CTG CAG CCG GAA GAT TTT GCG ACC TAT TAT TGC CAG <720
S   R   F   S   G   S   G   S   G   T   E   F   T   L   T   I   S   S   L   Q   P   E   D   F   A   T   Y   Y   C   Q

                                                                                >linker
                                                                                |
CAG AAC AAC AAC TGG CCG ACC ACC TTT GGT GCG GGC ACC AAA CTG GAA ATT AAA CGT GGA GGC GGT GGC AGC GGT GGG CGC GCC TCG GGC <810
Q   N   N   N   W   P   T   T   F   G   A   G   T   K   L   E   I   K   R   G   G   G   G   S   G   G   R   A   S   G

                >VHhu225
                |
GGA GGT GGC TCA GAA GTG CAG CTG GTT GAA AGC GGC GGT GGT CTG GTT CAG CCG GGT GGC AGC CTG CGT CTG AGC TGT GCG GCG AGC GGC <900
G   G   G   S   E   V   Q   L   V   E   S   G   G   G   L   V   Q   P   G   G   S   L   R   L   S   C   A   A   S   G

TTT AGC CTG ACC AAC TAT GGC GTG CAT TGG GTG CGT CAG GCA CCG GGC AAA GGC CTG GAA TGG CTG GGC GTG ATT TGG AGC GGC GGC AAC <990
F   S   L   T   N   Y   G   V   H   W   V   R   Q   A   P   G   K   G   L   E   W   L   G   V   I   W   S   G   G   N

ACC GAT TAT AAC ACC CCG TTT ACC AGC CGT TTT ACC ATT AGC CGT GAT AAC AGC AAA AAC ACC CTG TAT CTG CAG ATG AAC AGC CTG CGT <1080
T   D   Y   N   T   P   F   T   S   R   F   T   I   S   R   D   N   S   K   N   T   L   Y   L   Q   M   N   S   L   R

GCG GAA GAT ACC GCG GTG TAT TAT TGC GCG CGT GCG CTG ACC TAT TAT GAT TAC GAA TTT GCG TAT TGG GGC CAG GGC ACC ACC GTT ACG <1170
A   E   D   T   A   V   Y   Y   C   A   R   A   L   T   Y   Y   D   Y   E   F   A   Y   W   G   Q   G   T   T   V   T

            >linker             >VL323/A3hu3
            |                   |
GTC TCT AGC GGA GGC GGG GGA TCC GAG ATC GTG CTG ACA CAG AGC CCT GGC ACC CTG AGC CTG TCT CCA GGC GAA AGA GCC ACC CTG TCC <1260
V   S   S   G   G   G   G   S   E   I   V   L   T   Q   S   P   G   T   L   S   L   S   P   G   E   R   A   T   L   S

TGC AGA AGC AGC AAG AAC CTG CTG CAC AGC AAC GGC ATC ACC TAC CTG TAC TGG TAT CAG CAG AAG CCC GGC CAG GCC CCC AGA CTG CTG <1350
C   R   S   S   K   N   L   L   H   S   N   G   I   T   Y   L   Y   W   Y   Q   Q   K   P   G   Q   A   P   R   L   L

ATC TAC CAG ATG AGC AAC CTG GCC AGC GGC ATC CCC GAC AGA TTT TCT GGC AGC GGC TCC GGC ACC GAC TTC ACC CTG ACA ATC AGC AGA <1440
I   Y   Q   M   S   N   L   A   S   G   I   P   D   R   F   S   G   S   G   S   G   T   D   F   T   L   T   I   S   R

CTG GAA CCC GAG GAC TTC GCC GTG TAC TAC TGC GCC CAG AAC CTG GAA ATC CCC CGG ACC TTT GGC CAG GGC ACC AAG CTG GAA ATC AAG <1530
L   E   P   E   D   F   A   V   Y   Y   C   A   Q   N   L   E   I   P   R   T   F   G   Q   G   T   K   L   E   I   K

    NotI        >His-tag
    |           |
AGA GCG GCC GCC CAC CAT CAT CAC CAT CAC TAA
R   A   A   A   H   H   H   H   H   H   *
```

6.5.3 scDb4D5xhu225 (pSecTagAHis)

```
>Igk leader                                                                                                     >VH4D5
|                                                                                                               |
ATG GAG ACA GAC ACA CTC CTG CTA TGG GTA CTG CTG CTC TGG GTT CCA GGT TCC ACT GGT GAC GCG GCC CAG CCG GCC ATG GCC GAA GTG <90
M   E   T   D   T   L   L   L   W   V   L   L   L   W   V   P   G   S   T   G   D   A   A   Q   P   A   M   A   E   V

CAG CTC GTC GAA AGT GGC GGT GGA CTT GTG CAG CCT GGC GGT TCC CTC AGA CTG TCC TGT GCC GCG TCA GGC TTC AAC ATC AAG GAC ACG <180
Q   L   V   E   S   G   G   G   L   V   Q   P   G   G   S   L   R   L   S   C   A   A   S   G   F   N   I   K   D   T

TAC ATC CAC TGG GTG AGG CAA GCT CCT GGA AAG GGC TTG GAG TGG GTC GCT AGG ATC TAC CCG ACG AAC GGC TAC ACC AGG TAC GCT GAC <270
Y   I   H   W   V   R   Q   A   P   G   K   G   L   E   W   V   A   R   I   Y   P   T   N   G   Y   T   R   Y   A   D

TCA GTG AAG GGA AGG TTC ACG ATC AGT GCA GAC ACC AGC AAG AAC ACC GCA TAC CTC CAA ATG AAC TCC CTG AGA GCC GAG GAC ACC GCC <360
S   V   K   G   R   F   T   I   S   A   D   T   S   K   N   T   A   Y   L   Q   M   N   S   L   R   A   E   D   T   A

                                                                                                            >linker
                                                                                                            |
GTG TAC TAC TGC TCT CGT TGG GGT GGA GAT GGC TTC TAC GCT ATG GAC TAC TGG GGT CAA GGC ACA CTG GTG ACC GTC TCG AGT GGC GGT <450
V   Y   Y   C   S   R   W   G   G   D   G   F   Y   A   M   D   Y   W   G   Q   G   T   L   V   T   V   S   S   G   G

            >VLhu225
            |
GGC GGA TCG GAT ATT CAG CTG ACC CAG AGC CCG AGC TTT CTG AGC GCG AGC GTG GGC GAT CGT GTT ACC ATT ACC TGT CGT GCA AGC CAG <540
G   G   S   D   I   Q   L   T   Q   S   P   S   F   L   S   A   S   V   G   D   R   V   T   I   T   C   R   A   S   Q

AGC ATT GGC ACC AAC ATT CAT TGG TAT CAG CAG AAA CCG GGC AAA GCG CCG AAA CTG CTG ATT AAA TAT GCG AGC GAA AGC ATT AGC GGC <630
S   I   G   T   N   I   H   W   Y   Q   Q   K   P   G   K   A   P   K   L   L   I   K   Y   A   S   E   S   I   S   G

GTG CCG AGC CGT TTT AGC GGC AGC GGT AGC GGC ACC GAA TTT ACC CTG ACC ATT AGC AGC CTG CAG CCG GAA GAT TTT GCG ACC TAT TAT <720
V   P   S   R   F   S   G   S   G   S   G   T   E   F   T   L   T   I   S   S   L   Q   P   E   D   F   A   T   Y   Y

                                                                        >linker
                                                                        |
TGC CAG CAG AAC AAC AAC TGG CCG ACC ACC TTT GGT GCG GGC ACC AAA CTG GAA ATT AAA CGT GGA GGC GGT GGC AGC GGT GGG CGC GCC <810
C   Q   Q   N   N   N   W   P   T   T   F   G   A   G   T   K   L   E   I   K   R   G   G   G   G   S   G   G   R   A
```

```
                    >VHhu225
                    |
TCG GGC GGA GGT GGC TCA GAA GTG CAG CTG GTT GAA AGC GGC GGT GGT CTG GTT CAG CCG GGT GGC AGC CTG CGT CTG AGC TGT GCG GCG <900
S   G   G   G   G   S   E   V   Q   L   V   E   S   G   G   G   L   V   Q   P   G   G   S   L   R   L   S   C   A   A

AGC GGC TTT AGC CTG ACC AAC TAT GGC GTG CAT TGG GTG CGT CAG GCA CCG GGC AAA GGC CTG GAA TGG CTG GGC GTG ATT TGG AGC GGC <990
S   G   F   S   L   T   N   Y   G   V   H   W   V   R   Q   A   P   G   K   G   L   E   W   L   G   V   I   W   S   G

GGC AAC ACC GAT TAT AAC ACC CCG TTT ACC AGC CGT TTT ACC ATT AGC CGT GAT AAC AGC AAA AAC ACC CTG TAT CTG CAG ATG AAC AGC <1080
G   N   T   D   Y   N   T   P   F   T   S   R   F   T   I   S   R   D   N   S   K   N   T   L   Y   L   Q   M   N   S

CTG CGT GCG GAA GAT ACC GCG GTG TAT TAT TGC GCG CGT GCG CTG ACC TAT TAT GAT TAC GAA TTT GCG TAT TGG GGC CAG GGC ACC ACC <1170
L   R   A   E   D   T   A   V   Y   Y   C   A   R   A   L   T   Y   Y   D   Y   E   F   A   Y   W   G   Q   G   T   T

                >linker             >VL4D5
                |                   |
GTT ACG GTC TCT AGC GGA GGC GGG GGA TCC GAC ATC CAG ATG ACC CAG TCA CCC TCA AGC CTC AGT GCC AGC GTC GGA GAT AGA GTG ACC <1260
V   T   V   S   S   G   G   G   G   S   D   I   Q   M   T   Q   S   P   S   S   L   S   A   S   V   G   D   R   V   T

ATA ACG TGC CGA GCT TCT CAG GAT GTG AAC ACG GCA GTG GCT TGG TAT CAG CAA AAG CCT GGG AAA GCC CCA AAG CTG CTC ATC TAC TCC <1350
I   T   C   R   A   S   Q   D   V   N   T   A   V   A   W   Y   Q   Q   K   P   G   K   A   P   K   L   L   I   Y   S

GCA TCC TTC CTG TAT AGC GGA GTT CCA TCT AGG TTC TCA GGC TCT AGG TCT GGG ACC GAC TTC ACG CTG ACG ATC TCC TCC CTG CAA CCT <1440
A   S   F   L   Y   S   G   V   P   S   R   F   S   G   S   R   S   G   T   D   F   T   L   T   I   S   S   L   Q   P

                                                                                                        NOTI
                                                                                                        |
GAG GAC TTC GCC ACG TAC TAC TGC CAG CAG CAC TAC ACG ACT CCT CCA ACC TTC GGT CAG GGA ACG AAG GTC GAG ATC AAG CGT GCG GCC <1530
E   D   F   A   T   Y   Y   C   Q   Q   H   Y   T   T   P   P   T   F   G   Q   G   T   K   V   E   I   K   R   A   A

    >His-tag
    |
GCC CAC CAT CAT CAC CAT CAC TAA
A   H   H   H   H   H   H   *
```

6.5.4 scDb4D5x3M6 (pSecTagAHis)

```
>Igk leader                                                                                                     >VH4D5
|                                                                                                               |
ATG GAG ACA GAC ACA CTC CTG CTA TGG GTA CTG CTG CTC TGG GTT CCA GGT TCC ACT GGT GAC GCG GCC CAG CCG GCC ATG GCC GAA GTG <90
M   E   T   D   T   L   L   L   W   V   L   L   L   W   V   P   G   S   T   G   D   A   A   Q   P   A   M   A   E   V

CAG CTC GTC GAA AGT GGC GGT GGA CTT GTG CAG CCT GGC GGT TCC CTC AGA CTG TCC TGT GCC GCG TCA GGC TTC AAC ATC AAG GAC ACG <180
Q   L   V   E   S   G   G   G   L   V   Q   P   G   G   S   L   R   L   S   C   A   A   S   G   F   N   I   K   D   T

TAC ATC CAC TGG GTG AGG CAA GCT CCT GGA AAG GGC TTG GAG TGG GTC GCT AGG ATC TAC CCG ACG AAC GGC TAC ACC AGG TAC GCT GAC <270
Y   I   H   W   V   R   Q   A   P   G   K   G   L   E   W   V   A   R   I   Y   P   T   N   G   Y   T   R   Y   A   D

TCA GTG AAG GGA AGG TTC ACG ATC AGT GCA GAC ACC AGC AAG AAC ACC GCA TAC CTC CAA ATG AAC TCC CTG AGA GCC GAG GAC ACC GCC <360
S   V   K   G   R   F   T   I   S   A   D   T   S   K   N   T   A   Y   L   Q   M   N   S   L   R   A   E   D   T   A

                                                                                                                >linker
                                                                                                                |
GTG TAC TAC TGC TCT CGT TGG GGT GGA GAT GGC TTC TAC GCT ATG GAC TAC TGG GGT CAA GGC ACA CTG GTG ACC GTC TCG AGT GGC GGT <450
V   Y   Y   C   S   R   W   G   G   D   G   F   Y   A   M   D   Y   W   G   Q   G   T   L   V   T   V   S   S   G   G

            >VL3M6
            |
GGC GGA TCG CAG TCT GCC CTG ACA CAG CCT GCC AGC GTG TCC GGC AGC CCT GGC CAG AGC ATC ACA ATC AGC TGC ACC GGC ACC AGC AGC <540
G   G   S   Q   S   A   L   T   Q   P   A   S   V   S   G   S   P   G   Q   S   I   T   I   S   C   T   G   T   S   S

GAC GTG GGC AGC TAC AAC GTG GTG TCC TGG TAT CAG CAG CAC CCC GGC AAG GCC CCC AAG CTG ATC ATC TAC GAG GTG TCC CAG CGG CCC <630
D   V   G   S   Y   N   V   V   S   W   Y   Q   Q   H   P   G   K   A   P   K   L   I   I   Y   E   V   S   Q   R   P

AGC GGC GTG TCC AAC AGA TTC AGC GGC AGC AAG AGC GGC AAC ACC GCC AGC CTG ACC ATC AGC GGG CTG CAG ACC GAG GAC GAG GCC GAC <720
S   G   V   S   N   R   F   S   G   S   K   S   G   N   T   A   S   L   T   I   S   G   L   Q   T   E   D   E   A   D

                                                                                                  >linker
                                                                                                  |
TAC TAC TGC TCC AGC TAC GCC GGC AGC AGC ATC TTC GTG ATC TTC GGA GGT GGC ACC AAA GTG ACC GTG CTG GGA GGC GGT GGC AGC GGT <810
Y   Y   C   S   S   Y   A   G   S   S   I   F   V   I   F   G   G   G   T   K   V   T   V   L   G   G   G   G   S   G

                                >VH3M6
                                |
GGG CGC GCC TCG GGC GGA GGT GGC TCA GAA GTG CAG CTG CTG GAA AGC GGA GGC GGC CTG GTG CAG CCT GGC GGC TCT CTG AGA CTG AGC <900
G   R   A   S   G   G   G   G   S   E   V   Q   L   L   E   S   G   G   G   L   V   Q   P   G   G   S   L   R   L   S

TGT GCC GCC AGC GGC TTC ACC TTC AGC CAC TAC GTG ATG GCC TGG GTC CGA CAG GCC CCT GGC AAG GGA CTG GAA TGG GTG TCC AGC ATC <990
C   A   A   S   G   F   T   F   S   H   Y   V   M   A   W   V   R   Q   A   P   G   K   G   L   E   W   V   S   S   I

AGC AGC AGC GGC GGC TGG ACC CTG TAC GCC GAT AGC GTG AAG GGC CGG TTT ACC ATC AGC CGG GAC AAC AGC AAG AAC ACC CTG TAC CTG <1080
S   S   S   G   G   W   T   L   Y   A   D   S   V   K   G   R   F   T   I   S   R   D   N   S   K   N   T   L   Y   L

CAG ATG AAC AGC CTG CGG GCC GAG GAC ACC GCC GTG TAC TAC TGC ACC AGA GGC CTG AAG ATG GCC ACC ATC TTC GAC TAC TGG GGG CAG <1170
Q   M   N   S   L   R   A   E   D   T   A   V   Y   Y   C   T   R   G   L   K   M   A   T   I   F   D   Y   W   G   Q

                                >linker             >VL4D5
                                |                   |
GGC ACC CTG GTC ACA GTC TCG AGT GGA GGC GGG GGA TCC GAC ATC CAG ATG ACC CAG TCA CCC TCA AGC CTC AGT GCC AGC GTC GGA GAT <1260
G   T   L   V   T   V   S   S   G   G   G   G   S   D   I   Q   M   T   Q   S   P   S   S   L   S   A   S   V   G   D

AGA GTG ACC ATA ACG TGC CGA GCT TCT CAG GAT GTG AAC ACG GCA GTG GCT TGG TAT CAG CAA AAG CCT GGG AAA GCC CCA AAG CTG CTC <1350
R   V   T   I   T   C   R   A   S   Q   D   V   N   T   A   V   A   W   Y   Q   Q   K   P   G   K   A   P   K   L   L

ATC TAC TCC GCA TCC TTC CTG TAT AGC GGA GTT CCA TCT AGG TTC TCA GGC TCT AGG TCT GGG ACC GAC TTC ACG CTG ACG ATC TCC TCC <1440
I   Y   S   A   S   F   L   Y   S   G   V   P   S   R   F   S   G   S   R   S   G   T   D   F   T   L   T   I   S   S

CTG CAA CCT GAG GAC TTC GCC ACG TAC TAC TGC CAG CAG CAC TAC ACG ACT CCT CCA ACC TTC GGT CAG GGA ACG AAG GTC GAG ATC AAG <1530
L   Q   P   E   D   F   A   T   Y   Y   C   Q   Q   H   Y   T   T   P   P   T   F   G   Q   G   T   K   V   E   I   K
```

```
    NotI        >His-tag
    |           |
CGT GCG GCC GCC CAC CAT CAT CAC CAT CAC TAA
R   A   A   A   H   H   H   H   H   H   *
```

6.6 scTRAIL (pIRESpuro)

```
>VH leader                                                                                  >Flag-tag                    >linker
|                                                                                          |                            |
ATG GAC TGG ACC TGG CGC GTG TTT TGC CTG CTC GCC GTG GCT CCT GGG GCC CAC AGC CTC GAC GAT TAC AAA GAC GAT GAC GAT AAA GAA <90
M   D   W   T   W   R   V   F   C   L   L   A   V   A   P   G   A   H   S   L   D   D   Y   K   D   D   D   D   K   E

            >TRAIL 1
            |
TTC GGC GGA GGC CCC CAG AGA GTC GCC GCC CAC ATC ACC GGC ACC CGG GGC AGA AGC AAC ACC CTG AGC AGC CCC AAC AGC AAG AAC GAG <180
F   G   G   G   P   Q   R   V   A   A   H   I   T   G   T   R   G   R   S   N   T   L   S   S   P   N   S   K   N   E

AAG GCC CTG GGC CGG AAG ATC AAC AGC TGG GAG AGC AGC AGA AGC GGC CAC AGC TTT CTG AGC AAC CTG CAC CTG CGG AAC GGC GAG CTG <270
K   A   L   G   R   K   I   N   S   W   E   S   S   R   S   G   H   S   F   L   S   N   L   H   L   R   N   G   E   L

GTC ATC CAC GAG AAG GGC TTC TAC TAC ATC TAC AGC CAG ACC TAC TTC AGA TTC CAA GAA GAG ATC AAA GAG AAC ACC AAG AAC GAC AAG <360
V   I   H   E   K   G   F   Y   Y   I   Y   S   Q   T   Y   F   R   F   Q   E   E   I   K   E   N   T   K   N   D   K

CAG ATG GTG CAG TAC ATC TAC AAG TAC ACC AGC TAC CCC GAC CCC ATC CTG CTG ATG AAG TCC GCC CGG AAC AGC TGC TGG TCC AAG GAC <450
Q   M   V   Q   Y   I   Y   K   Y   T   S   Y   P   D   P   I   L   L   M   K   S   A   R   N   S   C   W   S   K   D

GCC GAG TAC GGC CTG TAC AGC ATC TAC CAG GGC GGC ATC TTC GAG CTG AAA GAG AAC GAC CGG ATC TTC GTG AGC GTG ACC AAC GAG CAC <540
A   E   Y   G   L   Y   S   I   Y   Q   G   G   I   F   E   L   K   E   N   D   R   I   F   V   S   V   T   N   E   H

                                                                  >G  >TRAIL 2
                                                                  |   |
CTG ATC GAC ATG GAC CAC GAG GCC AGC TTT TTC GGC GCA TTC CTG GTC GGC GGC GGA CCT CAG CGG GTG GCC GCC CAT ATT ACA GGC ACA <630
L   I   D   M   D   H   E   A   S   F   F   G   A   F   L   V   G   G   G   P   Q   R   V   A   A   H   I   T   G   T

AGA GGC CGG TCC AAC ACC CTG TCC TCC CCC AAC TCT AAG AAT GAA AAG GCC CTC GGG AGA AAG ATC AAC TCC TGG GAG TCC AGC CGC TCC <720
R   G   R   S   N   T   L   S   S   P   N   S   K   N   E   K   A   L   G   R   K   I   N   S   W   E   S   S   R   S

GGC CAC TCC TTT CTG TCC AAT CTG CAC CTG AGA AAT GGG GAG CTG GTC ATT CAC GAA AAG GGG TTT TAC TAT ATC TAC TCT CAG ACA TAC <810
G   H   S   F   L   S   N   L   H   L   R   N   G   E   L   V   I   H   E   K   G   F   Y   Y   I   Y   S   Q   T   Y

TTT AGG TTT CAG GAA GAA ATT AAA GAA AAT ACA AAG AAT GAT AAA CAG ATG GTC CAG TAT ATC TAT AAA TAC ACT TCC TAC CCT GAT CCT <900
F   R   F   Q   E   E   I   K   E   N   T   K   N   D   K   Q   M   V   Q   Y   I   Y   K   Y   T   S   Y   P   D   P

ATT CTG CTG ATG AAA AGC GCC AGA AAC AGC TGT TGG AGC AAG GAT GCC GAA TAT GGG CTC TAC TCT ATC TAC CAG GGG GGG ATT TTT GAA <990
I   L   L   M   K   S   A   R   N   S   C   W   S   K   D   A   E   Y   G   L   Y   S   I   Y   Q   G   G   I   F   E

CTT AAG GAG AAT GAC AGA ATC TTT GTG TCT GTG ACA AAT GAG CAT CTG ATT GAT ATG GAT CAC GAA GCC TCA TTC TTT GGA GCC TTT CTT <1080
L   K   E   N   D   R   I   F   V   S   V   T   N   E   H   L   I   D   M   D   H   E   A   S   F   F   G   A   F   L

        >G  >TRAIL 3
        |   |
GTG GGA GGG GGC CCA CAG AGG GTC GCC GCT CAC ATT ACA GGG ACC AGG GGC CGC AGC AAT ACC CTG TCC AGC CCG AAC TCC AAA AAT GAG <1170
V   G   G   G   P   Q   R   V   A   A   H   I   T   G   T   R   G   R   S   N   T   L   S   S   P   N   S   K   N   E

AAA GCG CTG GGG CGG AAG ATT AAT TCC TGG GAA AGC TCC AGA AGC GGG CAC TCC TTC CTC AGC AAT CTG CAT CTG CGC AAC GGG GAA CTC <1260
K   A   L   G   R   K   I   N   S   W   E   S   S   R   S   G   H   S   F   L   S   N   L   H   L   R   N   G   E   L

GTG ATT CAT GAG AAG GGA TTC TAT TAT ATC TAT TCC CAG ACA TAC TTC CGC TTC CAA GAG GAA ATT AAA GAG AAC ACT AAA AAC GAT AAA <1350
V   I   H   E   K   G   F   Y   Y   I   Y   S   Q   T   Y   F   R   F   Q   E   E   I   K   E   N   T   K   N   D   K

CAA ATG GTT CAA TAC ATC TAC AAA TAT ACC TCT TAC CCA GAT CCC ATC CTC CTC ATG AAG AGT GCC AGA AAC TCC TGC TGG TCT AAG GAT <1440
Q   M   V   Q   Y   I   Y   K   Y   T   S   Y   P   D   P   I   L   L   M   K   S   A   R   N   S   C   W   S   K   D

GCG GAA TAC GGA TTG TAC TCC ATC TAT CAA GGG GGA ATC TTT GAG TTG AAA GAA AAT GAT CGC ATT TTC GTG TCC GTC ACG AAT GAG CAC <1530
A   E   Y   G   L   Y   S   I   Y   Q   G   G   I   F   E   L   K   E   N   D   R   I   F   V   S   V   T   N   E   H

CTC ATA GAC ATG GAT CAT GAA GCG AGT TTC TTC GGG GCT TTC CTC GTG GGT TGA
L   I   D   M   D   H   E   A   S   F   F   G   A   F   L   V   G   *
```

6.7 EHD2-scTRAIL (pSecTagFLAG)

```
>Igk leader                                                                                 >FLAG-tag                    >linker
|                                                                                          |                            |
ATG GAG ACA GAC ACA CTC CTG CTA TGG GTA CTG CTG CTC TGG GTT CCA GGT TCC ACC GGT GAC TAC AAA GAC GAT GAC GAT AAA GCG GCC <90
M   E   T   D   T   L   L   L   W   V   L   L   L   W   V   P   G   S   T   G   D   Y   K   D   D   D   D   K   A   A

                    >EHD2
                    |
GCC GGG GGA AGC GGC GGT GAT TTC ACC CCC CCC ACA GTG AAG ATC CTC CAG AGC AGC TGT GAC GGC GGA GGC CAC TTC CCA CCT ACC ATC <180
A   G   G   S   G   G   D   F   T   P   P   T   V   K   I   L   Q   S   S   C   D   G   G   G   H   F   P   P   T   I

CAG CTG CTG TGT CTG GTG TCC GGC TAC ACC CCC GGC ACC ATC AAC ATC ACC TGG CTG GAA GAT GGA CAA GTG ATG GAC GTG GAC CTG AGC <270
Q   L   L   C   L   V   S   G   Y   T   P   G   T   I   N   I   T   W   L   E   D   G   Q   V   M   D   V   D   L   S

ACC GCC AGC ACC ACA CAG GAA GGC GAG CTG GCC TCT ACC CAG AGC GAG CTG ACA CTG AGC CAG AAG CAC TGG CTG AGC GAC CGG ACC TAC <360
T   A   S   T   T   Q   E   G   E   L   A   S   T   Q   S   E   L   T   L   S   Q   K   H   W   L   S   D   R   T   Y

                                                                                        >linker
                                                                                        |
ACC TGT CAA GTG ACC TAC CAG GGC CAC ACC TTC GAG GAC AGC ACC AAG AAG TGC GCC GAC AGC AAC GGA GGT TCA GGG GGC GCC TCG AGC <450
T   C   Q   V   T   Y   Q   G   H   T   F   E   D   S   T   K   K   C   A   D   S   N   G   G   S   G   G   A   S   S

        >TRAIL 1
        |
GGC GGC GGC CCC CAG AGA GTC GCC GCC CAC ATC ACC GGC ACC CGG GGC AGA AGC AAC ACC CTG AGC AGC CCC AAC AGC AAG AAC GAG AAG <540
G   G   G   P   Q   R   V   A   A   H   I   T   G   T   R   G   R   S   N   T   L   S   S   P   N   S   K   N   E   K
```

```
GCC CTG GGC CGG AAG ATC AAC AGC TGG GAG AGC AGC AGA AGC GGC CAC AGC TTT CTG AGC AAC CTG CAC CTG CGG AAC GGC GAG CTG GTC <630
A   L   G   R   K   I   N   S   W   E   S   S   R   S   G   H   S   F   L   S   N   L   H   L   R   N   G   E   L   V

ATC CAC GAG AAG GGC TTC TAC TAC ATC TAC AGC CAG ACC TAC TTC AGA TTC CAA GAA GAG ATC AAA GAG AAC ACC AAG AAC GAC AAG CAG <720
I   H   E   K   G   F   Y   Y   I   Y   S   Q   T   Y   F   R   F   Q   E   E   I   K   E   N   T   K   N   D   K   Q

ATG GTG CAG TAC ATC TAC AAG TAC ACC AGC TAC CCC GAC CCC ATC CTG CTG ATG AAG TCC GCC CGG AAC AGC TGC TGG TCC AAG GAC GCC <810
M   V   Q   Y   I   Y   K   Y   T   S   Y   P   D   P   I   L   L   M   K   S   A   R   N   S   C   W   S   K   D   A

GAG TAC GGC CTG TAC AGC ATC TAC CAG GGC GGC ATC TTC GAG CTG AAA GAG AAC GAC CGG ATC TTC GTG AGC GTG ACC AAC GAG CAC CTG <900
E   Y   G   L   Y   S   I   Y   Q   G   G   I   F   E   L   K   E   N   D   R   I   F   V   S   V   T   N   E   H   L

                                                                  >G  >TRAIL 2
                                                                  |   |
ATC GAC ATG GAC CAC GAG GCC AGC TTT TTC GGC GCA TTC CTG GTC GGC GGC GGA CCT CAG CGG GTG GCC GCC CAT ATT ACA GGC ACA AGA <990
I   D   M   D   H   E   A   S   F   F   G   A   F   L   V   G   G   G   P   Q   R   V   A   A   H   I   T   G   T   R

GGC CGG TCC AAC ACC CTG TCC TCC CCC AAC TCT AAG AAT GAA AAG GCC CTC GGG AGA AAG ATC AAC TCC TGG GAG TCC AGC CGC TCC GGC <1080
G   R   S   N   T   L   S   S   P   N   S   K   N   E   K   A   L   G   R   K   I   N   S   W   E   S   S   R   S   G

CAC TCC TTT CTG TCC AAT CTG CAC CTG AGA AAT GGG GAG CTG GTC ATT CAC GAA AAG GGG TTT TAC TAT ATC TAC TCT CAG ACA TAC TTT <1170
H   S   F   L   S   N   L   H   L   R   N   G   E   L   V   I   H   E   K   G   F   Y   Y   I   Y   S   Q   T   Y   F

AGG TTT CAG GAA GAA ATT AAA GAA AAT ACA AAG AAT GAT AAA CAG ATG GTC CAG TAT ATC TAT AAA TAC ACT TCC TAC CCT GAT CCT ATT <1260
R   F   Q   E   E   I   K   E   N   T   K   N   D   K   Q   M   V   Q   Y   I   Y   K   Y   T   S   Y   P   D   P   I

CTG CTG ATG AAA AGC GCC AGA AAC AGC TGT TGG AGC AAG GAT GCC GAA TAT GGG CTC TAC TCT ATC TAC CAG GGG GGG ATT TTT GAA CTT <1350
L   L   M   K   S   A   R   N   S   C   W   S   K   D   A   E   Y   G   L   Y   S   I   Y   Q   G   G   I   F   E   L

AAG GAG AAT GAC AGA ATC TTT GTG TCT GTG ACA AAT GAG CAT CTG ATT GAT ATG GAT CAC GAA GCC TCA TTC TTT GGA GCC TTT CTT GTG <1440
K   E   N   D   R   I   F   V   S   V   T   N   E   H   L   I   D   M   D   H   E   A   S   F   F   G   A   F   L   V

    >G  >TRAIL 3
    |   |
GGA GGG GGC CCA CAG AGG GTC GCC GCT CAC ATT ACA GGG ACC AGG GGC CGC AGC AAT ACC CTG TCC AGC CCG AAC TCC AAA AAT GAG AAA <1530
G   G   G   P   Q   R   V   A   A   H   I   T   G   T   R   G   R   S   N   T   L   S   S   P   N   S   K   N   E   K

GCG CTG GGG CGG AAG ATT AAT TCC TGG GAA AGC TCC AGA AGC GGG CAC TCC TTC CTC AGC AAT CTG CAT CTG CGC AAC GGG GAA CTC GTG <1620
A   L   G   R   K   I   N   S   W   E   S   S   R   S   G   H   S   F   L   S   N   L   H   L   R   N   G   E   L   V

ATT CAT GAG AAG GGA TTC TAT TAT ATC TAT TCC CAG ACA TAC TTC CGC TTC CAA GAG GAA ATT AAA GAG AAC ACT AAA AAC GAT AAA CAA <1710
I   H   E   K   G   F   Y   Y   I   Y   S   Q   T   Y   F   R   F   Q   E   E   I   K   E   N   T   K   N   D   K   Q

ATG GTT CAA TAC ATC TAC AAA TAT ACC TCT TAC CCA GAT CCC ATC CTC CTC ATG AAG AGT GCC AGA AAC TCC TGC TGG TCT AAG GAT GCG <1800
M   V   Q   Y   I   Y   K   Y   T   S   Y   P   D   P   I   L   L   M   K   S   A   R   N   S   C   W   S   K   D   A

GAA TAC GGA TTG TAC TCC ATC TAT CAA GGG GGA ATC TTT GAG TTG AAA GAA AAT GAT CGC ATT TTC GTG TCC GTC ACG AAT GAG CAC CTC <1890
E   Y   G   L   Y   S   I   Y   Q   G   G   I   F   E   L   K   E   N   D   R   I   F   V   S   V   T   N   E   H   L

ATA GAC ATG GAT CAT GAA GCG AGT TTC TTC GGG GCT TTC CTC GTG GGT TGA
I   D   M   D   H   E   A   S   F   F   G   A   F   L   V   G   *
```

6.8 Fc-scTRAIL (pSecTagFLAG)

```
>Igk leader                                                                                                 >FLAG-tag                       >linker
|                                                                                                           |                               |
ATG GAG ACA GAC ACA CTC CTG CTA TGG GTA CTG CTG CTC TGG GTT CCA GGT TCC ACC GGT GAC TAC AAA GAC GAT GAC GAT AAA GGC GGT <90
M   E   T   D   T   L   L   L   W   V   L   L   L   W   V   P   G   S   T   G   D   Y   K   D   D   D   D   K   G   G

            >hinge                                          >CH2
            |                                               |
GGC GGA TCA GGT ACC GAC AAA ACT CAC ACA TGC CCA CCG TGC CCA GCA CCT GAA CTC CTG GGG GGA CCG TCA GTC TTC CTC TTC CCC CCA <180
G   G   S   G   T   D   K   T   H   T   C   P   P   C   P   A   P   E   L   L   G   G   P   S   V   F   L   F   P   P

AAA CCC AAG GAC ACC CTC ATG ATC TCC CGG ACC CCT GAG GTC ACA TGC GTG GTG GTG GAC GTG AGC CAC GAA GAC CCT GAG GTC AAG TTC <270
K   P   K   D   T   L   M   I   S   R   T   P   E   V   T   C   V   V   V   D   V   S   H   E   D   P   E   V   K   F

AAC TGG TAC GTG GAC GGC GTG GAG GTG CAT AAT GCC AAG ACA AAG CCG CGG GAG GAG CAG TAC AAC AGC ACG TAC CGT GTG GTC AGC GTC <360
N   W   Y   V   D   G   V   E   V   H   N   A   K   T   K   P   R   E   E   Q   Y   N   S   T   Y   R   V   V   S   V

CTC ACC GTC CTG CAC CAG GAC TGG CTG AAT GGC AAG GAG TAC AAG TGC AAG GTC TCC AAC AAA GCC CTC CCA GCC CCC ATC GAG AAA ACC <450
L   T   V   L   H   Q   D   W   L   N   G   K   E   Y   K   C   K   V   S   N   K   A   L   P   A   P   I   E   K   T

                >CH3
                |
ATC TCC AAA GCC AAA GGG CAG CCC CGA GAA CCA CAG GTG TAC ACC CTG CCC CCA TCC CGG GAT GAG CTG ACC AAG AAC CAG GTC AGC CTG <540
I   S   K   A   K   G   Q   P   R   E   P   Q   V   Y   T   L   P   P   S   R   D   E   L   T   K   N   Q   V   S   L

ACC TGC CTG GTC AAA GGC TTC TAT CCC AGC GAC ATC GCC GTG GAG TGG GAG AGC AAT GGG CAG CCG GAG AAC AAC TAC AAG ACC ACG CCT <630
T   C   L   V   K   G   F   Y   P   S   D   I   A   V   E   W   E   S   N   G   Q   P   E   N   N   Y   K   T   T   P

CCC GTG CTG GAC TCC GAC GGC TCC TTC TTC CTC TAC AGC AAG CTC ACC GTG GAC AAG AGC AGG TGG CAG CAG GGG AAC GTC TTC TCA TGC <720
P   V   L   D   S   D   G   S   F   F   L   Y   S   K   L   T   V   D   K   S   R   W   Q   Q   G   N   V   F   S   C

                                                                                        >linker
                                                                                        |
TCC GTG ATG CAT GAG GCT CTG CAC AAC CAC TAC ACG CAG AAG AGC CTC TCC CTG TCT CCG GGT CAG GGG GGA AGC GGC GGT GGC TCG AGC <810
S   V   M   H   E   A   L   H   N   H   Y   T   Q   K   S   L   S   L   S   P   G   Q   G   G   S   G   G   G   S   S

        >TRAIL 1
        |
GGC GGC GGC CCC CAG AGA GTC GCC GCC CAC ATC ACC GGC ACC CGG GGC AGA AGC AAC ACC CTG AGC AGC CCC AAC AGC AAG AAC GAG AAG <900
G   G   G   P   Q   R   V   A   A   H   I   T   G   T   R   G   R   S   N   T   L   S   S   P   N   S   K   N   E   K

GCC CTG GGC CGG AAG ATC AAC AGC TGG GAG AGC AGC AGA AGC GGC CAC AGC TTT CTG AGC AAC CTG CAC CTG CGG AAC GGC GAG CTG GTC <990
A   L   G   R   K   I   N   S   W   E   S   S   R   S   G   H   S   F   L   S   N   L   H   L   R   N   G   E   L   V

ATC CAC GAG AAG GGC TTC TAC TAC ATC TAC AGC CAG ACC TAC TTC AGA TTC CAA GAA GAG ATC AAA GAG AAC ACC AAG AAC GAC AAG CAG <1080
I   H   E   K   G   F   Y   Y   I   Y   S   Q   T   Y   F   R   F   Q   E   E   I   K   E   N   T   K   N   D   K   Q
```

```
ATG GTG CAG TAC ATC TAC AAG TAC ACC AGC TAC CCC GAC CCC ATC CTG CTG ATG AAG TCC GCC CGG AAC AGC TGC TGG TCC AAG GAC GCC <1170
M   V   Q   Y   I   Y   K   Y   T   S   Y   P   D   P   I   L   L   M   K   S   A   R   N   S   C   W   S   K   D   A

GAG TAC GGC CTG TAC AGC ATC TAC CAG GGC GGC ATC TTC GAG CTG AAA GAG AAC GAC CGG ATC TTC GTG AGC GTG ACC AAC GAG CAC CTG <1260
E   Y   G   L   Y   S   I   Y   Q   G   G   I   F   E   L   K   E   N   D   R   I   F   V   S   V   T   N   E   H   L

                                                                  >G  >TRAIL 2
                                                                  |   |
ATC GAC ATG GAC CAC GAG GCC AGC TTT TTC GGC GCA TTC CTG GTC GGC GGC GGA CCT CAG CGG GTG GCC GCC CAT ATT ACA GGC ACA AGA <1350
I   D   M   D   H   E   A   S   F   F   G   A   F   L   V   G   G   G   P   Q   R   V   A   A   H   I   T   G   T   R

GGC CGG TCC AAC ACC CTG TCC TCC CCC AAC TCT AAG AAT GAA AAG GCC CTC GGG AGA AAG ATC AAC TCC TGG GAG TCC AGC CGC TCC GGC <1440
G   R   S   N   T   L   S   S   P   N   S   K   N   E   K   A   L   G   R   K   I   N   S   W   E   S   S   R   S   G

CAC TCC TTT CTG TCC AAT CTG CAC CTG AGA AAT GGG GAG CTG GTC ATT CAC GAA AAG GGG TTT TAC TAT ATC TAC TCT CAG ACA TAC TTT <1530
H   S   F   L   S   N   L   H   L   R   N   G   E   L   V   I   H   E   K   G   F   Y   Y   I   Y   S   Q   T   Y   F

AGG TTT CAG GAA GAA ATT AAA GAA AAT ACA AAG AAT GAT AAA CAG ATG GTC CAG TAT ATC TAT AAA TAC ACT TCC TAC CCT GAT CCT ATT <1620
R   F   Q   E   E   I   K   E   N   T   K   N   D   K   Q   M   V   Q   Y   I   Y   K   Y   T   S   Y   P   D   P   I

CTG CTG ATG AAA AGC GCC AGA AAC AGC TGT TGG AGC AAG GAT GCC GAA TAT GGG CTC TAC TCT ATC TAC CAG GGG GGG ATT TTT GAA CTT <1710
L   L   M   K   S   A   R   N   S   C   W   S   K   D   A   E   Y   G   L   Y   S   I   Y   Q   G   G   I   F   E   L

AAG GAG AAT GAC AGA ATC TTT GTG TCT GTG ACA AAT GAG CAT CTG ATT GAT ATG GAT CAC GAA GCC TCA TTC TTT GGA GCC TTT CTT GTG <1800
K   E   N   D   R   I   F   V   S   V   T   N   E   H   L   I   D   M   D   H   E   A   S   F   F   G   A   F   L   V

    >G  >TRAIL 3
    |   |
GGA GGG GGC CCA CAG AGG GTC GCC GCT CAC ATT ACA GGG ACC AGG GGC CGC AGC AAT ACC CTG TCC AGC CCG AAC TCC AAA AAT GAG AAA <1890
G   G   G   P   Q   R   V   A   A   H   I   T   G   T   R   G   R   S   N   T   L   S   S   P   N   S   K   N   E   K

GCG CTG GGG CGG AAG ATT AAT TCC TGG GAA AGC TCC AGA AGC GGG CAC TCC TTC CTC AGC AAT CTG CAT CTG CGC AAC GGG GAA CTC GTG <1980
A   L   G   R   K   I   N   S   W   E   S   S   R   S   G   H   S   F   L   S   N   L   H   L   R   N   G   E   L   V

ATT CAT GAG AAG GGA TTC TAT TAT ATC TAT TCC CAG ACA TAC TTC CGC TTC CAA GAG GAA ATT AAA GAG AAC ACT AAA AAC GAT AAA CAA <2070
I   H   E   K   G   F   Y   Y   I   Y   S   Q   T   Y   F   R   F   Q   E   E   I   K   E   N   T   K   N   D   K   Q

ATG GTT CAA TAC ATC TAC AAA TAT ACC TCT TAC CCA GAT CCC ATC CTC CTC ATG AAG AGT GCC AGA AAC TCC TGC TGG TCT AAG GAT GCG <2160
M   V   Q   Y   I   Y   K   Y   T   S   Y   P   D   P   I   L   L   M   K   S   A   R   N   S   C   W   S   K   D   A

GAA TAC GGA TTG TAC TCC ATC TAT CAA GGG GGA ATC TTT GAG TTG AAA GAA AAT GAT CGC ATT TTC GTG TCC GTC ACG AAT GAG CAC CTC <2250
E   Y   G   L   Y   S   I   Y   Q   G   G   I   F   E   L   K   E   N   D   R   I   F   V   S   V   T   N   E   H   L

ATA GAC ATG GAT CAT GAA GCG AGT TTC TTC GGG GCT TTC CTC GTG GGT TGA
  I   D   M   D   H   E   A   S   F   F   G   A   F   L   V   G   *
```

6.9 (ds)Db-scTRAIL (pSecTagFLAG)

(Ds)Db-scTRAIL constructs were generated by insertion of the respective (ds)Db sequences (see 6.2) as KpnI-NotI fragments into the sequence represented below (after KpnI-NotI digestion).

```
>Igk leader                                                                                  >FLAG-tag                    >linker
|                                                                                            |                            |
ATG GAG ACA GAC ACA CTC CTG CTA TGG GTA CTG CTG CTC TGG GTT CCA GGT TCC Acc ggT GAC TAC AAA GAC GAT GAC GAT AAA GGC GGT <90
M   E   T   D   T   L   L   L   W   V   L   L   L   W   V   P   G   S   T   G   D   Y   K   D   D   D   D   K   G   G

            KpnI    NotI>linker                    >TRAIL 1
            |       |                              |
GGC GGA TCA GGT ACC GCg gcc GCC GGG GGA AGC GGC GGC GGC CCC CAG AGA GTC GCC GCC CAC ATC ACC GGC ACC CGG GGC AGA AGC AAC <180
G   G   S   G   T   A   A   A   G   G   S   G   G   G   P   Q   R   V   A   A   H   I   T   G   T   R   G   R   S   N

ACC CTG AGC AGC CCC AAC AGC AAG AAC GAG AAG GCC CTG GGC CGG AAG ATC AAC AGC TGG GAG AGC AGC AGA AGC GGC CAC AGC TTT CTG <270
T   L   S   S   P   N   S   K   N   E   K   A   L   G   R   K   I   N   S   W   E   S   S   R   S   G   H   S   F   L

AGC AAC CTG CAC CTG CGG AAC GGC GAG CTG GTC ATC CAC GAG AAG GGC TTC TAC TAC ATC TAC AGC CAG ACC TAC TTC AGA TTC CAA GAA <360
S   N   L   H   L   R   N   G   E   L   V   I   H   E   K   G   F   Y   Y   I   Y   S   Q   T   Y   F   R   F   Q   E

GAG ATC AAA GAG AAC ACC AAG AAC GAC AAG CAG ATG GTG CAG TAC ATC TAC AAG TAC ACC AGC TAC CCC GAC CCC ATC CTG CTG ATG AAG <450
E   I   K   E   N   T   K   N   D   K   Q   M   V   Q   Y   I   Y   K   Y   T   S   Y   P   D   P   I   L   L   M   K

TCC GCC CGG AAC AGC TGC TGG TCC AAG GAC GCC GAG TAC GGC CTG TAC AGC ATC TAC CAG GGC GGC ATC TTC GAG CTG AAA GAG AAC GAC <540
S   A   R   N   S   C   W   S   K   D   A   E   Y   G   L   Y   S   I   Y   Q   G   G   I   F   E   L   K   E   N   D

                                                                                                                  >G  >TRAIL 2
                                                                                                                  |   |
CGG ATC TTC GTG AGC GTG ACC AAC GAG CAC CTG ATC GAC ATG GAC CAC GAG GCC AGC TTT TTC GGC GCA TTC CTG GTC GGC GGC GGA CCT <630
R   I   F   V   S   V   T   N   E   H   L   I   D   M   D   H   E   A   S   F   F   G   A   F   L   V   G   G   G   P

CAG CGG GTG GCC GCC CAT ATT ACA GGC ACA AGA GGC CGG TCC AAC ACC CTG TCC TCC CCC AAC TCT AAG AAT GAA AAG GCC CTC GGG AGA <720
Q   R   V   A   A   H   I   T   G   T   R   G   R   S   N   T   L   S   S   P   N   S   K   N   E   K   A   L   G   R

AAG ATC AAC TCC TGG GAG TCC AGC CGC TCC GGC CAC TCC TTT CTG TCC AAT CTG CAC CTG AGA AAT GGG GAG CTG GTC ATT CAC GAA AAG <810
K   I   N   S   W   E   S   S   R   S   G   H   S   F   L   S   N   L   H   L   R   N   G   E   L   V   I   H   E   K

GGG TTT TAC TAT ATC TAC TCT CAG ACA TAC TTT AGG TTT CAG GAA GAA ATT AAA GAA AAT ACA AAG AAT GAT AAA CAG ATG GTC CAG TAT <900
G   F   Y   Y   I   Y   S   Q   T   Y   F   R   F   Q   E   E   I   K   E   N   T   K   N   D   K   Q   M   V   Q   Y

ATC TAT AAA TAC ACT TCC TAC CCT GAT CCT ATT CTG CTG ATG AAA AGC GCC AGA AAC AGC TGT TGG AGC AAG GAT GCC GAA TAT GGG CTC <990
I   Y   K   Y   T   S   Y   P   D   P   I   L   L   M   K   S   A   R   N   S   C   W   S   K   D   A   E   Y   G   L

TAC TCT ATC TAC CAG GGG GGG ATT TTT GAA CTT AAG GAG AAT GAC AGA ATC TTT GTG TCT GTG ACA AAT GAG CAT CTG ATT GAT ATG GAT <1080
Y   S   I   Y   Q   G   G   I   F   E   L   K   E   N   D   R   I   F   V   S   V   T   N   E   H   L   I   D   M   D
```

```
                                                >G  >TRAIL 3
                                                |   |
CAC GAA GCC TCA TTC TTT GGA GCC TTT CTT GTG GGA GGG GGC CCA CAG AGG GTC GCC GCT CAC ATT ACA GGG ACC AGG GGC CGC AGC AAT <1170
H   E   A   S   F   F   G   A   F   L   V   G   G   G   P   Q   R   V   A   A   H   I   T   G   T   R   G   R   S   N

ACC CTG TCC AGC CCG AAC TCC AAA AAT GAG AAA GCG CTG GGG CGG AAG ATT AAT TCC TGG GAA AGC TCC AGA AGC GGG CAC TCC TTC CTC <1260
T   L   S   S   P   N   S   K   N   E   K   A   L   G   R   K   I   N   S   W   E   S   S   R   S   G   H   S   F   L

AGC AAT CTG CAT CTG CGC AAC GGG GAA CTC GTG ATT CAT GAG AAG GGA TTC TAT TAT ATC TAT TCC CAG ACA TAC TTC CGC TTC CAA GAG <1350
S   N   L   H   L   R   N   G   E   L   V   I   H   E   K   G   F   Y   Y   I   Y   S   Q   T   Y   F   R   F   Q   E

GAA ATT AAA GAG AAC ACT AAA AAC GAT AAA CAA ATG GTT CAA TAC ATC TAC AAA TAT ACC TCT TAC CCA GAT CCC ATC CTC CTC ATG AAG <1440
E   I   K   E   N   T   K   N   D   K   Q   M   V   Q   Y   I   Y   K   Y   T   S   Y   P   D   P   I   L   L   M   K

AGT GCC AGA AAC TCC TGC TGG TCT AAG GAT GCG GAA TAC GGA TTG TAC TCC ATC TAT CAA GGG GGA ATC TTT GAG TTG AAA GAA AAT GAT <1530
S   A   R   N   S   C   W   S   K   D   A   E   Y   G   L   Y   S   I   Y   Q   G   G   I   F   E   L   K   E   N   D

CGC ATT TTC GTG TCC GTC ACG AAT GAG CAC CTC ATA GAC ATG GAT CAT GAA GCG AGT TTC TTC GGG GCT TTC CTC GTG GGT TGA
R   I   F   V   S   V   T   N   E   H   L   I   D   M   D   H   E   A   S   F   F   G   A   F   L   V   G   *
```

6.10 scFv-EHD2-scTRAIL (pSecTagFLAG)

ScFv-EHD2-scTRAIL constructs were generated by insertion of the respective scFv sequences (see 6.1) as KpnI-NotI fragments into the sequence represented below (after KpnI-NotI digestion).

```
>Igk leader                                                                                 AgeI    >FLAG-tag                    >linker
|                                                                                           |       |                            |
ATG GAG ACA GAC ACA CTC CTG CTA TGG GTA CTG CTG CTC TGG GTT CCA GGT TCC ACC GGT GAC TAC AAA GAC GAT GAC GAT AAA GGC GGT <90
M   E   T   D   T   L   L   L   W   V   L   L   L   W   V   P   G   S   T   G   D   Y   K   D   D   D   D   K   G   G

            KpnI    NotI>linker                     >EHD2
            |       |                               |
GGC GGA TCA GGT ACC GCG GCC GCC GGG GGA AGC GGC GGT GAT TTC ACC CCC CCC ACA GTG AAG ATC CTC CAG AGC AGC TGT GAC GGC GGA <180
G   G   S   G   T   A   A   A   G   G   S   G   G   D   F   T   P   P   T   V   K   I   L   Q   S   S   C   D   G   G

GGC CAC TTC CCA CCT ACC ATC CAG CTG CTG TGT CTG GTG TCC GGC TAC ACC CCC GGC ACC ATC AAC ATC ACC TGG CTG GAA GAT GGA CAA <270
G   H   F   P   P   T   I   Q   L   L   C   L   V   S   G   Y   T   P   G   T   I   N   I   T   W   L   E   D   G   Q

GTG ATG GAC GTG GAC CTG AGC ACC GCC AGC ACC ACA CAG GAA GGC GAG CTG GCC TCT ACC CAG AGC GAG CTG ACA CTG AGC CAG AAG CAC <360
V   M   D   V   D   L   S   T   A   S   T   T   Q   E   G   E   L   A   S   T   Q   S   E   L   T   L   S   Q   K   H

                                                                                                                        >linker
                                                                                                                        |
TGG CTG AGC GAC CGG ACC TAC ACC TGT CAA GTG ACC TAC CAG GGC CAC ACC TTC GAG GAC AGC ACC AAG AAG TGC GCC GAC AGC AAC GGA <450
W   L   S   D   R   T   Y   T   C   Q   V   T   Y   Q   G   H   T   F   E   D   S   T   K   K   C   A   D   S   N   G

                                    >TRAIL 1
                                    |
GGT TCA GGG GGC GCC TCG AGC GGC GGC GGC CCC CAG AGA GTC GCC GCC CAC ATC ACC GGC ACC CGG GGC AGA AGC AAC ACC CTG AGC AGC <540
G   S   G   G   A   S   S   G   G   G   P   Q   R   V   A   A   H   I   T   G   T   R   G   R   S   N   T   L   S   S

CCC AAC AGC AAG AAC GAG AAG GCC CTG GGC CGG AAG ATC AAC AGC TGG GAG AGC AGC AGA AGC GGC CAC AGC TTT CTG AGC AAC CTG CAC <630
P   N   S   K   N   E   K   A   L   G   R   K   I   N   S   W   E   S   S   R   S   G   H   S   F   L   S   N   L   H

CTG CGG AAC GGC GAG CTG GTC ATC CAC GAG AAG GGC TTC TAC TAC ATC TAC AGC CAG ACC TAC TTC AGA TTC CAA GAA GAG ATC AAA GAG <720
L   R   N   G   E   L   V   I   H   E   K   G   F   Y   Y   I   Y   S   Q   T   Y   F   R   F   Q   E   E   I   K   E

AAC ACC AAG AAC GAC AAG CAG ATG GTG CAG TAC ATC TAC AAG TAC ACC AGC TAC CCC GAC CCC ATC CTG CTG ATG AAG TCC GCC CGG AAC <810
N   T   K   N   D   K   Q   M   V   Q   Y   I   Y   K   Y   T   S   Y   P   D   P   I   L   L   M   K   S   A   R   N

AGC TGC TGG TCC AAG GAC GCC GAG TAC GGC CTG TAC AGC ATC TAC CAG GGC GGC ATC TTC GAG CTG AAA GAG AAC GAC CGG ATC TTC GTG <900
S   C   W   S   K   D   A   E   Y   G   L   Y   S   I   Y   Q   G   G   I   F   E   L   K   E   N   D   R   I   F   V

                                                                                        >G   >TRAIL 2
                                                                                        |    |
AGC GTG ACC AAC GAG CAC CTG ATC GAC ATG GAC CAC GAG GCC AGC TTT TTC GGC GCA TTC CTG GTC GGC GGC GGA CCT CAG CGG GTG GCC <990
S   V   T   N   E   H   L   I   D   M   D   H   E   A   S   F   F   G   A   F   L   V   G   G   G   P   Q   R   V   A

GCC CAT ATT ACA GGC ACA AGA GGC CGG TCC AAC ACC CTG TCC TCC CCC AAC TCT AAG AAT GAA AAG GCC CTC GGG AGA AAG ATC AAC TCC <1080
A   H   I   T   G   T   R   G   R   S   N   T   L   S   S   P   N   S   K   N   E   K   A   L   G   R   K   I   N   S

TGG GAG TCC AGC CGC TCC GGC CAC TCC TTT CTG TCC AAT CTG CAC CTG AGA AAT GGG GAG CTG GTC ATT CAC GAA AAG GGG TTT TAC TAT <1170
W   E   S   S   R   S   G   H   S   F   L   S   N   L   H   L   R   N   G   E   L   V   I   H   E   K   G   F   Y   Y

ATC TAC TCT CAG ACA TAC TTT AGG TTT CAG GAA GAA ATT AAA GAA AAT ACA AAG AAT GAT AAA CAG ATG GTC CAG TAT ATC TAT AAA TAC <1260
I   Y   S   Q   T   Y   F   R   F   Q   E   E   I   K   E   N   T   K   N   D   K   Q   M   V   Q   Y   I   Y   K   Y

ACT TCC TAC CCT GAT CCT ATT CTG CTG ATG AAA AGC GCC AGA AAC AGC TGT TGG AGC AAG GAT GCC GAA TAT GGG CTC TAC TCT ATC TAC <1350
T   S   Y   P   D   P   I   L   L   M   K   S   A   R   N   S   C   W   S   K   D   A   E   Y   G   L   Y   S   I   Y

CAG GGG GGG ATT TTT GAA CTT AAG GAG AAT GAC AGA ATC TTT GTG TCT GTG ACA AAT GAG CAT CTG ATT GAT ATG GAT CAC GAA GCC TCA <1440
Q   G   G   G   I   F   E   L   K   E   N   D   R   I   F   V   S   V   T   N   E   H   L   I   D   M   D   H   E   A   S

                                >G  >TRAIL 3
                                |   |
TTC TTT GGA GCC TTT CTT GTG GGA GGG GGC CCA CAG AGG GTC GCC GCT CAC ATT ACA GGG ACC AGG GGC CGC AGC AAT ACC CTG TCC AGC <1530
F   F   G   A   F   L   V   G   G   G   P   Q   R   V   A   A   H   I   T   G   T   R   G   R   S   N   T   L   S   S

CCG AAC TCC AAA AAT GAG AAA GCG CTG GGG CGG AAG ATT AAT TCC TGG GAA AGC TCC AGA AGC GGG CAC TCC TTC CTC AGC AAT CTG CAT <1620
P   N   S   K   N   E   K   A   L   G   R   K   I   N   S   W   E   S   S   R   S   G   H   S   F   L   S   N   L   H

CTG CGC AAC GGG GAA CTC GTG ATT CAT GAG AAG GGA TTC TAT TAT ATC TAT TCC CAG ACA TAC TTC CGC TTC CAA GAG GAA ATT AAA GAG <1710
L   R   N   G   E   L   V   I   H   E   K   G   F   Y   Y   I   Y   S   Q   T   Y   F   R   F   Q   E   E   I   K   E
```

```
AAC ACT AAA AAC GAT AAA CAA ATG GTT CAA TAC ATC TAC AAA TAT ACC TCT TAC CCA GAT CCC ATC CTC CTC ATG AAG AGT GCC AGA AAC <1800
N   T   K   N   D   K   Q   M   V   Q   Y   I   Y   K   Y   T   S   Y   P   D   P   I   L   L   M   K   S   A   R   N

TCC TGC TGG TCT AAG GAT GCG GAA TAC GGA TTG TAC TCC ATC TAT CAA GGG GGA ATC TTT GAG TTG AAA GAA AAT GAT CGC ATT TTC GTG <1890
S   C   W   S   K   D   A   E   Y   G   L   Y   S   I   Y   Q   G   G   I   F   E   L   K   E   N   D   R   I   F   V

TCC GTC ACG AAT GAG CAC CTC ATA GAC ATG GAT CAT GAA GCG AGT TTC TTC GGG GCT TTC CTC GTG GGT TGA
S   V   T   N   E   H   L   I   D   M   D   H   E   A   S   F   F   G   A   F   L   V   G   *
```

6.11 scFv-Fc-scTRAIL (pSecTagFLAG)

ScFv-Fc-scTRAIL constructs were generated by insertion of the respective FLAG-scFv sequences from previously cloned pSecTagFLAG-scFv-EHD2-scTRAIL (see 6.10) as AgeI-NotI fragments into the sequence represented below (after AgeI-NotI digestion).

```
>Igk leader                                                                AgeI                NotI>linker
|                                                                          |                   |
ATG GAG ACA GAC ACA CTC CTG CTA TGG GTA CTG CTG CTC TGG GTT CCA GGT TCC ACC GGT ... ... ... GCG GCC GCA GGG GGA AGC GGC <180
M   E   T   D   T   L   L   L   W   V   L   L   L   W   V   P   G   S   T   G               A   A   A   G   G   S   G

    >hinge                                  CH2
    |                                       |
GGT GAC AAA ACT CAC ACA TGC CCA CCG TGC CCA GCA CCT GAA CTC CTG GGG GGA CCG TCA GTC TTC CTC TTC CCC CCA AAA CCC AAG GAC <270
G   D   K   T   H   T   C   P   P   C   P   A   P   E   L   L   G   G   P   S   V   F   L   F   P   P   K   P   K   D

ACC CTC ATG ATC TCC CGG ACC CCT GAG GTC ACA TGC GTG GTG GTG GAC GTG AGC CAC GAA GAC CCT GAG GTC AAG TTC AAC TGG TAC GTG <360
T   L   M   I   S   R   T   P   E   V   T   C   V   V   V   D   V   S   H   E   D   P   E   V   K   F   N   W   Y   V

GAC GGC GTG GAG GTG CAT AAT GCC AAG ACA AAG CCG CGG GAG GAG CAG TAC AAC AGC ACG TAC CGT GTG GTC AGC GTC CTC ACC GTC CTG <450
D   G   V   E   V   H   N   A   K   T   K   P   R   E   E   Q   Y   N   S   T   Y   R   V   V   S   V   L   T   V   L

CAC CAG GAC TGG CTG AAT GGC AAG GAG TAC AAG TGC AAG GTC TCC AAC AAA GCC CTC CCA GCC CCC ATC GAG AAA ACC ATC TCC AAA GCC <540
H   Q   D   W   L   N   G   K   E   Y   K   C   K   V   S   N   K   A   L   P   A   P   I   E   K   T   I   S   K   A

    >CH3
    |
AAA GGG CAG CCC CGA GAA CCA CAG GTG TAC ACC CTG CCC CCA TCC CGG GAT GAG CTG ACC AAG AAC CAG GTC AGC CTG ACC TGC CTG GTC <630
K   G   Q   P   R   E   P   Q   V   Y   T   L   P   P   S   R   D   E   L   T   K   N   Q   V   S   L   T   C   L   V

AAA GGC TTC TAT CCC AGC GAC ATC GCC GTG GAG TGG GAG AGC AAT GGG CAG CCG GAG AAC AAC TAC AAG ACC ACG CCT CCC GTG CTG GAC <720
K   G   F   Y   P   S   D   I   A   V   E   W   E   S   N   G   Q   P   E   N   N   Y   K   T   T   P   P   V   L   D

TCC GAC GGC TCC TTC TTC CTC TAC AGC AAG CTC ACC GTG GAC AAG AGC AGG TGG CAG CAG GGG AAC GTC TTC TCA TGC TCC GTG ATG CAT <810
S   D   G   S   F   F   L   Y   S   K   L   T   V   D   K   S   R   W   Q   Q   G   N   V   F   S   C   S   V   M   H

                                                                           >linker                                 >TRAIL 1
                                                                           |                                       |
GAG GCT CTG CAC AAC CAC TAC ACG CAG AAG AGC CTC TCC CTG TCT CCG GGT CAG GGG GGA AGC GGC GGT GGC TCG AGC GGC GGC GGC CCC <900
E   A   L   H   N   H   Y   T   Q   K   S   L   S   L   S   P   G   Q   G   G   S   G   G   G   S   S   G   G   G   P

CAG AGA GTC GCC GCC CAC ATC ACC GGC ACC CGG GGC AGA AGC AAC ACC CTG AGC AGC CCC AAC AGC AAG AAC GAG AAG GCC CTG GGC CGG <990
Q   R   V   A   A   H   I   T   G   T   R   G   R   S   N   T   L   S   S   P   N   S   K   N   E   K   A   L   G   R

AAG ATC AAC AGC TGG GAG AGC AGC AGA AGC GGC CAC AGC TTT CTG AGC AAC CTG CAC CTG CGG AAC GGC GAG CTG GTC ATC CAC GAG AAG <1080
K   I   N   S   W   E   S   S   R   S   G   H   S   F   L   S   N   L   H   L   R   N   G   E   L   V   I   H   E   K

GGC TTC TAC TAC ATC TAC AGC CAG ACC TAC TTC AGA TTC CAA GAA GAG ATC AAA GAG AAC ACC AAG AAC GAC AAG CAG ATG GTG CAG TAC <1170
G   F   Y   Y   I   Y   S   Q   T   Y   F   R   F   Q   E   E   I   K   E   N   T   K   N   D   K   Q   M   V   Q   Y

ATC TAC AAG TAC ACC AGC TAC CCC GAC CCC ATC CTG CTG ATG AAG TCC GCC CGG AAC AGC TGC TGG TCC AAG GAC GCC GAG TAC GGC CTG <1260
I   Y   K   Y   T   S   Y   P   D   P   I   L   L   M   K   S   A   R   N   S   C   W   S   K   D   A   E   Y   G   L

TAC AGC ATC TAC CAG GGC GGC ATC TTC GAG CTG AAA GAG AAC GAC CGG ATC TTC GTG AGC GTG ACC AAC GAG CAC CTG ATC GAC ATG GAC <1350
Y   S   I   Y   Q   G   G   I   F   E   L   K   E   N   D   R   I   F   V   S   V   T   N   E   H   L   I   D   M   D

                                            >G  >TRAIL 2
                                            |   |
CAC GAG GCC AGC TTT TTC GGC GCA TTC CTG GTC GGC GGC GGA CCT CAG CGG GTG GCC GCC CAT ATT ACA GGC ACA AGA GGC CGG TCC AAC <1440
H   E   A   S   F   F   G   A   F   L   V   G   G   G   P   Q   R   V   A   A   H   I   T   G   T   R   G   R   S   N

ACC CTG TCC TCC CCC AAC TCT AAG AAT GAA AAG GCC CTC GGG AGA AAG ATC AAC TCC TGG GAG TCC AGC CGC TCC GGC CAC TCC TTT CTG <1530
T   L   S   S   P   N   S   K   N   E   K   A   L   G   R   K   I   N   S   W   E   S   S   R   S   G   H   S   F   L

TCC AAT CTG CAC CTG AGA AAT GGG GAG CTG GTC ATT CAC GAA AAG GGG TTT TAC TAT ATC TAC TCT CAG ACA TAC TTT AGG TTT CAG GAA <1620
S   N   L   H   L   R   N   G   E   L   V   I   H   E   K   G   F   Y   Y   I   Y   S   Q   T   Y   F   R   F   Q   E

GAA ATT AAA GAA AAT ACA AAG AAT GAT AAA CAG ATG GTC CAG TAT ATC TAT AAA TAC ACT TCC TAC CCT GAT CCT ATT CTG CTG ATG AAA <1710
E   I   K   E   N   T   K   N   D   K   Q   M   V   Q   Y   I   Y   K   Y   T   S   Y   P   D   P   I   L   L   M   K

AGC GCC AGA AAC AGC TGT TGG AGC AAG GAT GCC GAA TAT GGG CTC TAC TCT ATC TAC CAG GGG GGG ATT TTT GAA CTT AAG GAG AAT GAC <1800
S   A   R   N   S   C   W   S   K   D   A   E   Y   G   L   Y   S   I   Y   Q   G   G   I   F   E   L   K   E   N   D

                                                                                                       >G  >TRAIL 3
                                                                                                       |   |
AGA ATC TTT GTG TCT GTG ACA AAT GAG CAT CTG ATT GAT ATG GAT CAC GAA GCC TCA TTC TTT GGA GCC TTT CTT GTG GGA GGG GGC CCA <1890
R   I   F   V   S   V   T   N   E   H   L   I   D   M   D   H   E   A   S   F   F   G   A   F   L   V   G   G   G   P

CAG AGG GTC GCC GCT CAC ATT ACA GGG ACC AGG GGC CGC AGC AAT ACC CTG TCC AGC CCG AAC TCC AAA AAT GAG AAA GCG CTG GGG CGG <1980
Q   R   V   A   A   H   I   T   G   T   R   G   R   S   N   T   L   S   S   P   N   S   K   N   E   K   A   L   G   R

AAG ATT AAT TCC TGG GAA AGC TCC AGA AGC GGG CAC TCC TTC CTC AGC AAT CTG CAT CTG CGC AAC GGG GAA CTC GTG ATT CAT GAG AAG <2070
K   I   N   S   W   E   S   S   R   S   G   H   S   F   L   S   N   L   H   L   R   N   G   E   L   V   I   H   E   K

GGA TTC TAT TAT ATC TAT TCC CAG ACA TAC TTC CGC TTC CAA GAG GAA ATT AAA GAG AAC ACT AAA AAC GAT AAA CAA ATG GTT CAA TAC <2160
G   F   Y   Y   I   Y   S   Q   T   Y   F   R   F   Q   E   E   I   K   E   N   T   K   N   D   K   Q   M   V   Q   Y
```

```
ATC TAC AAA TAT ACC TCT TAC CCA GAT CCC ATC CTC CTC ATG AAG AGT GCC AGA AAC TCC TGC TGG TCT AAG GAT GCG GAA TAC GGA TTG <2250
I   Y   K   Y   T   S   Y   P   D   P   I   L   L   M   K   S   A   R   N   S   C   W   S   K   D   A   E   Y   G   L

TAC TCC ATC TAT CAA GGG GGA ATC TTT GAG TTG AAA GAA AAT GAT CGC ATT TTC GTG TCC GTC ACG AAT GAG CAC CTC ATA GAC ATG GAT <2340
Y   S   I   Y   Q   G   G   I   F   E   L   K   E   N   D   R   I   F   V   S   V   T   N   E   H   L   I   D   M   D

CAT GAA GCG AGT TTC TTC GGG GCT TTC CTC GTG GGT TGA
H   E   A   S   F   F   G   A   F   L   V   G   *
```

6.12 scDb-EHD2-scTRAIL (pSecTagFLAG)

ScDb-EHD2-scTRAIL constructs were generated by insertion of the respective scDb sequences (see 6.5) as KpnI-NotI fragments into the sequence represented in 6.10 (after KpnI-NotI digestion).

List of Figures

List of Tables

Danksagung

Allen voran gilt mein Dank Prof. Dr. Roland Kontermann für die hervorragende Betreuung, die vielen Anregungen und hilfreichen Diskussionen, die Unterstützung insbesondere bei widersprüchlich erscheinenden Daten sowie das Vertrauen in meine Arbeit. Danke, dass ich in den letzten Jahren Teil deiner Gruppe sein durfte und es noch sein darf.

Herzlichen Dank an Prof. Dr. Ralf Takors für die Übernahme des Zweitgutachtens dieser Arbeit. Darüber hinaus danke ich Prof. Dr. Klaus Pfizenmaier, der wertvolle Anregungen zu dieser Arbeit geliefert hat, sowie Dr. Dafne Müller für hilfreiche Unterstützung in sowohl organisatorischen als auch wissenschaftlichen Fragen.

Weiterer Dank gilt unseren Kooperationspartnern für die inspirierende Zusammenarbeit im Rahmen des vom Bundesministerium für Bildung und Forschung finanzierten Projekts PREDICT, insbesondere Dr. Kristin Dickschen, Dr. Michael Block, Dr. Jens Schmid sowie Dr. Thomas Mürdter.

Ganz besonders danke ich meinen Kollegen und Freunden Sina Fellermeier, Dr. Felix Unverdorben, Dr. Oliver Seifert und Dr. Fabian Richter sowie allen „Kontermännern“, die wesentlich dazu beigetragen haben, die letzten Jahre zu einer ganz besonderen Zeit werden zu lassen. Liebe Sina, lieber Felix, danke für die vielen schönen Abende, die wir zu sechst außerhalb des Labors verbracht haben. Ich freue mich auf die vielen, die noch folgen werden. Liebe Sina, ich mache es mir an dieser Stelle einfach und schließe mich dir an: „von der besten Kollegin zu einer meiner wichtigsten Freundinnen.“ Mehr Worte braucht es wirklich nicht. Liebe Silvi, du hast mich am ersten Tag an dieser Uni angesprochen und seitdem nicht mehr aufgehört zu reden. Danke dafür, für deine Freundschaft und die vielen motivierenden Worte.

Zudem danke ich unseren TAs für ihre Unterstützung, insbesondere Nadine Heidel und Doris Göttsch. Vielen Dank an Alexandra Kraske und Beatrice Reiser sowie an alle Tierpflegerinnen, die im Laufe dieser Doktorarbeit für das Wohl meiner Mäuse gesorgt haben. Liebe Alex, danke für die Unterstützung im und außerhalb des Tierstalls.

An dieser Stelle möchte ich mich bei den wichtigsten Menschen bedanken, bei Harun und unseren Familien. Danke an meine Eltern. Danke für eure permanente bedingungslose Unterstützung, euer Verständnis und euren Glauben an mich. Ohne euch würde es diese Arbeit nicht geben. Danke an meine Schwester Tina, dafür ein Vorbild für mich zu sein und dafür mir die wundervollsten Patenkinder Yvonne und Ben geschenkt zu haben. Yvonne und Ben, ihr bereichert mein Leben und seid eine unglaubliche Motivation. Danke, Harun. Es gibt keine passenden Worte, die all deiner Unterstützung, deinem Verständnis, deiner Geduld, deinem Vertrauen in uns und deinem Glauben an mich gerecht werden. Çok teşekkür ederim.

Erklärung

Hiermit erkläre ich, dass die vorgelegte Dissertation und die darin gezeigten Daten von mir persönlich und ohne unrechtmäßige Hilfe angefertigt wurden. Alle genutzten Quellen sind entsprechend zitiert.

Declaration

I hereby declare that this thesis and the work presented in it are my own and have been prepared without any illegitimate help. All sources used have been quoted adequately.

Meike Hutt

Stuttgart, March 19, 2017

Conference contributions, publications, and patents

Conference contributions

02/2016 **Biologics & Biosimilars Congress, Berlin** | Poster presentation
08/2013 **International Congress of Immunology, Milan** | Poster presentation

Publications

Hutt, M., Seifert, O., Siegemund, M., Pfizenmaier, K., & Kontermann, R. E. Dimeric antibody-scTRAIL fusion proteins. In preparation.

Hutt, M., Seifert, O., Fellermeier, S., Schmitt, L. C., Siegemund, M., Pfizenmaier, K., & Kontermann, R. E. Tumor cell targeting with scFv-Fc-scTRAIL fusion proteins. In preparation.

Hutt, M., Färber-Schwarz, A., Unverdorben, F., Richter, F., & Kontermann, R. E. (2012). Plasma half-life extension of small recombinant antibodies by fusion to immunoglobulin-binding domains. *Journal of Biological Chemistry*, *287*(7), 4462–4469.

Hutt, M., Kulschewski, T., & Pleiss, J. (2012). Molecular modelling of the mass density of single proteins. *Journal of Biomolecular Structure and Dynamics*, *30*(3), 318–327.

Unverdorben, F., **Hutt, M.**, Seifert, O., & Kontermann, R. E. (2015). A Fab-selective immunoglobulin-binding domain from streptococcal protein G with improved half-life extension properties. *PLoS ONE*, *10*(10), 1–13.

Unverdorben, F., Richter, F., **Hutt, M.**, Seifert, O., Malinge, P., Fischer, N., & Kontermann, R. E. (2016). Pharmacokinetic properties of IgG and various Fc fusion proteins in mice. *mAbs*, *8*(1), 120–128.

Dickschen, K.; Jaeger, J.; **Hutt, M.**; Pollak, N.; Siegemund, M.; Seifert, O.; Kontermann, R. E.; Pfizenmaier, K., & Block, M. (2015). PBPK Modeling to Guide Experimental Design in Drug Development. *Journal of Pharmacokinetics and Pharmacodynamics, 42*(1), 75.

Unverdorben, F., Färber-Schwarz, A., Richter, F., **Hutt, M.**, & Kontermann, R. E. (2012). Half-life extension of a single-chain diabody by fusion to domain B of staphylococcal protein A. *Protein Engineering, Design and Selection*, *25*(2), 81–88.

Schmitt, L. C., Rau, A., Seifert, S., Honer, J., Schmid, S., **Hutt, M.**, Zantow, J., Hust, M., Dübel, S., Olayioye, M. A., & Kontermann, R. E. Inhibition of HER3 activation and tumor growth with a human antibody binding to a conserved epitope within domain III and IV. Submitted.

Siegemund, M., Seifert, O., Zarani, M., Džinić, T., De Leo, V., Göttsch, D., Münkel, S., **Hutt, M.**, Pfizenmaier, K., & Kontermann, R. E. (2016). An optimized antibody-single-chain TRAIL fusion protein for cancer therapy. *mAbs*, *8*(5), 879–891.

Patents

Kontermann, R., Schmitt, L., **Hutt, M.**, Seifert, O., Olayioye, M., Hust, M., Dübel, S., Zantow, J. (2016). Antigen-binding protein against HER3. 16188871.4.

Kontermann, R., Unverdorben, F., **Hutt, M.** (2011). Serum half-life extension using immunoglobulin binding domains. EP12762595.

Sahin, U., Kontermann, R., Pfizenmaier, K., Siegemund, M., **Hutt, M.**, Seifert, O. (2015). Single-chain TNF ligand family molecules and fusion proteins and derivatives thereof. EP16714290.